

**ASSESSMENT OF LATERAL FLOW AND BASE FLOW FOR EFFECTIVE
INTERVENTIONS IN WATER CONSERVATION**

By

JYOTHY NARAYANAN

(2016-28-004)



Department of Soil and Water Conservation Engineering

**KELAPPAJI COLLEGE OF AGRICULTURAL ENGINEERING AND
TECHNOLOGY**

TAVANUR-679573, MALAPPURAM (DT)

KERALA, INDIA

2021

**ASSESSMENT OF LATERAL FLOW AND BASE FLOW FOR EFFECTIVE
INTERVENTIONS IN WATER CONSERVATION**

By

JYOTHY NARAYANAN

(2016-28-004)

Thesis

Submitted in partial fulfilment of the requirement for the degree of

Doctor of Philosophy

In

Agricultural Engineering

(Soil and Water Engineering)

Faculty of Agricultural Engineering and Technology

Kerala Agricultural University



Department of Soil and Water Conservation Engineering

**KELAPPAJI COLLEGE OF AGRICULTURAL ENGINEERING AND
TECHNOLOGY**

TAVANUR-679573, MALAPPURAM (DT)

KERALA, INDIA

2021

DECLARATION

I, hereby declare that this thesis entitled “**ASSESSMENT OF LATERAL FLOW AND BASE FLOW FOR EFFECTIVE INTERVENTIONS IN WATER CONSERVATION**” is a bonafide record of research work done by me during the course of research and the thesis has not previously formed the basis for the award to me of any degree, diploma, associateship, fellowship or other similar title of any other University or Society.

Tavanur



Jyothy Narayanan
(2016-28-004)

CERTIFICATE

Certified that this thesis entitled “ASSESSMENT OF LATERAL FLOW AND BASE FLOW FOR EFFECTIVE INTERVENTIONS IN WATER CONSERVATION” is a record of research work done independently by Jyothy Narayanan (2016-28-004) under my guidance and supervision and that it has not previously formed the basis for the award of any degree, diploma, fellowship or associateship to her.



Dr. Sathian K. K.
(Major Advisor, Advisory Committee)
Professor & Head of SWCE and Dean
Kelappaji College of Agricultural Engineering and Technology
Tavanur

CERTIFICATE

We, the undersigned members of the advisory committee of Jyothy Narayanan (2016-28-004), a candidate for the degree of Doctor of Philosophy in Agricultural Engineering with major in Soil and Water Engineering, agree that the thesis entitled "ASSESSMENT OF LATERAL FLOW AND BASE FLOW FOR EFFECTIVE INTERVENTIONS IN WATER CONSERVATION" may be submitted by Jyothy Narayanan (2016-28-004), in partial fulfillment of the requirement for the degree.



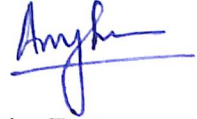
Dr. Sathian K.K
(Major Advisor, Advisory Committee)
Professor & Head of SWCE and Dean
KCAET, Tavanur



Dr. Abdul Hakim V.M
Professor (SWCE)
RARS Pattambi
Palakkad (DT)



Dr. Rema K.P
Professor and Head
Dept. of Irrigation and Drainage Engg.
KCAET, Tavanur



Dr. Anu Varughese
Assistant Professor
Dept of Irrig. and Drain. Engg.
KCAET, Tavanur



Dr. Suresh Kumar P.K
Professor
Dept. of Agricultural Engineering
College of Agriculture
KAU (PO), Thrissur

EXTERNAL EXAMINER



Dr. H.D Rank
Professor and Head
Dept. of Soil and Water Engg.
Junagarh Agricultural University
Junagadh, Gujarat

Retd. Scientist, CWRDM, Kerala, India for their intrinsic research enthusiasm and invaluable suggestions.

I would like to take the opportunity to present my incessant gratitude to **Dr. Deepak Swami**, *Assistant Professor*, School of Engineering, Indian Institute of Technology, Mandi, Himachal Pradesh, India for his unpretentious and unprejudiced help for the software access and its usage.

I am immensely thankful to **Dr. Sahila Beegum**, *Post-Doctoral Research Associate*, University of Nebraska Lincoln and USDA-Agricultural Research Service, Maryland, USA, for her generous support and suggestions.

I would like to place my special thanks to my junior **Er. Adarsh S S.**, for his sincere help and support during my research work. It would be my pleasure to thank my juniors **Er. Pooja M.R., Er. Pooja V Er. Md Majeed Pasha** and **Er. Mamatha Prabhakar**, for their immense support and constant motivation. I would also like to seize the opportunity to thank the field workers **Mr. Vasu** and **Mr. Natarajan** for their untiring contribution in installing the field set ups. I would like to thank **Mr. Shyam**, *Farm officer*, KCAET, Tavanur for his kind support. I would like to thank all the faculties and staff members of KCAET, Tavanur and from Krishi Vigyan Kendra, Malappuram for their timely suggestions, support and cooperation.

I am greatly beholden to my **parents** for their boundless support. With their blessings, prayers love and sacrifices, I have been able to accomplish this endeavor. I would like to thank my beloved husband **Mr. Anoop R.J** for bearing the patience, giving utmost care, support and help throughout this period.

Finally, I thank **all the people** who have supported me to complete the research work directly or indirectly.

Jyothy Narayanan

CONTENTS

Chapter No.	TITLE	Page No.
	LIST OF TABLES	i-ii
	LIST OF FIGURES	iii-x
	LIST OF PLATES	xi
I	INTRODUCTION	1
II	REVIEW OF LITERATURE	5
III	MATERIALS AND METHODS	44
IV	RESULTS AND DISCUSSION	88
V	SUMMARY AND CONCLUSION	192
	REFERENCES	
	ABSTRACT	
	PUBLICATION	

LIST OF TABLES

Table No.	TITLE	Page No.
3.1	Description of Experimental set ups for lateral flow monitoring	47
3.2	Description of Experimental set ups for lateral flow monitoring through salt (NaCl) tracer	48
3.3	Description of Experimental set ups for base flow monitoring	48
3.4	Physical specifications of TEROS12 sensors	54
3.5	Measurement specifications of TEROS12 sensors	55-56
3.6	Electrical and timing characteristics of TEROS12 sensors	56
3.7	Physical specifications of ZL6 data logger	57
4.1	Soil physical properties of site 1	92
4.2	Soil Physical Properties for Site 2	93
4.3	Soil Physical Properties for Site 3	94
4.4	Uniformity coefficient of sprinklers	95
4.5	Specifications of the butterfly sprinklers	95
4.6	Gravimetric soil moisture data analysis for experimental set up 1	96-97
4.7	Variation in lateral flow discharge through different soil profile depths during experimental set up 1	100-101
4.8	Gravimetric soil moisture data analysis for experimental set up 2	104-105
4.9	Variation in lateral flow discharge through different soil profile depths during experimental set up 2	108-109
4.10	Calibration functions for sensors	114
4.11	Volumetric water content analysis for experimental set up 3	115-116
4.12	Variation in lateral flow discharge through different soil profile depths during experimental set up 3	118
4.13	Rainfall data from 30/07/2019 to 29/08/2019	119-120
4.14	Volumetric water content analysis for experimental set up 4	120-123

4.15	Variation in lateral flow discharge through different soil profile depths during experimental set up 4	139-140
4.16	Variation of Lateral Flow Discharge with Temporal Variation of Volumetric Water content in Site 2 under Natural Rainfall Conditions (SW-Monsoon)	141-143
4.17	Rainfall records during September	145
4.18	Variation in lateral flow discharge through different soil profile depths during experimental set up 5	152
4.19	Variation of Lateral Flow Discharge with Temporal Variation of Volumetric Water content in Site 3 under Natural Rainfall Conditions	153-154
4.20	Average subsurface flow discharge through different soil profile depths recorded from three experimental sites under different experimental set ups.	155-156
4.21	True velocity of interflow from the salt breakthrough analysis in site 2 and site 3	165
4.22	Elevation head of observation wells 1 and 2	167
4.23	Stable isotope measurements	172
4.24	Material properties for water flow derived from Rosetta model	174

LIST OF FIGURES

Figure No.	TITLE	Page No.
3.1	The study area	44
3.2	Plan view of the experimental set up 1 installed at site 1	50
3.3	Plan view of the experimental set up 2 installed at site 2	52
3.4	Capacitance based TEROs12 sensor	53
3.5	ZL6 data logger	58
3.6	Plan view of the experimental set up 3 installed at site 2	63
3.7	Plan view of the experimental set up 4 installed at site 2	64
3.8	Plan view of the experimental set up 5 installed at site 3	65
3.9	Hypothetical soil column	67
3.10	Plan view of the experimental set up for tracer experiment in site 3	69
3.11	Plan view of the experimental set up for tracer experiment in site 2	71
3.12	Plan view of the experimental set up for groundwater flow monitoring	73
3.13	Plan view of the experimental set up for groundwater flow analysis using salt (KCl) tracer in site 1	75
3.14	Generalized structure for the first order decay reactions for three solutes	81
4.1	Recorded rainfall pattern for the years 2018 and 2019 in the study area	88
4.2	Contour map of experimental site 1	89
4.3	Slope map of experimental site 1	89
4.4	Contour map of experimental site 2	90
4.5	Slope map of experimental site 2	90
4.6	Contour map of experimental site 3	91
4.7	Slope map of experimental site 3	91
4.8	Gravimetric soil moisture content variations for experimental set up 1 on 8/02/2019 in site 1	98
4.9	Gravimetric soil moisture content variations for	99

	experimental set up 1 on 9/02/2019 in site 1	
4.10	Gravimetric soil moisture content variations for experimental set up 1 on 10/02/2019 in site 1	99
4.11	Gravimetric soil moisture content variations for experimental set up 1 on 11/02/2019 in site 1	100
4.12	Temporal variation of lateral flow discharge from 5/02/2019-6/02/2019 from three soil profile depths for experimental set up 1	102
4.13	Temporal variation of lateral flow discharge from 7/02/2019-8/02/2019 through three soil profile layers for experimental set up 1	102
4.14	Temporal variation of lateral flow discharge from 9/02/2019-10/02/2019 in three soil depths for experimental set up 1	103
4.15	Temporal variation of lateral flow on 11/02/2019 in three soil depths for experimental set up 1	103
4.16	Gravimetric soil moisture content variations for experimental set up 2 on day 4 in site 2	106
4.17	Gravimetric soil moisture content variations for experimental set up 2 on day 5 in site 2	106
4.18	Gravimetric soil moisture content variations for experimental set up 2 on day 6 in site 2	107
4.19	Gravimetric soil moisture content variations for experimental set up 2 on day 7 in site 2	107
4.20	Temporal variation of lateral flow discharge for the first 5 days from three soil profile depths for experimental set up 2	110
4.21	Temporal variation of lateral flow discharge for the last 5 days from three soil profile depths for experimental set up 2	110
4.22	Calibration curve for sensor 1 (for soil profile at 0-40 cm)	112
4.23	Calibration curve for sensor 2 (for soil profile at 40-80 cm)	113
4.24	Calibration curve for sensor 3 (for soil profile at 80-120 cm)	113

4.25	Temporal variation of % VWC in three soil profile depths during experimental set up 3 at site 2	117
4.26	Temporal variation of lateral flow discharge from three soil profile depths during experimental set up 3 at site 2	117
4.27	Temporal variation of % VWC in three soil profile depths during experimental set up 4 on 05/08/2019 at site 2	123
4.28	Temporal variation of % VWC in three soil profile depths during experimental set up 4 on 06/08/2019 at site 2	124
4.29	Temporal variation of % VWC in three soil profile depths during experimental set up 4 on 07/08/2019 at site 2	124
4.30	Temporal variation of % VWC in three soil profile depths during experimental set up 4 on 08/08/2019 at site 2	125
4.31	Temporal variation of % VWC in three soil profile depths during experimental set up 4 on 09/08/2019 at site 2	126
4.32	Temporal variation of % VWC in three soil profile depths during experimental set up 4 on 10/08/2019 at site 2	126
4.33	Temporal variation of % VWC in three soil profile depths during experimental set up 4 on 11/08/2019 at site 2	127
4.34	Temporal variation of % VWC in three soil profile depths during experimental set up 4 on 13/08/2019 at site 2	127
4.35	Temporal variation of % VWC in three soil profile depths during experimental set up 4 on 14/08/2019 at site 2	128
4.36	Temporal variation of % VWC in three soil profile depths during experimental set up 4 on 15/08/2019 at site 2	128

4.37	Temporal variation of % VWC in three soil profile depths during experimental set up 4 on 21/08/2019 at site 2	129
4.38	Temporal variation of % VWC in three soil profile depths during experimental set up 4 on 22/08/2019 at site 2	129
4.39	Temporal variation of % VWC in three soil profile depths during experimental set up 4 on 25/08/2019 at site 2	130
4.40	Temporal variation of % VWC in three soil profile depths during experimental set up 4 on 26/08/2019 at site 2	130
4.41	Temporal variation of % VWC in three soil profile depths during experimental set up 4 on 27/08/2019 at site 2	131
4.42	Temporal variation of % VWC in three soil profile depths during experimental set up 4 on 28/08/2019 at site 2	131
4.43	Temporal variation of lateral flow discharge from three soil profile depths during experimental set up 4 from 30/07/2019 – 31/07/2019 in site 2	133
4.44	Temporal variation of lateral flow discharge from three soil profile depths during experimental set up 4 from 01/08/2019 – 02/08/2019 in site 2	134
4.45	Temporal variation of lateral flow discharge from three soil depths during experimental set up 4 from 08/08/2019 to 09/08/2019 in site 2	135
4.46	Temporal variation of lateral flow discharge from three soil depths during experimental set up 4 from 09/08/2019 to 10/08/2019 in site 2	136
4.47	Temporal variation of lateral flow discharge from three soil depths during experimental set up 4 from 16/08/2019 to 17/08/2019 in site 2	137
4.48	Temporal variation of lateral flow discharge from three soil depths during experimental set up 4 from 18/08/2019 to 19/08/2019 in site 2	138
4.49	Daily lateral flow discharge from the three soil profile	144

	layers versus daily rainfall for the experimental set up 4 in site 2	
4.50	Temporal variation of % VWC in three soil profile depths during experimental set up 5 on 03/09/2019 at site 3	146
4.51	Temporal variation of % VWC in three soil profile depths during experimental set up 5 on 04/09/2019 at site 3	147
4.52	Temporal variation of % VWC in three soil profile depths during experimental set up 5 on 07/09/2019 at site 3	147
4.53	Temporal variation of % VWC in three soil profile depths during experimental set up 5 on 15/09/2019 at site 3	148
4.54	Temporal variation of % VWC in three soil profile depths during experimental set up 5 on 19/09/2019 at site 3	148
4.55	Temporal variation of % VWC in three soil profile depths during experimental set up 5 on 21/09/2019 at site 3	149
4.56	Temporal variation of % VWC in three soil profile depths during experimental set up 5 on 22/09/2019 at site 3	149
4.57	Temporal variation of lateral flow discharge from three soil profile depths during experimental set up 5 from 03/09/2019 to 04/09/2019 in site 3	150
4.58	Temporal variation of lateral flow discharge from three soil profile depths during experimental set up 5 from 07/09/2019 to 08/09/2019 in site 3	151
4.59	Daily lateral flow discharge from the three soil profile layers versus daily rainfall for the experimental set up 5 in site 3	154
4.60	Spatial and temporal variation of EC after salt tracer application on 14/10/2019	157
4.61	Spatial and temporal variation of % VWC after tracer application on 14/10/2019	158
4.62	Spatial and temporal variation of EC after tracer	159

	application on 19/10/2019	
4.63	Spatial and temporal variation of % VWC after tracer application on 19/10/2019	160
4.64	Spatial and temporal variation of % VWC after tracer application on 13/11/2019	161
4.65	Spatial and temporal variation of EC after tracer application on 13/11/2019	162
4.66	Spatial and temporal variation of % VWC after tracer application on 16/11/2019	164
4.67	Spatial and temporal variation of EC after tracer application on 16/11/2019	164
4.68	Pressure head variation in observation well 1	166
4.69	Pressure head variation in observation well 2	167
4.70	Hydraulic head variation of observation well 1 and 2	168
4.71	Temporal variation of electrical conductivity in injection well	169
4.72	Temporal variation of logarithmic tracer concentration in injection well	169
4.73	Weekly variation of groundwater flow	171
4.74	FE mesh with domain properties in HYDRUS-1D	174
4.75	(a) Temporal variation of simulated VWC (%) at three different observation nodes in site 2, (b) Temporal variation of simulated pressure head at three different observation nodes in site 2	176
4.76	Simulated and observed % VWC for soil depth of 0-40 cm in site 2	176
4.77	Simulated and observed % VWC for soil depth of 40-80 cm in site 2	177
4.78	Simulated and observed % VWC for soil depth of 80-120 cm in site 2	177
4.79	Temporal variation of cumulative flux across the line source trench in site 2	178
4.80	Soil water retention curve for soil materials at three different soil depths in site 2	179
4.81	Simulated two dimensional distribution of water content in the soil profile at t=0 in site 2	180

4.82	Simulated two dimensional distribution of water content in the soil profile at t =1 h after line application of water in site 2	180
4.83	Simulated two dimensional distribution of water content in the soil profile at t =4 h after line application of water in site 2	181
4.84	Simulated two dimensional distribution of water content in the soil profile at t =8 h after line application of water in site 2	181
4.85	Simulated two dimensional distribution of water content in the soil profile at t =12 h after line application of water in site 2	182
4.86	Simulated two dimensional distribution of water content in the soil profile at t =16 h after line application of water in site 2	182
4.87	Simulated two dimensional distribution of water content in the soil profile at t = 18 h after line application of water in site 2	183
4.88	Simulated two dimensional distribution of water content in the soil profile at t = 20 h after line application of water in site 2	183
4.89	Field set up for simulation of velocity of flow in shallow wells in site 1	185
4.90	Simulated salt (KCl) tracer breakthrough in monitoring well A at observation node N1 in site 1	186
4.91	Simulated and observed salt (KCl) tracer breakthrough in monitoring well A at site 1	186
4.92	Simulated two dimensional distribution of salt tracer in the soil profile at t=0 h in site 1	187
4.93	Simulated two dimensional distribution of salt tracer in the soil profile at t = 1 h in site 1	187
4.94	Simulated two dimensional distribution of salt tracer in the soil profile at t = 4 h in site 1	188
4.95	Simulated two dimensional distribution of salt tracer in the soil profile at t = 8 h in site 1	188
4.96	Simulated two dimensional distribution of salt tracer in the soil profile at t = 12 h in site1	189

4.97	Simulated two dimensional distribution of salt tracer in the soil profile at t = 16 h in site1	189
4.98	Simulated two dimensional distribution of salt tracer in the soil profile at t = 20 h in site1	190

LIST OF PLATES

Plate No.	TITLE	Page No.
3.1	Installation of experimental set up in site 1	51
3.2	Installation of TEROS 12 sensors in field for reliability check before calibration	59
3.3	Step-by-step procedure in calibration of TEROS12 sensor	61
3.4	Observation well and PVC pipe installation in site 1	72
3.5	Monitoring of base flow through salt tracer analysis and TEROS12 measurements	77

CHAPTER 1

INTRODUCTION

Water, the most essential resource which supports all forms of life exists on the earth in the space called hydrosphere. Out of the total water available on the Earth, the share of fresh water is very meagre and its availability is highly dynamic with respect to time and space. The unavailability of water to meet various lifesaving and economic activities worries people of all walks of life, countries whether rich or poor. As a result, topics related to water conservation and water management have become focused areas of research for the water scientists (Hydrologists). There is no second opinion that understanding the intricacies of the water cycle (Hydrological cycle) is the most essential prerequisite to plan any water scarcity mitigation plans.

Hydrosphere circumscribes the water on the surface of the planet, air and beneath the land surface where the water circulates through a maze of paths called hydrologic cycle. The hydrologic cycle has no beginning or end and incorporates numerous processes that occur continuously. Among the various processes occurring in the hydrologic cycle, the most hidden and complex process is the movement of water underneath the land surface through different pathways. Since soil is the major reservoir of fresh water and thus, the net interplay of the water moving down from surface to subsurface and the management of water from subsurface storage is very essential.

Water movement in the subsurface space exhibits inherent complexities. There is only limited knowledge available on the movement of water in the subsurface space as it is influenced by a number of forces and the heterogeneous characteristics of the substrata. The two major forces i.e. gravity and adhesion move the liquid water through the soil pores to facilitate the subsurface soil water. The soil water movement may either occur in the unsaturated zone of the subsurface or may undergo deep percolation into the zone of saturation. This partitioning of the water fundamentally depends upon the soil, its properties and the kinds of rock structures

present in the region. Scientifically, the unsaturated zone is highly complex and must be studied with an interdisciplinary approach (Nimmo, 2006)

Most literatures divide the infiltrated subsurface water into two zones, viz; zone of aeration and zone of saturation. Some of the infiltrated water that reaches a zone where all the pores in soil are filled with water is called as the *zone of saturation*. A part of the infiltrated water which will be held by the molecular attraction and surface tension to the walls of soil pores and does not reach the zone of saturation is termed as the *zone of aeration*. Further, the zone of aeration is fractioned into three parts: the belt of soil water/root zone, the intermediate belt / vadose or unsaturated zone and the capillary fringe.

The *root zone*, contains loose materials and soil, from where water evaporates into the atmosphere by the process of evapotranspiration. The *vadose zone* is an unsaturated zone mostly present above the aquifer, and is partly filled with air and water. The *capillary fringe* is present above the water table (zone of saturation) and contains the drawn up water obtained from the capillary action. The width of capillary fringe depends on the size of the micro pores of the soil. The depth of the zone of rock flowage is not accurately known but is generally estimated in several kilometres.

Depending upon the physiography of terrain and soil properties the infiltrated water may advance laterally or vertically through the soil matrix. The horizontal portion of moving water in the unsaturated zone is termed as lateral flow or interflow whereas; the deep percolation of water contributes to groundwater storage. The horizontal movement of water from the zone of saturation is called base flow or groundwater flow. In the case of steep hillslopes, lateral subsurface flow can be termed as *subsurface stormflow (SSF)* which is characterized by *translatory flow* due to macropores (Beven and German, 1982). It is mainly due to the presence of conductive soils with good humic content. However, in areas having dry climate and in areas with moderate slopes, SSF occurs whenever there is high rainfall or high

moisture content in the soil. The flow regimes in the vadose zone can be categorized into a uniform matrix flow and the non-uniform macropore /piped flow termed as preferential flow (Weiler *et al.*, 2003). The uniform matrix flow is a comparatively gradual and uniform movement of water alongside solutes through the soil. This kind of movement follows the *convective-dispersion theory*. Preferential flow, on the other hand represents a non-uniform and relatively faster movement of water through the soil domain. It is characterized by enhanced flux regions in such a way that the small fraction of soil media such as wormholes, holes from the roots and cracks takes part in most of the flow (Anderson and Burt, 1990). Preferential flow occurs either in such structures wherein water flows only under the gravitational action or in areas having higher degree of permeability as compared to nearby soil matrix. Hence, it is quite essential to identify the kind of lateral flow occurring in an area in order to understand the storage and soil dynamics of groundwater recharge.

Kerala, a southern peninsular state in India, has a strong influence of its geomorphology on its groundwater regime. The state is divided into three geographical divisions viz; the lowland, midland and the highlands. The midlands lie in between the highlands & lowlands and are characterized by undulating hills and valleys. The lowlands signify the coastal stretch in the state. In spite of abundant rainfall in the state, its ground water resources are limited due to the characteristic geomorphic setting and nature of the underlying geological formations (Pullare, 2012). More than 80 percent of the geographical area in the state is underlain by crystalline rocks which are lateralized in the midlands (Shaji , 2013). As laterites are highly porous lithological unit, the movement of water greatly depends on the topographical conditions. Thus, the physiographical and lithological conditions in the state promote quick drainage of rain water into the Arabian Sea thereby reducing the residence time of available groundwater. Although, the State receives an average annual rainfall of 3000 mm which is almost three times of that received by the whole country the baseline water stress (withdrawal/total supply) is constantly increasing (Aayog, 2019). With, more than 60 percent of the total State's population depending

solely on the available groundwater, the groundwater table is declining at a greater pace than ever before. The wells are becoming a seasonal source of water. The physiographical, hydrogeological and emerging anthropogenic conditions in the State have further aggravated the prevailing situation. It became more evident when the State was classified among the poor scorers in water resource management, according to the composite water management index (CWMI) provided by NITI Aayog for the financial year 2017-18. In sloping terrains with high permeability, a considerable amount of lateral flow has also been reported (Sathian and Syamala, 2009). Thus, it is essential to carry out a comprehensive study on the subsurface movement of water for suggesting effective interventions for water conservation in such extensive situation of the state.

The detailed review of references reveals very little information and insufficient explanation on the movement of water through the intermediate vadose zone and zone of saturation under a laterite terrain. Moreover, the interactive effect of interflow and groundwater flow has not been addressed adequately for a laterite terrain. Concurrently, a detailed analysis, quantification and simulation of lateral and groundwater flow for a laterite terrain is unavailable.

Thus, the present study focalizes to render a detailed insight into the interflow and base flow with the following objectives:

1. **To estimate the lateral flow and base flow of the selected lateritic terrains.**
2. **To model the lateral flow and base flow for using in different lateritic terrains.**
3. **To suggest better interventions for ground water recharge and storage.**

CHAPTER 2

REVIEW OF LITERATURE

2.1 GENERAL

This chapter encompasses various research reviews and their contributions in carrying out the present study. The chapter will foreground upon the prominent results obtained through various research works that had aided in understanding the significance of soil moisture studies, automated soil moisture sensors and their soil specific calibration, their eminence in monitoring spatial and temporal variation in interflow and significance of lateral subsurface flow in ground water recharge.

The chapter will also focus onto the various studies that were made to understand the movement of soil moisture in different soil profiles and it's monitoring using tracers. The groundwater recharge and its discharge being the most significant subject in the study area due to the presence of charnockite bedrock system, the chapter does include the past studies focused upon the monitoring of groundwater flow rate using natural and artificial tracers. Additionally, the research works related to the modelling of these two major hydrological processes viz; lateral flow and base flow are also included in this chapter for having better information towards the two major hydrological systems.

2.2 SIGNIFICANCE OF SOIL MOISTURE STUDIES

Nyberg (1996) conducted a study for a catchment of area 6300 m² on the Swedish west coast to analyse variation in soil moisture content spatially. The main objective of this research was to describe the lateral variability of soil water content at different spatial scales. A Time Domain Reflectometer (TDR) was used to create catchment wide mappings of soil water. The estimations were done for the soil layers between 0-15 cm and 0-30 cm depth. A three-component mixing model was used for estimating the water content from the TDR measurements. Both traditional statistics and geostatistics were used to analyse the results. The spearman rank correlation was

calculated between soil water content at the catchment scale and other properties, such as the topographic indices, thickness of the humus layer and distance to the nearest tree. The results depicted no significant correlation between the water content at single points and the distance to the nearest tree or to the thickness of the humus layer. But, there were significant correlations noted between water content and elevation and slope. It was also found that there was a great spatial variability in the moisture content even within small distances. It was concluded from the study that the variability of water content in closed basin was large, mainly as an effect of the topography and of the soil conditions.

Grayson *et al.* (1997) did a study in Australia to observe soil moisture patterns under various conditions. The state of soil moisture varied between dry and wet. The lateral movement of water through both surface and subsurface pathways was found to be predominant in the wet phase. It was identified and named as nonlocal control. The other state of soil moisture which was denoted as dry state included vertical fluxes, with soil properties and only local terrain influencing spatial patterns. It was denoted as local control. The interchange between the soil moisture states was explained in the form of predominance of lateral over vertical water fluxes and the other way round. It was concluded from the study that hydraulic conductivity decreases with depth in temperate areas of Australia. The spatial patterns of soil moisture showed two preferred states and took relatively short period for transition.

Crave and Gascuel-Oudou (1997) analysed the influence of topography on time and space distribution of soil surface water content in an area of 1.3 km² within a catchment of Coet- Dan at Brittany in France. Four field surveys were performed. A total of 400 samples were collected from soil profile depth of 5 cm during the survey. The obtained measurements and topography characteristics were analysed for any relation between them. A topographic index was used in the study to explain the structural data. The index was defined as the difference in elevation of the sample

point and stream point. Thus, it was found from the study that topography and spatial distribution of soil controlled the spatial distribution of surface water content.

Qiu *et.al* (2001) carried out the investigation on effect of land use and topography on soil moisture in a sloppy hill of the Loess plateau in China. Biweekly soil moisture measurements were conducted for soil profile depths of 0–5, 10–15, 20–25, 40–45 and 70–75 cm. It was done by correlation analysis and detrended canonical correspondence analysis (DCCA). It was found from the analysis of the time-averaged soil moisture profile type and quantitative indices were correlated to one another. It was found that different environmental factors play an important role in effecting different soil moisture and its profile features. It was found that the of soil moisture content profile type was notably correlated to the land use in study area. Additionally, the profile gradient (G_i) and the profile variability (VP_i) were influenced by topography. A new index called profile gradient of soil water (G_i) was developed in this research to determine the lateral and vertical redistribution of soil water.

Gomez-Plaza *et al.* (2001) analysed the factors regulating the spatial distribution of soil water content in a small semiarid watershed located in south east Spain in Murcia region. The experiment was carried out at two different locations. The first was the burnt area with sparse vegetation and the other was the unburned area with more vegetation cover. The factors which were found to affect the soil water content in the burnt area included soil texture and slope. These factors were considered as local controls. Further, the factors that affected soil moisture in the unburnt area were related to the vegetation cover in semi-arid environment. In the vegetated zone the spatial variation in the soil moisture content was best explained by the upslope contributing area, its aspect, soil profile curvature and depth of soil. Considerable variations were noticed in the physiological activity of the vegetation cover under the influence of these factors. This study was focused on two objectives. The first was to explore the main factors determining soil moisture trends in semi-

arid environments, the role of plant cover in soil moisture models, and how these factors affected soil moisture content. The second objective was to enhance the physical importance of field indices in semi-arid zones by introducing factors that are usually not taken into account in these indices. The study found that the spatial variability of soil moisture and the factors that regulated this variation had a major influence on the spatial variability of soil moisture. The results were found apt for both vegetated and non-vegetated zones. The study also showed that the factors which need consideration while analyzing the soil moisture patterns relied on the study area environment and the vegetal canopy. The developed indices in the study merged the effect of lateral flow in the unsaturated zone and topographic convergence on soil moisture.

Western *et al.* (2004) interpreted the correlation in terms of space between soil moisture and prevailing hydrological processes in the small watersheds of Australia (Tarrawarra and Point Nepean) and New Zealand (Mahurangi River Basin). In this study soil samples from five different sites were analysed for the soil moisture patterns and its geostatistical properties. Time domain reflectometry (TDR) was used to collect soil moisture from all sites, allowing for comparisons between sites without complications related to differences in methodology. During the study, a seasonal variation was found in the spatial variance of soil moisture and average water content of all sites. A systematic relationship was established between the differences in variability associated with the mean spatial soil moisture. This relationship varies between sites. It was found that these differences were due to variations in the seasonal patterns of controlling processes. It was found that these patterns were responsible for the seasonal variations in the mean spatial soil moisture content, especially lateral flow processes. A comparison of the soil moisture correlation lengths with that of field attributes was done, and subsequently sites were identified, where the soil moisture variation matched the topography spatially. The controlling processes depended upon the catchment conditions. The results suggested that

similar pattern in soil moisture variation recurred when similar conditions in the catchment were developed.

Wilson *et al.* (2004) identified and quantified variability sources in temporal and spatial observations of soil moisture. Data of soil moisture proved reliable in terms of temporal and spatial coverage. During the study, the temporal variance was found to be five times greater than the spatial variance. Additionally, it was found that seasonality played a dominant role in bringing the temporal variability at experimental sites. The study also concluded that these variations are climate dependent and are not applicable with limited water storage in the soil.

Brocca *et al.* (2007) investigated the soil moisture spatial variability in central Italy. The research involved carrying out investigations in experimental plots located in Central Italy. Spot measurements were carried out during the experimentation. Time Domain Reflectometer (TDR) was used to measure near-surface volumetric water in the study area. The area of measurement extended from 9 to 8800 m². The investigations for the soil moisture pattern in the site were repeated periodically to analyse the pattern of moisture as function of wetness conditions. The test results showed that the probability distribution for soil moisture can be assumed that is normal in flat areas. Further, in case of normalized soil moisture too the probability distribution can be assumed normal in gentle slope areas. A general decreasing trend was observed in the variance with increase in the mean moisture content. Geostatistical analysis confirmed it during the research. It was also established that the natural logarithm of the specific upslope area increases when the water volume in the soil increases and proved as an efficient spatial predictor for the near-surface soil moisture. Thus, it was established through the study that, the surface and subsurface lateral redistribution of water can be assumed to play a vital role in the spatial arrangement of soil moisture in an area.

2.3 LATERAL FLOW ANALYSIS

McCord and Stephens (1987) investigated lateral flow of moisture under sandy slopes without an obvious impeding layer. The study was carried out in a minor drainage basin on the Sevilleta National Wildlife Refuge. The study area was adequately equipped with soil monitoring instrument to determine natural ground-water recharge. To comprehend the effect of topography on water flow paths in the vadose zone of medium aeolin sand, analysis of collected soil moisture data was done. Neutron scattering technique was adopted to obtain soil moisture data. The data for hydraulic head were obtained using tensiometers. Additionally, delineation of flow paths in the vadose zone of a sandy hillslope was conducted using tracer experiments. The results established the presence of a strong lateral component of unsaturated flow in the hillslope even when the sub-soil layers had lower permeability. Tracer experiments conducted in the study using bromide exhibited that lateral flow of moisture took place under the hillslope during infiltration. The experiments also showed occurrence of soil moisture redistribution in a uniform sandy profile even when soil horizons were low-permeable. It was found through the study that the concentration of accumulated moisture can cause a notable raise soil-moisture flux at greater depths below the lowland. Thus, through the research it was concluded that in soil-moisture budgets are important and thus, be taken into consideration in case of undulating terrain.

Miyazaki (1988) analysed the flow of water in unsaturated soils on graded slopes. The study was conducted in an unsaturated area to measure water discharge on graded slopes with crushed coarse material. Measurements were made using a sloping soil container placed under the rain simulator. At the interface of two different soil layers an extended refraction was applied to the flow, utilizing a jump condition and suitable assumptions of hydraulic conductivity for soil materials. The purpose of the study was to gain insight into the effects of changing permeability on water flow in unsaturated soil. It was found through the study that the lateral flow

occurs in the direction of inclined interface and advancement of the wetting front ceases, when the plants or gravel layer is sandwiched in slopes of sandy loams soil and plants/gravel layer. During a steady percolation it was found that the lateral flow of water occurred at the inclined interface. The continuation of drainage was found to be obstructed in the slopes due to the presence of sandwiched plants/gravel.

Jackson (1992) measured the infiltration process on the slope and lateral descent in the vadose zone. The flow close to the ground surface and behind the wetting front was found to gradually ascend to vertical during the study in homogeneous and isotropic soil. In case of anisotropic soils, it was found that the height gradient became vertical, but the anisotropy diverted flow to bring up an inclined component of flow, the size of which depended on the degree of anisotropy. It was found through the study that in homogeneous soils of hillslope, drainage occurred in soils both isotropic and anisotropic, as shallow flow of water laterally in vadose zone. Any anisotropy in the downslope was found to enhance the lateral flow downslope the hill, which caused shallow flow vectors during drainage which were found to be practically parallel to the surface. The simulations were coupled with McCord results. A very high ratio of constant anisotropy was found e.g. 10 or < 10 caused notable lateral flow downslope the hill during wetting. Further, the simulations which were conducted numerically in the study substantiated Zaslavsky and Sinai's (1981b) and Philip's (1991) findings. It has been found that an isotropic homogeneous slope during wetting contributes to lateral flow, but does so during drying, as suggested by Zaslavsky and Sinai (1981b).

Woods *et al.* (1996) performed study across a hillside. The study involved probing variation in the subsurface flow. The study involved monitoring subsurface flow through thirty troughs located across the base of forested hillslope at Maimai in New Zealand. The experimental period for the study was 110 days. Measurements of extended dry periods and intense rainfall were recorded. The surface topography was found to be the main governing factor in deciding the flows. A steady relation

was found in between the portion of the total flow taken by each trough and the net flow from the hillside. The spatial variation in the flow suggested that 1-2 meter long troughs were inadequate to estimate total subsurface flow from the hillside or small catchments. In between the adjacent troughs large variations in flow rates were found which indicated that the subsurface flow can't be measured just by the length of trough multiplied the estimated length of stream in case of a small catchment.

Spatial variability of subsurface flow alters over time, depending on the total flow from the hillside; at the study site. The results suggested that data for small troughs are very difficult to extrapolate to larger scales, and the problem is more severe for changing flow conditions. Wider troughs improve the reliability, but account must still be taken of topographic features.

Freer (2002) studied subsurface stormflow in a bedrock topography. The study site was considered to be the Mount Panola Research Watershed (PMRW) in Georgia. An extensive study was carried out to monitor flow beneath the surface. Additionally response of the water table along with digital terrain analysis (DTA) was carried out for analyzing surface and subsurface features. A trench of dimensions (20 m x 48 m) on a granitic bedrock system was surveyed. Trench sections of length 2 m and macropores were monitored during three rainstorms. Matrix flow was observed from hillside during every storm. Flow through the macropores was noted during two larger rainstorms. The study showed a delayed water flow relative to precipitation and stream flow. Subsurface storm flow, peak flow and presence of macropores were noticed from the deeper sections of the trench. Ground and bedrock surface elevations were measured in a grid pattern to obtain detailed map of two surfaces.

High variability was recorded in the timing of subsurface storm flow, its peak flow, macropore flow volume and recession characteristics when the measurements were done along the artificial trench face. During the rainstorm's wetter periods, responses between water table, trench flow and bedrock indices improved. It was due to the increased hydrological connection in the hillslope. The results obtained

from the study showed that local bedrock topography play a vital role in understanding the runoff generation mechanism, especially in the areas where the bedrock surface is relatively impermeable. The results obtained through the study showed that topography of the bedrock governs the subsurface storm flow response. Moreover, it was also found that the topography of the ground surface is a poor predictor.

Kumar (2004) formulated a subsurface soil moisture transport model using the Richard's equation. For layer-averaged data of lateral flow, explicit expressions were derived for the contribution of layered lateral transport of scattering, gravity, diffusion and curvature-induced convergence of the Earth's surface. Furthermore, a formulation to analyse averaged soil moisture transport was also developed in this study using Richard's equation. The formulation accounted for lateral flow of water as well as dispersion phenomenon as a result of variation. It became clear from the study that for certain slope ranges and soil properties, the lateral flow can occur in significant amounts. Although the dispersion terms were small but they accounted for notable flux when considered over large areas. It was found significantly in areas with heterogeneous soil properties. Through the study it became clear that land surface curvature also contributes the lateral moisture flux. Moreover, if such contributions are ignored it can result in significant error in the model. It may lead to inaccurate predictions or error in calibration of parameters.

Kim *et al.* (2005) measured the effect of antecedent soil moisture content on the shallow lateral flow in a forested hillslope. A soil pit of width 5 m was constructed and instrumented in British Columbia, at the foot of a forested hillslope. The processes of subsurface flow were studied throughout the course of three typical fall rainstorms having low intensities. Various antecedent moisture circumstances were analysed. The outflow was captured horizon of organic soil. Measurement was done using a trough. Additionally, the discharge from the mineral horizon was also calculated for three different sections of the soil pit. It was noted that the lateral

outflow which was measured for the storms preceding the dry conditions did not contribute much to the water table. The level of the water table did not raise upto the organic horizon. Further, the lateral flow discharge recorded from the biological horizon was 400 times less than the outflow recorded during a later storm with wet antecedent conditions. It was clear from the study that shallow lateral flow plays a significant role of potential factor in storm runoff in forested sites. The flow at the interface of organic and mineral soils interface may also contribute to a web of interconnected pathways for preferential flow during wetter antecedent conditions.

Sinai and Dirksen (2006) determined flow of water laterally in the upper of unsaturated section of sloping soil due to precipitation through laboratory experiment evidence. For the experiment water was applied at the rate of hundred times lesser than the saturated hydraulic conductivity. The water was applied on fine sand having horizontal and v-shaped surfaces. Subsequently the regimes of flow were analysed near the soil surface as well as in the soil bulk with the help of dyes. Visual analysis of flow lines, streaks and wet fronts was carried out using photographs. The analysis was done through a glass wall that runs vertically. The direction of the flow was always found perpendicular when analysed near wetting fronts. It was due to the dominant matrix potential gradients. Thus, it was found that the flow direction was in upslope direction when the dry sloping sand had an early wetting. During the analysis it was found that the lateral movement of water decayed with soil depth, but was the highest close to the soil's surface. The experiments conducted in present study verified the theory of predicting the unsaturated flow of water in a sloping soil is due to the dynamics of rainfall only. The difference in the texture of soil or anisotropy played least role in the lateral flow movement. This phenomenon observed through the study proved to have a vital inference in understanding hydrology of hillslope, desert agriculture, management of agriculture and mechanisms involved in surface runoff and erosion. Through this study the explanation given by Jackson (1992), about the occurrence of unsaturated lateral flow in downslope only upon the cessation of rainfall was proved to be partially correct. It

was proved that the essential situation for the lateral flow to occur is reducing rainfall intensity instead of a lack of flow at the soil's surface. Significant lateral flow conditions were observed under such conditions.

Vereecken *et al.* (2008) explored and reviewed measurements of soil moisture content in the vadose zone. The study was focused on a large scale (field and catchment). The study was conducted due to the increasing ability and instrumentation in soil moisture measurement with unparalleled resolution, both spatially and temporally at different scales. In this review study various state of art of soil moisture measurement has been highlighted to estimate soil hydraulic properties, the measurement of fluxes related to water and energy and methods to understand temporal and spatial dynamics soil moisture with various soil profiles. Certain arguments related to easy access to field sites and databases under surveillance having detailed information about hydrological flux variability and its parameters which included their upscale values have been also included in the present review.

Van Schaik (2008) investigated preferential flow on the hillslope and its effect on the hydrology of hillslope in a semi-arid watershed in Dehesas. This study was aimed to quantify preferential flow from the in a semi-arid Dehesa landscape. The data required for the quantification involved piezometric data, soil moisture content, precipitation and total outflow. The variation in soil moisture content in the soil profile during the transition from the dry to the wet season concluded that preferential infiltration into the soil occurs. A rapid increase in the water level of piezometer was noticed during high intensity rainfall in the study area. Sometimes the water level also reached the soil surface. The raised water level dropped to the bedrock level within few hours to days depending upon the catchment conditions. It was noted through the study that even when the soil matrix was not wet, water layer built up. It was postulated that at this stage the transient water table present in the large pores drained partly into the matrix. Also, transient water table partly filled up the irregularities of bedrock thereby creating subsurface flow into the channels. It was

noticed that drainage from the macropores to the matrix and rock formations reduced when the matrix of the soil was wetter. Additionally the study showed that in a hillslope hydrology water can move through the fine matrix as well as macropore domain. These domains had its own characteristics, however they also interact dependent upon their moisture contents. In the study macropore contributed 13 % to the total discharge for high intensity rainfall event whereas for a low rainfall event, macropore had a contribution of 80 % of total discharge. During the large rainfall events, surface runoff suppressed the fraction of subsurface discharge. It was found that during high intensity discharge events overland flow had the dominance.

Hopp and McDonnell (2009) identified the dominant controls responsible for the subsurface flow generation. The parameters involved were depth of soil, slope angle, permeability of existing bedrock in the area, size of the storm & interactions between storms. This study involved a systematic investigation to discover the interactions between dominant controls and their effects on subsurface storm generation. Investigations were done using virtual experiments through three dimensional physical based finite element models. A hillslope at Panola was considered for the study. Virtual experiments were prepared and used in the analysis. The framework for series of virtual experiments was created using the surface and subsurface topography and stormflow details for the site. Parameterization for soil and bedrock properties was done on the basis of field analysis and measurements. At varied combinations of slope types in the site saturation of subsurface was a common feature of hillslope behaviour. During the analysis it was found that an unexpected hydrograph peak times were caused by the interactions between depth of soil, size of the storm and slope angle. The interactions between the controls led to a better understanding of connectivity due to process controls. The study led to an understanding of connectivity through process controls. It was inferred through the study that in order to characterize hillslope functions, it is essential to understand and characterize soil-bedrock permeability.

Anderson *et al.* (2009) determined the velocity of subsurface flow characterized with preferential lateral flow in a hillslope. The study involved determining the interaction between lateral velocities of tracer, length of the hillslope and storm indicators using tracers. The boundary conditions and slope length determined the subsurface velocities. The recorded velocities of subsurface flow were closely associated to 1-h rainfall intensity. Contrary to many studies on subsurface flow estimation, the measured flow velocities were only little correlated to volume of storms or previous soil moisture conditions. This study exhibited that in monitoring the average subsurface flow velocity, understanding reliability in hillslope preferential flow is important. Tracer results were used to estimate the correlation between velocities of tracer and explanatory parameters. The independent parameters involved length of the slope, inflow rate at steady state, piezometer response and characteristics of the storm. The findings from the study showed that the network of preferential flow did not depend upon the soil matrix. Additionally, it was also found that most of the subsurface flows were recorded during storms. It was noted that subsurface flow velocity was higher at short distance (12 m) as compared to larger distances (30 m). This was noted through the study that stream paths were more connected on shorter distances as compared to longer distances due to ephemeral nature of the connections. The study thus inferred that in monitoring the average subsurface flow velocity, connectivity in the network of hillslope preferential flow play an important role.

Lu *et al.* (2011) measured the direction of unsaturated flow in a homogeneous and isotropic hillslope. The study showed that within the hillslope upslope and vertical downslope lateral flow occurs concurrently at varying depths due to time varying rainfall. Temporal and spatial variation in the subsurface flow (upslope or downslope) was shown to greatly depend on the wetting and drying in the hillslope. The study inferred that history of rainfall is inadequate in defining the flow regime of subsurface flow. The condition of wetting and drying defines the subsurface direction of flow. Upslope lateral flow was noticed during the study when a certain

point in the hillslope got subjected to a sudden increase in moisture. Similarly, a downward vertical flow was witnessed during the study during a steady or small change in soil moisture content. It was found that regardless of the steady rainfall conditions, the force of gravity and constant pressure boundary conditions will produce lateral downslope movement of saturated groundwater in hillslope with isotropic and homogeneous characteristics.

Lv *et al.* (2013) investigated the unsaturated lateral flow conditions of the downward slope and the effects of the slope angle on the movement of soil moisture. The study involved investigating the effects of various angles of slope on movement of soil moisture. It was done in an isotropic and homogeneous soil tank through drying processes. Three different experiments were carried out with varying slope angles. Research results demonstrated that the rate of downward lateral flow was influenced by the rate of drainage. The flow was found to be parallel to the surface of the slope. In addition, the component of flow perpendicular to the incline surface was found to be least affected by inclination changes. The angle of slope greatly affected the flow component perpendicular to the surface of the slope in the interlayer.

Ghasemizade and Schirmer (2013) reviewed the contribution of subsurface flow in the hydrological cycle. In this study, the authors focused on the contribution of subsurface flow. Different suggested mechanisms, considering their applicability, strengths and inadequacies for subsurface flow monitoring and analysis had been discussed. Additionally, tracer experiments and their applications have been elaborated. Further, the study has also outlined various challenges in modelling interactions between surface and subsurface flows. Future targets were also highlighted.

Teschemacher *et al.* (2019) investigated lateral subsurface flow experimentally. The experiments were dependent on type of soil cultivation and land use. It was found through the study that generation of surface flow, subsurface flow and land use distribution greatly influenced the flood events in the site. Three sites

were selected to set up experimental set ups. All the three sites had similar topographic and soil characteristics. Three different land use types were set up in the sites. It included cropland, grassland and forest cover. Various parameters considered for the study were soil moisture content, generated surface runoff, soil moisture tension, observations of stream discharge and subsurface lateral flow. It was found that large volumes of flow were recorded in the grassland whereas low subsurface flow discharges were recorded from the cropland. The average response times recorded for forest site, grassland and cropland site were 6 h, 12.4 h and 20.9 h respectively. The greatest heterogeneity was observed in the forest site. Grassland site showed the lowest variability in vertical direction. The lowest vertical variability was observed at the grassland site. Greater vertical variations were noticed during rain-induced events instead of thawing events. Vegetation cover and changes in soil management influenced the subsurface flow volume distribution in the cropland site. It resulted in vertical flow in opposing shares. It was noticed during the study that the generation of subsurface flow varied in all the three sites. Forest site witnessed subsurface flow in the form of macropore flow. It was supported by smaller response times in case of intensive rain events and greater variability spatially. However, subsurface flow in the cropland site was caused by the matrix flow caused due to soil tillage on a regular basis. In the grassland site, subsurface flow was contributed by both matrix and macropore flow. In the grassland the type of the flow was found to be dependent on the event characteristics. The assumptions made from the study were completely based on event response times and on the flow volumes. It was found that inadequate amount of data restricted generalized conclusions. Nevertheless, it became clear from the study different land use types contributed to different subsurface flow volumes. The study highlighted the effective representation of subsurface flow in a realistic manner for effective working of hydrological models. Subsequently, the hydrological models can be used for the land use evaluation and its effect on flood generation process.

2.4 SOIL MOISTURE SENSORS IN SUBSURFACE FLOW ASSESSMENT

Dean *et al.* (1987) developed a capacitance sensor operating at 150 MHz. The study involved sensor design and performance analysis. Advanced electronic component technology was used in the study to obtain reliable sensitive probe for field measurements in real time. The capacitance based sensor was developed as an integrated system to measure soil moisture content, access tube installation and calibration. The probe was found to be precise, economical, easy to use, lightweight and sensitive. It was found through the study that the capacitance probe had greater resolution in the measurement of soil moisture content vertically. However, radial penetration of probe needed greater care to avoid any air gaps which may cause error. Further scope in optimization of electrode geometry was presented in the study.

Malicki *et al.* (1992) determined unsaturated soil water characteristics from undisturbed soil cores. It was done through Time Domain Reflectometer (TDR) with soil moisture miniprobe. The study involved detailed description on the construction of soil moisture miniprobe. Operating characteristics of TDR were also explained in the study. The experimental set up involved a laboratory stand having undisturbed soil cores. A set of TDR miniprobe and mini tensiometers used for the measurement of unsaturated water flow have also been described. The results presented TDR as a reliable instrument for monitoring the flow of water in the unsaturated zone.

Fen-Chong *et al.* (2004) used capacitive sensor based apparatus to estimate the dielectric constant and liquid water content in a porous media. A technique which relied on the dielectric properties of matter was used in the research. It was found to be an efficient method as water, and soil minerals have different dielectric constants which made it easier to identify them. Analysis of oven dried soil samples allowed the estimation of dielectric constant of the sample as a function of sample water amount. The described methodology in the study was found to be more compatible than other techniques.

Evelt *et al.* (2006) compared various soil moisture sensors through laboratory experiments. Experiment was carried out on three soil columns. Various sensors used in the study were the Trime T3 tube probe, Sentek EnviroSCAN, EM methods, Diviner 2000, TDR and Delta-T PR1/6 profiler. The clay content in the three soil profiles ranged from 17 to 48 %. The study involved measurements of soil moisture content in three phases i.e., before, during and after the wetting of soil column. During the study it was found that TDR was more accurate after using the factory calibrations as compared to other EM systems. Incorrect measurements were given by the EM systems for both saturated and air-dry conditions of soil. The Delta-T PR1/6 was found to be inaccurate. The Trime T3, Diviner 2000 and EnviroSCAN provided roughly accurate values.

Merlin *et al.* (2007) analysed different calibration methods for a soil moisture sensor. Stevens Hydraprobe ® dielectric soil sensor was tested with different calibration approaches. The sensor which operates at 50 MHz was tested with National Airborne Field Experiment (NAFE) data. The study was done to understand and determine the effect of various soil types and soil temperature on the sensor. The applicability of general calibration equation was also assessed for the sensor. A comparison between the factory calibrated sensor readings and gravimetric measurements showed that the sensor lost its sensitivity above 25 % of soil moisture content in clay. The study showed that the root mean square error (RMSE) was decreased from 4.0 % to 3.3 % with the loss corrected equation.

Chow *et al.* (2009) performed an assessment on the performance of soil water content sensors in the field. The study was carried out in New Brunswick, maritime region in Canada. Nine capacitance based soil water sensors were installed in the site having sandy loam soil. Gravimetric method of soil water estimation was adopted as reference. Irrespective of the depth of installation and regimes of soil water the Trase, CS615 and Troxler were proved to be best after factory calibration. The root mean square error recorded was 16.93 %, 15.78 % and 17.65 % respectively for the

three sensors. The r^2 values recorded were 0.7, 0.75 and 0.65 respectively for the three sensors. Three sensors including MP917, Gopher and TRIME were the worst performers even with factory calibration. Root mean square error values obtained were 26.57, 20.41 and 45.76 respectively. The r^2 values recorded were 0.72, 0.78 and 0.65 respectively for the three sensors. Additionally the other three sensors i.e. Netafim, Gypsum and WaterMark needed frequent calibration for the soil in study area.

Francesca *et al.* (2010) performed comparison of instrumentation performances for ECH2O probes, EC-5 soil moisture sensors. The study did a comparison of both sensors to the gravimetric data. The comparisons were also done in between sensor to sensor using their capacitive measurements under field conditions. In the field, two experiments were carried out in two different kinds of soil. The results exhibited that all the sensors gave acceptable results after calibration. It was found that same calibration equation was suitable for both kinds of soil. The recorded root mean square error was in the range of 2.5 % to 3.6 %. A conclusion was drawn from the analysis that variations in the result were due to combination of factors. Installation of the probes was found to be difficult in the soil due to the geometry of sensors. EC-5 sensor was found to be most reliable due to its short prongs which assisted in easy installation and no air gap in between the instrument and soil. The experimental site having the soil rich in skeleton exhibited greater values of root mean square error than the site having homogeneous soil. The study also revealed that ECHO2O and EC-5 sensors both worked efficiently with the same calibration equation. The study showed that all the soil moisture sensors were suitable for a medium-long period. Also, the sensors with small dimensions were reliable and easy to use in homogenous soil. It became clear from the study that due to soil temperature and solar radiation diurnal oscillations were recorded in soil moisture content data. These variations were believed to be due to water vapour flux in the soil pores instead of any measuring error. Further studies were also advised in the study.

Hardie *et al.* (2013) used a multi-sensory capacitance probe to monitor soil moisture. The probe was mounted inside vertically rammed access tube. Preferential flow events were determined in terms of its occurrence, wetting front and depth of flow. It was noticed in the study that preferential flow was dependent on the antecedent moisture content of the study area instead of rainfall. When the soil moisture storage was below 226 mm occurrence of preferential was noted. The study suggested the application of high temporal frequency measurements of moisture in soil for the areas where preferential flow are responsible for shallow groundwater contamination due to agrochemicals. Although the accuracy of high temporal frequency soil monitoring systems are reliable but lack in quantifying the flow, identification of flow with a high pre-existing moisture content and inaccuracy caused due to artificial voids created during access tube installation in stony soils.

Matula *et al.* (2016) analysed soil moisture sensors which were cheaply available and were usually used with FDR or impedance sensors. Five commercially available sensors were ECH2O TE, ECH2O EC-10, ThetaProbe ML2x, ECH2O EC-20 and ECH2O EC-5. All the sensors were examined under controlled laboratory conditions in loess and silica sand. Calibration of the sensor was done under conditions ranging from dry to saturated in both pristine and salty water. Nine consecutive soil water contents were used for the calibration. A statistical evaluation was also done in the study using ANOVA with a significance level of 0.05. Gravimetric measurements were used as a reference in statistical analysis. It became clear with the study that calibrated sensors resulted in more accurate results. Total variation obtained was as follows: material (18 % contribution), sensor type (29 % contribution), dry bulk density (11 % contribution) and calibration (42 % contribution). ECH2O EC-5 and ECH2O TE performed well in even saline conditions. Within a wide range of water content, all other sensors operated admirably in the soil. The measurement accuracy was found to increase with increasing value of dry bulk density. This relation emphasized that there need to be a good contact between the sensor and soil. ECH2O EC-5, ECH2O TE and

ThetaProbe were found to be efficient in saline conditions. Factory calibrations proved to produce more accurate results for ThetaProbe sensor.

Gao *et al* (2018) used high-frequency capacitance principle for designing a soil moisture sensor. The designed sensor involved a data processor, five types of sensing probes and accessories. Sensory probes were equipped with copper rings of low resistance. A simulator of high frequency was used to simulate the sensing probes. Signal frequency division was carried out along with conditioning. For the same a circuit of parallel resonance of controlled voltage oscillator was used. The frequency related signals were processed using a data processor for soil moisture sensing of soil profile. At soil depths of 20 cm, 30 cm and 50 cm real time soil moisture detection was carried out using the sensor. Online inversion for soil depth range of 0-100 cm was also performed during the study. A degree of fitting i.e. r^2 equal to 0.99 was recorded in between volumetric moisture content of soil and sensor's measuring frequency. The consistency of the sensor was evaluated from the relative error, which was 0-1.17 %. The degree of fitting and root mean square error was found to be 0.96 and 0.04 respectively when the results obtained from field tests were compared to the observed soil moisture values. The value of degree of fitting and relative error was found to be 0.85 and <5 % respectively when measured values were compared with that of the Diviner2000. It was found through the study that the sensor proved to be reliable in precise agricultural irrigation. It had greater accuracy and stable performance at low cost. It had good operability and high integration.

Datta *et al.* (2018) analysed soil moisture sensors for their performance. Five soil moisture sensors were selected namely, CropX, CS655, GS1, TDR315 and SM100. In two irrigated cropping systems the sensors were analysed for their accuracy. The cropping systems were located in southwest and central Oklahoma. Cropping systems had variable levels of clay content and soil salinity. It was exhibited from the study that at the sites where there was low level of clay and salinity, the sensors performed accurately whereas at the site with higher levels of

salinity and clay content, none of the sensors performed efficiently. Rosetta model, sensor and laboratory based were considered and investigated as different approaches for determining the thresholds of soil moisture which were needed for scheduling irrigation (wilting point and field capacity). It was discovered that Rosetta model estimated the closest value for wilting point and field capacity when compared with the laboratory measured data. Also the results were found to be independent of the number and type of input parameters. The study involved the estimation of a critical parameter used in effective irrigation scheduling, called soil moisture depletion. It was calculated from the readings obtained from the sensor and estimates of field capacity. All the sensors responded satisfactorily to the wetting and drying events. Three sensors which had an acceptable performance in irrigation management at the site having low clay content and low salinity were namely, CS655, TDR315 and GSI. It was drawn on the basis of root mean square error values. Sites with high clay content and high salinity exhibited higher values of RMSE which were almost eight times higher than estimated in low salinity and low clay content sites. TDR315 recorded high levels of noise due to high values of salinity. It was made clear through the study that for reliable estimates it is necessary to always carry out site specific calibrations in soil moisture sensors.

2.5 LATERAL FLOW MONITORING

Germann and Beven (1981) used soil water potential concept to measure the volume of a macropore system. The study involved analyzing the influence of macropore system on the soil's capacity of infiltration. Two undisturbed soil samples of large size were taken under the investigation. The two soil samples had volume of macropores equal to 0.01 and 0.045. The hydraulic conductivity was measured after fully draining the soil sample from being in fully saturation condition. At this point it was assumed that the soil macropores had no water. The measurements showed that at this stage a decrease by factors of 18 and 4.3 in hydraulic conductivity had reached. Thus, the effect of macropore flow was established in the movement of

water. It became clear that macropores have a great impact on the flow of water in soils. Further studies were suggested in the study to better understand the dynamics of macropore and its effect on soil water movement.

McLaughlin (1981) reviewed dyes and their use as soil water. The review study stressed upon the fact that there are no ideal tracers which can follow the exact movement of water. It was found that one sulphonic acid group usually plays to be an essential component in the tracer dyes which are high in their performance as soil water tracers. This was found to be correct for both fluorescent as well as non-fluorescent tracers. Dyes are believed to have greater potential than radioisotopes, salt tracers and biological tracers.

Ghodrati and Jury (1990) analysed preferential flow of water directly through numerous field plot experiments. It was done with the help of dye which stained the flow pathways. The study involved spatial structure characterization of preferential flow pathways, investigation of patterns traced by dyes to understand the soil structure and selection of irrigation methods on the basis of patterns of preferential flow of water and solutes. It was found that preferential flow pathways contributed to the transportation of solutes which were applied to the field plots. It was done through the analysis of distribution patterns of dyes. The flow pattern which was observed after the application of dyes showed both vertical as well as lateral pathways of soil water movement along the tortuous path. The observed flow patterns were structureless which proved that preferential flow is not confined only to the soils having continuous void spaces.

Germann *et al.* (1984) analysed the macropore structure and its role in water distribution in soil profile. Bromide was used to trace the soil water movement. Both lateral as well as vertical movement was observed during the study. Bromide profiles

were analysed to characterize the macroporosity which proved to be an effective method.

McIntosh *et al.* (1999) analysed preferential flow and its temporal patterns. Hydrometric analysis was performed for the analysis. Tracer was used throughout the study. Large undisturbed soil cores of length 38 cm and diameter of 30 cm were obtained from the study area located in the Panola mountain research watershed in Georgia. Chlorine and bromide were used as soil water tracers. It was found that the breakthrough of tracer was affected by rainfall intensity and structure of soil. Rainfall intensities of 20 mm/h and 40 mm/h were applied to the soil cores. The soil cores were extracted from a hillslope soil and residual clay soil on the ridge. It was found that for both the rainfall intensities preferential flow was recorded in clay core and not in the hillslope core. It was due to the presence of macro-channels in the core which are common in structured clay soil. Tensiometer was used to monitor preferential flow. Additionally, outflow and breakthrough curves during both rainfall intensities were used to interpret the preferential flow. The study showed that preferential flow occurred through macro channels and continued till the flow rate in them was greater than the absorption occurring in the surrounding matrix. The study showed that tracer recovery and its mass balance were influenced by exchange of tracer and water in between macro channels and soil matrix. They were also found to be functions of rainfall intensity and soil structure.

Kung *et al.* (2000) carried out field experiments to quantify contaminant transport. The study involved field experiments to identify preferential pathways through which transportation of contaminants was occurring. Experimental plots were tile- drained and the site had silt loam soil. The experimental site was in Butlerville in Indiana. Tracers having flouorbenzoic acids were used. The preliminary study involved analyzing three fluorobenzoic acid i.e. *o*-trifluoromethylbenzoic acid, pentafluorobenzoic acid and 2,6-difluorobenzoic acid. It

was inferred from the study that the tracers had fast arrival time and higher recovery rate which confirmed the presence of larger pores. Additionally, the study showed that with the wetting of soil during rainfall events in the study area the movement of water and contaminant transportation shifted towards larger pores of preferential flow pathways.

Flury and Wai (2003) conducted a review on various dye tracers. The review emphasized on the types, role and importance of dye tracers as hydrological tracers specifically in vadose zone. The review covered information on various dyes as well as non-dye tracers. The chemical properties of tracer dyes have been described. Suitable recommendations have been made related to the use and handling of tracer dyes. A toxicological assessment has also been discussed regarding tracer dyes when used in tracing the hydrological processes.

Kienzler and Naef (2008) performed field experiments to analyse subsurface stormflow and discussed the 'old water paradox'. Four different hillslopes were considered for the experimentation. Experiments were carried out both during sprinkler water application as well under natural rainfall conditions. Sprinkling water that has been artificially traced and ^{222}Rn were utilized to trace the soil water movement. Water during both event and pre-event were estimated using the same. It was inferred from the study that occurrence and amount of pre-event water varied at different hillslopes. It was found dependent on the mode of feeding water in the site. Subsequently, the saturated patches of soil matrix contributed to larger pores where the event water and old water got mixed. Hydrometric and tracer estimations were done along with soil investigations to get to know SSF formation in different sites. ^{222}Rn proved to be an efficient tracer in monitoring fractions of pre-event water with high temporal resolution. The study showed that low pre-event water was produced when precipitation directly feeds on the preferential flow paths. When the rainwater fed on the saturated zones of soil, a portion of the pre-event water was more and

subsurface stormflow was delayed. The study clearly stated that significant quantity of pre-event water was present in shallow soil profile which gets released from the saturated and small patches of soil matrix. This kind of localized saturation has the potential to trigger preferential flow and rapid transport of pre-event water down the slope. The results from the study emphasized that it is common to have an exchange in between subsurface flow and overland flow which can produce rapid responses of discharge in hillslopes. Thus, the study explained the concept of pre-event water as 'old water paradox'.

Kienzler and Naef (2008) carried out sprinkling experiments to analyse temporal variation in subsurface stormflow formation. Three replicating experimental slopes were considered with varying degrees of intensity of rainfall and antecedent precipitation. Hydrometric measurements with tracer experiments were conducted in the study. Varying changes in precipitation intensity and preceding precipitation regulated the subsurface stormflow response. The effect of antecedent precipitation on SSF formation and its reaction was found to be dependent on the fact that how the hillslope allowed the formation of SSF. Least variation was found in SSF rates with the variation in intensity of precipitation. However, subsurface flow rates responded to different precipitation intensities in terms of its timing and relevance. The reason inferred from the study was that the subsurface flow and soil saturation occurred both within the top soil as well as above the soil-bedrock interface due to varying precipitation intensities. A correlation between the antecedent precipitation and antecedent soil moisture was established and was found to affect the runoff response. Thus, the study suggested having in depth knowledge of SSF and its variability spatially in order to correctly apply the parameters such as antecedent precipitation index at catchment scale. A non-linearity was noted in the effect of precipitation intensity and SSF generation. Thus, for the hydrological modelling a detailed knowledge in precipitation-intensity and SSF is needed.

Anderson (2009) used excavation and dye staining to estimate the spatial pattern and morphology of preferential flow network. The experiment was carried out on a large area of 30 m. The viability of outstretching small scale experiments on dye staining to hillslope scale was also assessed. Analysis was done on preferential lateral flow paths which were found to be active during steady-state flow conditions. Their interactions with soil matrix were also assessed. The velocity of flow was calculated for each cross-section in the hillslope. The results were compared to the applied tracer measurements. Investigations were also carried out to assess the relationship between preferential flow paths and contributing area. To find the lateral preferential flow pathways, velocity of flow in every cross section and the connections between their features a food dye tracer was used. The dye pattern on analysis stated that the information regarding connection between every single preferential pathway was provided by saturated flow. It was found through the study that preferential flow paths had an influence on the redistribution of organic material and fine sand within the study site. It was evident due to the erosion and deposition of soil in the area. It was found that largest and the highest connected soil pores were present in the areas having concave surface topography. It was found from the experiments that the obtained findings can assist highly in defining solute transport, soil development, slope stability and subsurface flow generation.

Wienhofer *et al.* (2009) analysed flow paths of both unsaturated and saturated zones in a forest hillslope. The study was carried out in Australian Alps. The analysis was done using salt tracers and fluorescent dye. The experiments revealed that preferential flow was occurring from soil pipes and cracks and these structures were found active during the tracer transportation in the hillslope. The study revealed a positive correlation between transient flows of tracer to tracer concentration during natural rainfall conditions. The study was able to demonstrate preferential flow, its features and its effects on subsurface stormflow both qualitatively and quantitatively in the catchment. Additionally, the study emphasized that to model hillslope scale

processes, a detailed investigation of various parameters and structures are needed. The salts used in the study were sodium chloride and sodium bromide. The fluorescent dyes involved sulforhodamine and uranine. The dyes and salts were found to be efficient tracers for a distance of upto 44.2 m and 32.4 m respectively. Analysis of fluorescence tracers were done in natural precipitation conditions. Breakthrough of the tracer was measured through breakthrough curves which were estimated in site. The high temporal resolution measurements were beneficial in assessing the transient flow of fluorescence tracers. Dyes proved to be better water tracers during the rainfall as salt tracers experienced dilution which deterred the estimations through electrical conductivity and ion chromatography. However, salt proved as efficient water tracers during simulated rainfall conditions. Electrical conductivity readings were easily captured and also complete tracer recovery was achieved. The study showed that tracers must be chosen with care as per their interplay with the soil.

Udayakumar *et al.* (2015) used well hydrograph analysis to understand the water shortage due to quick drainage of water in lateritic formations in west coast of India. The study involved estimation of net and gross recharge components. Forty two wells over the watershed were selected having different diameters and depths. An equation to estimate the recession was developed to foretell the level of water in the wells at a specific time of the dry season. Specific yield of wells were estimated using recession curves. The shallow well recession was recorded as 0.003 and 0.001 for deep wells. The specific yield varied from 0.013 to 0.036. Recorded subsurface flow from the watershed on average was 0.09 m/yr. The fraction of annual rainfall contribution as subsurface flow was 2.78 %. Well hydrograph analysis was used to quantify the recharge and subsurface flow. The study emphasized the adoption of semi pervious surface barriers to maintain water levels in the watershed for long duration during summer season.

Du *et al.* (2016) analysed the interflow over perched aquifer present within a sandy clay loam argillic horizon. The study site was located at the Savannah River site in coastal plain of South Carolina. The catchment was forested with low relief. The topography and its influence on the generation of interflow in the area were estimated. Various parameters used in the study involved measuring the soil moisture, trench flows, soil hydraulic properties, streamflow and shallow groundwater behaviour. The study showed that perching of water occurred within and above the argillic horizons and interflow was found to be infrequent. It was due to micro topographic relief and depression storage. It was found that through the soil anomalies percolation rate was higher which reduced the role of interflow. Further, the study concluded that 60 mm of cumulative rainfall threshold was needed to produce interflow in the area.

2.6 MONITORING OF BASE FLOW

Harrington *et al.* (2002) estimated the recharge rates from flood outs of ephemeral rivers. The study was carried out in Ti-Tree basin of central Australia. The site had arid environment. Carbon-14 concentrations in groundwater taken from the boreholes were used to determine the recharge rates. Environmental Chloride was also collected from the groundwater samples specifically from the areas where the water entered the saturated zone to estimate recharge rate at that point in the study area. The study showed that only the intense rainfall events of about 150 mm/month to 200 mm/month contributed to recharge in the basin. The findings in the study provided suitable implications for ground water resource management. The stable isotope and chloride proved to be efficient water tracers and showed that the basin got recharged only during intense rainfall events of intensities 150 mm/month and 200 mm/month.

Deshpande *et al.* (2003) undertook isotope analysis of river and groundwater samples from the south Indian Peninsula through oxygen and hydrogen isotopes. The

study was carried out to provide a framework for the hydrological studies in future. It was done by characterizing the nature of isotopes in the near surface water sources. The study revealed depleted isotopic concentrations in north east monsoon dominated areas when compared with south west monsoon dominated areas. A secondary evaporation was suggested when the regression line of ^{18}O -D for local precipitation was found to be lower. It was found during the study that Western Ghats played an important role in distribution control of isotopes along the west coast region.

Lee and Kim (2007) estimated seasonal contribution of precipitation in recharging groundwater at North Han River basin in Korea. Oxygen and hydrogen stable isotopes were used in the study. The study involved comparison of signatures of stable isotopes. It was found that in the study area precipitations were important source of groundwater recharge during both dry and rainy season. It was found through the isotopic signature comparisons. During the study the stream water showed isotopic signature similar to that of the groundwater. It indicated major contribution of groundwater into the stream. Downstream flood control dams showed lower values of deuterium when compared to upstream water sources. It indicated secondary evaporative enrichment. The results obtained during the study provided basis for suitable resources for groundwater and stream water management within the basin. The study also revealed that summer monsoon rains contributed only in half of the groundwater replenishment. However, precipitation during the dry season contributed the remainder of the fraction of groundwater. Same regression line as that of groundwater was followed by the stream waters. It showed that groundwater discharge was the major contributor to the streams in the study area. The water samples of flood control dam showed excess values of deuterium which was due to the evaporation.

Larocque *et al.* (2009) analysed groundwater flow in heterogeneous aquifers. The study was carried out using tracers. Uncertainty, bias and various hydraulic approaches of tracer were also assessed in the study. To simulate the groundwater

flow, transport of radioactive tracers and pumping tests 2-dimensional synthetic aquifers were used with varied levels of heterogeneity. It was found that with the variation in hydraulic conductivity both bias and uncertainty too varied. Moreover, when a tracer of decay rate as same as that of groundwater residence time was used the non-linearity in the concentration-time relationship was reduced. It was concluded from the study that the bias depended on the half-life period of tracer, variations of the flow field and duration of pumping tests.

Devlin *et al.* (2012) illustrated the benefits of ground velocity measurements. Three experiments were performed in the study. The first study involved multilevel point level measurement probes and conventional methods for the measurement. The second method included mapping of velocity field of groundwater through PVPs. The PVPs in the second test assumed homogeneity in the aquifer and provided higher values of velocities than expected. This led to better illustration of heterogeneity in the aquifer when modelled in a 3-D model. In the last and third study which was a bio-stimulation model, changes were noticed in the permeability of aquifer down the gradient. Through the study PVPs were proved to be an essential tool for the hydrogeologist. These devices are easy to construct, inexpensive and reliable.

Harrington *et al.* (2014) carried out a research in continuation of a previous work which was conducted in Fitzroy River. The River comes among one of the perennial rivers in Australia. The study involved tracking the discharge of groundwater through geophysics and tracers. Various tracers used in the study were ^4He , ^{222}Rn , $^{87}\text{Sr}/^{86}\text{Sr}$ and major ions. Sampling of groundwater and river water was done synoptically at regional -scale. Subsequently, tracer behaviour in the river was modelled. An airborne electromagnetic survey was used to acquire sections of vertical conductivity. The survey provided an insight in the aquifer architecture related to the source and general quality analysis of water. The tracer data indicated that a preferential discharge of groundwater was occurring to the river from a depth

of 300 m beneath the surface. The study concluded that analyzing different environmental tracers greatly increases the understanding of interaction processes in between groundwater and surface water. Also when these analysis are done in association with geophysical techniques.

Essouayed *et al.* (2019) used the Direct Velocity Tool (DVT) to estimate groundwater velocity. The study involved measurement of Darcy flux using DVT. The measurements were done at centimetre scale and the results were obtained within few minutes. The coefficient of correlation obtained was 0.99, when laboratory results were compared with results obtained from DVT.

2.7 MODELLING OF LATERAL FLOW

Beven and Germann (1982) analysed subsurface stormflow in a hillslope of East Twin Brook catchment in United Kingdom. Analytical solutions based on kinematic approximations were given for subsurface stormflow. The analysis was done in both saturated as well unsaturated zone. The analysis of unsaturated zone was done during drainage as well as wetting. The analytical model used proved to be flexible and easy to access for performing a distributed and physically based modelling in catchments which are steep and has permeable soils.

Sloan and Moore (1984) predicted subsurface flow in Coweeta Hydrologic Laboratory. Five mathematical models were used for the prediction and a comparison was also made from the discharge values obtained from a prior experiment done on the uniform sloping soil trough. The models used were based on Richard's equation, two simple storage-discharge models following Boussinesq equation and kinematic wave and a kinematic wave model. The models used were economical and provided subsurface response and position of water table. The results obtained in the study emphasized field verifications after modelling the process as these models may not be the base for validating and testing other models.

The simpler models like kinematic storage model was found to be more accurate when compared to other complex models.

Peters and Klavetter (1988) evaluated isothermal movement of water using a continuum model. The study involved analyzing the isothermal movement of water in fractured, porous medium which is slowly changing and unsaturated medium. The model was used to evaluate the vadose zone in Yucca Mountain. It was done to find any potential repository. Both macroscopic and microscopic level of approach has been used to develop the model. The water movement was also assessed in the fractured rock mass. The assumptions adopted were that pressure heads in matrix and rock fractures are same and in perpendicular plane of flow. A single flow equation was obtained for the fractured rock mass. The two approaches were also used to measure saturation and relative permeability using the available hydrologic data for matrix and bedrock. To calculate water flow through fractured medium a continuum model with assumptions was developed. The assumption was that the pressure head in matrix and fractures were same in the direction perpendicular to the flow. The study stated that the same model can be used for another hydrologic system if the stated assumptions hold for the area.

Wood *et al.* (1988) analysed spatial variability effects and also reported the results of an investigation carried out in Coweeta River basin. Modelling of the hydrologic response for the catchment was also analysed. For the same a modified version of TOPMODEL was used which had the ability to model both saturation excess runoff and infiltration excess. The model incorporated the parameters such as rainfall, spatial variability of soils and topography. The study concluded that when the catchment hydrologic responses were considered Representative Elementary Area (REA) existed. Further, in determining REA it was found that length of rainfall was a secondary aspect in the determination of size of REA.

Gerke and Van Genuchten (1993) studied the flow of water in saturated zone and solute transportation in fractured rocks. The study involved development of a dual porosity model. Two models i.e. less permeable matrix pore system and fractured pore system were involved as two overlaying continua. It was assumed that water was mobile in both the pore systems. The convection-dispersion equation described the solute transport. First order rate equations were used to simulate solute and water transfer. Both convective and diffusive components were included in the solute transportation. Galerkin finite element model was used to numerically solve two coupled systems of differential equations which were non-linear and partial. The results obtained from the simulations showed that during transient water flow solute leaching had a complex flow through the unsaturated and saturated porous media. It was found through sensitivity studies that it is essential to have accurate measurements of hydraulic conductivity. The present model proved to be efficient to simulate preferential flow using the chemical and physical characteristics of the medium.

Liu *et al.* (1998) modelled flow as well as water transportation through the connected fractures. The study was based on the hypothesis that in the study area only a fraction of linked fractures took part in water conductivity. The study revealed that in Topopah Spring welded unit of Yucca Mountain about 18-27 % connected fractures were present.

Jacques *et al.* (2003) coupled HYDRUS-1D and PHREEQC to analyse multicomponent reactive transport. HYDRUS-1D was used to simulate movement of water, multiple solutes and heat in variably-saturated heterogeneous soil. The soil was subjected to varied boundary and atmospheric conditions. PHREEQC was used to simulate chemical systems and reactions such as mineral precipitation, surface complexation and speciation etc. Simulated results obtained from this coupled model were verified by comparing with the calculations done by the independent model.

The results obtained from the coupled model also were in correlation with CRUNCH. The study revealed that the coupling of PHREEQC and HYDRUS 1D allowed simulation of various physical, chemical and biological processes.

Twarakavi and Simunek (2008) assessed the unsaturated flow package of HYDRUS for MODFLOW to simulate one dimensional problem. Evaluations and comparisons were made in between the developed package with other contemporary models. HYDRUS package was fully incorporated with MODFLOW. The recharge fluxes at water table were provided by HYDRUS whereas MODFLOW provided the groundwater table location to HYDRUS. The provided location of groundwater table was used as bottom boundary condition. Three case studies were used for the analysis. The experiments involved one-dimensional infiltration, two dimensional recharge of water table and a regional groundwater flow problem which was hypothetical in nature. Comparison was done in between the developed package and MODFLOW packages like UZFI, REC-ET and VSF. It was found that the newly developed software package was more accountable and reliable than other MODFLOW packages. It was found from the study that VSF package provided best accuracy in case of small scale problems.

Xu *et al.* (2017) analysed HYDRUS 2D model and its performance in modelling movement of soil wetting front in loess soil column under constant water head condition. The simulation was carried out under different soil properties. HYDRUS 2D was found good in simulating soil water movements in loess soil. The recorded simulation relative errors were found to be less than 15 %. Moreover, mean relative error was found to be $< 5 \%$ and $R^2 > 40.9$.

Dandekar *et al.* (2018) assessed groundwater recharge and recharge flux in a semi-arid region. HYDRUS-1D and MODFLOW were used for the assessment. The results from the study showed that the recharge flux when calculated cumulatively varied from 20.1 cm to 23.43 cm. Average groundwater recharge was found to be

22.2 cm. Surface runoff was found to vary from 3.39 cm to 14.36 cm. Reference evapotranspiration when measured was found to vary from 37.19 cm to 45 cm. A water table rise of 1.46 m was expected through the results by retaining the surface water in the study area. Thus, the study revealed that the combination of these models was reliable.

Dominguez-Nino *et al.* (2020) found the most appropriate configuration of HYDRUS-3D for simulating the soil water dynamics in a drip-irrigated orchard. Rosetta model parameterized the simulations and these were compared with the results of HYPROP + WP4C. Validation was done on a seasonal scale using results obtained from neutron probe and tensiometers. The findings of the study discovered that soil moisture measurements were found in best agreements with parameterizations obtained from HYPROP + WP4C. It was found that near the drippers simulations had best fit as compared to that outside wetting pattern and at 80 cm depths.

2.8 MODELLING OF BASE FLOW

Brouyere (2003) modelled solute exchange using a numerical approach. The solute exchange was studied between a well and the aquifer that surrounds it. It was done for a better tracer test interpretation in the field. Equations for the mass balance of water and tracer were used in this study. Integration of these equations was done over the volume of well water. A numerical solution was proposed through SUFT3D for the groundwater flow in 3-dimension. This allowed modelling of tracer mass flux which was non-uniformly distributed along the well screens. Validation was done through field experiments. The model included all processes influencing the solute exchange between well and surrounding aquifer.

Leterme *et al.* (2012) used Richard's based soil water balance model HYDRUS 1D to simulate groundwater recharge and its sensitivity to various climatic conditions. Meteorological time series from analogue stations were used for the

study. The study utilized four analogue stations. Variation in the potential evapotranspiration was found to be +8 % to +82 %. The average annual precipitation variation was found to be -42 % to 5. These results were obtained when comparisons were made from the then present day climatic situation. The results obtained for the study area were found to be in confirmation with the field data.

Assefa *et al.* (2013) performed recharge modelling by integrating modelling tools and field data. The research was carried out to investigate spatially and temporally varying groundwater recharge in North Okanangan. The softwares used were ArcGIS TM, HYDRUS 1D and Rosetta. Field experiments were carried out and parameters like soil moisture, climatic data and soil temperature were estimated in the field. The parameters were fed in the models for the recharge modelling. The simulation of snow pack, soil temperature and soil moisture for a time period of one year was done using public version of HYDRUS-1D. Model performance was evaluated using soil hydraulic parameters derived from ROSETTA and field data. Subsequently, the results were coupled with ArcGISTM. It was used to produce recharge maps throughout the watershed. The study revealed that the 25 years of daily discharge results estimated the average recharge of 77.86 mm/year. The results obtained from the models when compared to in situ observed data showed good relation. Further, a statistical analysis revealed the degree of extrapolation that can be done in the field site results. Robustness of the methodology adopted in the study was proved from the statistical analysis.

Leterme *et al.* (2013) produced a groundwater model for Nete catchment by coupling HYDRUS-1D and MODFLOW software packages. The study aimed at improving the simulations of hydrological processes at near surface. The study also included analyzing the spatial and temporal variabilities in groundwater recharge rates. The study revealed good correlation of the simulated results with field observations.

Pathak *et al.* (2014) assessed groundwater flow in an inclined porous media. Dupit's assumptions were used to form the governing partial differential equation. Three cases with different slopes and boundary conditions were discussed. Graphical as well as numerical simulation was done in MATLAB. It was concluded from the study that the level of water table free surface can be efficiently measured using the explained approach in study at different distances.

Simunek (2015) showed the application of HYDRUS-1D in giving a mathematical description of hydrological processes occurring in Lommel in Belgium. A 1 m deep soil profile was considered with no or grass cover on it. The transient water flow was modelled using HYDRUS. The study demonstrated that the fraction of water returned to atmosphere was more from the grass covered soil profile. It was due to transpiration. Conversely, the bare soil had more fraction of water contributing to groundwater recharge.

Tonkul *et al.* (2019) used the numerical model, HYDRUS-1D to determine groundwater recharge in a sub-basin of Gediz basin in Turkey. The study involved calculation of aquifer recharge due to precipitation, core sampling for characterization of soil and characterization of aquifer properties. The study revealed that 10 % of annual rainfall contributed to recharge. An average recharge value obtained was 43.09 mm. Coefficient of recharge was also represented for the research area. It was derived from the study that HYDRUS-1D model can efficiently simulate vertical movement of water through the soil profile. Further, it proved to be an efficient tool in determining soil moisture content both spatially and temporally in order to predict recharge rates.

2.9 INTERVENTIONS FOR GROUND WATER RECHARGE

Ishida *et al.* (2011) provided a detailed review on the underground dams, its basics and construction throughout the world. The study also involved various

threats to groundwater recharge and hurdles involved in the sustainable use of groundwater.

Udayakumar and Mayya (2014) analysed semi-impervious subsurface barriers and their suitability in lateritic formations to control the lateral flow. Using composite soil having the required clay and lateritic soil percentage, a subsurface barrier (SSB) was built in a known watershed. It was ensured to keep the hydraulic conductivity of soil mix in the range of 10^{-6} to 10^{-7} cm/s. Level of water in nearby observation wells were observed prior and after the construction of the barrier. The study revealed high performance of subsurface barriers in keeping high groundwater levels in both its upstream and downstream. The study also revealed that for preparing a suitable subsurface barrier in lateritic soil the percentage of gravel must be less than 20 % and for that of silt and clay it must be more than 40 %.

The above compiled literature review has been an attempt to cover all the research done in lateral flow and base flow monitoring. Various studies based on different methods of lateral and base flow monitoring including salt tracers, dyes, radioisotopes and natural isotopes have been mentioned. Simulation of these two hydrological processes plays a vital role in defining and adopting effective interventions for water conservation. Thus, research with the support of software that can be used for simulating both unsaturated and saturated zone in a soil profile have also been mentioned in the literature review. However, the existing literature lacks a clear explanation of lateral flow movement of water in the root zone of laterite terrain. It may be due to its very limited geographical spread in a global scenario. The laterite midlands of Kerala receive an average annual rainfall of 3000 mm but, experiences water shortage during the post monsoon period. The present study will contribute in describing the major factors that are accountable for reducing the residence time of soil water in the laterite terrain of Kerala. The research study will enable to interpret the lateral movement of water under varying water application methods. The importance of capacitance based sensor in in-situ soil water content

measurement and its calibration for site specific soil performed in the present study will assist the researchers in performing efficient and less-laborious soil water estimation in the real time. The salt tracer analysis performed in the study area will define its suitability and reliability in tracing lateral movement of water. Estimation of base flow through the analysis of hydraulic head variation and tracers performed in the present study will provide an understanding of shallow base flow movement and calculation of its apparent horizontal velocity in the laterite terrain. Additionally, simulation of both lateral and base flow performed in the present research work will establish the importance of simulating such complex hydrological processes in order to suggest suitable water conservation measures.

CHAPTER 3

MATERIALS AND METHODS

3.1 GENERAL

The chapter involves detailed descriptions of materials used and field investigations carried out for the monitoring of subsurface flow of water in laterite terrain. The determination of vital site specific soil characteristics and a comprehensive methodology for the determination of lateral flow and base flow have been described explicitly under the following sections.

3.2 DESCRIPTION OF THE STUDY AREA

The study was carried out in Kelappaji College of Agricultural Engineering and Technology (KCAET) campus, Tavanur (Malappuram District), Kerala in India, as shown in figure 3.1. It is situated at latitude of $10^{\circ} 51'18''$ N and longitude and $75^{\circ} 59'11''$ E with an altitude of 10 m above the Mean Sea Level (MSL). The terrain is lateritic in nature, having sandy loam texture and gentle slope.

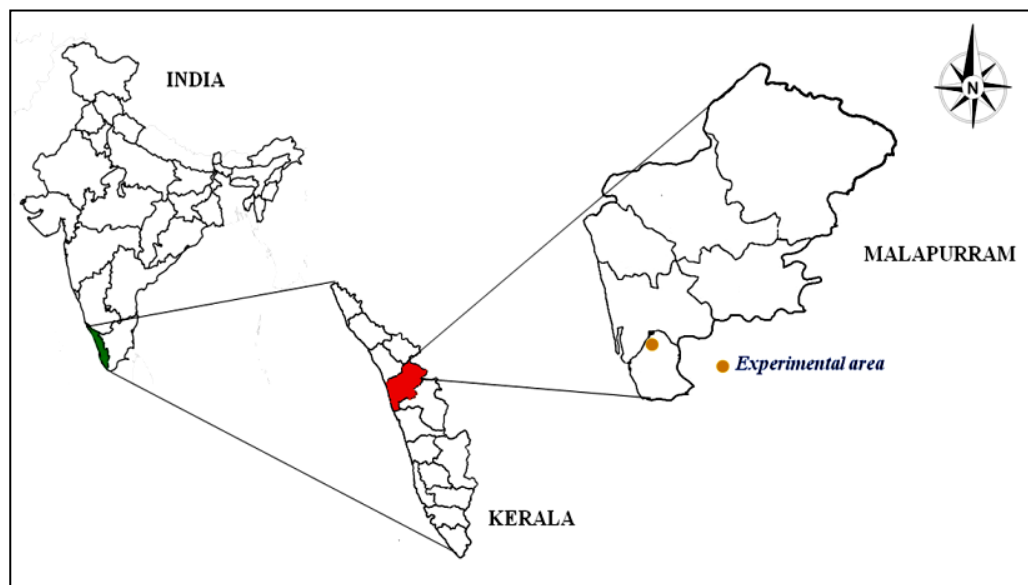


Figure 3.1 The study area

The average annual rainfall received in the study area for a period of last 30 years (1989-2019) was 2600 mm. The annual average maximum and minimum temperature of the area ranges between 31 °C to 26 °C. The area is rich in vegetation with deep and dense rooted plants.

3.3 MEASUREMENT OF DAILY RAINFALL

The monthly rainfall pattern for the period 2018-19 was recorded using a non-recording Symon's rain-gauge installed at the meteorological observatory in the college campus. The daily measurements of rainfall were recorded at 8:30 am (IST).

3.4 SITE SELECTION CRITERION

The following criterions were considered for the site selection:

1. Terrain with gentle slope
2. Minimal through fall
3. Availability of water source and electrical power.
4. Suitability for tracer studies
5. Availability of open wells for base flow monitoring

Based on the above mentioned elements, 3 sites were selected as site 1, site 2, and site 3.

3.5 CONTOUR AND SLOPE MAPPING FOR THE EXPERIMENTAL SITES

Contour and slope maps were developed for all the three experimental sites using total station surveying.

3.6 DETERMINATION OF SOIL PHYSICAL PROPERTIES IN EXPERIMENTAL SITES

The various soil properties which were determined to support the study of monitoring of sub-surface flow analysis are as follows:

1. Initial moisture content

2. Dry density
3. Particle density/Specific gravity
4. Porosity
5. Void ratio
6. Textural classification

All the above mentioned properties were determined at room temperature in Soil and Water Engineering lab situated in the K.C.A.E.T college campus after in-situ soil sample collection. The soil properties enlisted above were determined specifically for each site from three soil profile depths of 0-40 cm, 40-80 cm and 80-120 cm. This was done to obtain an overview of the various hydrological processes occurring across the soil horizon. The initial soil moisture content was determined for the three soil profile depths in each site. The measurements were taken in the laboratory using the conventional gravimetric method. The bulk and particle density of the soil profiles were measured using the core cutter and the pycnometer respectively. Further, the grain size distributions in the three soil profile depths were determined using sieve analysis method for all the three experimental sites. The soil profile properties at depths of 0-40 cm, 40-80 cm and 80-120 cm were determined three times each for obtaining averaged values and thus, for better representative results. The basic chemical properties of the site specific soil viz. electrical conductivity and pH were obtained by employing COM-80 TDS/EC meter and pH meter respectively.

3.7 INSTALLATION OF THE EXPERIMENTAL SETUPS IN EXPERIMENTAL SITES

Separate experimental set ups were installed to investigate lateral flow and base flow/groundwater flow. The lateral flow or interflow assessment was conducted in three sites with different experimental set ups as described in table 3.1. The spatial and temporal variation of interflow was analysed from three different soil profile depths of 0-40 cm, 40-80 cm and 80-120 cm. Furthermore, salt tracer studies were

conducted in site 2 and site 3 using sodium chloride (NaCl) through the experimental set ups as described in table 3.2. Base flow monitoring in site 1 was carried out through the experimental set ups as described in table 3.3. Potassium chloride (KCl) was used as the tracing element to assess the groundwater flow through salt breakthrough analysis in the monitoring wells.

Table 3.1 Description of Experimental set ups for lateral flow monitoring

S.No.	Site number	Name of experimental set up	Mode of water application	Methodology adopted for monitoring of lateral flow
1	Site 1	Experimental set up 1	Water application through a single butterfly sprinkler	Gravimetric measurements
2	Site 2	Experimental set up 2	Intermittent application of water through a 30 cm deep line source trench	Gravimetric measurements
		Experimental set up 3	Instantaneous application of water through a 50 cm deep line source trench	TEROS 12- Capacitance based soil moisture sensors
		Experimental set up 4	Natural rainfall	TEROS 12- Capacitance based soil moisture sensors
3	Site 3	Experimental set up 5	Natural rainfall	TEROS 12- Capacitance based soil moisture sensors

Table 3.2 Description of Experimental set ups for lateral flow monitoring through salt (NaCl) tracer

S.No.	Site number	Name of experimental set up	Methodology adopted for tracer application
1	Site 3	Experimental set up 6	Application of 500 l of salt (NaCl) solution @ 0.12g/l of salt through instantaneous application
		Experimental set up 7	Application of 1000 l of salt (NaCl) solution @0.12g/l of salt through instantaneous application
2	Site 2	Experimental set up 8	Instantaneous application of salt (NaCl) solution with 1x Background Electrical Conductivity (BEC)
		Experimental set up 9	Instantaneous application of salt (NaCl) solution with 3x Background Electrical Conductivity (BEC)

Table 3.3 Description of Experimental set ups for base flow monitoring

S.No.	Site number	Name of experimental set up	Methodology adopted for base flow monitoring
1	Site 1	Experimental set up 10	Measurement of hydraulic head variation between two observation wells.
		Experimental set up 11	Instantaneous application of salt (KCl) tracer in injection well and its breakthrough analysis in monitoring wells

3.7.1 Measurement of uniformity coefficient and discharge for different sprinklers

In order to simulate the rainfall in site1 using sprinklers, uniformity/distribution coefficient of three different sprinklers viz; pop-up sprinkler, micro-sprinkler and

butterfly sprinkler were analysed individually. Uniformity coefficient was determined using the catch can method.

Uniformity coefficient is calculated using equation 3.1.

$$CU = \left(1 - \frac{\sum_{i=1}^n |Xi|}{mn} \right) \times 100 \quad (3.1)$$

Where

CU – Uniformity coefficient

m – Average application rate

n – Total number of observation points

|Xi| – Numerical deviation of individual observations from average application

To evaluate the water losses during the process of sprinkling, it is necessary to measure the discharge from the sprinkler head under the operating pressure. The pressure and discharge of the sprinkler head were measured before and after the test run. Pressure is measured by a pressure gauge. The discharge is measured by connecting flexible tubes on the sprinkler nozzle and collecting the discharge in a container for a specific period.

3.7.2 Installation of experimental set up 1 at site 1

The experiment for lateral flow monitoring at site 1 was carried out during the post monsoon season of the year. The area under consideration was of 78 m² with a general slope of 5 percent. The contributing area was 60 m² as shown in figure 3.2.

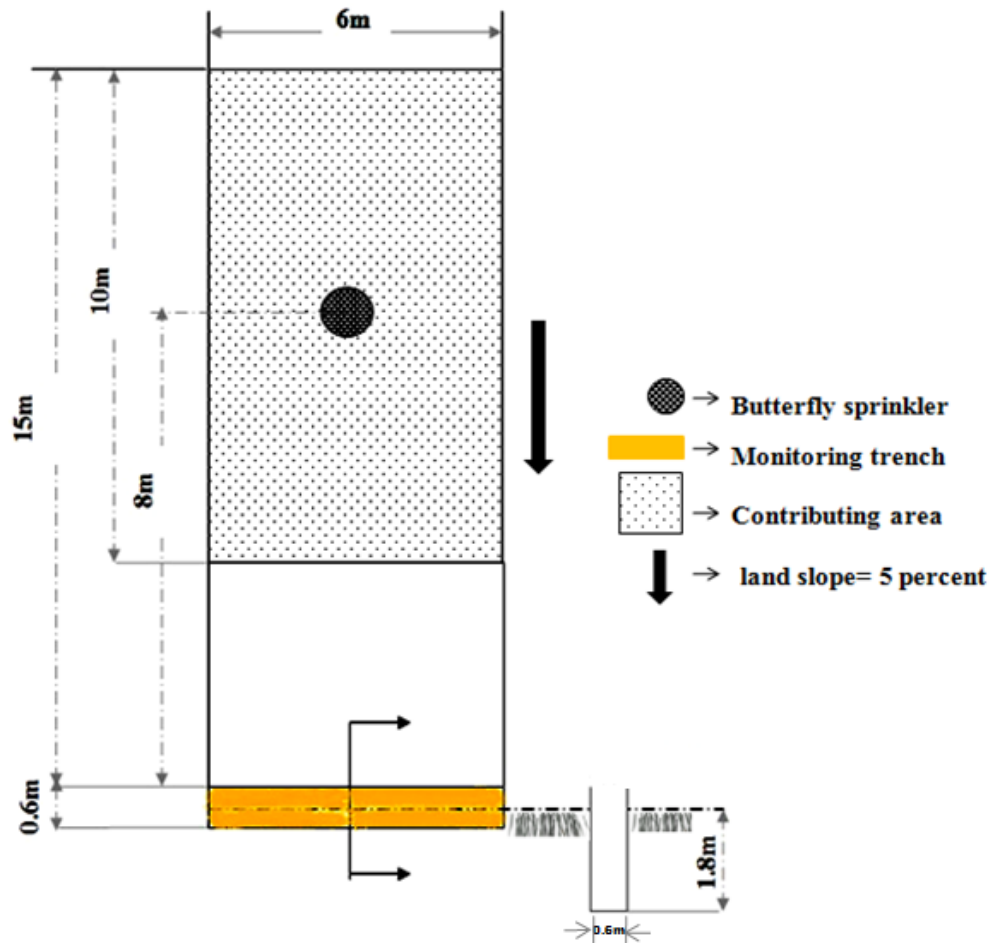


Figure 3.2 Plan view of the experimental set up 1 installed at site 1

The site was first well protected by enclosing it with barriers so as to prevent trespassing, livestock and wild animals straying. A trench of length 6 m, width 0.6 m and depth 1.8 m was dug at the downslope of the site with at most care, so as to prevent any major soil disturbance in experimental set up. A tin sheet having thickness of 14 gauges (1.628 mm) and length of 5 m was, tilted towards the depth of trench, was inserted on the monitoring face of trench at a depth of 1.2 m from the soil surface as shown in plate 3.1. A can for collecting water was kept at one end of the tin sheet in the monitoring trench.



Plate 3.1 Installation of experimental set up in site 1

The trench was covered with a tarpaulin sheet to prevent the direct fall of water from the sprinklers into the trench. Pipelines and ancillary connections to install the sprinkler were set in the field to derive water from the irrigation line installed in the nearby farm. A disc type filter was provided in between to prevent the clogging of sprinkler. A butterfly sprinkler was erected at the center of the experimental site at a distance of 8 m from the downslope trench. A pressure gauge was also installed in the line to measure the pressure. Continuous irrigation was carried out for twelve hours in a day at an operating pressure of 1 kg/cm^2 using a centrifugal pump of 1 HP power. A spray diameter of 10 m and a uniformity coefficient of 90.90 % were achieved in the study site. The height of the lateral was adjusted maintaining a trade-off between uniform wetting of the site and no direct fall into the trench. Soil samples for the gravimetric analysis were collected in steel cans at every 2 h interval. The soil samples in the can were carefully placed in the oven for 24 hours at 105°C . The experiment was carried out for seven days in succession. The experiment was focused to provide an insight in the changing flow pattern of water in soil matrix throughout the day and its effect on the lateral flow rate.

3.7.3 Installation of experimental set up 2 at site 2

The experimental set up 2 was a rectangular area of dimension (4 m x 2 m) with slight vegetation in the form of grass cover. Slope of the land measured was 8 percent. The experimental set up 2 involved periodic line application of water to induce interflow through the soil matrix as shown in figure 3.3.

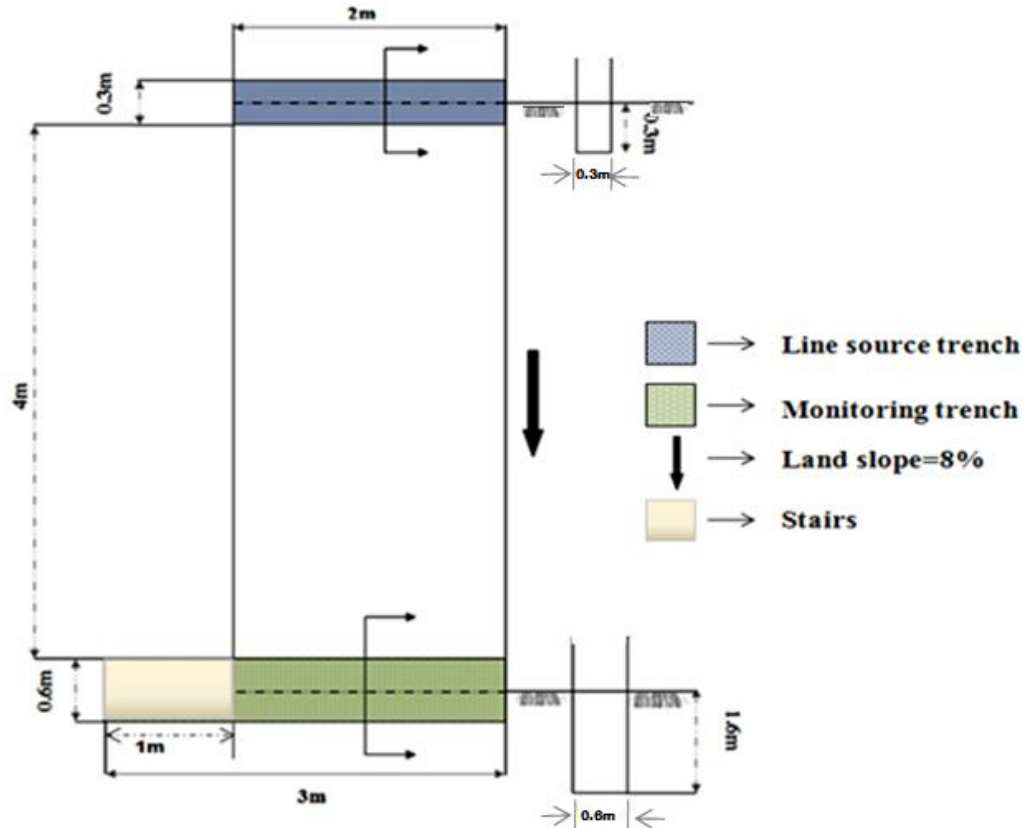


Figure 3.3 Plan view of the experimental set up 2 installed at site

Thus, two trenches were dug across the slope length, one as the line source of water application and other as monitoring trench to quantify the incoming lateral flow down the trench. The two trenches were constructed at a distance of 4 m apart. The dimensions (L x W x D) of the line source trench and monitoring trench were (2 m x 0.3 m x 0.3 m) and (3 m x 0.6 m x 1.6 m) respectively. The volume of water to be poured into the line source trench was calculated based on the volume of the line source trench. Subsequently, filling of the line source trench was started early in the

morning so as to minimize the evaporation losses. Intermittent application of water into the line source trench was carried out in such a way that pouring of water into the line source trench was done once the applied water had permeated the soil. The experiment was carried out for a period of 12 h in a day. The total duration of the experiment was 10 days. During the day time the line source trench was covered with a white polyhouse sheet to prevent the evaporation losses. Soil samples from the monitoring trench were collected from three different soil profile depths viz; 0-40 cm, 40-80 cm and 80-120 cm. Subsequently, a gravimetric moisture content analysis and interflow quantification was done from the corresponding gravimetric moisture content increase recorded in a day. The experiment gave an idea about the movement of soil water through the soil profiles when the water was allowed to move through a trench of depth 30 cm under periodic application.

3.7.4 Calibration of capacitance based moisture sensors TEROS12

TEROS 12 sensor as illustrated in figure 3.4 is a METER Group product. Three TEROS 12, capacitance based moisture sensors were used for determining the real time moisture variation and its movement in the experimental sites.

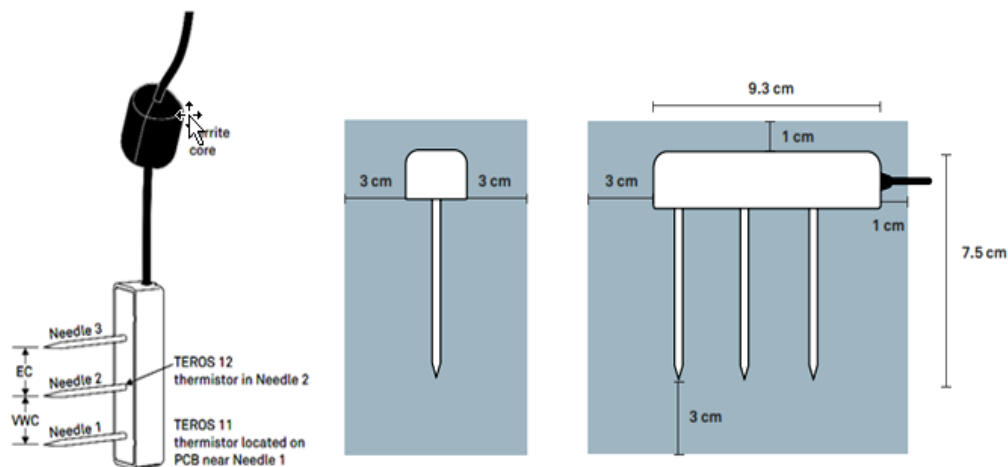


Figure 3.4 Capacitance based TEROS 12 sensor

Unlike gravimetric soil moisture analysis, volumetric water content measurements using TEROS 12 sensors are easier to record and can provide real time temporal variations in volumetric water content of the soil. TEROS 12 sensors have three needles. Soil moisture is measured in between needle 1 and needle 2.

Table 3.4 Physical specifications of TEROS12 sensors

PHYSICAL SPECIFICATIONS	
Dimensions	Length: 9.4 cm (3.70 in) Width: 2.4 cm (0.95 in) Height: 7.5 cm (2.95 in)
Needle length	5.5 cm (2.17 in)
Cable length	5 m (standard) 75 m (maximum custom cable length)
Cable diameter	0.165±.004 (4.20±.10mm) with min. jacket of .030 (.76 mm)
Connector types	3.5-mm stereo plug connector or stripped and tinned wires
Stereo plug connector diameter	3.50 mm
Conductor gauge	22 AWG/24 AWG drain wire

The sensor measures electrical conductivity (EC) between needle 2 and needle 3. A thermistor is incorporated to determine the temperature variations. TEROS 12 sensor has low power requirement. It measures the dielectric permittivity or the ability of medium (soil) to get polarized by creating an electromagnetic field. The physical and measurement specifications of TEROS 12 sensors are described in table 3.4 and table 3.5 respectively.

The electrical and timing characteristics of TEROS 12 sensors are described in table 3.6. An oscillating wave of 70 MHz is supplied by the sensor to the sensor

needles, which gets charged depending upon the dielectric property of medium. The charge time taken by the needles is recorded by the TEROS 12 microprocessor and provides the output in the raw value based on the dielectric property of the substrate. The raw value is converted to volumetric water content (VWC) by a using Topp's equation (Topp *et al.*1980). The configuration for the TEROS 12 moisture sensors and its data collection is done by the ZL6 data logger.

Table 3.5 Measurement specifications of TEROS 12 sensors

MEASUREMENT SPECIFICATIONS	
Volumetric water content (VWC)	<p>Range: Mineral soil calibration: 0.00–0.70 m³/m³ Soilless media calibration: 0.0–1.0 m³/m³ Apparent dielectric permittivity (ϵ_a): 1 (air) to 80 (water)</p> <p>NOTE: The VWC range is determined by the medium to which the sensor has been calibrated to.</p> <p>Resolution: 0.001 m³/m³</p> <p>Accuracy: Generic calibration: ± 0.03 m³/m³ ($\pm 3.00\%$ VWC) typical in mineral soils that have solution EC <8 dS/m. Medium specific calibration: ± 0.01–0.02 m³/m³ (± 1–2% VWC) in any porous medium Apparent dielectric permittivity (ϵ_a): 1–40 (soil range) , ± 1 ϵ_a (unitless) 40–80, 15% of measurement.</p>

MEASUREMENT SPECIFICATIONS	
Dielectric measurement frequency	70 MHz
Temperature	Range: -40 to 60 °C
Bulk electrical conductivity (EC_b)	Range: 0 to 20 dS/m (bulk) Resolution: 0.001 dS/m Accuracy: +/- (5% +0.01 dS/m) from 0 to 10 dS/m +/- 8% from 10 to 20 dS/m

Table 3.6 Electrical and timing characteristics of TEROS12 sensors

ELECTRICAL AND TIMING CHARACTERISTICS	
Supply voltage (VCC) to GND	Minimum: 4.0 VDC Typical: NA Maximum: 15.0 VDC
Digital input voltage (logic high)	Minimum: 2.8 V Typical: 3.6 V Maximum: 3.9 V
Digital input voltage (logic low)	Minimum: -0.3 V Typical: 0.0 V Maximum: 0.8 V
Digital output voltage (logic high)	Minimum NA Typical 3.6 V
Operating temperature range	Minimum: -40 °C Typical: NA Maximum: +60 °C

Table 3.7 Physical specifications of ZL6 data logger

PHYSICAL SPECIFICATIONS	
Dimensions	Length: 14.9 cm (5.9 in) Width: 6.3 cm (2.5 in) Height: 25.0 cm (9.9 in)
Enclosure material	Weather-, impact-, and UV-resistant polymer
Enclosure rating	IP56, NEMA 3R
Sensor input ports	6 (supports METER analog, digital, or pulse sensors)
Sensor port type	3.5-mm stereo plug connector
Memory type	Non-volatile flash, full data retention with loss of power
Data storage	ZL6 Basic: 2 MB (20,000 to 30,000 records depending on configuration) ZL6 and ZL6 Pro: 8 MB (40,000 to 80,000+ records depending on configuration)
Battery capacity	ZL6 Basic: 6 AA alkaline batteries ZL6 and ZL6 Pro: 6 AA NiMH or alkaline batteries
Battery life	Alkaline: 3–12 months depending on configuration NiMH: 3+ years with unobstructed view of sun. Charging through solar energy harvesting or USB
Operating temperature range	Minimum: –40 °C Maximum: +60 °C

ZL6 logger is a plug-n-play data logger for field research works depicted in figure 3.5. A weather resistant enclosure houses the data logger thereby making the device compatible for long term outdoor operations.

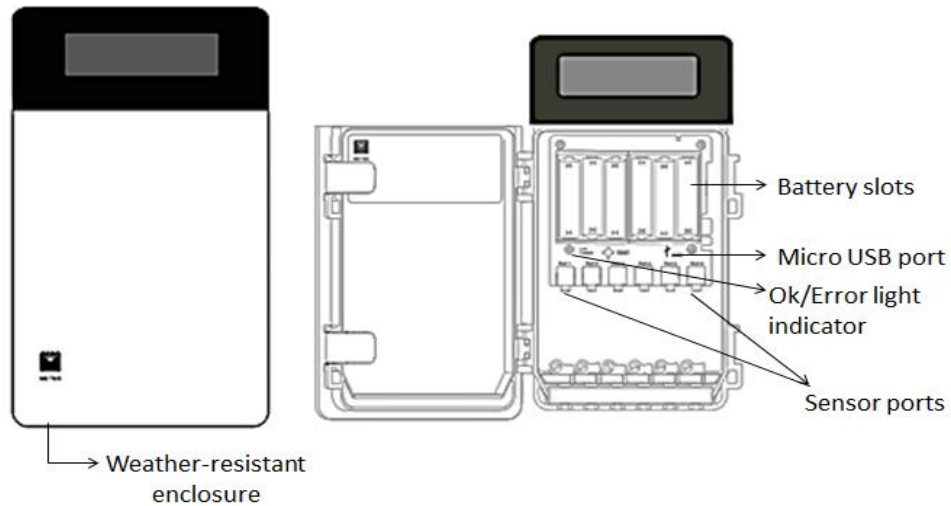


Figure 3.5 ZL6 data logger

The enclosure of data logger is made up of UV resistant polymer with an enclosure rating of IP56y, NEMA 3R. The physical specifications of ZL6 data logger are described in table 3.7. The collected data from the logger can be transmitted to the ZENTRA cloud web service via cellular communication which is furnished in the ZENTRA Utility software. Six sensor input ports are provided in the data logger which can support six different METER analog, digital or pulse sensors at the same time. Simple user interface software to configure and download the data from ZL6 logger is ZENTRA Utility, which was downloaded from metergroup.com. ZENTRA Utility can set all the configuration parameters required for the logger and can carry out real time sensor measurements at the study site. The capacitance based soil moisture sensor TEROS 12 has been already company calibrated for mineral soils and soilless media. However, the sensor has not been calibrated for its accuracy in the laterite terrain at different soil profiles with varying soil aggregation and texture. Hence, the moisture sensor was first calibrated for the site specific soils before being used for monitoring moisture movement. Calibration and validation of three TEROS 12 sensors were performed in five phases.



Plate 3.2 Installation of TEROS12 sensors in field for reliability check before calibration

The first phase was to install the TEROS 12 capacitance based soil moisture sensors along with ZL6 data logger at the study site as illustrated in plate 3.2. The three TEROS 12 moisture sensors were marked as 1, 2 and 3 as per the sequence of their insertion in different soil depths.

The tines of the moisture sensors were carefully inserted in all the three profile depths at the study site. The insertion was carried out carefully at the trench face, avoiding the bending or breakage of the sensor tines, specifically at 40-80 cm and 80-120 cm soil profile depths where, clods of lateritic clay and compaction in soil respectively, were potent. The stereo plug connector of the moisture sensors were connected to sensor input ports inside the ZL6 data logger. The TEROS 12 sensor comes standard with a 5 m long cable. Thus, the excess cable was secured so as to prevent the cables from rodent damage.

Data logger was configured through ZENTRA Utility interface. Subsequently, the sensor configuration was done, by providing a measurement interval of fifteen minutes and the sensor type information was supplied to the respective ports. Desired preferences for the volumetric water content, temperature and electrical conductivity measurements were set through the ZENTRA Utility interface. ZL6 logger was checked for its proper installation by checking the OK green light in the logger.

Subsequently, the sensor readings were scanned for all the three depths at different time to obtain the real time soil moisture data and were noted down.

The second phase was field data acquisition for the gravimetric moisture content analysis. Soil samples from the three profile depths of 0-40 cm, 40-80 cm and 80-120 cm in the site were collected carefully from the vicinity of the installed TEROS 12 sensors. Discreet soil sample collection was done with least/ no disturbance to the moisture sensors and thereby, assuring representative sampling, from the volume of influence of moisture sensor at the same time. The samples were taken after noting down the sensor readings so as to ensure no discrepancy in the sensor data. Soil samples were secured in moisture cans with appropriate moisture can number. The samples were kept in an oven at a temperature of 105 °C for 24 hours after removing their lids. Mandatory calculations and comparisons were done among the results obtained from both the phases of experiment.

The third phase included the soil sample preparation for calibration of sensor as shown through plate 3.3. Following the comparative analysis of the volumetric water content determined by TEROS 12 and that from the gravimetric method, soil sample from the first profile depth of 0-40 cm was taken for the sensor calibration. The calibration method preferred was the Method A of soil specific calibration for METER soil moisture sensors. It is a method recommended by the METER group for higher accuracy and is based on weighing the entire sample of calibration. The collected soil sample from the study site was air-dried for 24 hours. The air dried sample was run through a sieve of 2 mm size after breaking the larger clods. A plastic container of size 29.5 cm x 22.5 cm x 12 cm (L x W x H) was used as a calibration container. The container was packed with the soil as per the field bulk density, of 0-40 cm soil depth. This was done using the dry density value which was calculated through the core sample analysis in the laboratory.



Plate 3.3 Step-by-step procedure in calibration of TEROS12 sensor

Subsequently, the air dried soil was packed upto a height of 8 cm in the plastic container in such a way, that it matched the field bulk density of soil. The procedure was carried out gradually by adding the soil in layers and its compaction after every layer so as to minimize the voids. TEROS 12 moisture sensor was inserted vertically directly into the soil, filled in the container, avoiding any air gaps between the sensor tines and the soil. Some additional soil was put on and around the sensor and on its plastic base. Raw moisture data from the sensor was then collected and noted. Soil sample of about 15 g was collected in the moisture can and was kept in the oven for gravimetric moisture content determination. Water was added in the dry soil to about ten percent of the total soil volume to raise the volumetric water content by ten percent. The soil was thoroughly mixed by overturning, until the mixture became homogeneous. The soil sample was filled again into the plastic calibration container in layers and with each layer light compaction was done to minimize the voids. Raw value of raised volumetric water content was noted after inserting the moisture sensor

into the soil. At this point sensor to sensor variation was also determined using sensor 2.

The procedure was repeated to yield five calibration points. The calibration of sensor 1 was opted for the first soil profile depth of 0-40 cm. Similar procedure was followed for the sensor 2 and sensor 3 for soil profile depths of 40-80 cm and 80-120 cm, considering their respective dry densities. Proper care was taken to maintain the same bulk density of the sample throughout the calibration process, by packing the soil sample in the calibration container to the same height while raising the volumetric water content. The whole procedure was carried out at room temperature. Raw data from the sensor obtained via ZENTRA Utility was tabulated in the calibration chart.

In the fourth phase, integration of TEROS 12 moisture sensor with ZENTRA cloud software was done. Once the calibration function is determined for all the three moisture sensors specific for the respective soil profile depths, it can be applied to the METER sensor data. Further, the calibration function was applied using ZENTRA Cloud software. The new calibration function was added through the system settings tab in cloud software. Coefficients of new calibration function were added in the TEROS 12 moisture sensor section along with ancillary data obtained from field analysis. Once the coefficients for new calibration function were fed in the ZENTRA Cloud, validation was carried out.

The fifth phase concluded the validation of the generated calibration function. The developed calibration function was validated by determining the different water contents in the site specific soil samples. The first soil profile depth of 0-40cm at the study site represents sandy loam type of soil and the other two depths contain loamy sand. The calibration procedure as prescribed in TEROS 12 user manual resulted in calculated coefficients which were put in the calibration equation via ZENTRA cloud software. The validation was performed for all the three profile depths with varying moisture content soil samples: oven dried, air dried, samples with volumetric water

contents of 20 %, 30 % and 40 % respectively. The calibration and validation of the sensors were carried out for the soils at site 2 and site 3.

3.7.5 Installation of experimental set up 3 at site 2

The experimental set up 3 at site 2, as shown in figure 3.6 was set to investigate the effect of greater exposed surface area of soil profile and pulse application of water on the lateral flow discharge rate. The moisture sensors were kept installed at same points on trench face as they were during the experimental set up 2. The line source trench was constructed 2 m apart from the monitoring trench. The volume of water applied in line source trench was equal to the volume of line source trench and the volume of soil column in between the two trenches.

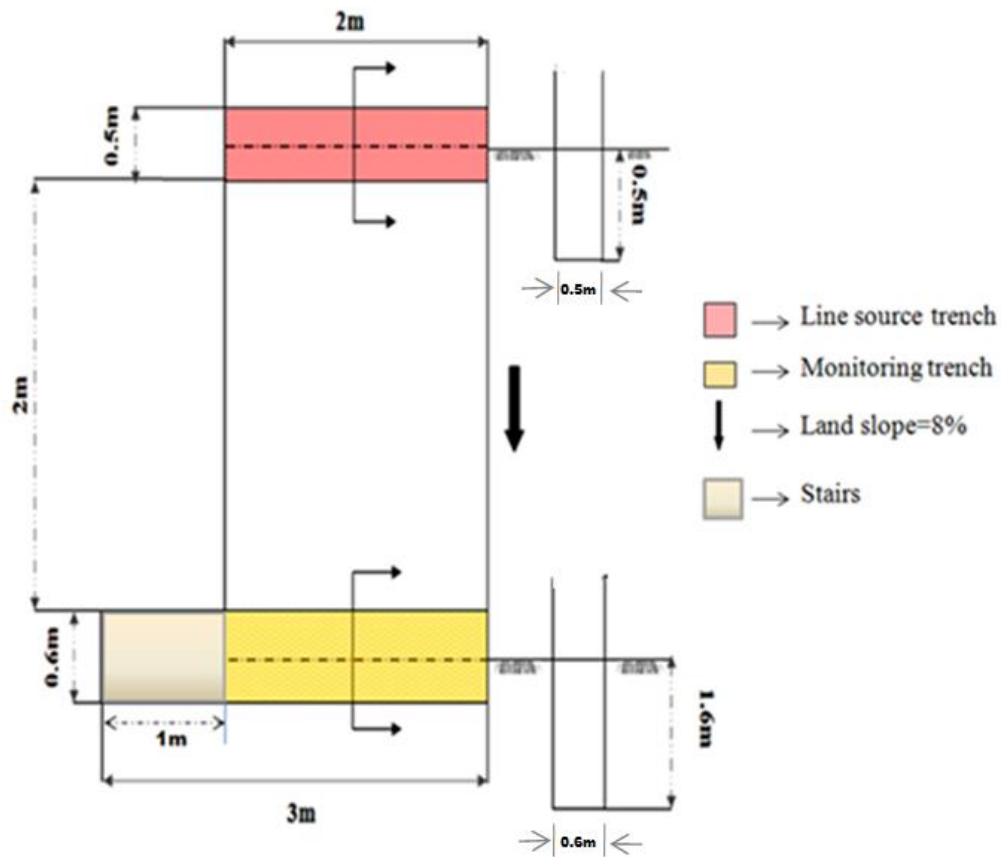


Figure 3.6 Plan view of the experimental set up 3 installed at site 2

Thus, a volume of 1200 litres of water was applied from 13:00 hrs in the line source trench. The change in the volumetric water content was recorded at the monitoring trench face by TEROS 12 sensors. Data logger was set to record the data at every 1 h interval for the day starting from the time of pulse application of water in line source trench. The volumetric water content recorded from the three soil profile depths depicted the time at which interflow was attributable at the monitoring trench face.

3.7.6 Installation of experimental set up 4 at site 2

The experimental set up 4 was installed in site 2 and is represented by figure 3.7. It was to assess lateral flow discharge under natural rainfall conditions.

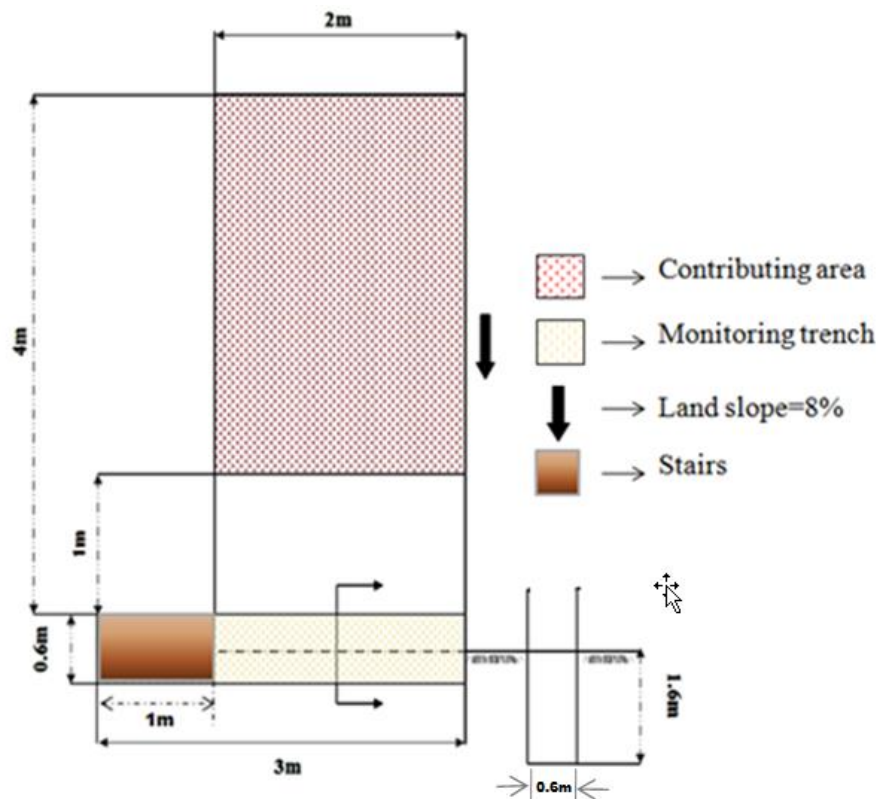


Figure 3.7 Plan view of the experimental set up 4 installed at site 2

The considered area of contribution was 6 m^2 , with a plot size of dimension (4 m x 2 m). A plastic sheet placed over a wooden frame was used to cover the monitoring trench. The 1 m upslope of monitoring trench was covered with tarpaulin sheet along with the trench to prevent it from the direct rainfall. The three moisture sensors recorded change in volumetric water content from the soil profile depths of 0-40 cm, 40-80 cm and 80-120 cm. The total duration of experiment was 26 days with data collection intensity at every 1 h interval throughout the experimental period.

3.7.7 Installation of experimental set up 5 at site 3

The experimental set up 5 as shown in figure 3.8 was installed to quantify interflow discharge at site 3 under natural rainfall conditions.

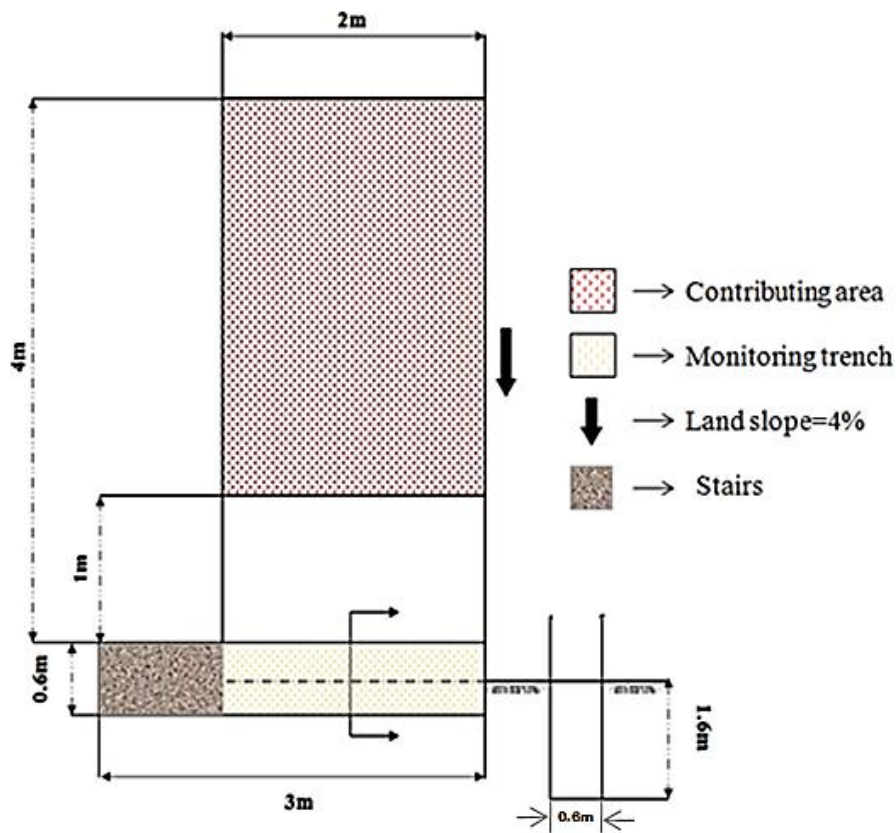


Figure 3.8 Plan view of the experimental set up 5 installed at site 3

The area under consideration in site 3 was 12 m² with the least vegetation as compared to other two experimental sites. Slope of the land was 4 percent.

A wooden frame of bamboo branches was made above the monitoring trench to cover it with a plastic sheet preventing direct rainfall into the monitoring trench. Three calibrated TEROS12 sensors were carefully inserted into three different soil profile depths i.e. at 0-40 cm, 40-80 cm and 80-120 cm in the monitoring trench. All the sensors were connected to ZL6 data logger through cables. The data retrieving interval was set at every 1h through the Zentra Utility interface.

3.8 DETERMINATION OF LATERAL FLOW

Among the five installed experimental set ups, the soil moisture measurement in experimental set up 1 and 2 was done by determining the gravimetric moisture content (GMC) for the three soil profile depths. The estimated GMC was converted to volumetric water content using equation 3.2 and equation 3.3.

$$\theta = wx\rho_d \quad (3.2)$$

Where,

$$\rho_d = (1 - n)G\rho_w \quad (3.3)$$

Where,

' θ ' is volumetric water content in %

' w ' is gravimetric moisture content in %

ρ_d is dry density of soil in g/cm³

' n ' is porosity

G is specific gravity of soil

ρ_w is density of water which is taken equal to 1 g/cm³

Volumetric water content (VWC) of three soil profile layers at depths of 0-40 cm, 40-80 cm and 80-120 cm was directly measured by TEROS 12 capacitance based sensors for the experimental set ups 3, 4 and 5.

The hypothesis adopted for the interflow quantification in the present research relates the temporal variation in volumetric water content to movement of water through the soil matrix.

A soil column of unit volume as shown in figure 3.9 is considered and the length, width and height of the soil column are represented as 'L', 'W' and 'H' respectively. Thus, volume of water, 'V₁' present in the soil column at time, t=i will be given by equation 3.4.

$$V_1 = L \times H \times W \times \theta_i \text{ cubic units} \quad (3.4)$$

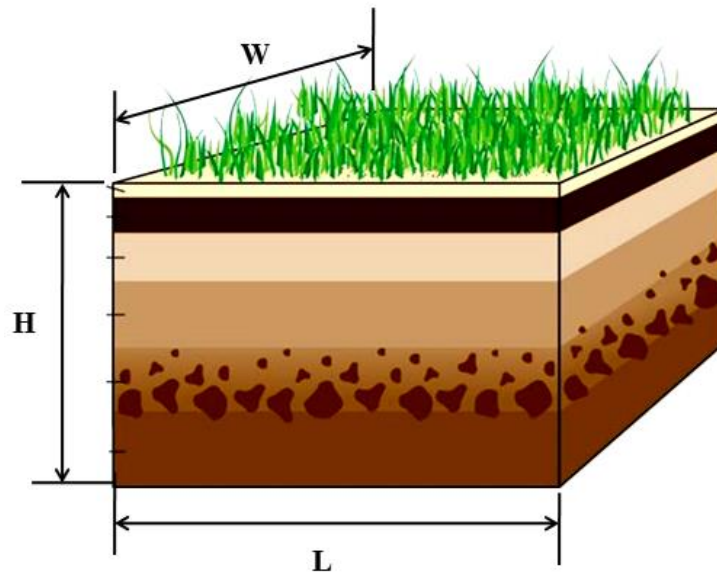


Figure 3.9 Hypothetical soil column

Where,

' θ ' is volumetric water content of the soil

After a period of time ' $i+n$ ', if the volumetric water content increases to ' θ_j ', then the volume of water present in the soil column, 'V₂' can be obtained using equation 3.5.

$$V_2 = L \times H \times W \times \theta_j \text{ cubic units} \quad (3.5)$$

Therefore, the volume of water ' V ' entered into the soil column in time ' t ', can be determined using equation 3.7 simplified from equation 3.6.

$$V = V_2 - V_1 \text{ cubic units} \quad (3.6)$$

Or

$$V = L \times H \times W(\theta_j - \theta_i) \text{ cubic units} \quad (3.7)$$

Subsequently, if the calculated discharge rate of lateral flow through a cross-sectional area ' A ' is represented as ' Q ' then the pore velocity is given by equation 3.8

$$v = \frac{Q}{A \times \text{porosity}} \quad (3.8)$$

3.9 LATERAL FLOW MEASUREMENTS USING SALT TRACER (NaCl)

Common salt (NaCl) was used to trace the lateral flow movement of water in site 3 and site 2. Each site involved two sets of tracer experiments under pulse application of tracer solution. The tracer breakthrough was recorded from three soil profile depths using TEROS 12 sensors. The required tracer mass concentration for the site specific soil was suggested by Division of Isotope Facility, *CWRDM, Calicut, Kerala* after the analysis of background electrical conductivity of sample water. It was suggested through the laboratory experiments, to raise electrical conductivity of final tracer solution upto three times than that of the background electrical conductivity. At site 3, salt tracer analysis was carried out with two different volumes of tracer solution and its effect was assessed on the salt breakthrough pattern at the monitoring trench face during the south-west monsoon. It was also done to validate the effect of pre-saturated soil matrix on the dispersion of tracer (NaCl) particles. In site 2, salt tracer analysis for interflow determination was conducted with two different mass concentration of tracer (NaCl) during the post-monsoon season.

The experiment was also done to validate the suitability of suggested tracer mass concentration, for efficient salt breakthrough analysis by TEROS 12 sensors in the laterite terrain under experimentation.

3.9.1 Lateral flow measurement using salt tracer in site 3

The first experiment was carried out on 14th October 2019. A rainfall depth of 40.1 mm was recorded at the experimental site on 13th October 2019. Thus, no prior soil saturation was conducted for tracer application. The experimental set up as shown in figure 3.10 involved a tracer application trench and monitoring trench. The tracer (NaCl) solution was applied in the tracer application trench and variations in electrical conductivity (EC) and Volumetric Water Content (VWC) were recorded at monitoring trench face by TEROS 12 sensors.

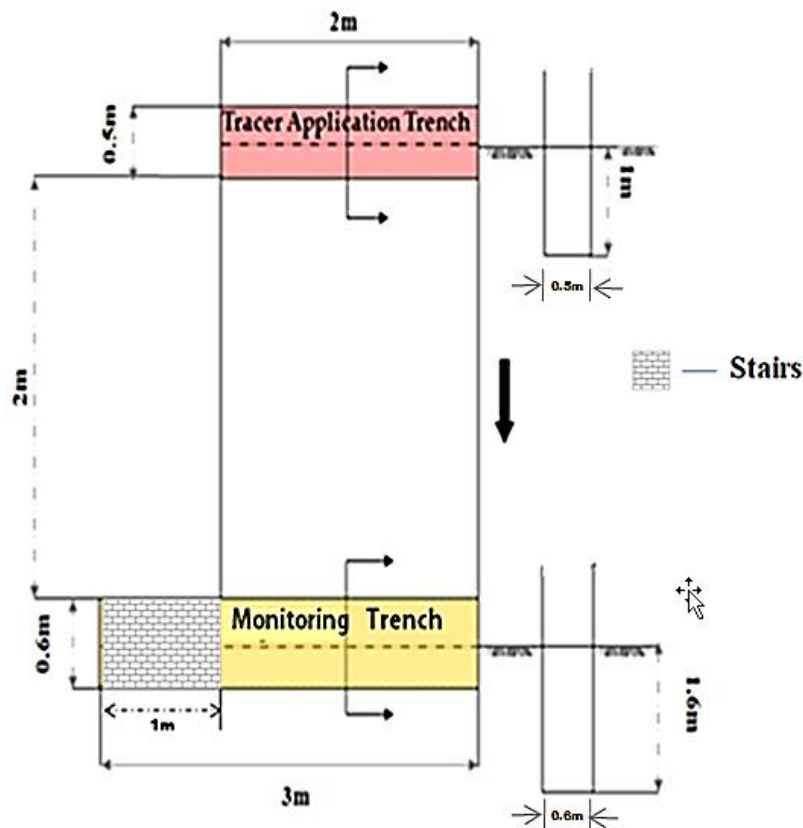


Figure 3.10 Plan view of the experimental set up for tracer experiment in site 3

Mass estimation of salt tracer to be applied was done using the equation 3.9 given by Martel (1913).

$$M/c = 23(LQ)^{0.97} \quad (3.9)$$

Where M is mass in g , c is peak concentration in g/m^3 , L is the distance in m and Q is discharge in the monitoring trench. The equation is a two-step process. First is to calculate M/c , and the second is to identify the suitable peak tracer concentration target. The suitable peak concentration is a contextual selection based on the tracer's detectability against expected background, the possibility of high concentrations, and the implications of failing to detect a tracer (Worthington and Smart, 2016). For the present study the target for a salt trace was taken as 10.

Thus, the mass concentration will be

$$\begin{aligned} M/c &= 23(2 \times 0.000208)^{0.97} \\ &= 0.0120 \text{ g/ppm} \end{aligned}$$

Further, the target for the salt trace was applied as 10 ppm which gave the tracer mass as 0.12 g/litre of water.

Subsequently, a volume of water equal to the volume of tracer application trench, i.e. 500 litres with a salt (NaCl) tracer mass of 60 g was applied in the field through tracer application trench. The second experiment at site 3 was conducted with 1000 l volume of water and salt tracer (NaCl) mass of 120 g.

3.9.2 Lateral flow measurement using salt tracer in site 2

The experimental set up at site 2 as shown in figure 3.11 involved a tracer application trench of 50 cm depth and a monitoring trench of depth 160 cm. Lateral flow measurement in site 2 was analysed under the application of two different salt tracer mass concentrations. Three TEROS12 sensors were installed at soil profile depths of 0-40 cm, 40-80 cm and 80-120 cm on the monitoring trench face.

The first experiment was carried out with 48 g of solute (NaCl) dissolved in 1200 l of water. The second experiment for lateral flow analysis through salt (NaCl) tracer was done with 96 g of solute in 800 l of water.

The experiment was conducted to analyse the variation in interflow movement and its detection by TEROS 12 sensors with varying salt tracer mass concentrations.

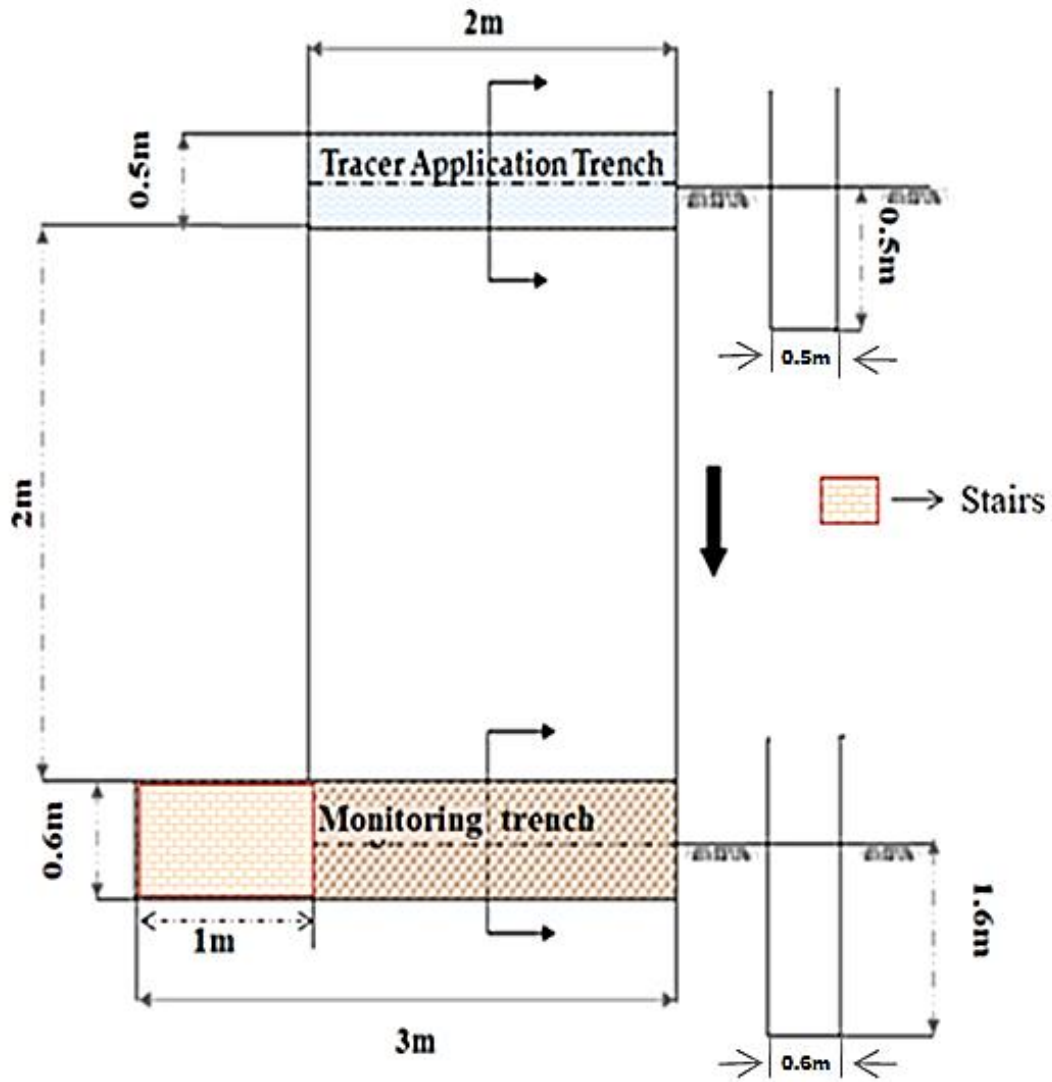


Figure 3.11 Plan view of the experimental set up for tracer experiment in site 2

3.10 GROUND WATER FLOW MONITORING

3.10.1 Groundwater monitoring through pressure head measurement

The experiment was carried out in site 1. Two observation wells were first dug at a distance of 7 m apart from each other. The operation was performed using handheld earth auger as shown in plate 3.4. At a depth of 4.19 m for first well and 4.90 m for the second well, water table was observed and digging was halted. Excess mud was scrapped off and poured out through an industry made hollow iron cylinder with scrapers at the bottom and a metal ball inside it. The metal ball provided the required weight to the cylinder for pouring out the mud out of the observation wells. The metal ball provided the required weight to the cylinder for pouring out the mud out of the observation wells. A PVC pipe of length and diameter 5 m and 0.09 m respectively was inserted down in both the observation wells. The PVC pipe was provided with slits along 2 m of its bottom length on three sides and a perforated end cap at the bottom.

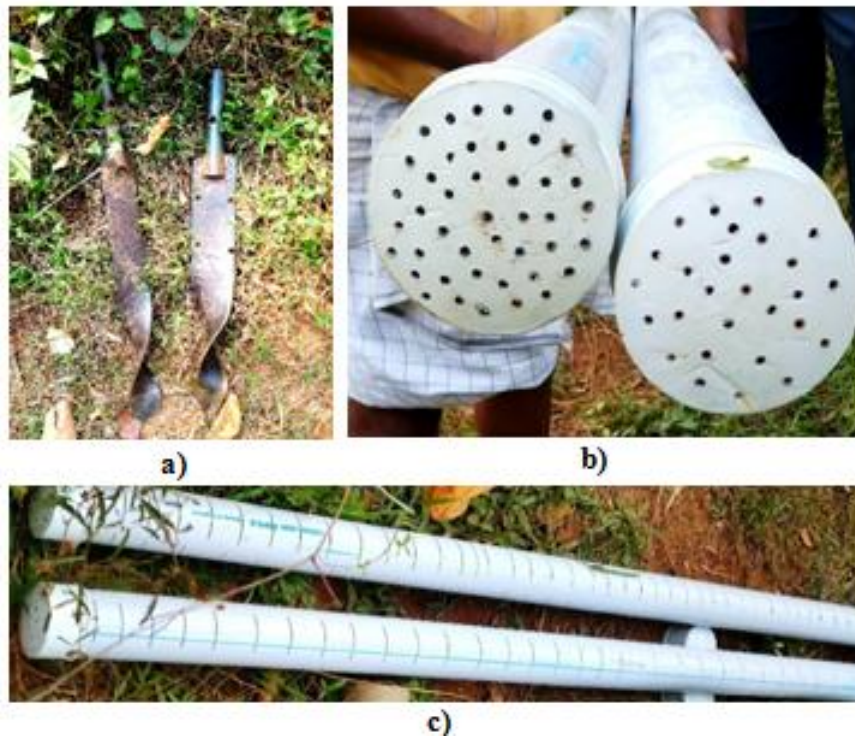


Plate 3.4 Observation well and PVC pipe installation in site 1

The installation was carried out during the pre-monsoon season from 24th February 2019 to 2nd March 2019. Figure 3.12 represents the plan view of the experimental set up for groundwater flow monitoring.

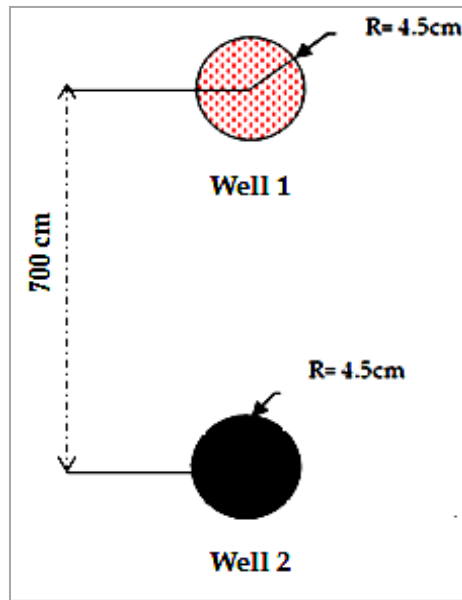


Figure 3.12 Plan view of the experimental set up for groundwater flow monitoring

The weekly peizometric head measurements were recorded for both the observation wells from 26th February 2019 to 9th September 2019. The total hydraulic head for two wells were calculated using equation 3.9.

$$H = H_p + H_e + H_v \quad (3.9)$$

Where,

H= Hydraulic Head

H_p = Pressure Head

H_e = Elevation Head

H_v = Velocity Head (considered negligible in case of base flow)

∴ for groundwater studies hydraulic head is given by equation 3.10,

$$H = H_p + H_e \quad (3.10)$$

Pressure head was measured by measuring the water level in the observation wells.

Elevation Head for observation wells were calculated as

$$H_e = SE_{msl} - D \quad (3.11)$$

Where,

H_e = Elevation Head

SE_{msl} = Elevation of the site above mean sea level

D = Depth of the observation well

3.10.2 Groundwater monitoring through salt tracer (KCl) analysis

An experimental set up for salt (KCl) tracer analysis was made ready in site 1 and is represented by figure 3.13. Three observation wells were dug in between well 1 and well 2. The wells were named as A, B and C. The depths of the observation wells A, B and C were 4.13 m, 3.90 m and 4.13 m respectively.

PVC pipes of lengths 5 m were inserted in all the three wells. The excess pipe length was cut as required for the experimentation. Prior to insertion, horizontal slits were made on the pipes upto 2 m height of the pipe from its bottom. Perforated end caps were fixed at the bottom of the PVC pipes.

Well 1 was opted as the injection well and other three wells were chosen for monitoring base flow. Potassium chloride (KCl) was used as a tracer agent. As K^+ ions have least interaction with the sediment particles (Mastrocicco *et al.*, 2011). KCl was considered as the best and easily available tracing compound for the experiment in the site specific laterite terrain. Prior to tracer application, the following preparatory measures were carried out.

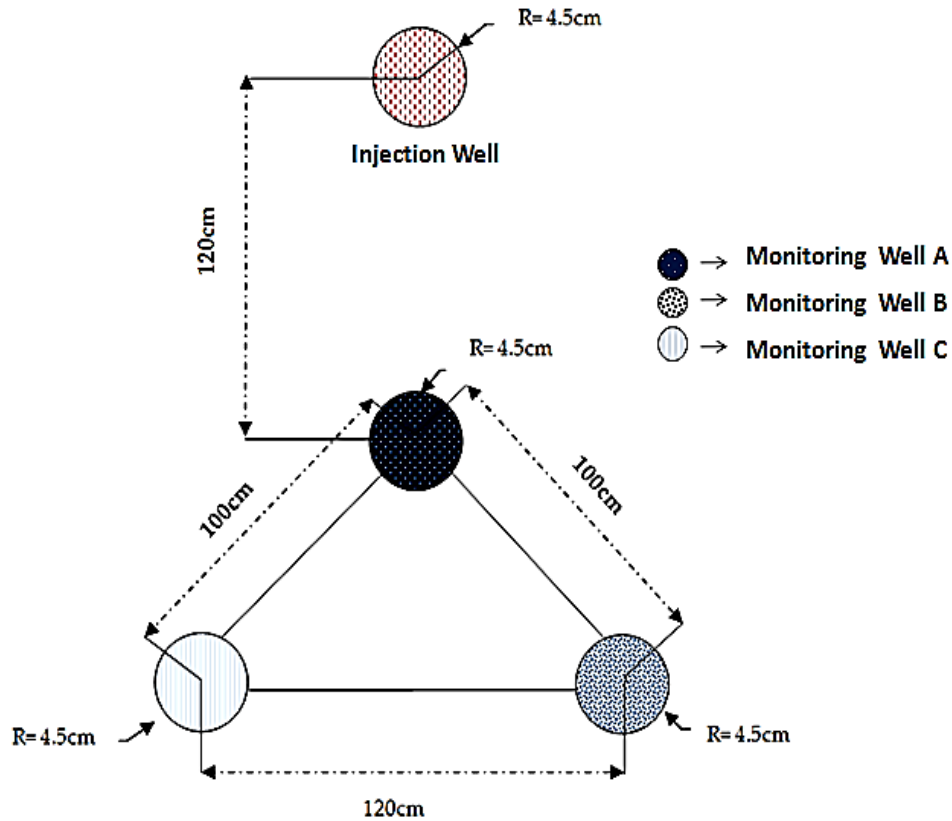


Figure 3.13 Plan view of the experimental set up for groundwater flow analysis using salt (KCl) tracer in site 1

1. A PVC pipe having similar horizontal perforation pattern as that of the wells A, B and C was inserted into observation well 1/injection well.
2. A hollow PVC pipe was obtained to inject the tracer directly into well 1 and for thorough mixing of tracer.
3. Mass of KCl to be injected into the observation well was determined depending upon the volume of water in the injection well and its background electrical conductivity.

4. Nine grams of KCl was kept in oven at a temperature of 90°C for half an hour to remove any clods.
5. Salt tracer (KCl) was allowed to cool down upto room temperature.
6. Potassium chloride (KCl) solution was made in 1l of distilled water.
7. Three marked TEROS12 moisture sensors were inserted down into the observation wells A, B and C through the PVC pipes to record the variation in electrical conductivities and volumetric water contents temporally. The moisture sensors were connected to the ZL6 data logger.

The following procedure was followed to trace the base flow in real time:

1. The KCl solution was poured rapidly into well 1 through the hollow PVC pipe. It was done by inserting the hollow tube completely into the first outer perforated tube.
2. The hollow tube was bobbed up and down immediately after pouring KCl solution and was rotated 2-3 times to ensure complete mixing. The hollow tube was removed within 2 minutes after thoroughly bobbing it in the well.
3. Observations of the temporally varying electrical conductivity was recorded continuously in every 5 minutes interval simultaneously for well A, B and C. The observations were done by the TEROS12 sensors and were recorded in ZL6 data logger as shown in plate 3.5.



Plate 3.5 Monitoring of base flow through salt tracer analysis and TEROS12 measurements

A point dilution test was used for single observation well analysis. The rate of tracer dilution is used to calculate linear velocity. The study is based on the simple hypothesis that decreasing tracer concentration is proportionate to both apparent velocity in test section and Darcy velocity in the aquifer (Piccinini et.al, 2016, Gomo, 2019). The point dilution method for horizontal flow velocity determination was used for injection well 1. The rate of flow of water Q , was calculated using equation 3.10 as per (Halevy et. al 1967).

$$Q = \frac{U}{t} \ln \frac{C_0}{C} \quad (3.10)$$

Where,

U = Borehole dilution volume

t = Time elapsed between the start of initial activity C_0 and the start of C

Further, the linear flow velocity v , was calculated utilizing the relationship shown in equation 3.11.

$$v = \frac{Q}{hd} \quad (3.11)$$

Where,

h = height of the water column in observation well

d = diameter of observation well

Equation 3.10 can be further solved in terms of diameter only by substituting Q from equation 3.9 which will give velocity as shown by equation 3.12.

$$v = \frac{Q}{hd} = \frac{U}{t} \ln \frac{C_0}{C} \cdot \frac{1}{hd} = d \left[\frac{\pi}{4} \cdot \frac{1}{t} \ln \frac{C_0}{C} \right] \quad (3.12)$$

Again, from Darcy's law we can deduce the equation 3.13

$$\frac{Q}{A} = -K \frac{\Delta h}{L} \quad (3.13)$$

Where, Δh is the hydraulic head difference and L is distance between injection well and monitoring well A respectively.

Combining equation 3.11 and 3.13 we get the relation for hydraulic conductivity given by equation 3.14

$$K = -v \left(\frac{L}{\Delta h} \right) \quad (3.14)$$

3.11 NATURAL ISOTOPE ANALYSIS OF GROUNDWATER

Isotope ratios of hydrogen ($^2\text{H} / ^1\text{H}$) or oxygen ($^{18}\text{O} / ^{16}\text{O}$) in natural waters provide ideal conservative tracer approaches for hydrological cycle research (Kumar *et al.* 2008). Natural water has isotopic levels of $^2\text{H} / ^1\text{H} \sim 156$ ppm, $^{18}\text{O} / ^{16}\text{O} \sim 2000$ ppm and $^3\text{H} / ^1\text{H} \sim 10^{-18}$. Isotope fractionation is caused by water condensation and evaporation (Gat, 1996). These variations in the isotope ratios, When measured in relation to ocean water, they generate signatures that can be used to identify the stage

at which any given stretch of water is part of the hydrological cycle. Thus, water samples from different water bodies in and near the experimental sites were collected during pre and post monsoon season in the state. Water samples from two open wells, two observation wells, pond, river and soil water from 80-120 cm depth were collected. Analysis for hydrogen and oxygen isotopes was carried out at CWRDM, Calicut Kerala.

3.12 SIMULATION OF LATERAL FLOW AND BASE FLOW OF WATER

A two dimensional simulation of lateral flow and base flow of water occurring in the site specific laterite terrain was done using HYDRUS 2D. The software was accessed from Indian Institute of Technology (IIT), Mandi, Himachal Pradesh through remote desktop using Any Desk- a remote desktop application. It was carried out with the support of School of Engineering, IIT Mandi, Himachal Pradesh. License ID 2574 was utilized for the access.

The HYDRUS programme solves numerically the Richards's equation for variably saturated flow of water and advection-dispersion equations for both heat and solute transport. A sink term is included in the flow equation to account for water uptake by plant roots. HYDRUS can be used to investigate the movement of water and solutes in unsaturated, partially saturated, or fully saturated porous media. The programme is capable of handling flow regions with irregular boundaries. The flow region itself could be made up of non-uniform soils with varying degrees of local anisotropy. The 2-D simulations of interflow and base flow for the present research were carried out by simulating the flow of water and solute (KCl) transport through the soil matrix respectively. The system's overall computational environment is defined by the main programme unit of the HYDRUS Graphical User Interface (GUI). A project manager, as well as pre- and post-processing units, is included in the main module. The pre-processing unit specifies all of the parameters required to run the HYDRUS FORTRAN codes, grid generators for rectangular and hexahedral transport domains that are relatively simple, a grid generator for complex two-

dimensional domains with unstructured finite element meshes, a brief listing of soil hydraulic properties, as well as a Rosetta Lite programme for calculating soil hydraulic properties from soil textural data.

The post-processing unit is made up of simple x-y graphics that are used to display the hydraulic properties of the soil graphically, as well as output in the form of distributions versus time of a specific variable at selected observation points, and actual or cumulative water and solute fluxes across a specific type of boundary. The post-processing unit also includes options for displaying simulation results by means of contour maps, isolines, spectral maps, and velocity vectors, and/or by animation using both contour and spectral maps.

The governing flow equation for simulating variably saturated flow in HYDRUS 2D is given by the modified form of Richard's equation as given by equation 3.15. A two- and/or three-dimensional isothermal uniform Darcian flow of water in a variably saturated rigid porous medium are considered and it is assumed that the air phase plays an insignificant role in the liquid flow process.

$$\frac{\partial \theta}{\partial t} = \frac{\partial}{\partial x_i} \left[K \left(K_{ij}^A \frac{\partial h}{\partial x_j} + K_{iz}^A \right) \right] - S \quad (3.15)$$

Where,

θ is volumetric water content in [L^3L^{-3}]

h is the pressure head in [L]

S is a sink term in [T^{-1}]

x_i ($i=1, 2$) are the spatial coordinates in [L]

t is time in [T]

K_{ij}^A are components of a dimensionless anisotropy tensor K^A

K is the unsaturated hydraulic conductivity function in [LT^{-1}] given by equation 3.16

$$K(h, x, y, z) = K_s(x, y, z) K_r(h, x, y, z) \quad (3.16)$$

Where,

K_r is the relative hydraulic conductivity

K_s is the saturated hydraulic conductivity

The governing transport equation for non-equilibrium transport of solutes is given by Fickian-based convection dispersion equation. The equation assumes that the solutes are transported by convection and dispersion in the liquid phase. A first-order decay reaction for three solutes (A, B and C) is generalized through a structure Simunek *et al.*, (1999) as represented in figure 3.14.

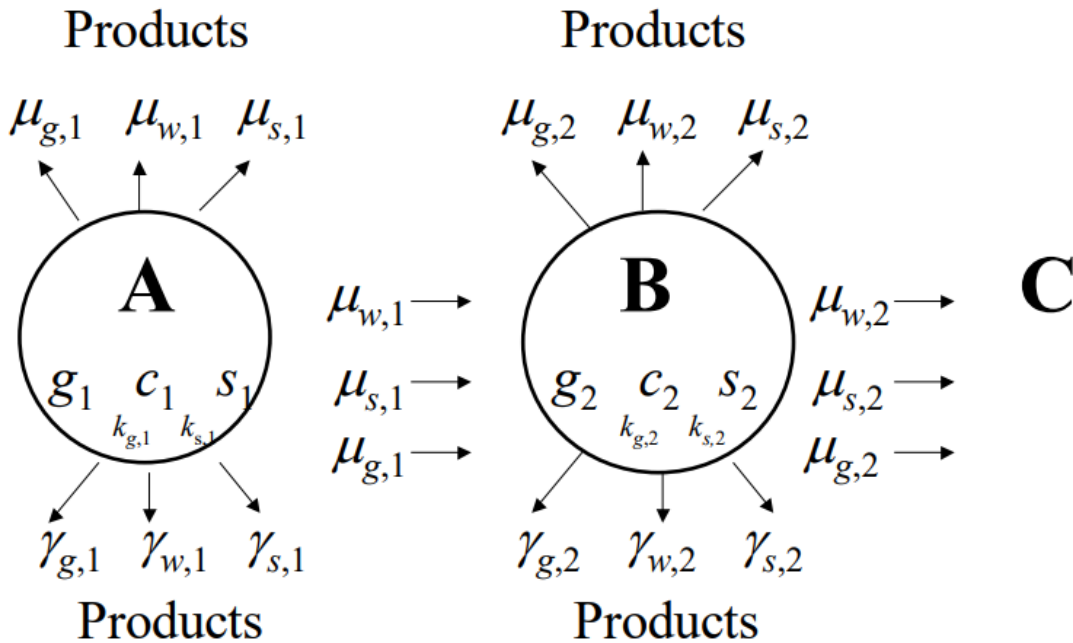


Figure 3.14 Generalized structure for the first order decay reactions for three solutes

Where,

c, s, and g represent concentrations in the liquid, solid, and gaseous phases, respectively.

s, w, and g refer to solid, liquid and gaseous phases, respectively. Straight arrows represent the different zero-order (γ) and first-order (μ , μ') rate reactions, and circular arrows (k_g , k_s) indicate equilibrium distribution coefficients between phases.

The partial differential equations governing non-equilibrium chemical transport of solutes involved in a sequential first-order decay chain during transient water flow in a variably saturated rigid porous medium are taken as given by equation 3.17 and equation 3.18.

$$\begin{aligned} \frac{\partial \theta c_1}{\partial t} + \frac{\partial \rho s_1}{\partial t} + \frac{\partial a_v g_1}{\partial t} = \frac{\partial}{\partial x_i} \left(\theta D_{ij,1}^w \frac{\partial c_1}{\partial x_j} \right) + \frac{\partial}{\partial x_i} \left(a_v D_{ij,1}^g \frac{\partial g_1}{\partial x_j} \right) - \frac{\partial q_i c_1}{\partial x_i} - S c_{r,1} - \\ - (\mu_{w,1} + \mu_{w,1}) \theta c_1 - (\mu_{s,1} + \mu_{s,1}) \rho s_1 - (\mu_{g,1} + \mu_{g,1}) a_v g_1 + \gamma_{w,1} \theta + \gamma_{s,1} + \gamma_{g,1} a_v \end{aligned} \quad (3.17)$$

$$\begin{aligned} \frac{\partial \theta c_k}{\partial t} + \frac{\partial \rho s_k}{\partial t} + \frac{\partial a_v g_k}{\partial t} = \frac{\partial}{\partial x_i} \left(\theta D_{ij,k}^w \frac{\partial c_k}{\partial x_j} \right) + \frac{\partial}{\partial x_i} \left(a_v D_{ij,k}^g \frac{\partial g_k}{\partial x_j} \right) - \frac{\partial q_i c_k}{\partial x_i} - \\ - (\mu_{w,1} + \mu_{w,k}) \theta c_k - (\mu_{s,k} + \mu_{s,k}) \rho s_k - (\mu_{g,k} + \mu_{g,k}) a_v g_k + \mu_{w,k-1} \theta c_{k-1} + \\ + \mu_{s,k-1} \rho s_{k-1} + \mu_{s,k-1} a_v g_{k-1} + \gamma_{w,k} \theta + \gamma_{s,k} \rho + \gamma_{g,k} a_v - S c_{r,k} \quad k \in (2, n_s) \end{aligned} \quad (3.18)$$

Where c , s , and g are solute concentrations in the liquid [ML^{-3}], solid [MM^{-1}], and gaseous [ML^{-3}], phases, respectively; q_i is the i -th component of the volumetric flux density [LT^{-1}], ' μ_w ', ' μ_s ', and ' μ_g ' are first-order rate constants for solutes in the liquid, solid, and gas phases [T^{-1}], respectively; ' μ_w ', ' μ_s ', and ' μ_g ' are similar first-order rate constants providing connections between individual chain species, ' γ_w ', ' γ_s ', and ' γ_g ' are zero-order rate constants for the liquid [$\text{ML}^{-3}\text{T}^{-1}$], solid [T^{-1}], and gas [$\text{ML}^{-3}\text{T}^{-1}$] phases, respectively; ρ is the soil bulk density [ML^{-3}], a_v is the air content [L^3L^{-3}], S is the sink term in the water flow equation (2.1), c_r is the concentration of the sink term [ML^{-3}], D_{ij}^w is the dispersion coefficient tensor [L^2T^{-1}] for the liquid phase, and D_{ij}^g is the diffusion coefficient tensor [L^2T^{-1}] for the gas phase. As before, the subscripts w , s , and g correspond with the liquid, solid and gas phases, respectively; while the subscript k represents the k th chain number and n_s is the number of solutes involved in the chain reaction. The indicial notation used in this report assumes summations over indices i and j ($i, j = 1, 2$), but not over index k . The

nine zero- and first-order rate constants may be used to represent a variety of reactions or transformations including biodegradation, volatilization, and precipitation.

HYDRUS assumes non-equilibrium interaction between the solution (c) and adsorbed (s) concentrations, and equilibrium interaction between the solution (c) and gas (g) concentrations of the solute in the soil system. The adsorption isotherm relating s_k and c_k is described by a generalized nonlinear equation of the form given by equation 3.19 and equation 3.20.

$$s_k = \frac{k_{s,k} c_k^{\beta_k}}{1 + \eta_k c_k^{\beta_k}} k\epsilon(2, n_s) \quad (3.19)$$

$$\frac{\partial s_k}{\partial t} = \frac{k_{s,k} \beta_k c_k^{\beta_k - 1}}{(1 + \eta_k c_k^{\beta_k})^2} \frac{\partial c_k}{\partial t} + \frac{c_k^{\beta_k}}{1 + \eta_k c_k^{\beta_k}} \frac{\partial k_{s,k}}{\partial t} - \frac{k_{s,k} c_k^{2\beta_k}}{(1 + \eta_k c_k^{\beta_k})^2} \frac{\partial \eta_k}{\partial t} + \frac{k_{s,k} c_k^{\beta_k} \ln c_k}{(1 + \eta_k c_k^{\beta_k})^2} \frac{\partial \beta_k}{\partial t} \quad (3.20)$$

Where $k_{s,k}$ [$L^3 M^{-1}$], β_k [-] and η_k [$L^3 M^{-1}$] are empirical coefficients. The Freundlich, Langmuir, and linear adsorption equations are special cases of equation (3.18). When $\beta_k=1$, equation (3.18) becomes the Langmuir equation, when $\eta_k=0$, equation (3.18) becomes the Freundlich equation, and when both $\beta_k=1$ and $\eta_k=0$, equation (3.18) leads to a linear adsorption isotherm. Solute transport without adsorption is described with $k_{s,k}=0$. While the coefficients $k_{s,k}$, β_k , and η_k in equation (3.18) are assumed to be independent of concentration, they are permitted to change as a function of time through their dependency on temperature. The concentrations g_k and c_k are related by a linear expression of the form given in equation 3.21.

$$g_k = k_{g,k} c_k k\epsilon(1, n_s) \quad (3.21)$$

Where $k_{g,k}c_k$ is an empirical constant [-] equal to $(K_H R_u T^A)^{-1}$ [Stumm and Morgan, 1981] in which K_H is Henry's Law constant [$MT^2M^{-1}L^{-2}$], R_u is the universal gas constant [$ML^2T^{-2}K^{-1}M^{-1}$] and T^A is absolute temperature [K].

3.12.1 Two dimensional simulation of interflow in unsaturated zone of soil matrix

Among the various experimental set ups described for interflow analysis and its quantification in different experimental sites, the set up described in section 3.7.5 was used for the 2-D simulation. Since, the point application of water through the trench was comparatively more controlled spatially and temporally, simulation using HYDRUS 2D was considered to be more rendering. The various input parameters for the simulation of lateral flow of water are described as follows:

1. Selection of type of geometry- A general two-dimensional geometry with a vertical XZ plane was opted to define the geometry of experimental set up in HYDRUS 2D.
2. Time information- As the analysis was carried out for a period of 11 hours, time units was fed in terms of hours. The initial and final time provided was 0th and 24thhour respectively. A single time varying boundary condition was defined which represented the variable water head in line source application trench.
3. Initial condition and soil hydraulic model - HYDRUS-2D software facilitates input option both in terms of pressure head as well as water content. As, in the present field research, TEROS 12 measurements had been used, thus the initial conditions were fed in terms of water content.

A single porosity model given by Van Genuchten - Mualem was used to define the movement of water through the site specific soil matrix.

4. Water flow parameters- The parameters for the soil hydraulic models are entered into the HYDRUS 2D water flow parameters dialogue window. The soil hydraulic parameters for the site specific soil were estimated through neural network prediction. The programme employs neural network-based pedotransfer functions (PTFs). Schaap *et al.*, (2001) to predict Van Genuchten [1980] water retention parameters and the saturated hydraulic conductivity (K_s) based on textural information. The HYDRUS code is inbuilt coupled with the Rosetta Lite DLL (Dynamically Linked Library) which was developed by Marcel Schaap at the U.S. Salinity Laboratory (Schaap *et al.*, 2001). Rosetta implements pedotransfer functions (PTFs) which predict Van Genuchten's (1980) water retention parameters and the saturated hydraulic conductivity (K_s) in a hierarchical manner from soil textural class, the soil textural distribution, bulk density and one or two water retention points as input.

Thus, soil textural and bulk density information estimated through the field experimentation were provided as input for all the three soil profile depths.

5. Time variable boundary condition- A variable head value of 50 cm was provided as input, to represent the total applied volume of water in the 50 cm deep line source trench. This applied volume of water was a pulse application thus, with time the total head varied as per the infiltration capacity of site specific soil.

6. Creation of domain geometry and surfaces - A two-dimensional geometry representing the experimental set up in field was created through points and lines in the view window of HYDRUS 2D. The coordinates of the points were selected according to the land slope in between the line source trench and monitoring trench. Subsequently, three planar surfaces were generated for the domain representing three soil layers at depths of 0-40 cm, 40-80 cm and 80-120 cm. Surface generation is required for the initiation of finite element mesh.

7. Finite element mesh refinement - A finite element mesh refinement was applied to the points defining line source trench and monitoring trench. It is done to increase the accuracy of resulting solution.

8. Materials on geometric objects- Three different materials representing the three soil profile depths of different physical properties in the site were defined under this command.

9. Selection of observation nodes and initial condition specifications - HYDRUS 2D provides the option for locating the observation nodes from where the measurements are extracted. For the present research, observation node depths represented the soil depths at which TEROS12 sensors were inserted. The initial volumetric water content recorded by the sensors for the three soil profile depths were specified for the domain.

10. Boundary conditions - For simulating the lateral movement of water occurring at site 2 three different boundary conditions were specified. A variable head boundary condition was chosen for the receding water head level in line source trench after water application. Boundary condition of free drainage and no flux was specified for monitoring trench and rest of the domain/borders respectively.

The calculated results after model simulation can be viewed under the options of 'Results - Graphical display' and 'Results – Other information'. Under the graphical display option results are displayed by means of contour maps, isolines, isobands, isosurfaces, colour points, colour edges, spectral maps, and/or velocity vectors and/or by animation using both contour and spectral maps. The 'other information' involves the additional information, such as boundary fluxes and/or soil hydraulic properties which are displayed using x-y graphs

3.12.2 Two dimensional simulation of base flow

The simulation of base flow was done by simulating the solute (KCl) transport through injection well to monitoring well A. In addition to the input parameters described in section 3.10.1, the following solute information was specified for simulating solute transport in HYDRUS 2D.

1. Solute transport and solute information - The basic information regarding the solute transport is entered in the solute transport dialog window. Crank Nicholson scheme and Galerkin finite elements were specified under time weighing and space weighing schemes respectively. The Time Weighting Scheme specifies the temporal weighing coefficient that will be used in the numerical solution of the transport equation. The temporal weighing coefficient is equal to 0.5 for a Crank-Nicholson time-centered implicit scheme. The solute information was specified in terms of number of solutes, pulse duration and mass units. As the number of solute used during the experiment was one, it was specified as 1 and the pulse duration was specified in terms of day as equal to 0.006 days. Tortuosity factor and water content dependence dialog boxes were checked. Tortuosity factor allowed molecular diffusion coefficients in the water and gas phases to be multiplied by a tortuosity factor according to Millington and Quirk, (1961). The initial condition for the solute transport was given in terms of liquid phase concentrations.

2. Solute transport parameters - The soil specific parameters were defined according to the site specific soil. Solute specific parameters were kept default. As the distance between the injection well and monitoring well was 1.2 m, it was assumed that the solute had no/minimum adsorption and reaction with the soil material.

CHAPTER 4

RESULTS AND DISCUSSIONS

4.1 GENERAL

The chapter involves the core findings of the research, derived from the methodology applied, in order to collect and analyse the detailed information regarding two major hydrological processes occurring in the site viz; lateral flow and base flow. The results obtained are presented and discussed in sequence.

4.2 RAINFALL PATTERN IN THE STUDY AREA

The State of Kerala experienced a severe flood in the year 2018. Simultaneously, an abnormally high rainfall was recorded in the experimental site as well. Figure 4.1 shows the monthly rainfall pattern recorded in the experimental site for the years 2018 and 2019. The total monthly rainfall recorded for August month in year 2018 was 1104.3 mm, which was the highest among the months.

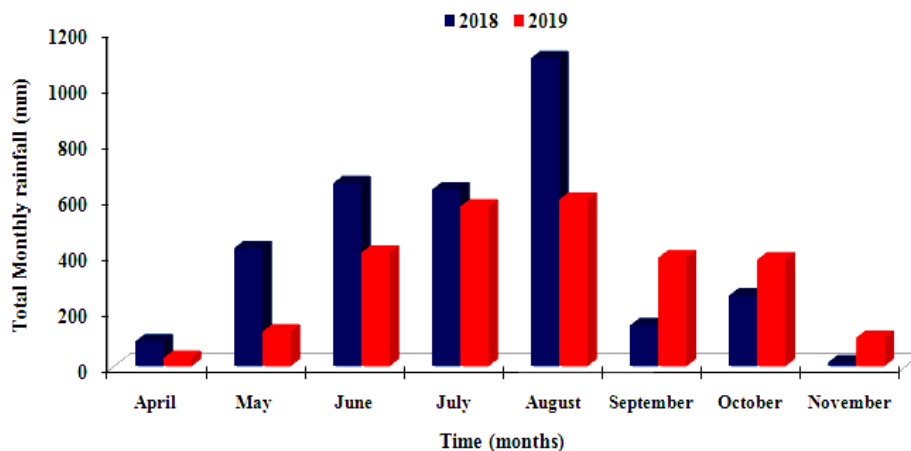


Figure 4.1 Recorded rainfall pattern for the years 2018 and 2019 in the study area

The foremost set up for monitoring subsurface flow at site 1 was damaged due to the flooding of the site and trench. The total rainfall recorded for the year 2018 was 3322.4 mm. Contrarily the year 2019 recorded total rainfall of 2615.05 mm only. The highest daily rainfall recorded was 143.2 mm on 20th July 2019. There was no

significant pattern of rainfall in the experimental site when the rainfall data for the years 2018 and 2019 were compared.

4.3 SITE SPECIFIC CONTOUR AND SLOPE MAPS

Total station surveying was done for developing site specific contour maps. for all the three sites. The maps are shown in figure 4.2, 4.3, 4.4, 4.5, 4.6, and 4.7.

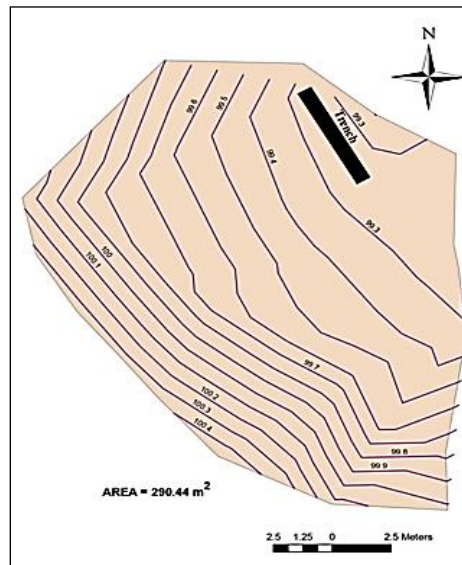


Figure 4.2 Contour map of experimental site 1

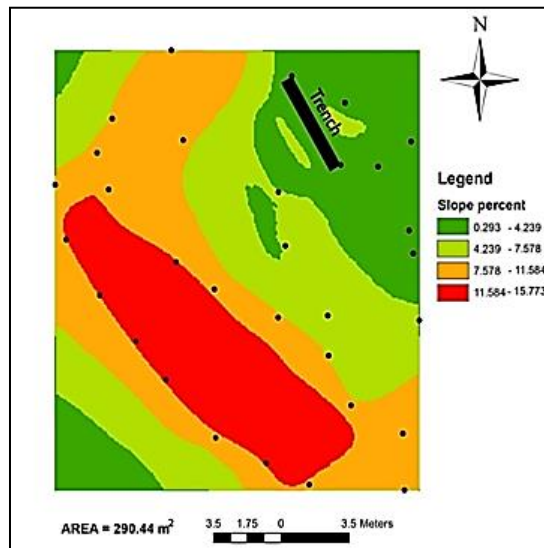


Figure 4.3 Slope map of experimental site 2

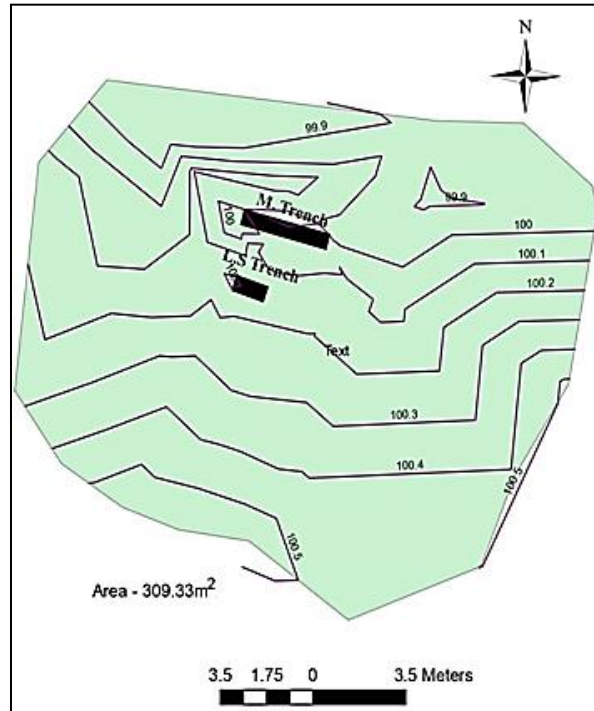


Figure 4.4 Contour map of experimental site 2

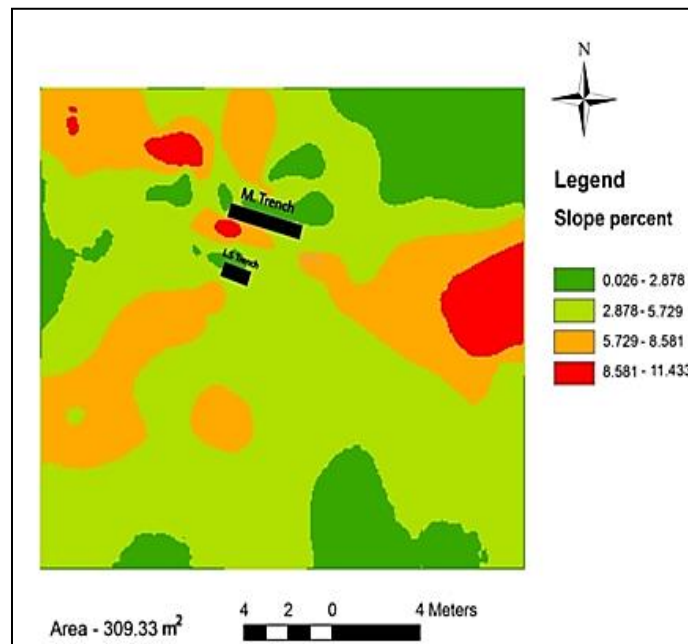


Figure 4.5 Slope map of experimental site 2

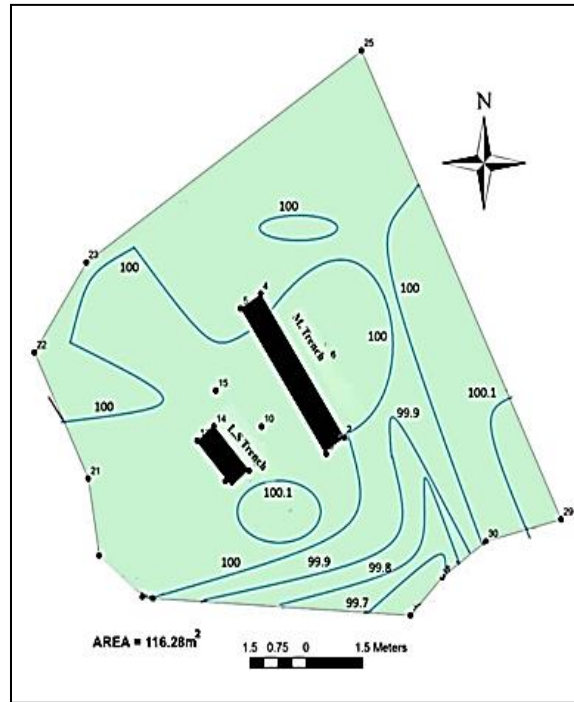


Figure 4.6 Contour map of experimental site 3

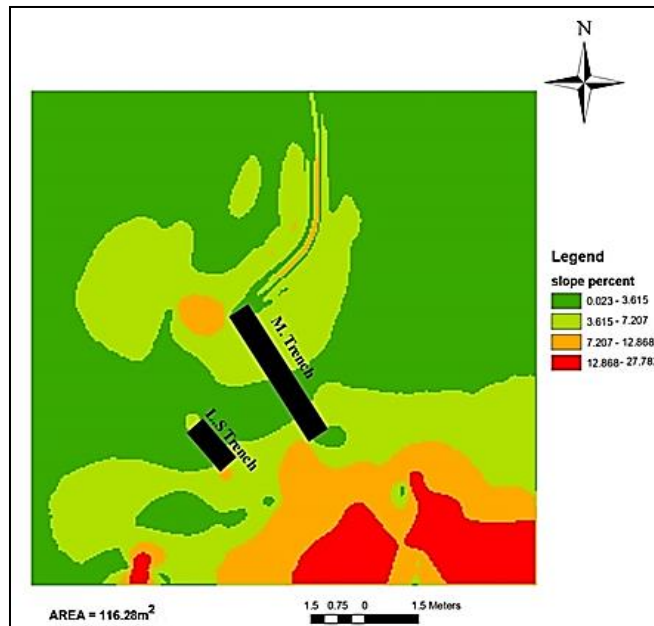


Figure 4.7 Slope map of experimental site 3

4.4 PHYSICAL PROPERTIES OF SOIL IN EXPERIMENTAL SITES

The soil physical properties of site 1 revealed an increase in the bulk density with increasing depth as shown in table 4.1. Thus, soil compaction with increasing soil depth was observed in the experimental sites. Subsequently, increasing specific gravity was noted with the increase in soil depth representing finer soil layer at a depth of 80-120 cm as compared to first two soil horizons. It can be attributed to the presence of inorganic soil particles and increased density of minerals with the depth.

Table 4.1 Soil physical properties of site 1

S.No.	Physical Properties	Site 1		
		0-40 cm	40-80 cm	80-120 cm
1	Initial Soil Moisture Content (%)	18	15	17
2	Dry Density (g/cm ³)	1.16	1.54	1.56
3	Specific Gravity	2.41	2.51	2.64
4	Porosity (n)	0.52	0.39	0.40
5.	Voids Ratio (e)	1.08	0.63	0.67
6	Soil Texture	Sandy Loam	Sandy Loam	Loamy Fine Sand
7	Sand (%)	66.00	61.20	72.39
8	Silt (%)	30.57	37.98	25.63
9	Clay (%)	3.43	0.82	1.98

The soil layer at a depth of 0-40 cm had the highest porosity as compared to the other two depths. This may be due to the presence of rich organic matter and coconut tree roots along with grass present in the site.

The soil physical properties in site 2 showed an unconventional pattern of dry density variation along the increasing depth as shown in table 4.2. The site was covered with vegetation in the form of grass and medium-rooted shrubs.

Soil horizon at depth of 40-80 cm represented the least bulk density of 1.11 g/cm³ as compared to other two depths. It was justified as the soil layer at depth of 40-80 cm had the highest porosity and sandy loam soil.

Table 4.2 Soil Physical Properties for Site 2

S.No.	Physical Properties	Site 2		
		0-40 cm	40-80 cm	80-120 cm
1	Initial Soil Moisture Content (%)	25	20	17
2	Dry Density (g/cm ³)	1.23	1.11	1.26
3	Specific Gravity	2.42	2.49	2.54
4	Porosity (n)	0.49	0.55	0.50
5.	Voids Ratio (e)	0.96	1.22	1
6	Soil Texture	Loam Fine Sand	Sandy Loam	Sandy Loam
7	Sand (%)	76.46	75.03	71.36
8	Silt (%)	18.40	19.70	22.47
9	Clay (%)	5.14	5.27	6.17

Soil properties in site 3 were very similar in characteristics as observed at site 1 as shown in table 4.3. Site 3 had least vegetation as compared to other two sites.

Table 4.3 Soil Physical Properties for Site 3

S.No.	Physical Properties	Site 3		
		0-40 cm	40-80 cm	80-120 cm
1	Initial Soil Moisture Content (%)	10	12	15
2	Dry Density (g/cm ³)	0.93	1.19	1.81
3	Specific Gravity	2.37	2.53	2.60
4	Porosity (n)	0.60	0.52	0.30
5	Void Ratio (e)	1.5	1.08	0.42
6	Soil Texture	Sandy Loam	Sandy Loam	Loamy Fine Sand
7	Sand (%)	64.00	62.20	73.50
8	Silt (%)	32.77	36.00	24.50
9	Clay (%)	3.23	1.80	2.0

4.5 LATERAL FLOW DETERMINATION THROUGH GRAVIMETRIC MOISTURE CONTENT MEASUREMENTS

4.5.1 Determination of Uniformity Coefficient of Sprinklers

The selection of sprinkler was done considering inducement of interflow through light to moderate intensity simulated rainfall, with maximum uniformity coefficient. Thus, among three available sprinklers, butterfly sprinkler was found to be most appropriate for the present study. Maximum uniformity coefficient of 90.87 % was recorded for butterfly sprinkler as tabulated in table 4.4.

Table 4.4 Uniformity coefficient of sprinklers

Type of Sprinkler	Uniformity Coefficient (%)
Pop-up sprinkler	63
Micro Sprinkler	59.84
Butterfly Sprinkler	90.873

The specification of butterfly sprinkler has been represented in table 4.5. The sprinkler was used at operating pressure of 1kg/cm^2 and discharge rate 660 lph was obtained for simulating rainfall in site 1.

Table 4.5 Specifications of the butterfly sprinklers

Pressure (kg/cm^2)	Discharge (lph)	Radius of coverage (m)
1.0	660	5.0
1.5	780	5.2
2.0	900	5.35

4.5.2 Lateral flow measurement for experimental set up 1

The rainfall simulation for inducing lateral flow was carried out with a butterfly sprinkler. The experiment was carried out for 12 hours in a day from 6:00 am to 6:00 pm (IST) for seven consecutive days. Total water application rate of butterfly sprinkler was 660 l/h. Total area under consideration was 78 m^2 , thus the depth of water applied through the sprinkler in the site was 8.46 mm/h. Accordingly, depth of water applied throughout the in-situ experimentation for 12 hours was obtained as 101.52 mm/12 h or mm/day (as per experimental hours). The experiment did not yield direct measurable discharge through the trench face and hence, gravimetric moisture content measurements (GMC) were taken from three soil profiles at depths of 0-40 cm, 40-80 cm and 80-120 cm. A volume of $6.09\text{ m}^3/\text{day}$ of water was applied to an area of 60 m^2 . Thus total volume of water applied for duration of seven days was obtained as 42.638 m^3 or 42638 l. The gravimetric soil moisture content

variation to obtain the total daily interflow discharge was computed for the experimental period of seven days and is shown in table 4.6. The daily recorded moisture content showed different patterns of variation along the three soil depths.

Table 4.6 Gravimetric soil moisture data analysis for experimental set up 1

Date	Depth (cm)	Time (h)	Gravimetric Moisture Content (%)	Change in Gravimetric Moisture Content (%)	Change in Volumetric Water Content (%)
9/02/2019	0-40	6:00	22.21	-	-
		8:00	25.55	3.34	3.86
		10:00	23.45	-2.1	-2.43
		12:00	23.79	0.34	0.39
		14:00	21.03	-2.76	-3.19
		16:00	20.61	-0.42	-0.49
		18:00	23.34	2.73	3.16
	40-80	6:00	23.71	-	-
		8:00	20.27	-3.44	-5.27
		10:00	23.94	3.67	5.62
		12:00	21.52	-2.42	-3.71
		14:00	21.5	-0.02	-0.03
		16:00	22.11	0.61	0.93
		18:00	23.32	1.21	1.85
	80-120	6:00	28.74	-	-
		8:00	25.97	-2.77	-4.39
		10:00	27.68	1.71	2.71
		12:00	23.26	-4.42	-7.00
		14:00	25.35	2.09	3.31
		16:00	24.26	-1.09	-1.73
		18:00	28.86	4.6	7.29

Date	Depth (cm)	Time (h)	Gravimetric Moisture Content (%)	Change in Gravimetric Moisture Content (%)	Change in Volumetric Water Content (%)
10/02/2019	0-40	6:00	21.93	-	-
		8:00	22.77	0.84	0.97
		10:00	22.37	-0.4	-0.46
		12:00	23.74	1.37	1.58
		14:00	25.47	1.73	2.00
		16:00	25.14	-0.33	-0.38
		18:00	22.47	-2.67	-3.09
	40-80	6:00	25.1	-	-
		8:00	20.3	-4.8	-7.35
		10:00	20.94	0.64	0.98
		12:00	22.55	1.61	2.46
		14:00	21.55	-1	-1.53
		16:00	22.45	0.9	1.38
		18:00	21.22	-1.23	-1.88
	80-120	6:00	25.09	-	-
		8:00	25.51	0.42	0.67
		10:00	34.31	8.8	13.94
		12:00	27.08	-7.23	-11.45
		14:00	24.53	-2.55	-4.04
		16:00	24.64	0.11	0.17
		18:00	27.14	2.5	3.96

On the first day of experiment all the three soil depths on the trench face gave a varying pattern in soil moisture increase and then decrease. This may be attributed to

the diurnal evapotranspiration occurring in the first two soil depths and the capillary movement of water at third depth in the site.

The diurnal variation of surface albedo is asymmetric around midday. Soil moisture and thermal diffusivity have a nonlinear relationship. The thermal diffusivity will first increase with soil moisture, then decreases after reaching its maximum (Roxy et.al. 2010). This phenomenon was also noticed and justified in the present study through the daily gravimetric soil moisture content analysis and is shown in figure 4.8, figure 4.9, figure 4.10 and figure 4.11. Nearly, same pattern of moisture content variation was experienced at soil depth of 80-120 cm. The visible macropores on the trench face can be potential indicator of preferential flow path ways in the site. This phenomenon can be attributed to the sudden upsurge of moisture content and discharge observed at depth of 80-120 cm on 10th and 11th February 2019. With the advancement of experiment day by day, the pattern of soil moisture content variation and discharge became more dynamic in all the three soil profile depths as represented in table 4.7.

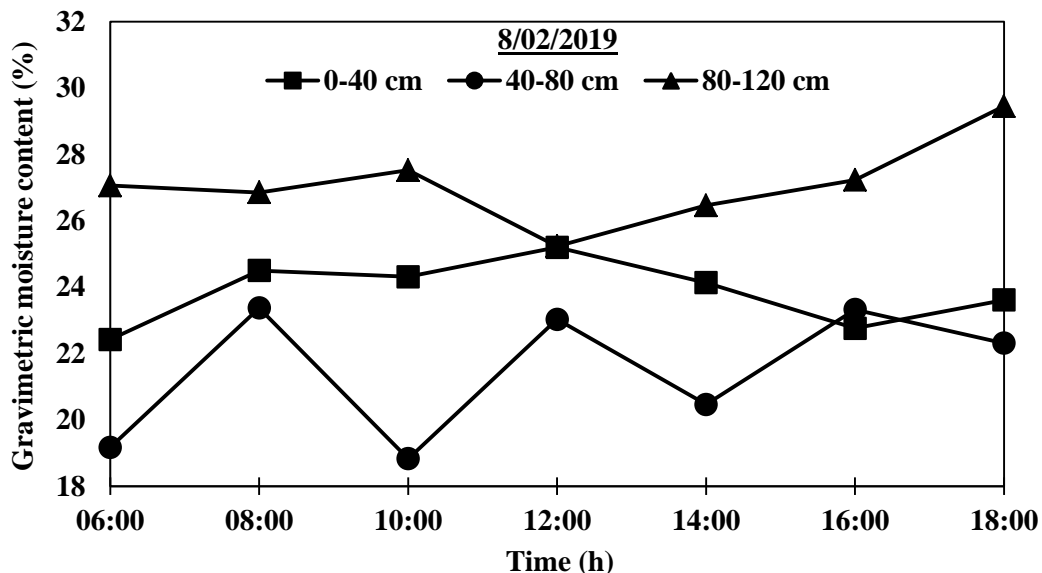


Figure 4.8 Gravimetric soil moisture content variations for experimental set up 1 on 8/02/2019 in site 1

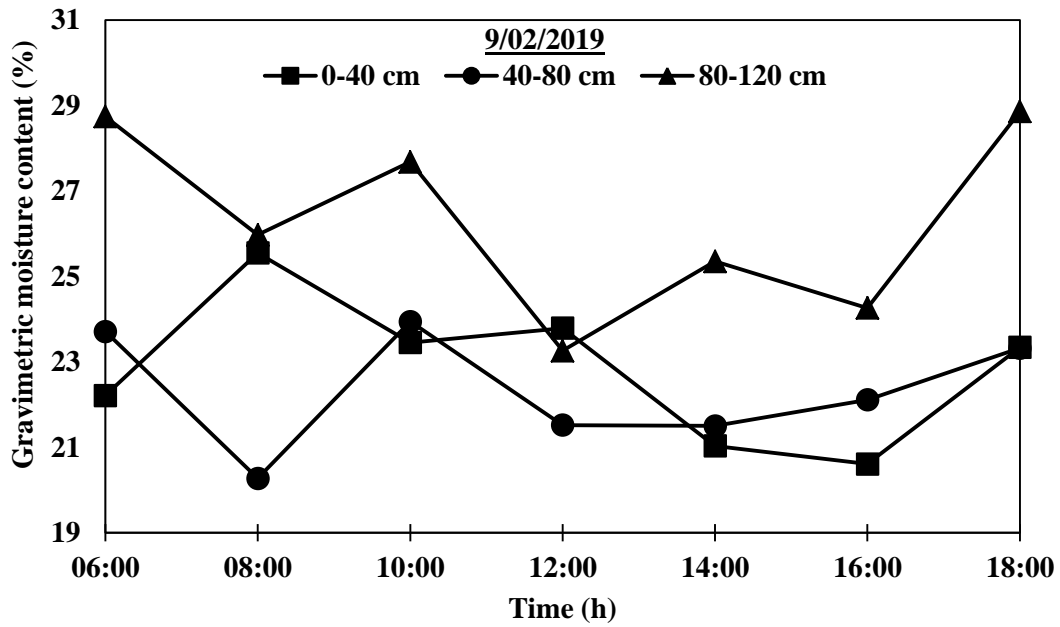


Figure 4.9 Gravimetric soil moisture content variations for experimental set up 1 on 9/02/2019 in site 1

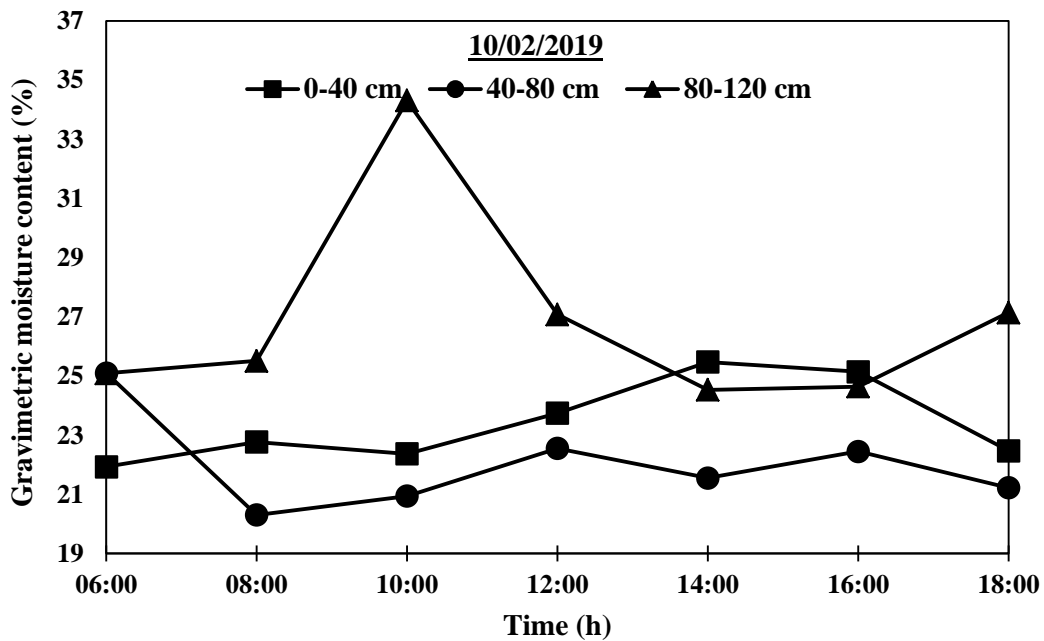


Figure 4.10 Gravimetric soil moisture content variations for experimental set up 1 on 10/02/2019 in site 1

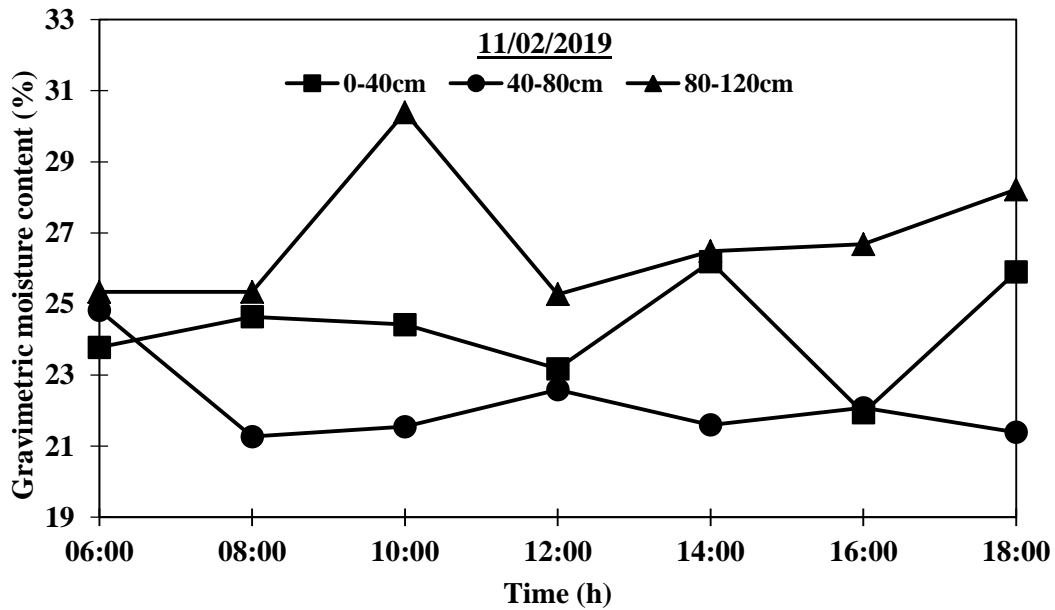


Figure 4.11 Gravimetric soil moisture content variations for experimental set up 1 on 11/02/2019 in site 1

Table 4.7 Variation in lateral flow discharge through different soil profile depths during experimental set up 1

Date	Depth (cm)	Average Lateral Flow Rate ($l/m^2/h$)
5/02/2019	0-40	7.15
	40-80	9.06
	80-120	8.21
6/02/2019	0-40	16.54
	40-80	15.22
	80-120	18.87
7/02/2019	0-40	10.29
	40-80	6.12

Date	Depth (cm)	Average Lateral Flow Rate (l/m²/h)
7/02/2019	80-120	16.66
8/02/2019	0-40	7.38
	40-80	28.90
	80-120	9.53
9/02/2019	0-40	12.39
	40-80	14.09
	80-120	21.84
10/02/2019	0-40	8.22
	40-80	8.08
	80-120	23.06
11/02/2019	0-40	15.13
	40-80	4.62
	80-120	12.48

Thus, a total lateral flow for the entire cross section of the soil for the experimental site was estimated to be 1151.4 l, 1288.42 l and 1870.12 l from soil layers having depths of 0-40 cm, 40-80 cm and 80-120 cm respectively for a period of seven days. This accounted for a total of 4309.90 l of lateral flow volume in seven days of experiment and it was 10.10 % of the simulated rainfall. The temporal variation of lateral flow discharge has been shown from figure 4.12 to 4.15. The highest lateral flow discharge was recorded on 10/02/2019 from 80-120 cm soil depth. A negative discharge represents draining off water from the specific soil depth. An average discharge rate through the respective cross sectional areas were

calculated as 67.34 l/m²/day, 76.69 l/m²/day and 111.31 l/m²/day for soil depths of 0-40 cm, 40-80 cm and 80-120 cm respectively.

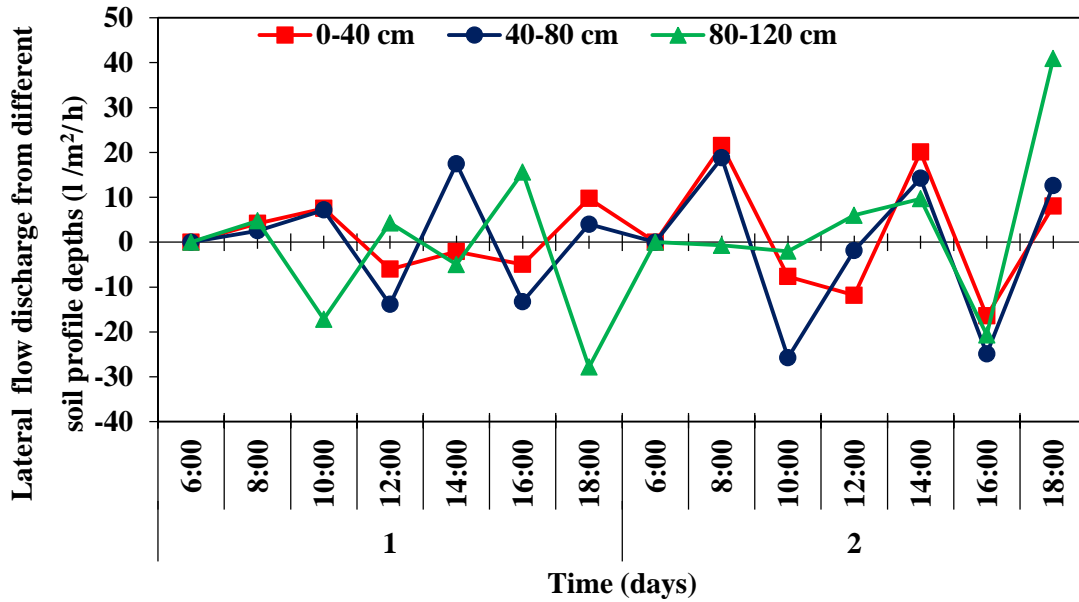


Figure 4.12 Temporal variation of lateral flow discharge from 5/02/2019-6/02/2019 from three soil profile depths for experimental set up 1

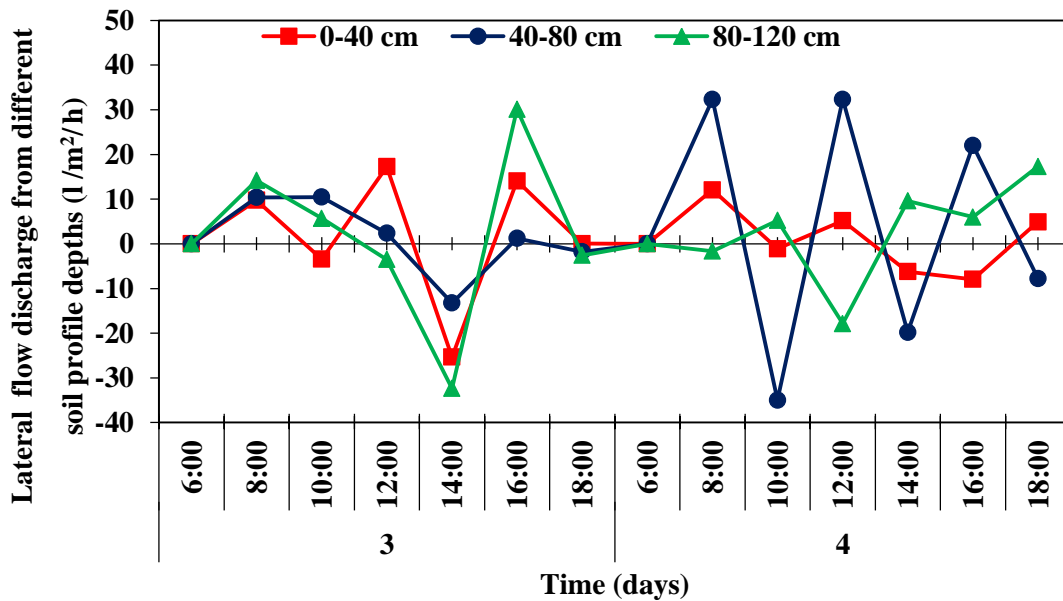


Figure 4.13 Temporal variation of lateral flow discharge from 7/02/2019-8/02/2019 through three soil profile layers for experimental set up 1

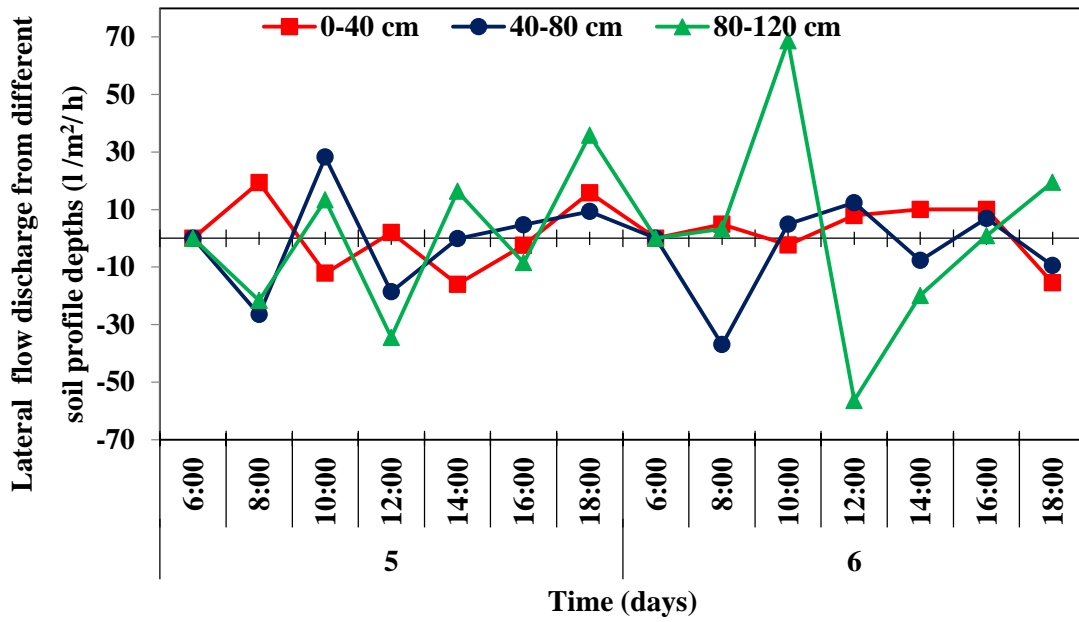


Figure 4.14 Temporal variation of lateral flow discharge from 9/02/2019-10/02/2019 in three soil depths for experimental set up 1

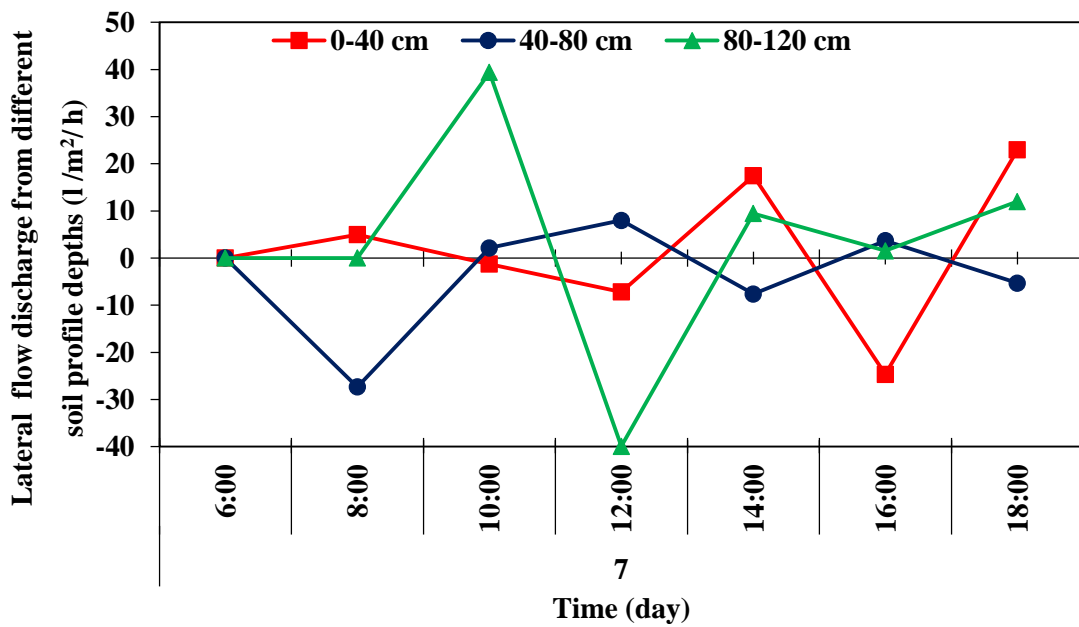


Figure 4.15 Temporal variation of lateral flow on 11/02/2019 in three soil depths for experimental set up 1

4.5.3 Lateral Flow Measurement for experimental set up 2

Lateral flow analysis through experimental set up 2 in site 2 involved the estimation of soil moisture variation during line source application of water through a 30 cm deep trench. It was done in a way that the trench was completely filled throughout the day time. A periodic application of water during the experiment ensured that, the water infiltration and its replenishment into the line source trench followed the same rate. Sample collection for gravimetric analysis was done from monitoring trench at every 4 hour interval from all the three soil depths starting at 6:00 am till 6:00 pm. The experiment was carried out for ten days from 24/05/2019 to 2/06/2019. The soil moisture data analysis to obtain the total daily interflow discharge was computed for the experimental period of ten days and is shown in table 4.8.

Table 4.8 Gravimetric soil moisture data analysis for experimental set up 2

Day	Depth (cm)	Time (h)	Gravimetric Moisture Content (%)	Change in Gravimetric Moisture Content (%)	Change in Volumetric Water Content (%)
3	0-40	6:00	21.54	-	-
		10:00	26.15	4.61	5.68
		14:00	26.20	0.05	0.06
		18:00	24.69	-1.51	-1.86
	40-80	6:00	22.56	-	-
		10:00	27.80	5.24	5.86
		14:00	27.84	0.04	0.04
		18:00	26.92	-0.92	-1.03
	80-120	6:00	22.73	-	-

Day	Depth (cm)	Time (h)	Gravimetric Moisture Content (%)	Change in Gravimetric Moisture Content (%)	Change in Volumetric Water Content (%)
3	80-120	10:00	28.53	5.8	7.36
		14:00	27.24	-1.29	-1.63
		18:00	27.21	-0.03	-0.03
4	0-40	6:00	23.89	-	-
		10:00	27.20	3.31	4.08
		14:00	24.50	-2.7	-3.33
		18:00	23.45	-1.05	-1.29
	40-80	6:00	25.80	-	-
		10:00	26.42	0.62	0.69
		14:00	28.24	1.82	2.03
		18:00	26.50	-1.74	-1.94
	80-120	6:00	28.23	-	-
		10:00	30.20	1.97	2.50
		14:00	28.72	-1.48	-1.87
		18:00	28.70	-0.02	-0.02

The gravimetric soil moisture content variations for the representative days during the experimental period have been shown from figure 4.16 to figure 4.19. With the progression of experiment a deeper infiltration of water was observed in the site.

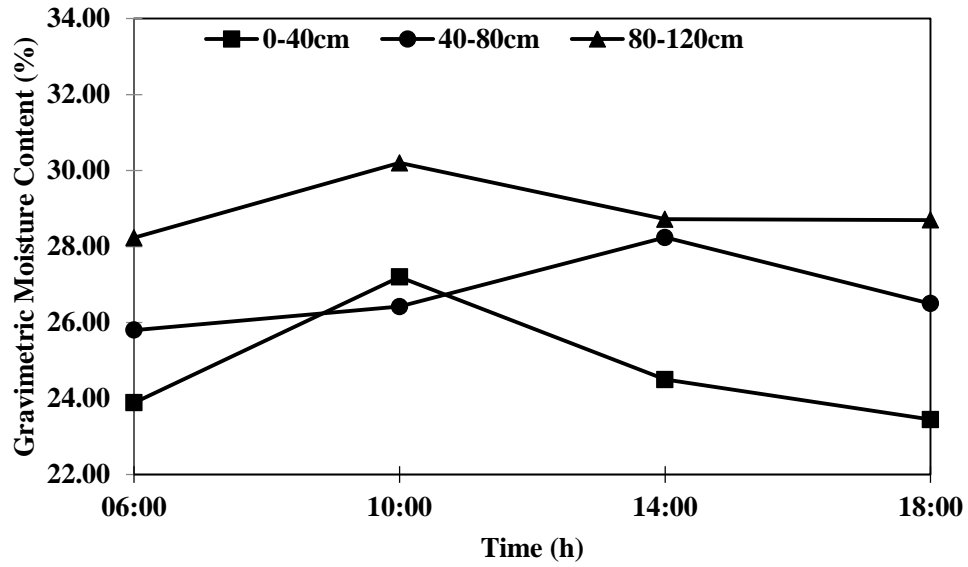


Figure 4.16 Gravimetric soil moisture content variations for experimental set up 2 on day 4 in site 2

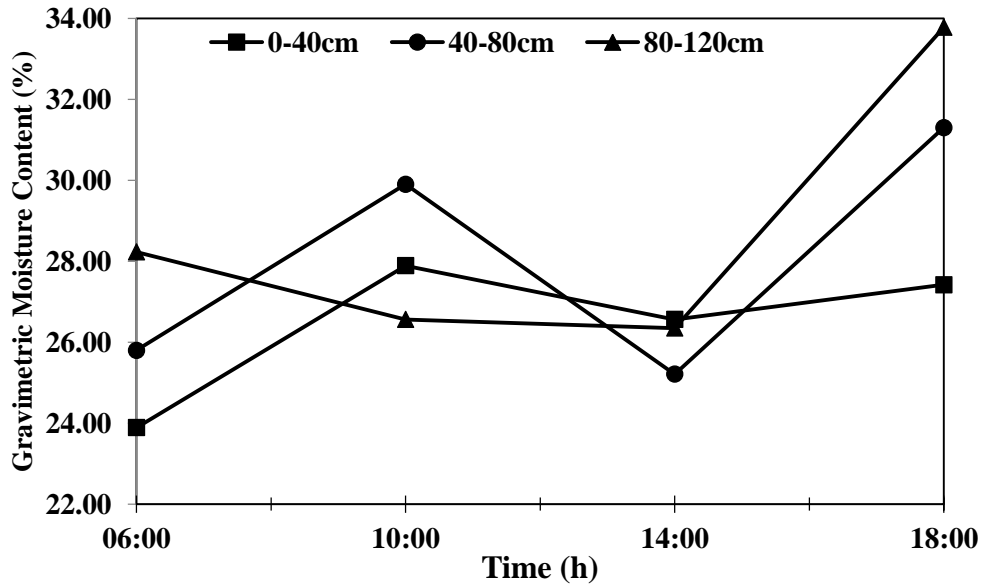


Figure 4.17 Gravimetric soil moisture content variations for experimental set up 2 on day 5 in site 2

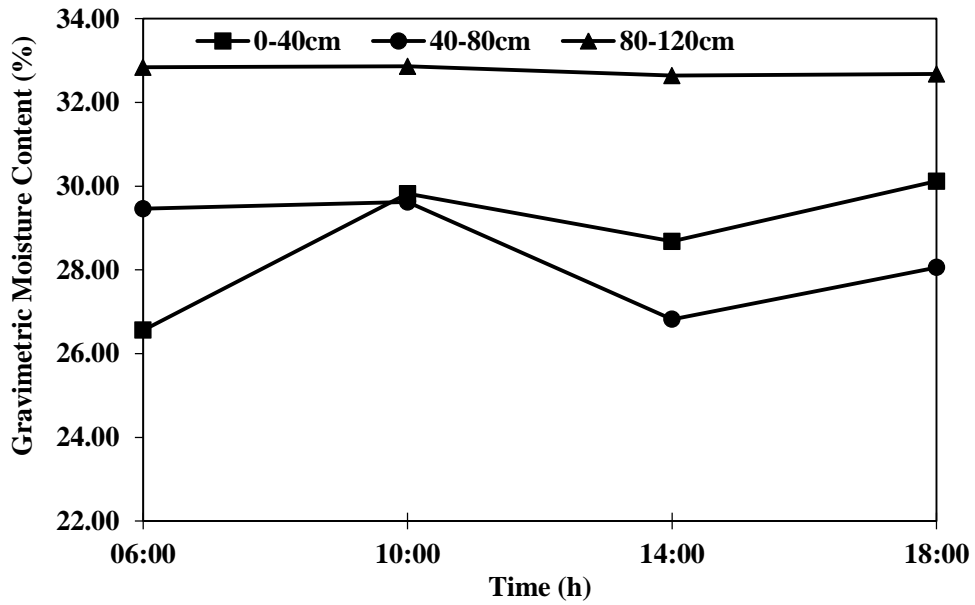


Figure 4.18 Gravimetric soil moisture content variations for experimental set up 2 on day 6 in site 2

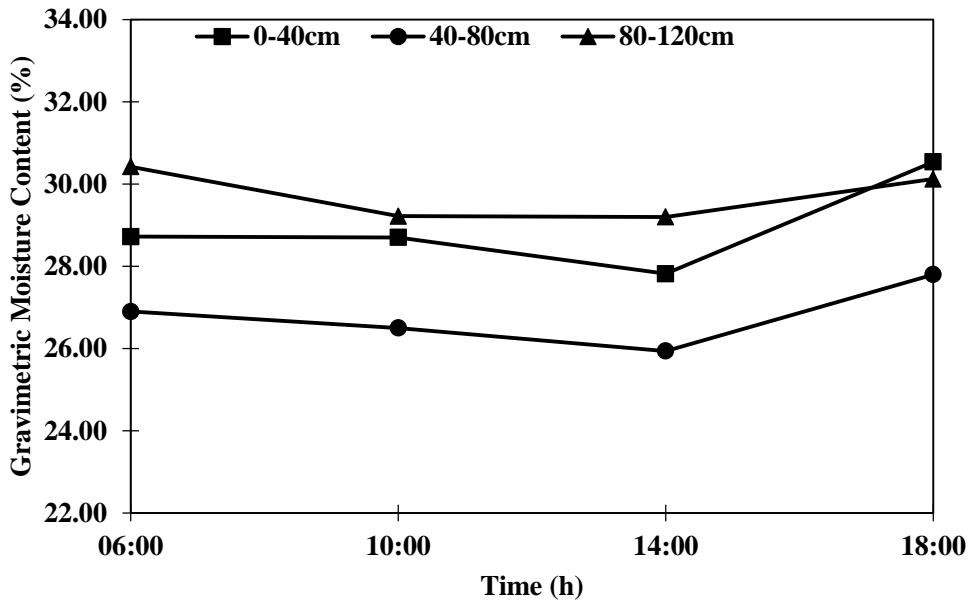


Figure 4.19 Gravimetric soil moisture content variations for experimental set up 2 on day 7 in site 2

The variation in lateral flow discharge through different soil profile depths during experimental set up 2 has been shown in table 4.9. It became evident with the progression of experiment that the volume of water required to replenish the line source trench kept on reducing. It was apparently due to gradual pore saturation in the soil. It can also be attributed to the presence of larger pores at deeper soil depths. The hourly temporal variation of lateral flow discharge for the first and last five days of experimental duration has been represented by figure 4.20 and figure 4.21.

Table 4.9 Variation in lateral flow discharge through different soil profile depths during experimental set up 2

Day	Depth (cm)	Average Lateral Flow Rate ($l/m^2/h$)
1	0-40	1.90
	40-80	1.85
	80-120	2.52
2	0-40	1.27
	40-80	3.05
	80-120	2.14
3	0-40	1.45
	40-80	2.16
	80-120	2.85
4	0-40	2.46
	40-80	3.71
	80-120	1.86
5	0-40	1.10

Day	Depth (cm)	Average Lateral Flow Rate ($l/m^2/h$)
5	40-80	2.34
	80-120	2.05
6	0-40	1.88
	40-80	1.22
	80-120	0.92
7	0-40	0.51
	40-80	0
	80-120	0
8	0-40	0.82
	40-80	0.27
	80-120	1.72
9	0-40	2.39
	40-80	0.86
	80-120	0.25
10	0-40	3.17
	40-80	3.75
	80-120	1.72

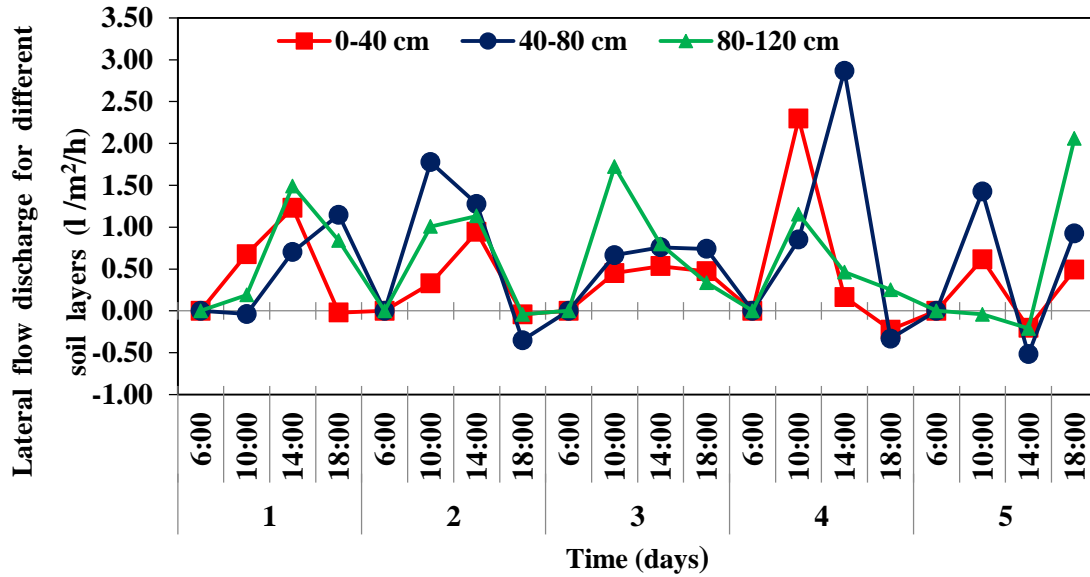


Figure 4.20 Temporal variation of lateral flow discharge for the first 5 days from three soil profile depths for experimental set up 2

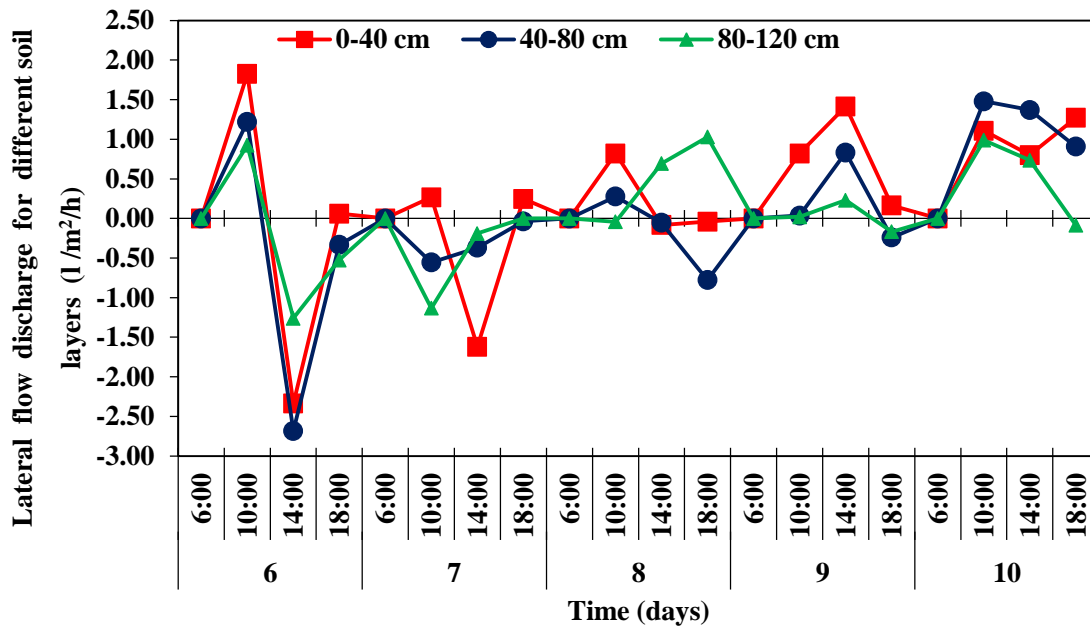


Figure 4.21 Temporal variation of lateral flow discharge for the last 5 days from three soil profile depths for experimental set up 2

Lateral flow discharge through the first layer of soil depth, 0-40 cm didn't show any appreciable increase as compared to other two soil depths. Discharge reported from 80-120 cm soil depth was the highest among the three depths under observation. Total volume of water applied in 10 days of experiment at site 2 through line source application trench was 7188 *l*.

Lateral subsurface flow through a cross-sectional area of (2 m x 0.4 m) throughout the experimental period of ten days were 83.54 *l*, 106.82 *l* and 148.68 *l* at soil depths of 0-40 cm, 40-80 cm, and 80-120 cm respectively. Thus, in ten days of experiment total lateral flow obtained from 1.6 m deep soil profile was calculated as 339.04 *l*. The percentage interflow contribution out of the total interflow generated from soil depths of 0-40 cm, 40-80 cm and 80-120 cm were determined as 24.64 %, 31.50 % and 43.85 % respectively. Out of the total water applied through the line source trench 4.71 % was recorded as interflow from monitoring trench face of length 2 m and depth of 1.6 m. The lateral flow discharge calculated was both positive and negative during the experimental period. The negative discharge implied the draining of laterally infiltrated water to deeper depths or in the adjacent soil layers which were not along the slope of experimental set up. Interflow discharge from first two soil depths followed approximately the same pattern in its variation during the day. However, the lateral flow discharge through 40-80 cm of depth was greater and faster as compared to the interflow discharge from 0-40 cm of soil layer. The average calculated lateral flow discharge rate from the three cross-sectional areas were 10.44 *l* /m² /day, 13.35 *l* /m² /day and 14.58 *l* /m² /day for soil depths of 0-40 cm, 40-80 cm and 80-120 cm respectively. Increased rate of discharge with depth represented higher vertical infiltration of water. This may be due to the application of water at a lower level than the ground surface. The phenomenon was tested and validated through further experiments.

4.6 LATERAL FLOW MEASUREMENT USING CAPACITANCE BASED MOISTURE SENSORS TEROS 12

4.6.1 Calibration of TEROS12 Soil Moisture Sensors

The comparison between the moisture measurements taken by gravimetric analysis and TEROS 12 moisture sensor showed variations. Thus, in order to obtain precise measurements, sensor calibration was performed using Calibration A method used for the TEROS 12 moisture sensor by the METER group. Figure 4.22, figure 4.23 and figure 4.24 show the calibrated curve obtained after the calibration.

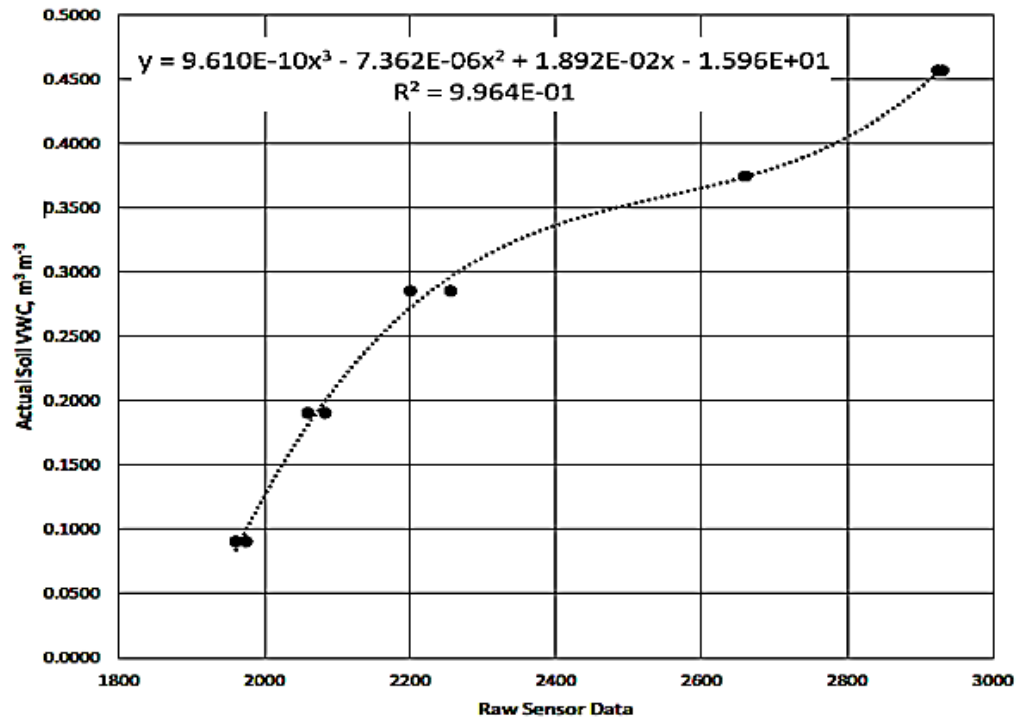


Figure 4.22 Calibration curve for sensor 1 (for soil profile at 0-40 cm)

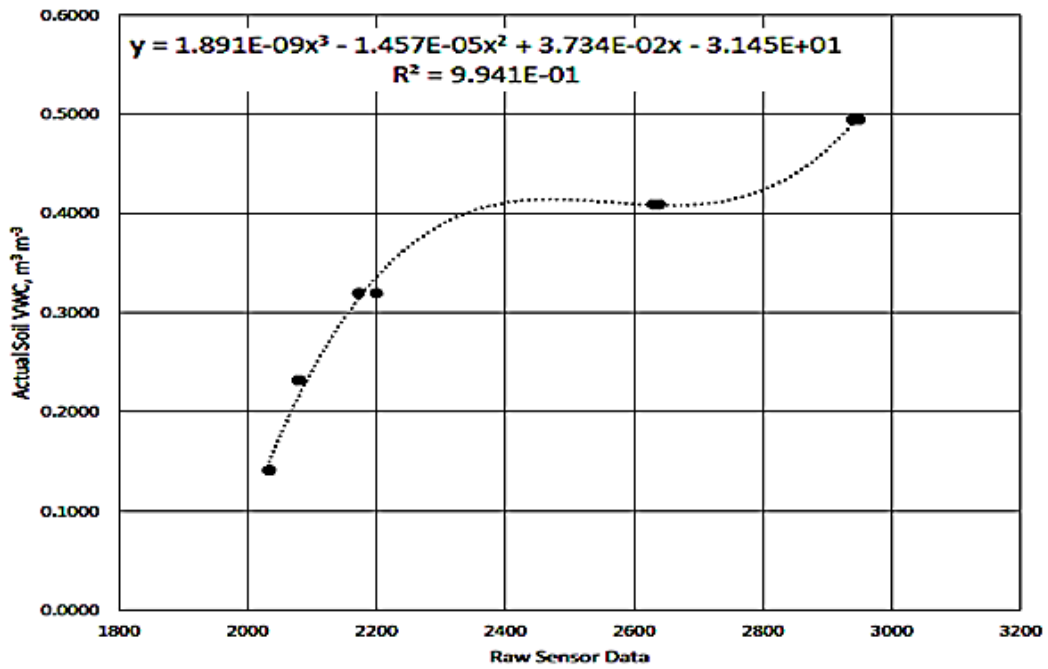


Figure 4.23 Calibration curve for sensor 2 (for soil profile at 40-80 cm)

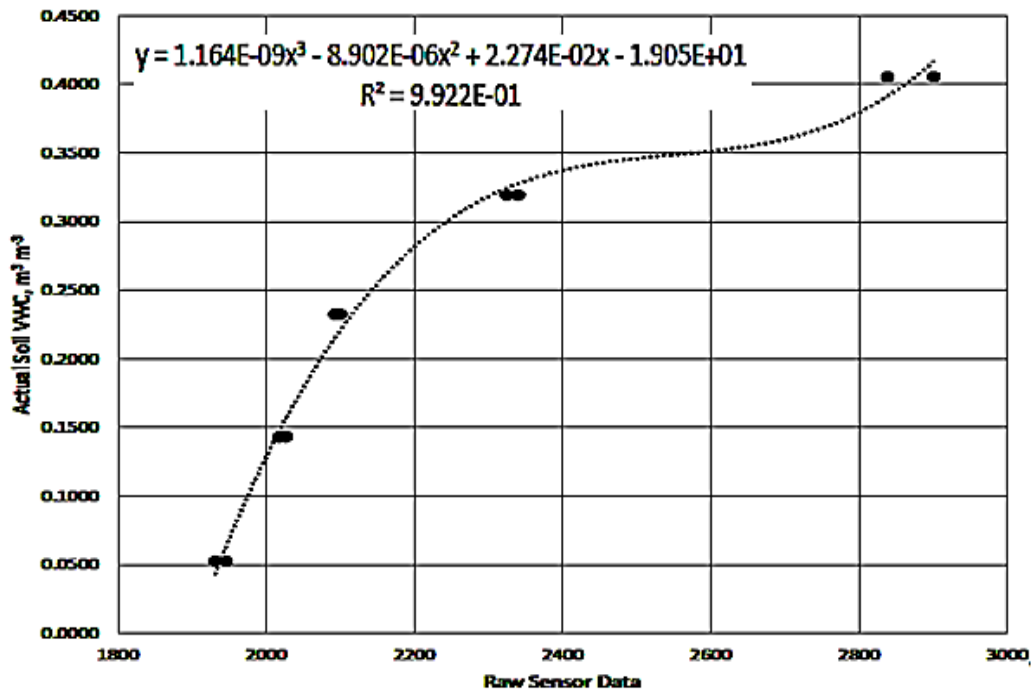


Figure 4.24 Calibration curve for sensor 3 (for soil profile at 80-120 cm)

The calibration resulted in equations with calculated coefficients for all the three soil depths of the trench separately which are shown in table 4.10.

Table 4.10 Calibration functions for sensors

Sensor	Calibration Equation	R ²
1	$y = (9.610E - 10)x^3 - (7.362E - 06)x^2 + (1.892E - 02)x - (1.596E + 01)$	99.6
2	$y = (1.891E - 09)x^3 - (1.457E - 05)x^2 + (3.734E - 02)x - (3.145E + 01)$	99.4
3	$y = (1.164E - 09)x^3 - (8.902E - 06)x^2 + (2.274E - 02)x - (1.905E + 01)$	99.2

4.6.2 Validation of Developed Calibrated Function

The percentage deviation in volumetric water content observations recorded by TEROS 12 sensors, when compared to gravimetric results for the experimental site were changed from (+5.1 %), (+7.0 %) (-3.0 %) to (+1.7 %), (+3.9 %) and (-1.8 %) for the soil profile at depths of 0-40 cm, 40-80 cm and 80-120 cm respectively after calibration. Thus, the moisture measurement by the capacitance based TEROS 12 moisture sensor was improved.

4.6.3 Lateral Flow Measurement for experimental set up 3

The experimental set up 3 was set to investigate the effect of infiltration from a trench with ponded water through a deeper soil cross-section on the lateral flow discharge rate in site 2. The sensors were installed at same points on trench face as they were during the experimental set up 2. Water was applied to a trench of 50 cm depth having a length of 2 m. It involved applying the volume of water equal to the volume of trench. The monitoring of volumetric water content variation with time for the three soil profiles was done using the calibrated capacitance based sensors,

TEROS 12. The moisture variations recorded at the three soil depths represented the time at which interflow was reaching the monitoring trench face. Exactly after four hours of water application, an increment in volumetric water content was recorded by the sensor at soil depth of 0-40 cm. Moisture increment of 0.35 % was recorded in between 16:45 pm to 17:00 pm. A major upsurge of 0.66 % in volumetric water content was observed at 17:30 pm. However, the wetting of soil at 40-80 cm depth followed a uniform or steady pattern of % VWC increase starting between 16:00 pm and 16:45 pm. The moisture sensor recorded only minor arbitrary variations at soil depth of 80-120 cm. Thus, the experiment strongly displayed the interflow occurrence in site 2 within 4 hours of line application of water. The major variation in % VWC on the monitoring trench face was observed from soil layers at depths of 0-40 cm and 40-80 cm. The temporal variation of % VWC in three soil profile depths during experimental set up 3 at site 2 has been represented by figure 4.25. A rapid increase and decrease was observed in the hourly interflow discharge, recorded from the soil layer at depth of 40-80 cm. The hourly variation of lateral flow discharge for the three soil profiles have been represented in figure 4.26.

Table 4.11 Volumetric water content analysis for experimental set up 3

Day	Depth (cm)	Time (h)	Volumetric Water Content (%)	Change in Volumetric Water Content (%)
1	0-40	13:00	37.644	-
		14:00	37.648	0.004
		15:00	37.625	-0.023
		16:00	37.609	-0.016
		17:00	37.621	0.012
		18:00	39.622	2.001
		19:00	40.154	0.532
		20:00	40.204	0.050
		21:00	40.212	0.008

	Depth (cm)	Time (h)	Volumetric Water Content (%)	Change in Volumetric Water Content (%)
	0-40	22:00	40.212	0
		23:00	40.189	-0.023
	40-80	13:00	38.137	-
		14:00	38.152	0.015
		15:00	38.125	-0.027
		16:00	38.117	-0.008
		17:00	38.164	0.047
		18:00	38.331	0.167
		19:00	38.571	0.24
		20:00	39.149	0.578
		21:00	39.839	0.69
		22:00	40.169	0.33
		23:00	40.348	0.179
	80-120	13:00	33.214	-
		14:00	33.202	-0.012
		15:00	33.168	-0.034
		16:00	33.168	0
		17:00	33.179	0.011
		18:00	33.183	0.004
		19:00	33.202	0.019
		20:00	33.179	-0.023
		21:00	33.183	0.004
		22:00	33.171	-0.012
		23:00	33.214	0.043

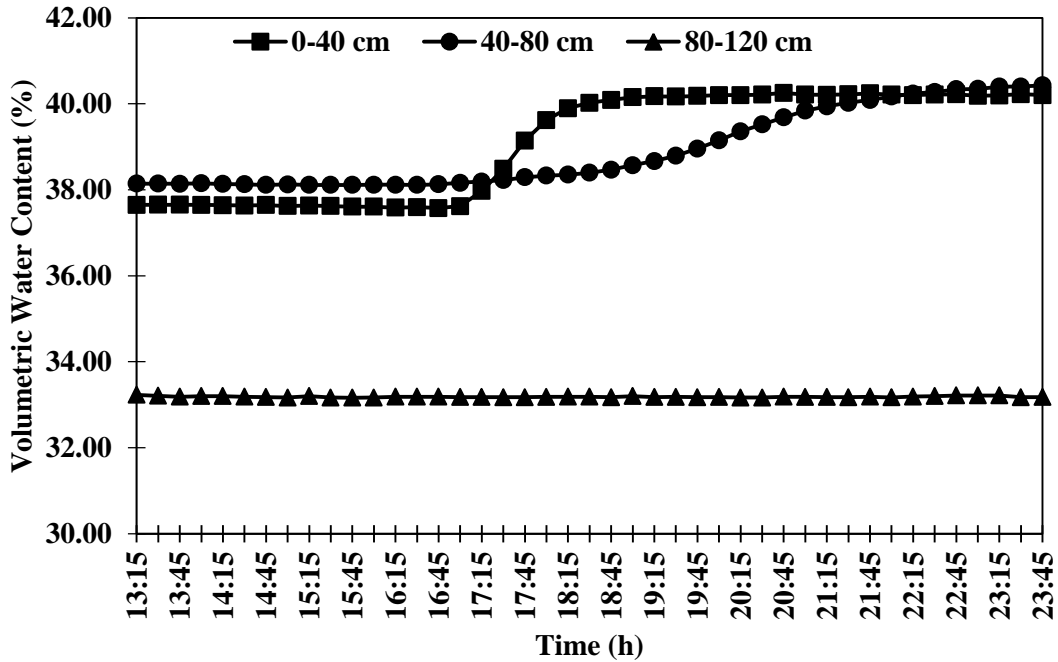


Figure 4.25 Temporal variation of %VWC in three soil profile depths during experimental set up 3 at site 2

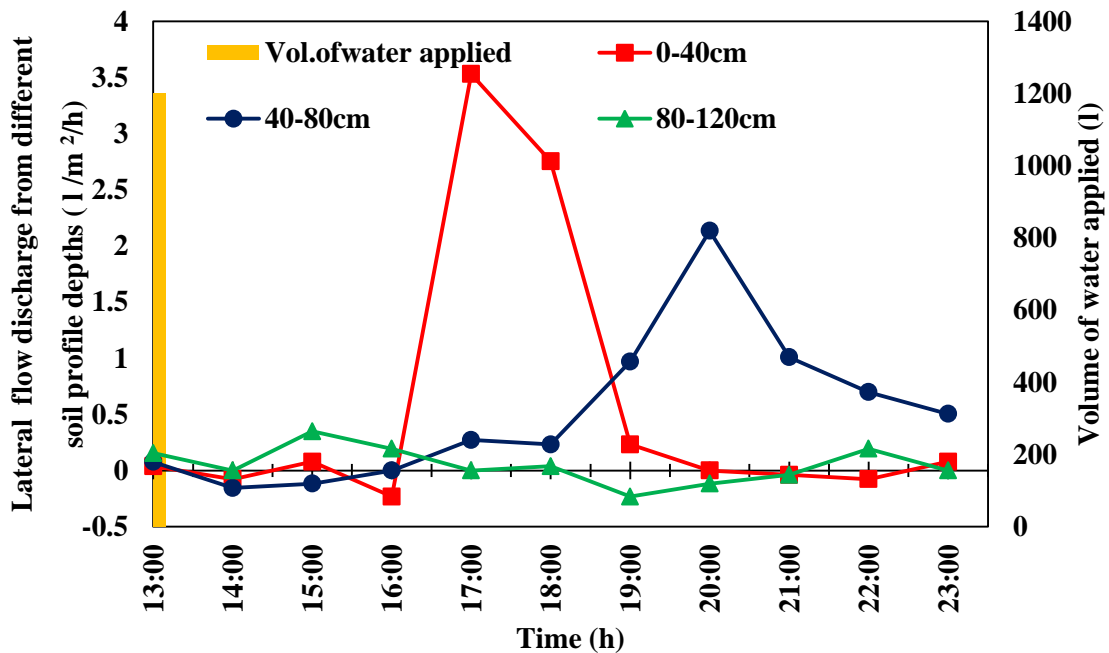


Figure 4.26 Temporal variation of lateral flow discharge from three soil profile depths during experimental set up 3 at site 2

The variation in the lateral flow discharge during experimental set up 3 is given in table 4.12. The first two soil profiles contributed greater lateral flow.

Table 4.12 Variation in lateral flow discharge through different soil profile depths during experimental set up 3

Day	Depth (cm)	Average Lateral Flow Rate ($l/m^2/h$)
1	0-40	2.36
	40-80	2.04
	80-120	0.07

The recorded variation in moisture content was obtained when the distance between line source trench and monitoring trench was reduced to 2 m and depth of line source trench was increased to 50 cm. The random variation in % GMC recorded in the prior experiment of 30 cm line source trench can also be attributed to the uneven slope of land inclusion in between line source and monitoring trench which was adjusted in the present experiment by reducing the distance between trenches. The total lateral flow discharge calculated was 22.50 *l*, 18.80 *l* and 1.64 *l* from 0-40 cm, 40-80 cm and 80-120 cm soil depths respectively. Thus, percentage contribution as interflow out of the total applied water was obtained as 1.87 %, 1.56 % and 0.13 % from 0-40 cm, 40-80 cm and 80-120 cm of soil profile depths respectively. Out of the total interflow recorded, from three soil depths at the monitoring trench face, soil depths of 0-40 cm, 40-80 cm and 80-120 cm contributed 52.39 %, 43.78 % and 3.8 % respectively. The rate of discharge calculated through the soil matrix was 28.12 $l/m^2/day$, 23.50 $l/m^2/day$ and 2.05 $l/m^2/day$ from soil depths of 0-40 cm, 40-80 cm and 80-120 cm respectively. A 12 hour experimental period has been represented as a day in the present experiment. The seepage velocity obtained was 5.7 cm/day, 4.27 cm/day and 0.41 cm/day for soil depths of 0-40 cm, 40-80 cm and 80-120 cm respectively.

4.6.4 Lateral Flow Measurement for experimental set up 4

The daily rainfall recorded from 30/07/2019 to 29/08/2019 is given in table 4.13. The experimental site received heavy rainfall during the month of August in the year 2019. With a monthly total of 597.85 mm. On 6th August 2019 the site received 107.4 mm rainfall. Daily rainfall recorded on 30/07/2019, 31/07/2019, 04/08/2019 and 05/08/2019 were 2 mm, 5.6 mm, 9.2 mm and 13.6 mm respectively. The sensor was set on 30th July 2019 and the sensor recordings were started at 13:00 h. The computed change in volumetric water content for experimental set up 4 is given in table 4.14.

Table 4.13 Rainfall data from 30/07/2019 to 29/08/2019

S.no	Date	Rainfall (mm)
1	30-Jul-19	2
2	31-Jul-19	5.6
3	4-Aug-19	9.2
4	5-Aug-19	13.6
5	6-Aug-19	107.4
6	7-Aug-19	35.6
7	8-Aug-19	19.2
8	9-Aug-19	19
9	10-Aug-19	20
10	11-Aug-19	5.4
11	12-Aug-19	41.4
12	14-Aug-19	19.6
13	15-Aug-19	1.2
14	16-Aug-19	1.4
15	17-Aug-19	1.45
16	18-Aug-19	0.2
17	20-Aug-19	2.4

S.no	Date	Rainfall (mm)
18	21-Aug-19	1.4
19	22-Aug-19	36
20	23-Aug-19	21.4
21	24-Aug-19	36.4
22	25-Aug-19	21.4
23	26-Aug-19	56.4
24	27-Aug-19	36.6
25	28-Aug-19	8.6
26	29-Aug-19	72.6

Table 4.14 Volumetric water content analysis for experimental set up 4

Date	Depth (cm)	Time (h)	Volumetric Water Content (%)	Change in Volumetric Water Content (%)
6/08/2019	0-40	0:00	37.124	0
		1:00	37.116	-0.008
		2:00	37.132	0.016
		3:00	37.136	0.004
		4:00	37.14	0.004
		5:00	37.132	-0.008
		6:00	37.12	-0.012
		7:00	37.132	0.012
		8:00	37.124	-0.008
		9:00	37.144	0.02
		10:00	37.151	0.007
		11:00	37.14	-0.011
		12:00	37.093	-0.047
		13:00	37.124	0.031
14:00	37.116	-0.008		

Date	Depth (cm)	Time (h)	Volumetric Water Content (%)	Change in Volumetric Water Content (%)
6/08/2019	0-40	15:00	37.167	0.051
		16:00	37.322	0.155
		17:00	41.054	3.732
		18:00	41.267	0.213
		19:00	41.407	0.14
		20:00	41.992	0.585
		21:00	41.849	-0.143
		22:00	41.608	-0.241
		23:00	41.511	-0.097
	40-80	0:00	31.294	-10.217
		1:00	31.29	-0.004
		2:00	31.294	0.004
		3:00	31.275	-0.019
		4:00	31.286	0.011
		5:00	31.278	-0.008
		6:00	31.278	0
		7:00	31.282	0.004
		8:00	31.294	0.012
		9:00	31.278	-0.016
		10:00	31.275	-0.003
		11:00	31.306	0.031
		12:00	31.282	-0.024
		13:00	31.278	-0.004
		14:00	31.271	-0.007
		15:00	31.236	-0.035
		16:00	31.251	0.015
		17:00	31.546	0.295

Date	Depth (cm)	Time (h)	Volumetric Water Content (%)	Change in Volumetric Water Content (%)
6/08/2019	40-80	18:00	36.767	5.221
		19:00	36.95	0.183
		20:00	38.734	1.784
		21:00	38.16	-0.574
		22:00	37.256	-0.904
		23:00	36.694	-0.562
	80-120	0:00	37.031	0.337
		1:00	37.031	0
		2:00	37.05	0.019
		3:00	37.05	0
		4:00	37.031	-0.019
		5:00	37.05	0.019
		6:00	37.074	0.024
		7:00	37.07	-0.004
		8:00	37.089	0.019
		9:00	37.062	-0.027
		10:00	37.078	0.016
		11:00	37.058	-0.02
		12:00	37.054	-0.004
		13:00	37.043	-0.011
		14:00	37.035	-0.008
		15:00	37.05	0.015
		16:00	37.043	-0.007
		17:00	37.299	0.256
		18:00	38.202	0.903
	19:00	38.722	0.52	
20:00	40.103	1.381		

Date	Depth (cm)	Time (h)	Volumetric Water Content (%)	Change in Volumetric Water Content (%)
6/08/2019	80-120	21:00	40.154	0.051
		22:00	39.979	-0.175
		23:00	39.824	-0.155

Soil at depth of 40-80 cm showed rapid variations in percentage volumetric water content with time as compared to other soil profile depths. The days with representative % VWC variation at different soil depths in conjunction with the rainy as well as the consecutive days have been shown from figure 4.27 to figure 4.42.

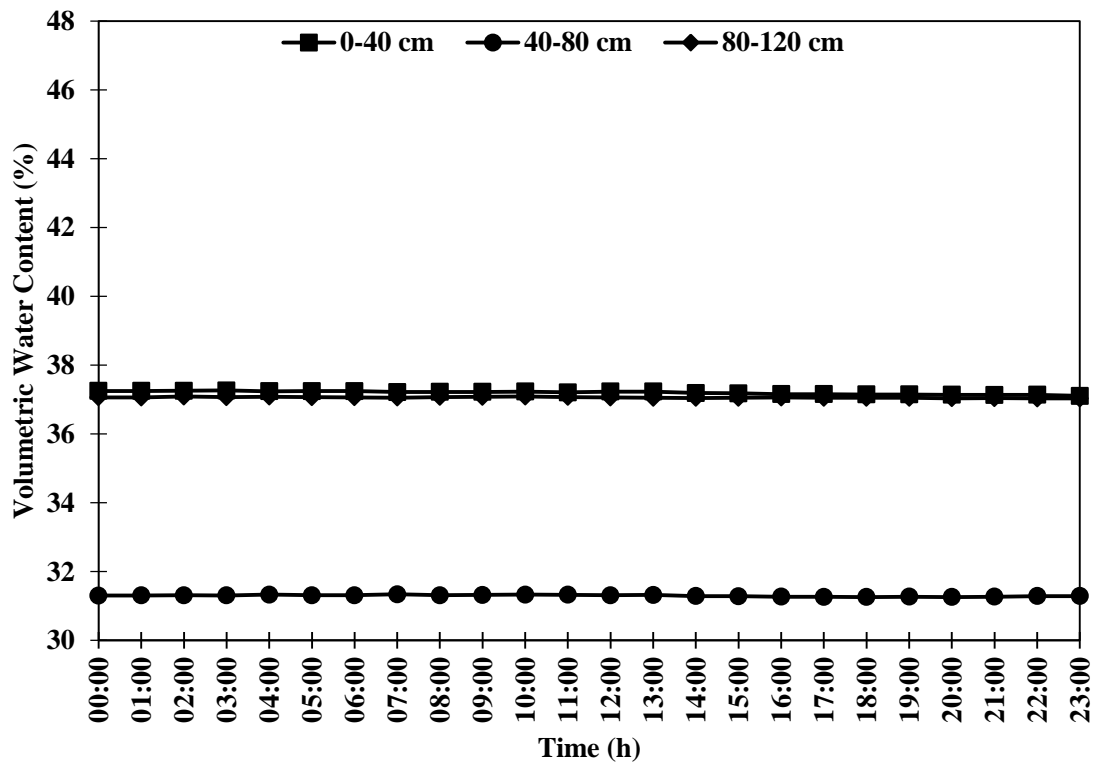


Figure 4.27 Temporal variation of %VWC in three soil profile depths during experimental set up 4 on 05/08/2019 at site 2

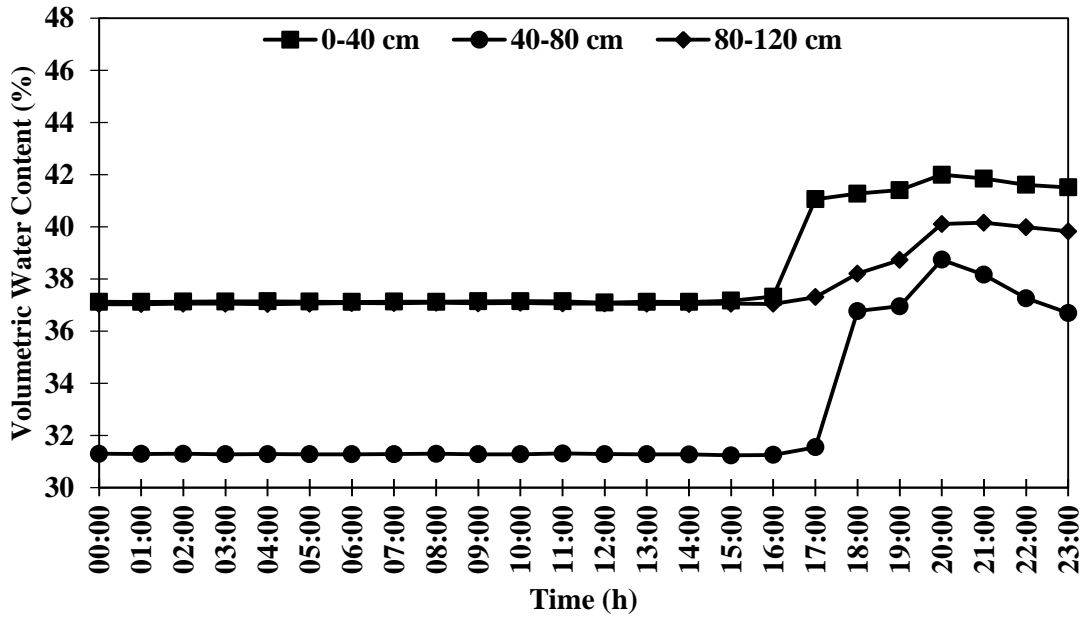


Figure 4.28 Temporal variation of %VWC in three soil profile depths during experimental set up 4 on 06/08/2019 at site 2

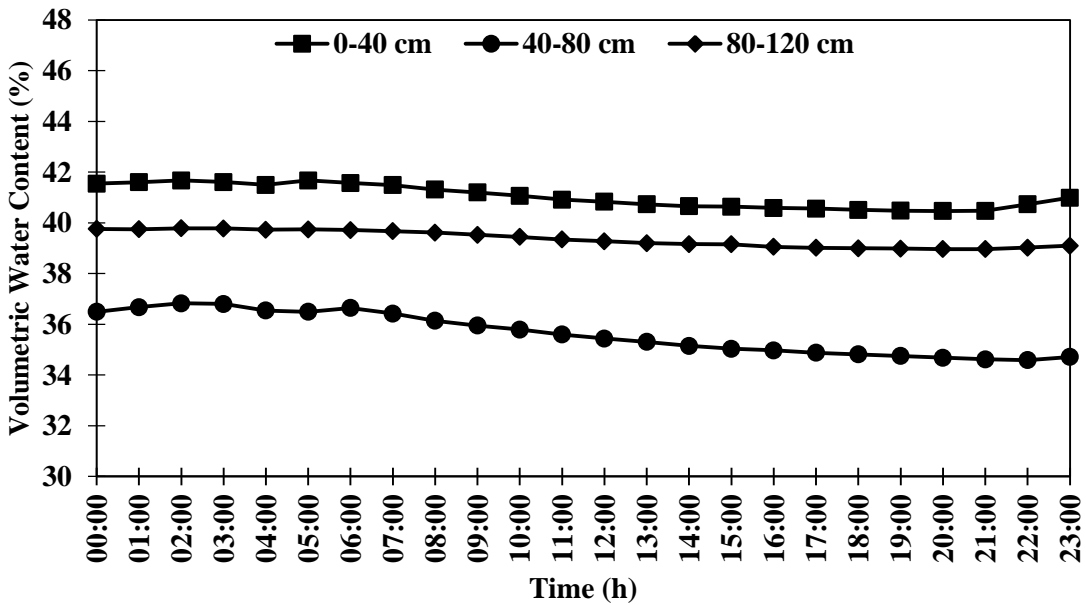


Figure 4.29 Temporal variation of %VWC in three soil profile depths during experimental set up 4 on 07/08/2019 at site 2

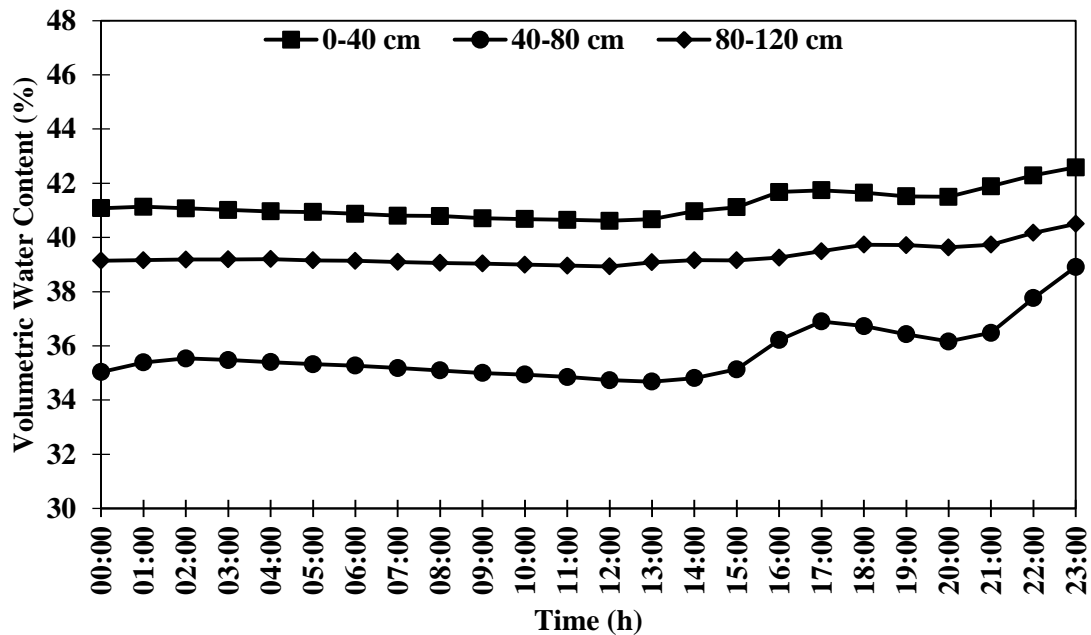


Figure 4.30 Temporal variation of %VWC in three soil profile depths during experimental set up 4 on 08/08/2019 at site 2

A downpour of 10.7 cm was recorded in the site on 6th August 2019. Lateral flow discharge recorded through a cross-sectional area of (2 m x 0.4 m) was 38.81 l and 18.56 l from soil depths of 0-40 cm, 40-80 cm and 80-120 cm respectively. A rapid increase in % VWC was observed on 6th August 2019 from 17:00 h to 21:00 h at first 40 cm layer of soil depth. The soil layers at depths of 40-80 cm and 80-120 cm recorded a raise in % VWC at 18:00 h and 19:00 h respectively. A percentage increase of 3.73 %, 5.22 % and 0.52 % in VWC was recorded from soil depths of 0-40 cm, 40-80 cm and 80-120 cm respectively at the above-mentioned time durations. The sudden raise in % VWC and draining of infiltrated water was observed at second soil depth throughout the monsoon season representing its higher porosity. A total lateral flow discharge from 40-80 cm of soil depth contributed 50.2 % of the total subsurface flow received on that day at the monitoring trench face.

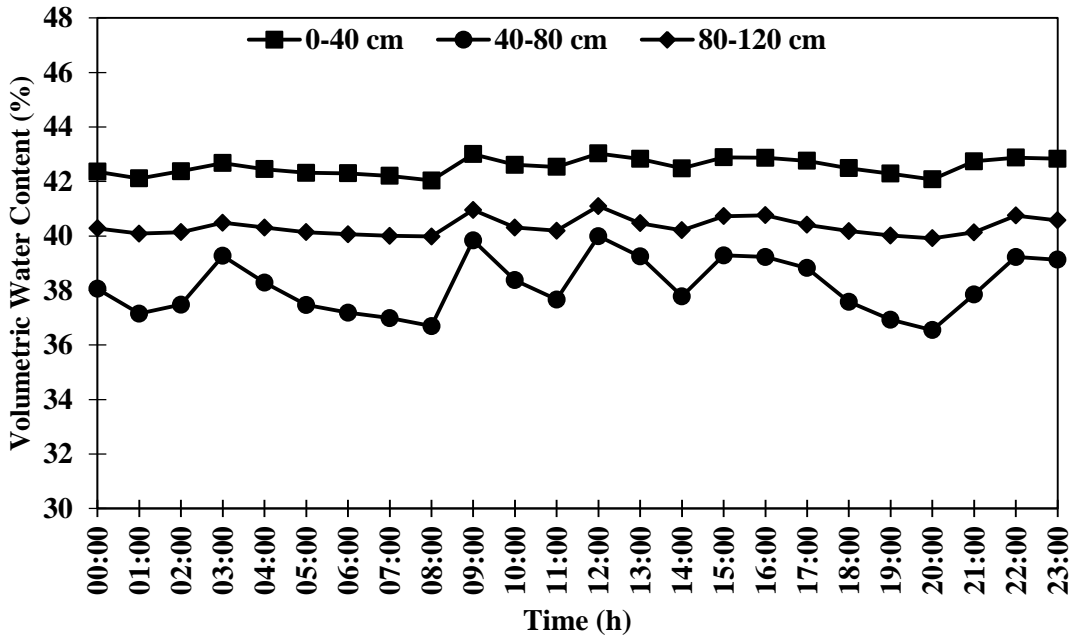


Figure 4.31 Temporal variation of %VWC in three soil profile depths during experimental set up 4 on 09/08/2019 at site 2

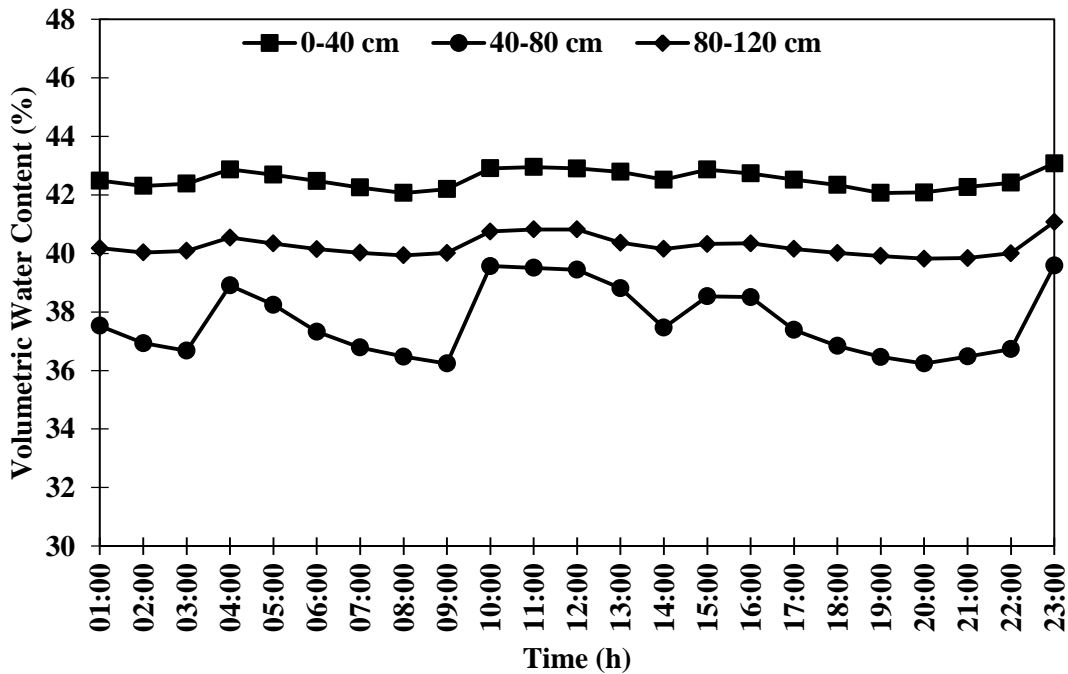


Figure 4.32 Temporal variation of %VWC in three soil profile depths during experimental set up 4 on 10/08/2019 at site 2

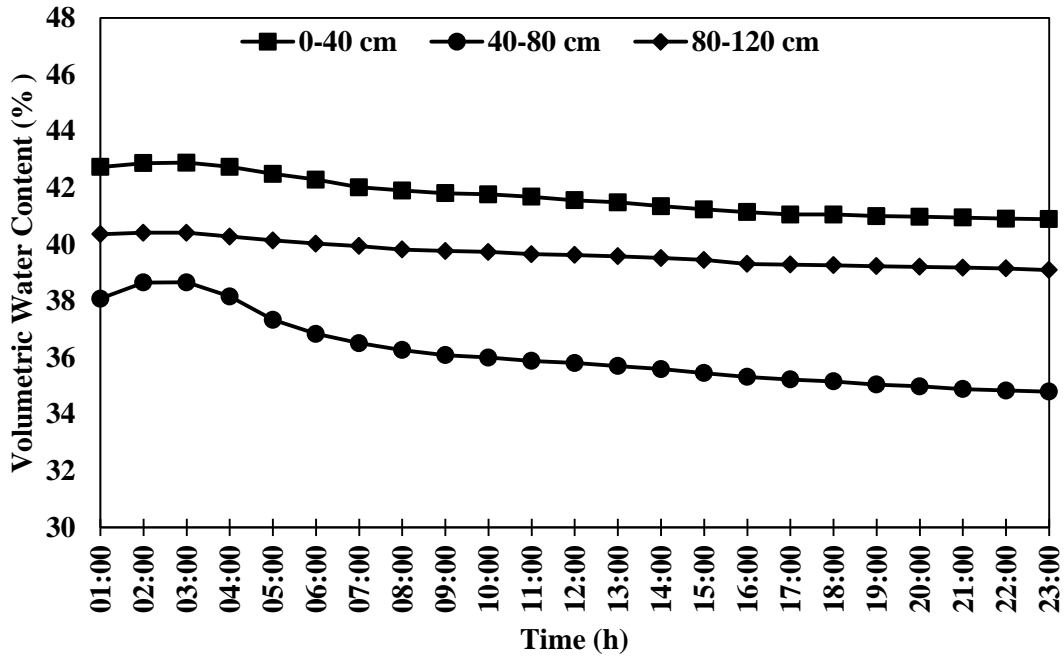


Figure 4.33 Temporal variation of % VWC in three soil profile depths during experimental set up 4 on 11/08/2019 at site 2

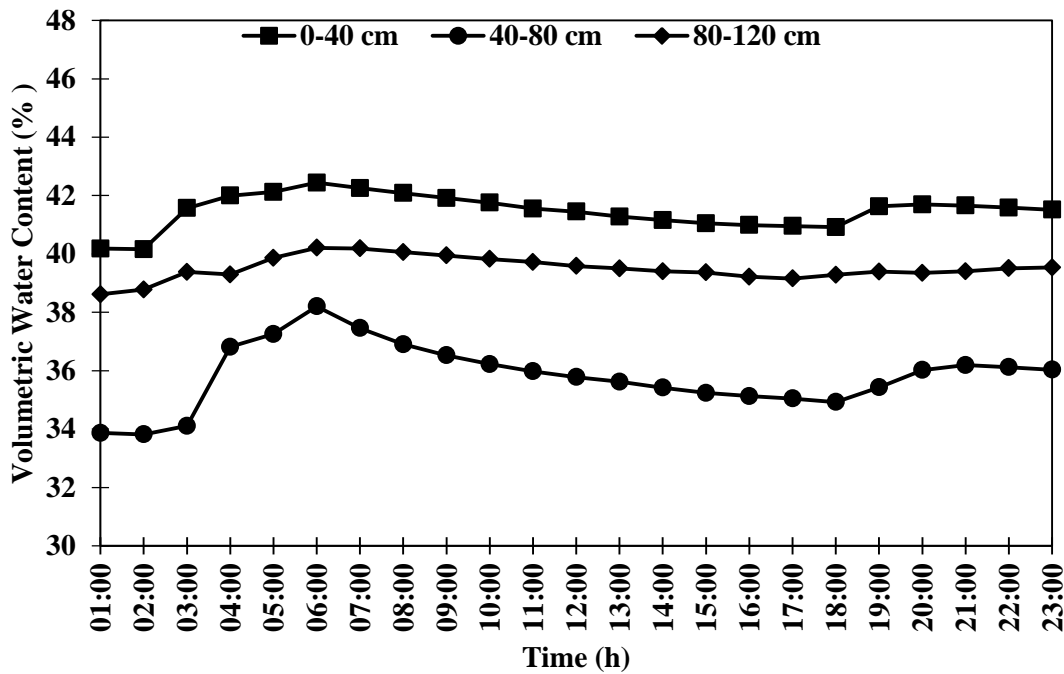


Figure 4.34 Temporal variation of % VWC in three soil profile depths during experimental set up 4 on 13/08/2019 at site 2

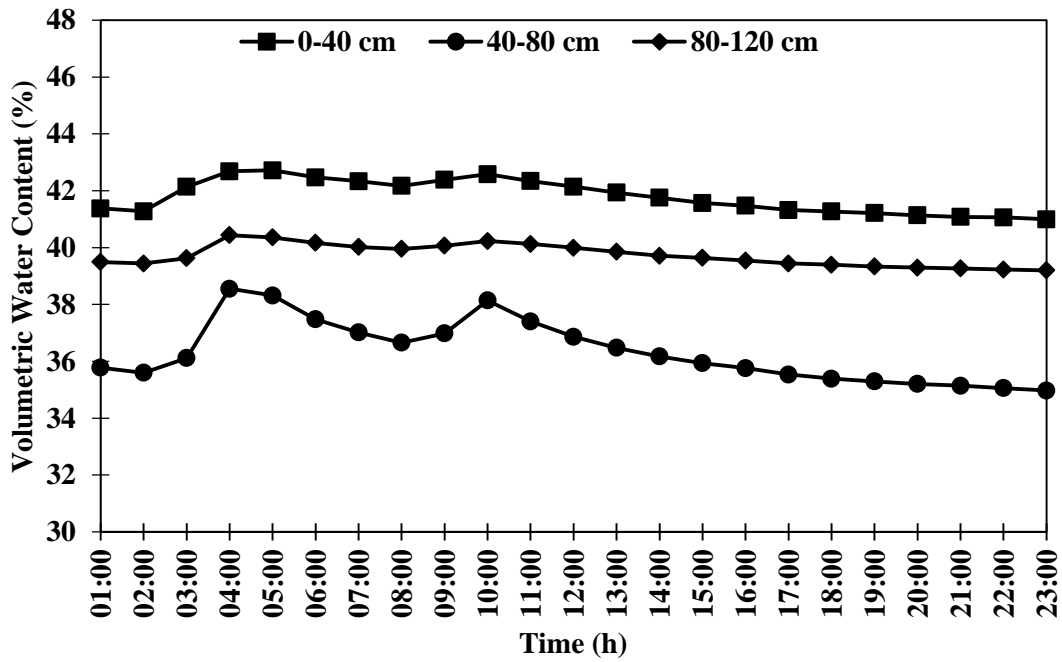


Figure 4.35 Temporal variation of % VWC in three soil profile depths during experimental set up 4 on 14/08/2019 at site 2

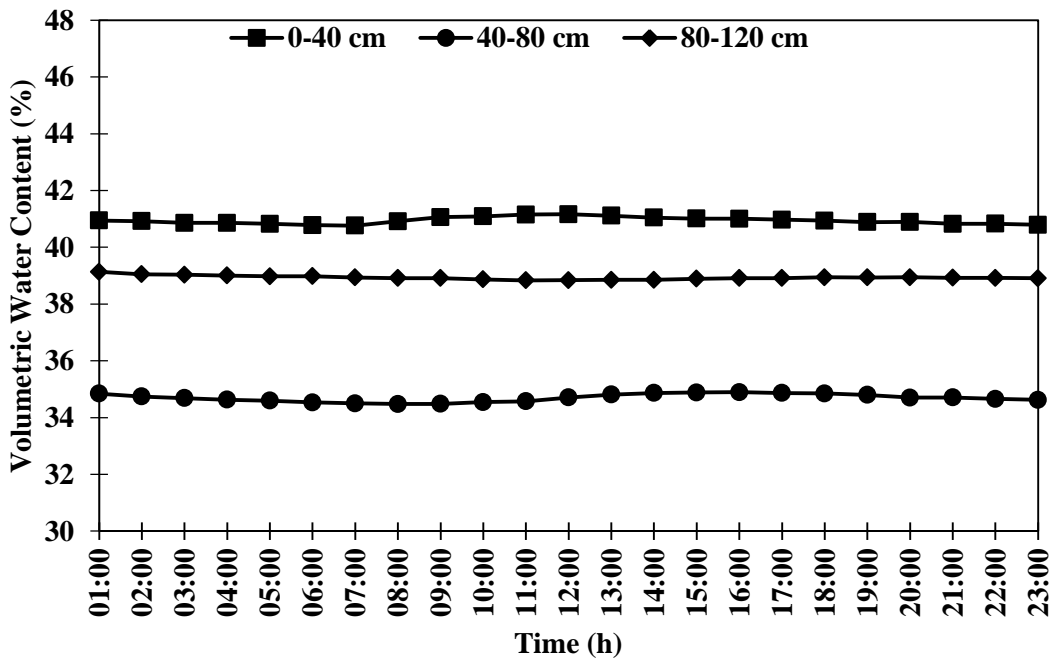


Figure 4.36 Temporal variation of % VWC in three soil profile depths during experimental set up 4 on 15/08/2019 at site 2

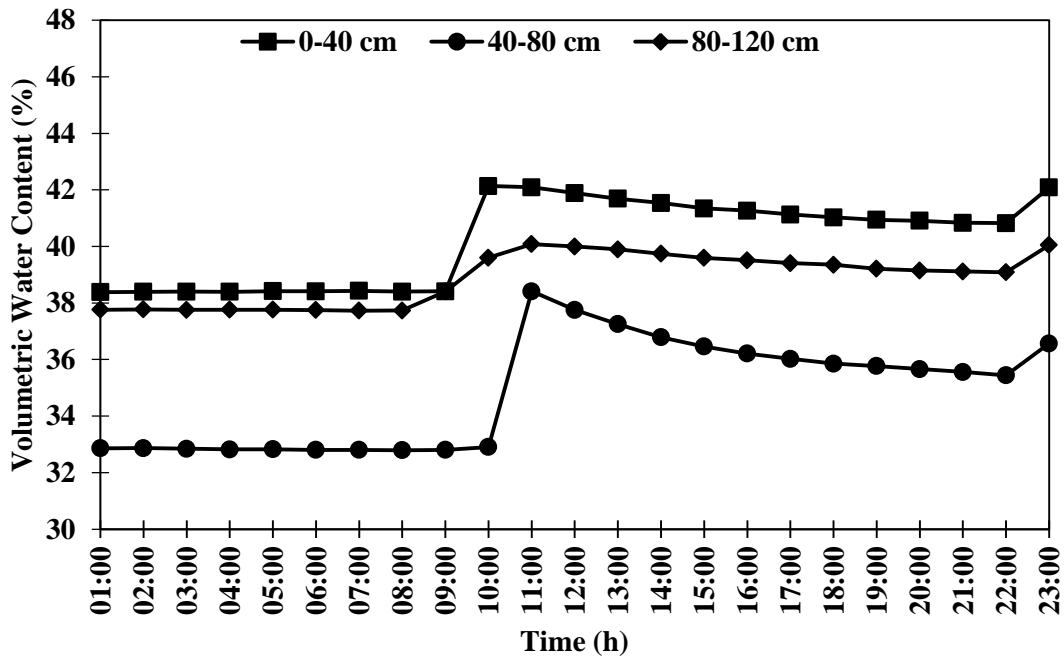


Figure 4.37 Temporal variation of % VWC in three soil profile depths during experimental set up 4 on 21/08/2019 at site 2

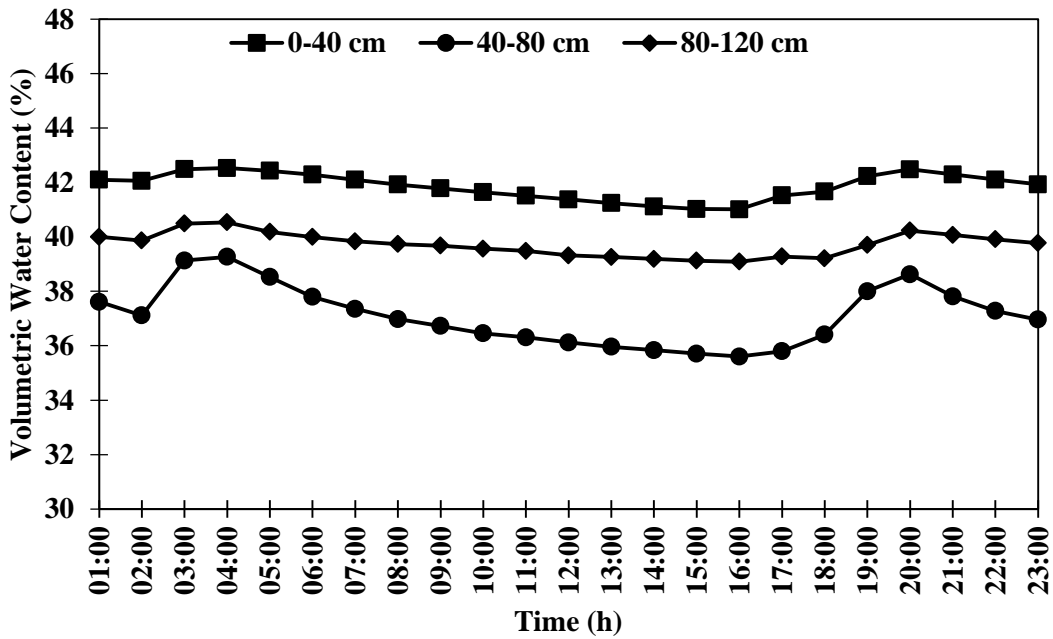


Figure 4.38 Temporal variation of % VWC in three soil profile depths during experimental set up 4 on 22/08/2019 at site 2

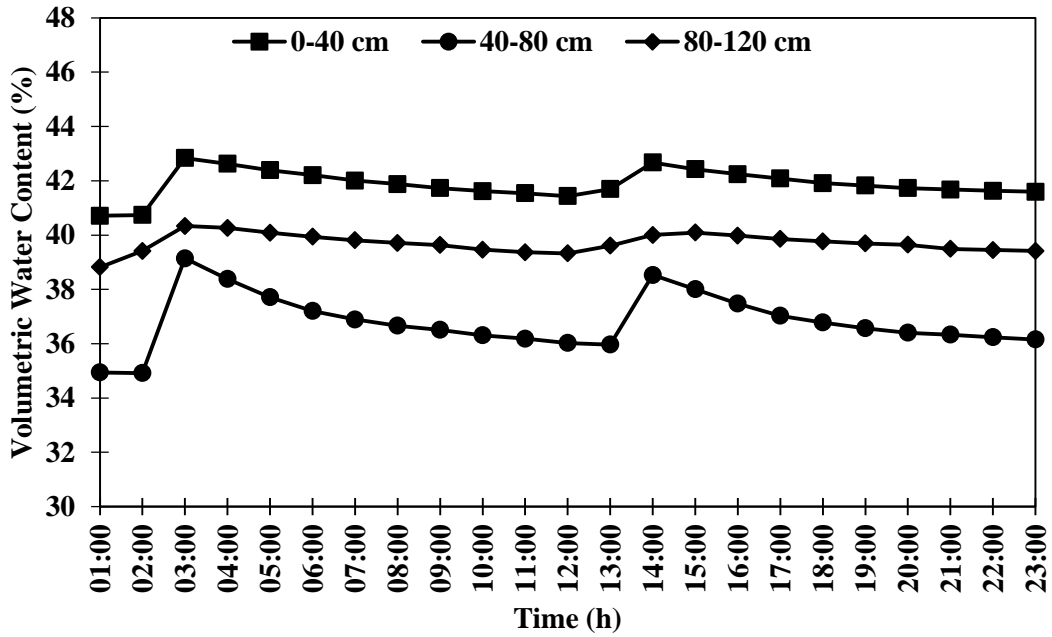


Figure 4.39 Temporal variation of % VWC in three soil profile depths during experimental set up 4 on 25/08/2019 at site 2

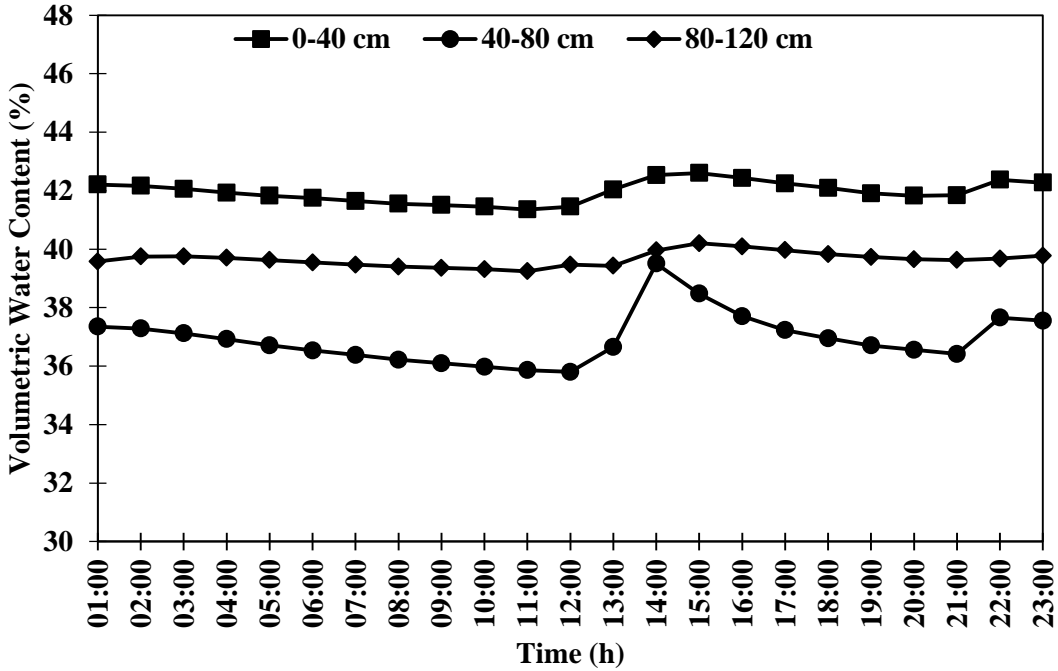


Figure 4.40 Temporal variation of % VWC in three soil profile depths during experimental set up 4 on 26/08/2019 at site 2

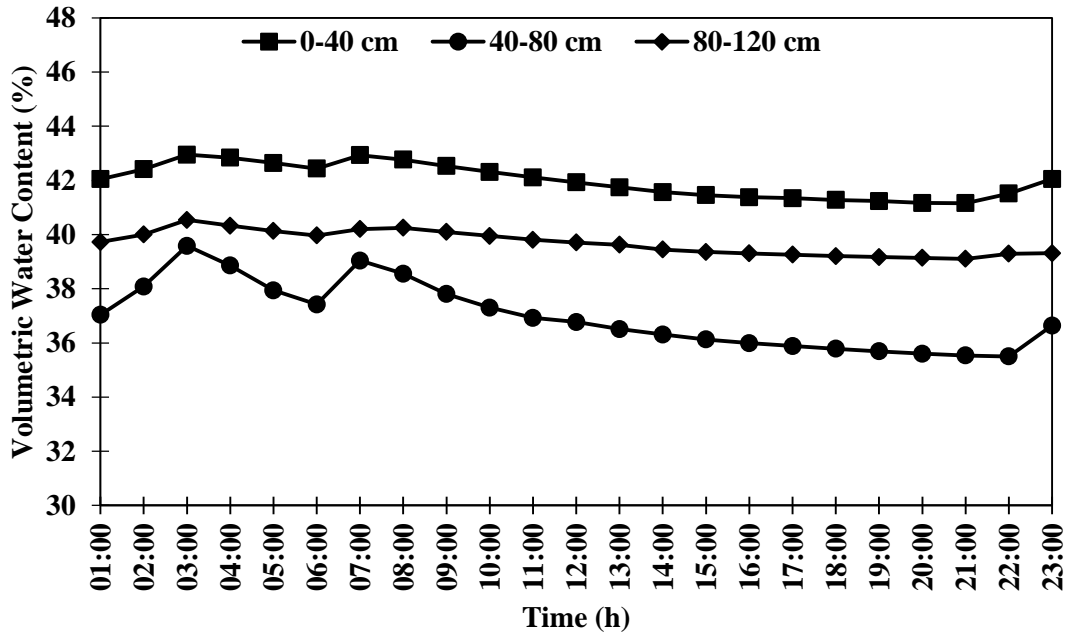


Figure 4.41 Temporal variation of % VWC in three soil profile depths during experimental set up 4 on 27/08/2019 at site 2

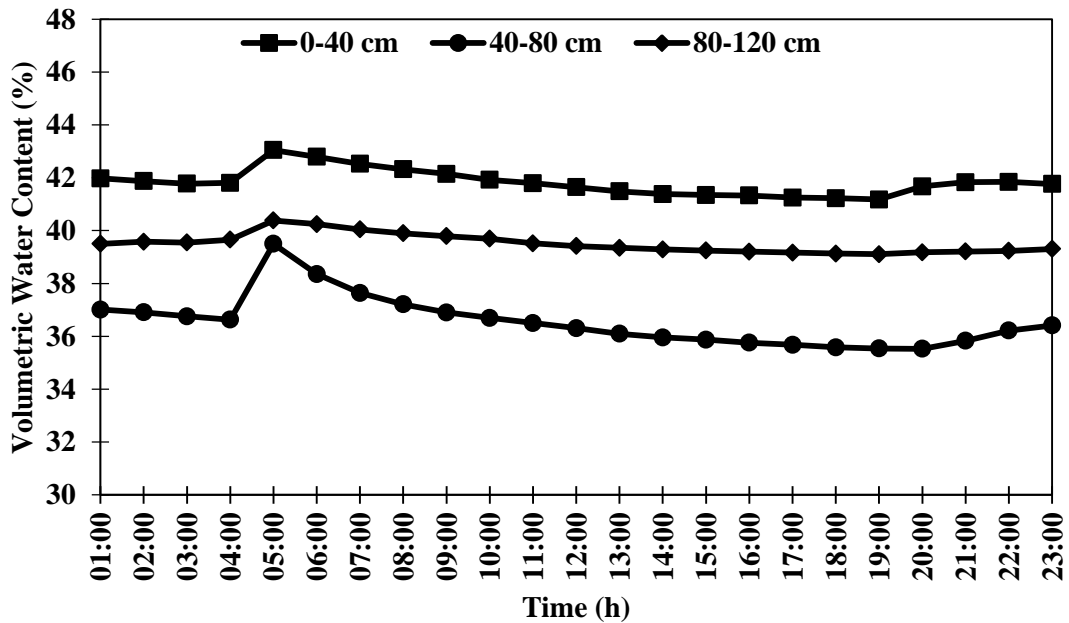


Figure 4.42 Temporal variation of % VWC in three soil profile depths during experimental set up 4 on 28/08/2019 at site 2

By analyzing the temporal variation in percentage volumetric water content at three soil depths from the monitoring trench face, it was revealed that there was no instant upsurge in the moisture content during the first few days of rainfall. It denotes absence of any major macropores in the site upto a depth of 1.6 m and thus, the chances of preferential flow to occur was minimal. Once the soil was nearly saturated, soil at depth of 40-80 cm exhibited rapid variations in its volumetric water content as compared to other two soil depths. The TEROS 12 observations of hourly variations in % VWC also signified temporal occurrence of rainfall in the site. The total rainfall depth recorded from 30/07/2019 to 29/08/2019 was 595.45mm. The total subsurface flow calculated for the similar duration was 281.6 l, 686.24 l and 235.11 l from soil depths of 0-40 cm, 40-80 cm and 80-120 cm respectively. The seepage velocity of flow calculated, assuming unit width of soil column were obtained as 2.3 cm/day, 5.0 cm/day and 1.8 cm/day from soil depths of 0-40 cm, 40-80 cm and 80-120 cm respectively. The hourly temporal variation of subsurface flow discharge during the experimental period was analysed for the three soil depths under observation and is shown from figure 4.43 to figure 4.48. Rapid and moderate variations in lateral flow discharge were observed throughout the days from 30/07/2019 to 5/08/2019. The hourly variations in the lateral flow discharge clearly represented the sudden outflow from the second soil profile depth due to the greater soil porosity. An upsurge was noticed in the total lateral flow discharge on 9th and 10th August 2019. It can be attributed to the periodical discharge of interflow at the trench face in every hour unlike discharge occurred on 6th August 2019. This may be due to the pores of upper soil getting close to saturation due to the continuous rain. The average lateral flow discharge through the different soil profile depths is given in table 4.15.

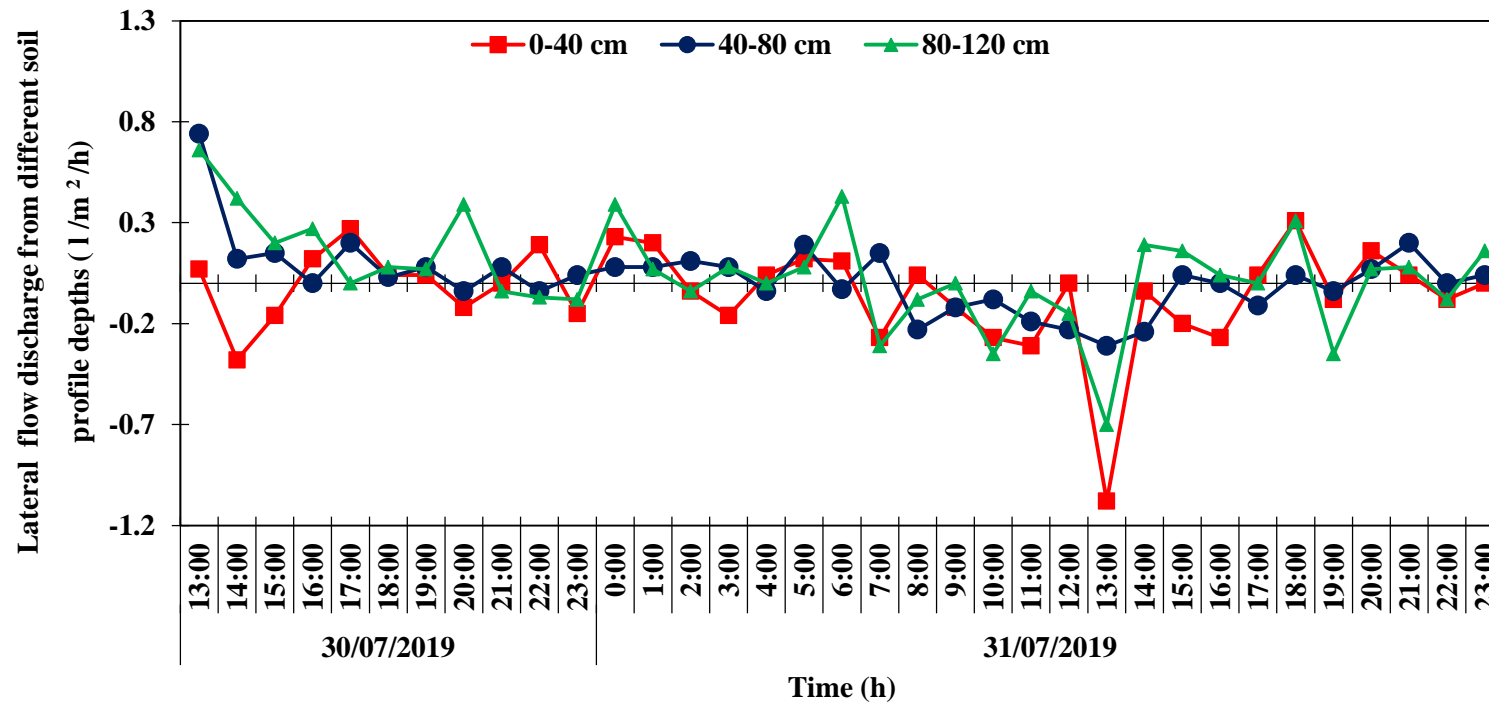


Figure 4.43 Temporal variation of lateral flow discharge from three soil profile depths during experimental set up 4 from 30/07/2019 – 31/07/2019 in site 2

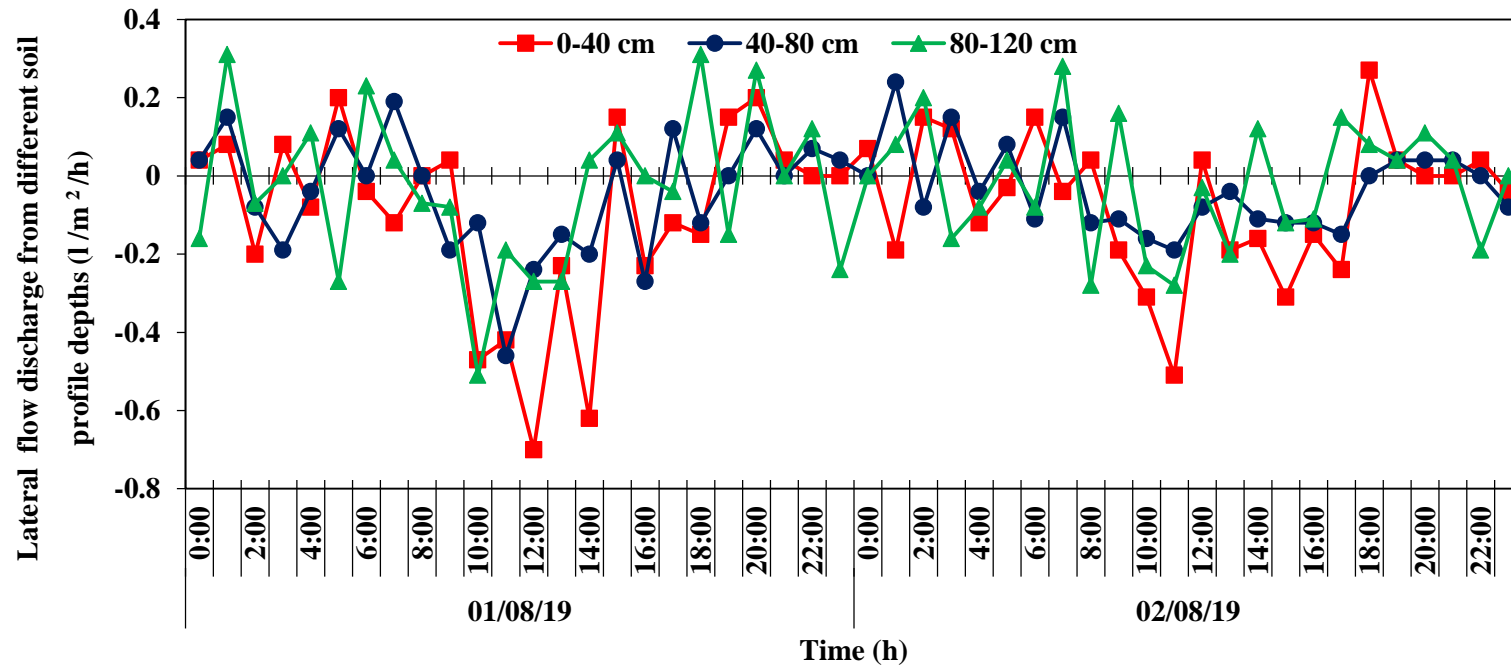


Figure 4.44 Temporal variation of lateral flow discharge from three soil profile depths during experimental set up 4 from 01/08/2019 – 02/08/2019 in site 2

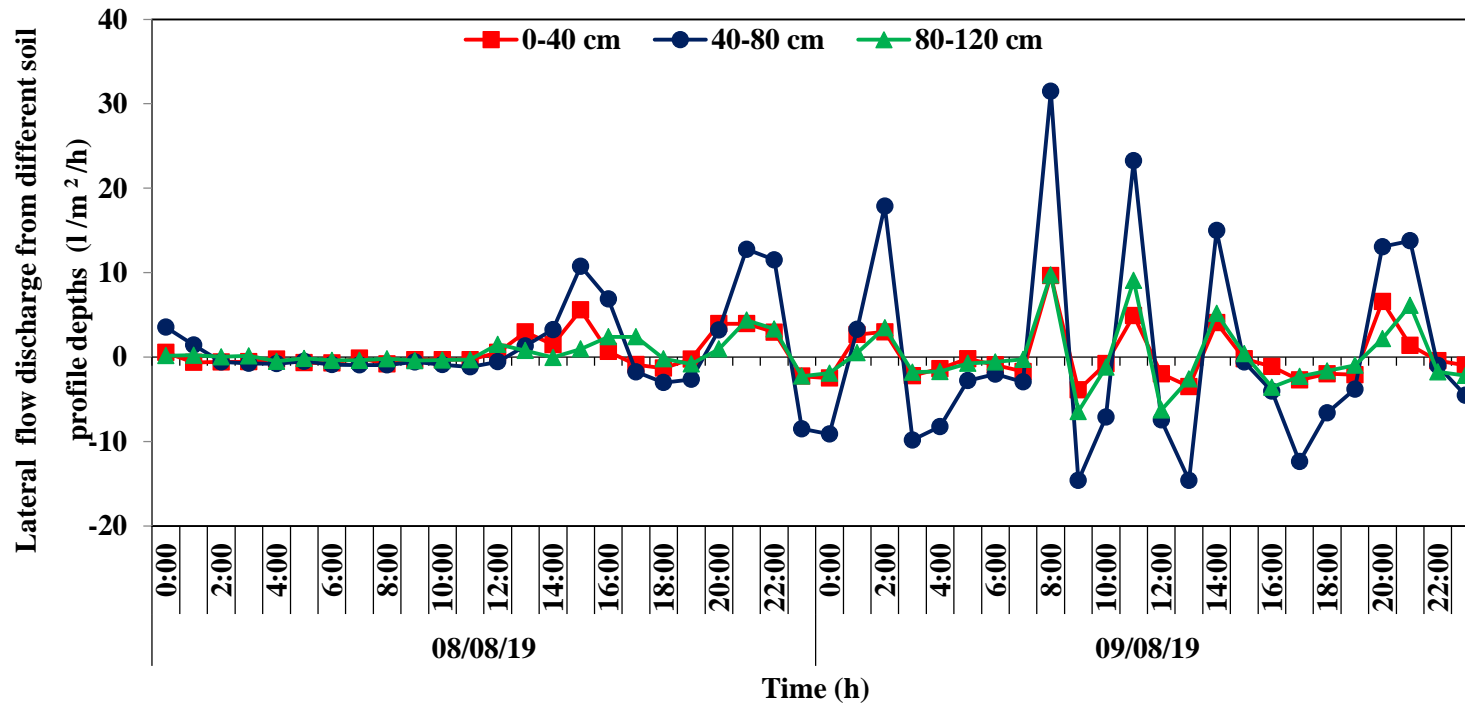


Figure 4.45 Temporal variation of lateral flow discharge from three soil depths during experimental set up 4 from 08/08/2019 to 09/08/2019 in site 2

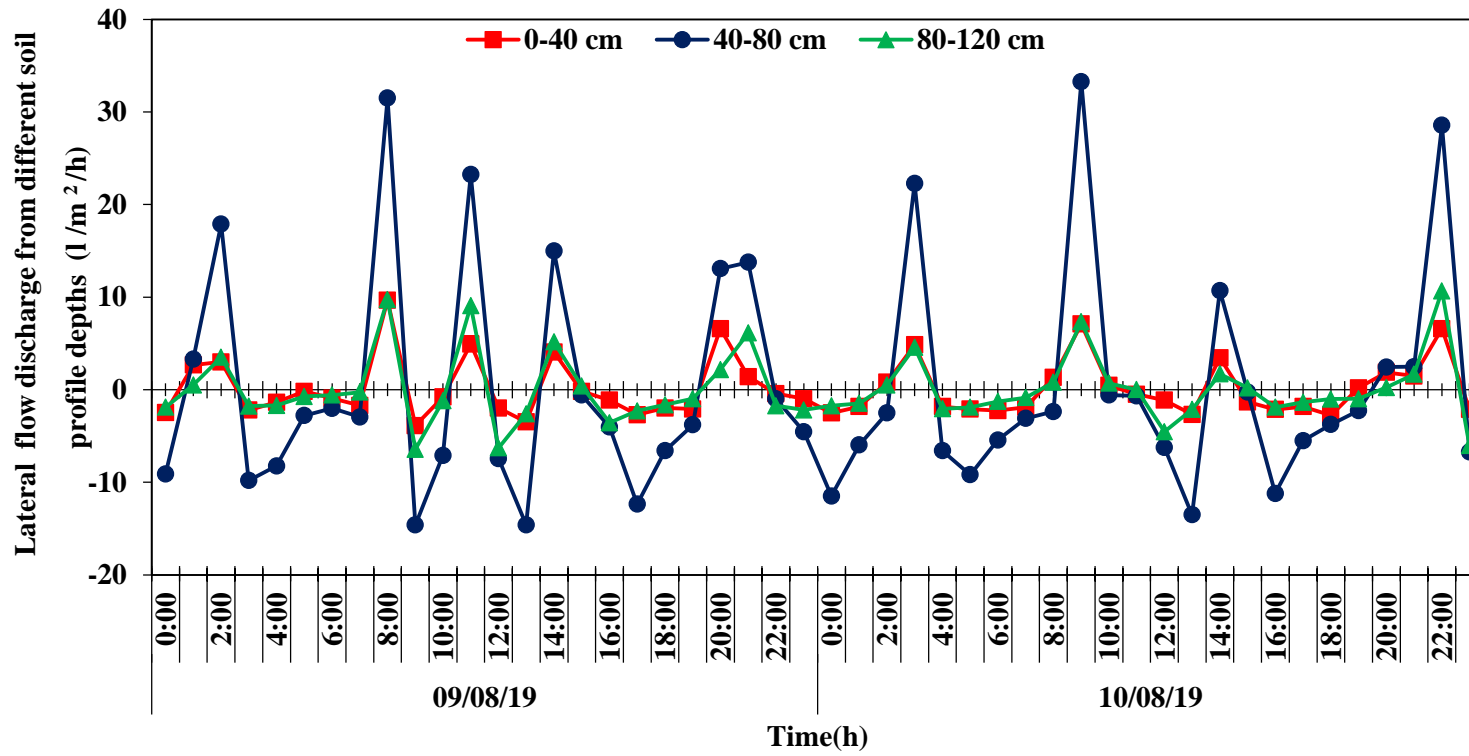


Figure 4.46 Temporal variation of lateral flow discharge from three soil depths during experimental set up 4 from 09/08/2019 to 10/08/2019 in site 2

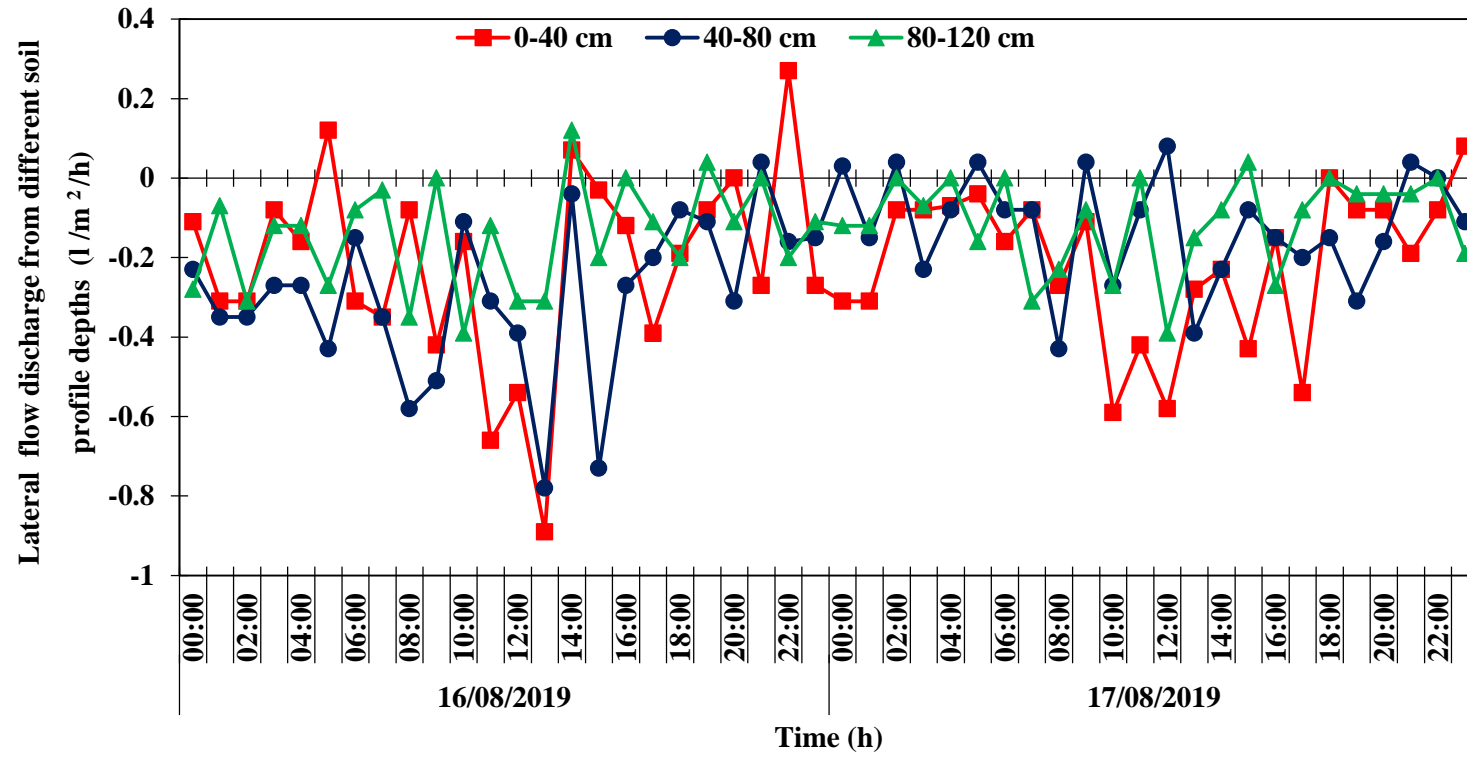


Figure 4.47 Temporal variation of lateral flow discharge from three soil depths during experimental set up 4 from 16/08/2019 to 17/08/2019 in site 2

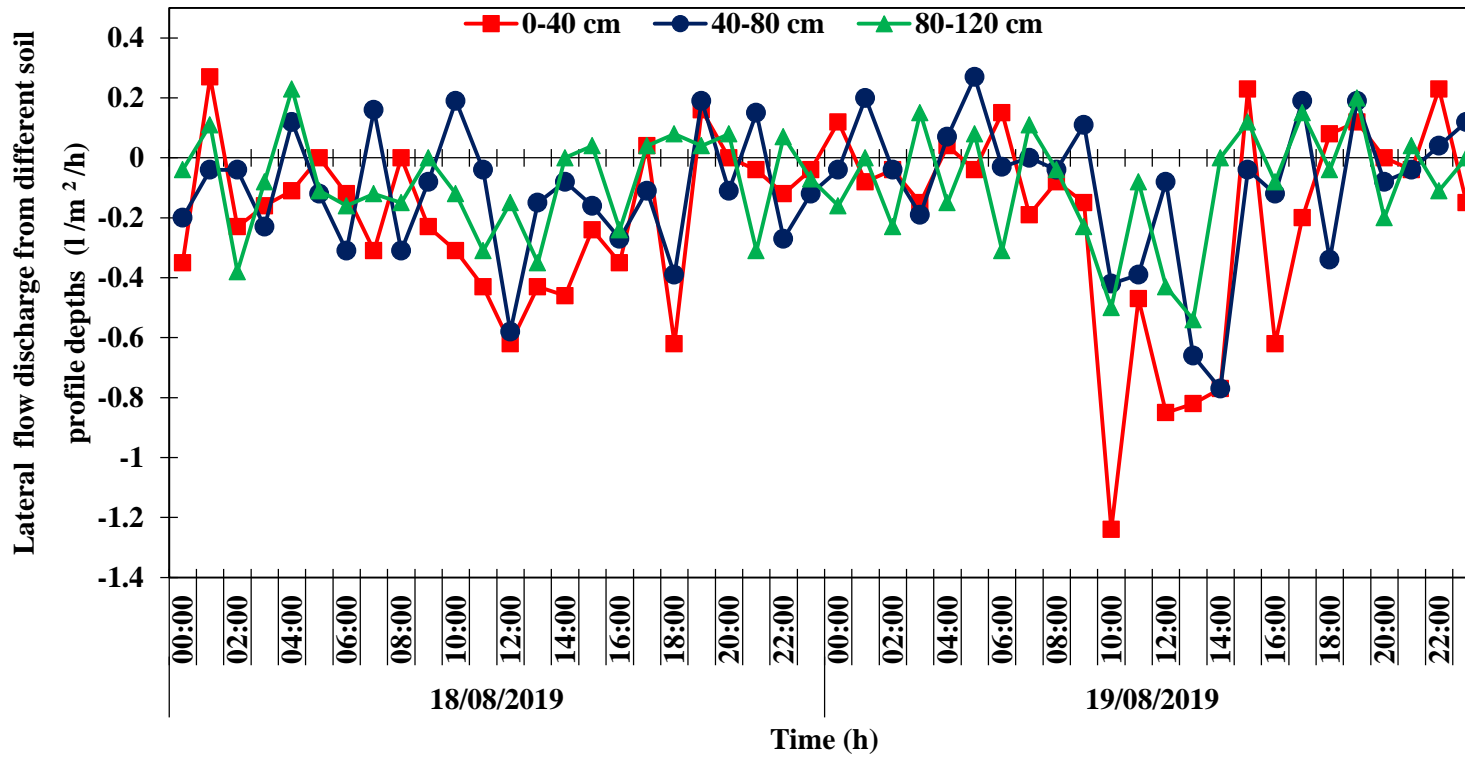


Figure 4.48 Temporal variation of lateral flow discharge from three soil depths during experimental set up 4 from 18/08/2019 to 19/08/2019 in site 2

Table 4.15 Variation in lateral flow discharge through different soil profile depths during experimental set up 4

Date	Average lateral flow discharge ($l/m^2/h$) at depths of		
	0-40 cm	40-80 cm	80-120 cm
30-07-19	0.12	0.18	0.30
31-07-19	0.13	0.10	0.17
01-08-19	0.11	0.10	0.17
02-08-19	0.10	0.11	0.12
03-08-19	0.13	0.11	0.11
04-08-19	0.15	0.11	0.10
05-08-19	0.09	0.10	0.13
06-08-19	3.58	7.56	2.93
07-08-19	1.30	1.87	0.39
08-08-19	2.52	6.08	1.45
09-08-19	4.94	16.82	4.58
10-08-19	2.81	16.62	3.13
11-08-19	0.78	2.89	0.27
12-08-19	0.12	0.10	0.06
13-08-19	4.38	8.07	2.12
14-08-19	3.72	11.10	3.19
15-08-19	0.68	0.47	0.15
16-08-19	0.15	0.04	0.08

Date	Average lateral flow discharge ($l/m^2/h$) at depths of		
	0-40 cm	40-80 cm	80-120 cm
17-08-19	0.08	0.05	0.04
18-08-19	0.16	0.16	0.09
19-08-19	0.14	0.14	0.12
20-08-19	0.12	0.15	0.12
21-08-19	6.59	9.47	3.85
22-08-19	3.23	8.63	3.74
23-08-19	2.15	6.16	1.60
24-08-19	2.48	11.99	3.34
25-08-19	7.84	23.53	4.01
26-08-19	2.66	14.66	1.55
27-08-19	4.59	10.45	1.91
28-08-19	3.88	9.39	1.47
29-08-19	0.15	0.00	0.08

The variation of lateral flow discharge conformed to the temporal variation of volumetric water content in Site 2 under natural rainfall conditions which can be seen in table 4.16. The experiments carried out with three different experimental set ups in site 2 elucidated the effect of varied soil profiles and their properties on soil water movement in a laterite terrain. The experiments exhibited the pattern of intermolecular movement of water and its variation in the soil strata under simulated rainfall and natural rainfall conditions.

Table 4.16 Variation of Lateral Flow Discharge with Temporal Variation of Volumetric Water content in Site 2 under Natural Rainfall Conditions (SW-Monsoon)

Date	Time	Depths of Soil layers					
		0-40 cm		40-80 cm		80-120 cm	
		VWC (%)	Discharge (l/m ² /h)	VWC (%)	Discharge (l/m ² /h)	VWC (%)	Discharge (l/m ² /h)
6/8/2019	15:00	37.16	0.51	31.236	0	37.05	0.15
	17:00	41.054	37.32	31.546	0	37.299	2.56
	18:00	41.267	2.13	36.767	52.21	38.202	9.03
	19:00	41.407	1.4	36.95	1.83	38.722	5.2
	20:00	41.992	5.85	38.734	17.84	40.103	13.81
8/8/2019	14:00	40.968	2.98	34.812	1.32	39.161	0.78
	15:00	41.116	1.48	35.138	3.26	39.157	0
	16:00	41.674	5.58	36.213	10.75	39.254	0.97
	17:00	41.74	0.66	36.903	6.9	39.494	2.4
	20:00	41.496	0	36.162	0	39.634	0
	21:00	41.891	3.95	36.484	3.22	39.731	0.97
	22:00	42.287	3.96	37.76	12.76	40.169	4.38
	23:00	42.582	2.95	38.912	11.52	40.503	3.34

Date	Time	Depths of Soil layers					
		0-40 cm		40-80 cm		80-120 cm	
		VWC (%)	Discharge (l/m ² /h)	VWC (%)	Discharge (l/m ² /h)	VWC (%)	Discharge (l/m ² /h)
10/8/2019	3:00	42.384	0.81	36.678	0	40.084	0.51
	4:00	42.869	4.85	38.905	22.27	40.542	4.58
	9:00	42.194	1.32	36.236	0	40.014	0.81
	10:00	42.904	7.1	39.564	33.28	40.747	7.33
	11:00	42.95	0.46	39.506	0	40.817	0.7
	15:00	42.865	3.45	38.536	10.71	40.32	1.7
	21:00	42.268	1.87	36.48	2.44	39.839	0.23
	22:00	42.415	1.47	36.728	2.48	40.006	1.67
	23:00	43.075	6.6	39.583	28.55	41.073	10.67
13/09/2019	2:00	40.161	0	33.819	0	38.777	1.63
	3:00	41.569	14.08	34.11	2.91	39.382	6.05
	4:00	41.996	4.27	36.814	27.04	39.292	0
	5:00	42.12	1.24	37.252	4.38	39.863	5.71
	6:00	42.438	3.18	38.202	9.5	40.212	3.49
	19:00	41.628	0	34.429	5.04	39.393	1.08
	20:00	41.697	0.69	36.023	5.94	39.347	0

Date	Time	Depths of Soil layers					
		0-40 cm		40-80 cm		80-120 cm	
		VWC (%)	Discharge (l/m ² /h)	VWC (%)	Discharge (l/m ² /h)	VWC (%)	Discharge (l/m ² /h)
14/08/2019	3:00	42.136	0	36.116	5.2	39.626	1.86
	4:00	42.683	5.47	38.552	24.36	40.437	8.11
	5:00	42.718	0.35	38.319	0	40.359	0
	8:00	42.171	0	36.659	0	39.952	0
	9:00	42.384	2.13	36.981	3.22	40.068	1.16
	10:00	42.586	2.02	38.144	11.63	40.231	1.63
21/08/2019	8:00	38.40	0	32.795	0	37.733	0.04
	9:00	38.412	0.12	32.807	0.12	38.408	6.75
	10:00	42.136	37.24	32.908	1.01	39.603	11.95
	11:00	42.089	0	38.412	55.04	40.084	4.81
	22:00	40.825	0	35.441	0	39.083	0
	23:00	42.085	12.6	36.569	11.28	40.049	9.66

The graph of daily lateral flow discharge versus daily rainfall for the experimental set up under natural rainfall condition in site 2 as represented by figure 4.49 showed similar variations throughout the experimental duration in the site.

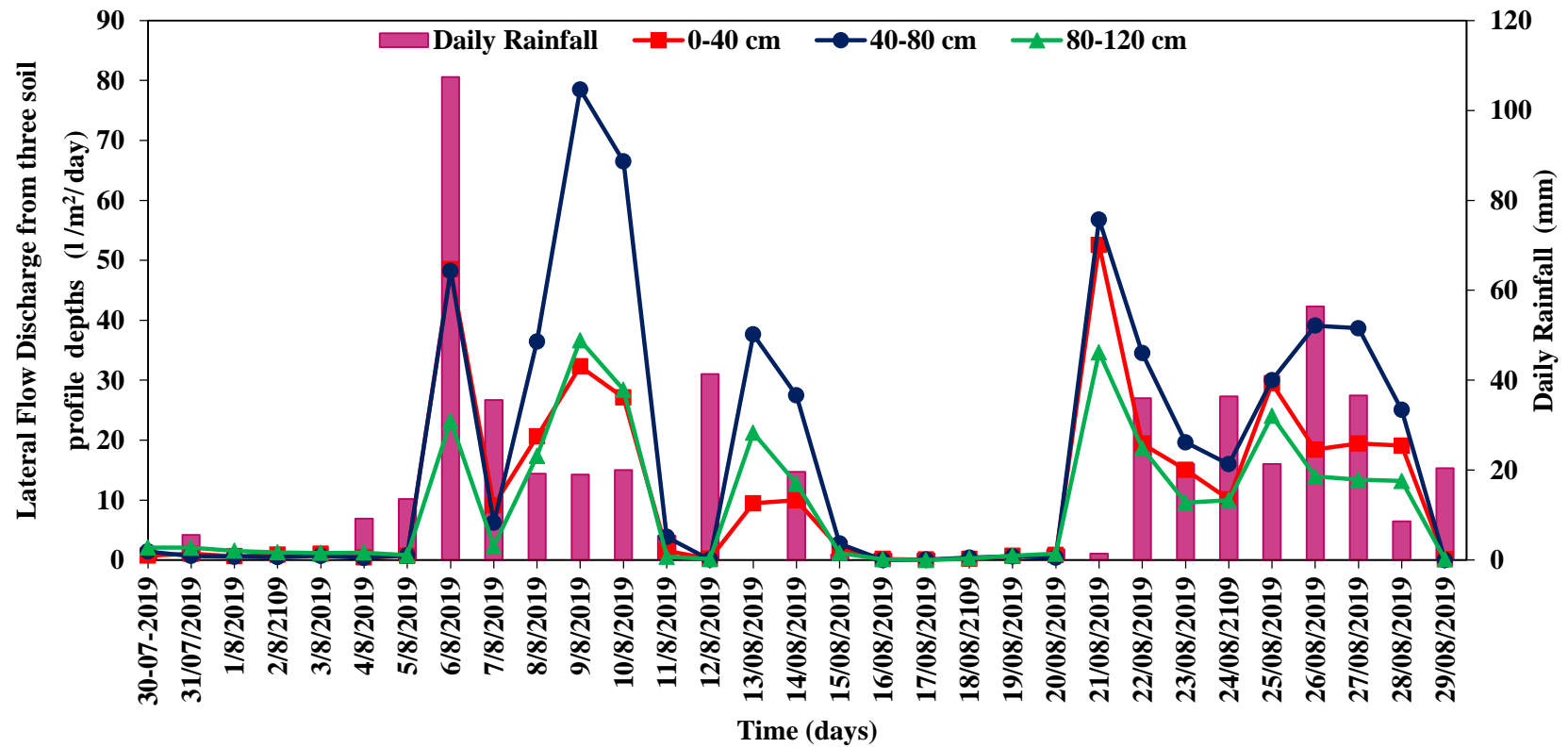


Figure 4.49 Daily lateral flow discharge from the three soil profile layers versus daily rainfall for the experimental set up 4 in site 2

4.6.5 Lateral flow measurement for experimental set up 5

The experimental set up was installed to analyse interflow during natural rainfall in site 3. The vegetation was sparse in the site unlike in site 1 and site 2. The total rainfall received by the site during experimental period was less as compared to that, received during the prominent south west monsoon period as shown in table 4.17. The experiment was carried out to monitor the % VWC variations recorded by TEROS 12 from a site having different soil physical properties compared to site 1 and site 2. The temporal variations in percentage volumetric water content were recorded in site 3 for soil profile depths of 0-40 cm, 40-80 cm and 80-120 cm. The site had shown delayed response to the rainfall. The days which recorded significant variations in volumetric water content during the experimental period have been shown from figure 4.50 to figure 4.56.

Table 4.17 Rainfall records during September

S.No	Date	Rainfall (mm)
1	01/09/2019	15.6
2	02/09/2019	15.8
3	7/9/2019	16.8
4	08/09/2019	18
5	09/09/2019	15.2
6	10/09/2019	19.6
7	11/09/2019	13
8	12/09/2019	20.4
9	19/09/2019	14
10	22/09/2019	8

An increase in volumetric water content of the subsurface soil on monitoring trench face was recorded on 4/09/2019 at soil depth of 0-40 cm and 40-80 cm. An increase of 0.8 % was observed at first 40 cm depth in between 2:00 am to 3:00 am. A total % VWC increase of 0.76 % was recorded at soil depth of 40-80 cm in between 2:00 am to 6:00 am on 4/09/2019. However, at soil depth of 80-120 cm the % VWC recorded from 4:00 am to 23:00 pm was just 0.03 %. It may be attributed to the good water holding capacity of clay particles at soil depth of 80-120 cm. Two successive non-rainy days witnessed depletion in % VWC at first two depths. Conversely, the third depth retained its moisture increase with abruptly small variations in % VWC. During entire experiment, the expected subsurface flow was not obtained proportional to the north-east monsoon received. It may be due to the surface runoff generated as a result of least vegetation in the site. The hourly variation of lateral flow discharge from three soil profile depths during experimental set up 5 showed majority of dips in the discharge. The discharge for representative days has been shown by figure 4.57 and figure 4.58.

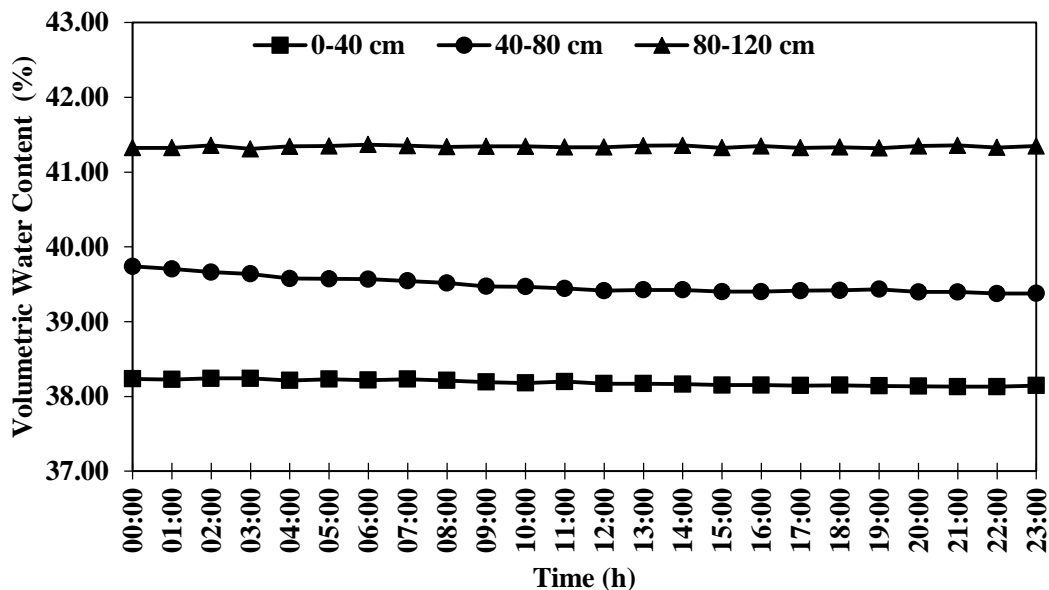


Figure 4.50 Temporal variation of % VWC in three soil profile depths during experimental set up 5 on 03/09/2019 at site 3

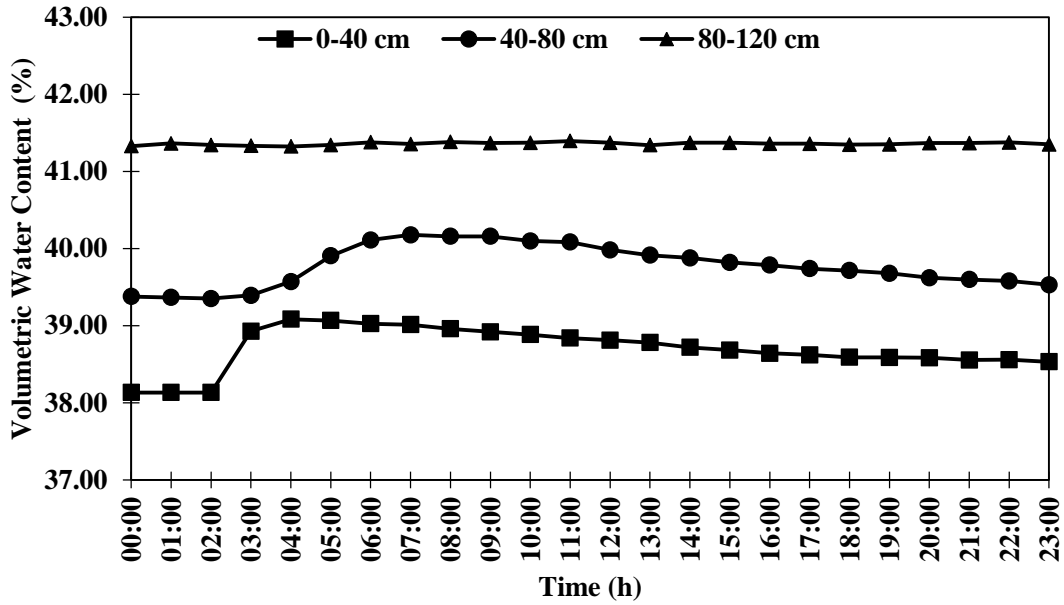


Figure 4.51 Temporal variation of % VWC in three soil profile depths during experimental set up 5 on 04/09/2019 at site 3

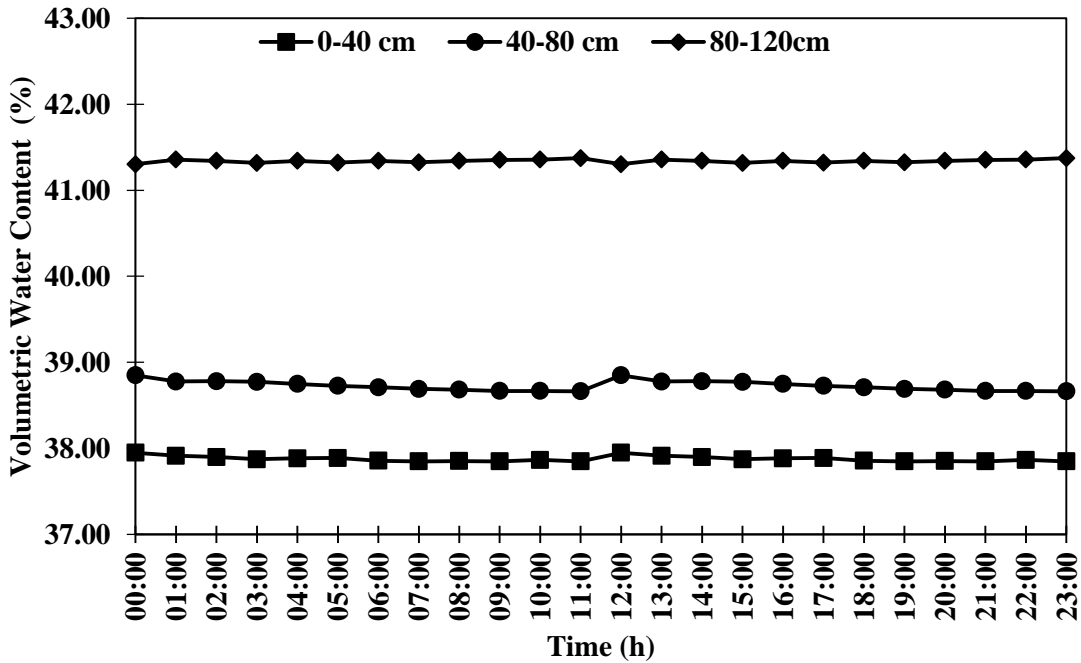


Figure 4.52 Temporal variation of % VWC in three soil profile depths during experimental set up 5 on 07/09/2019 at site 3

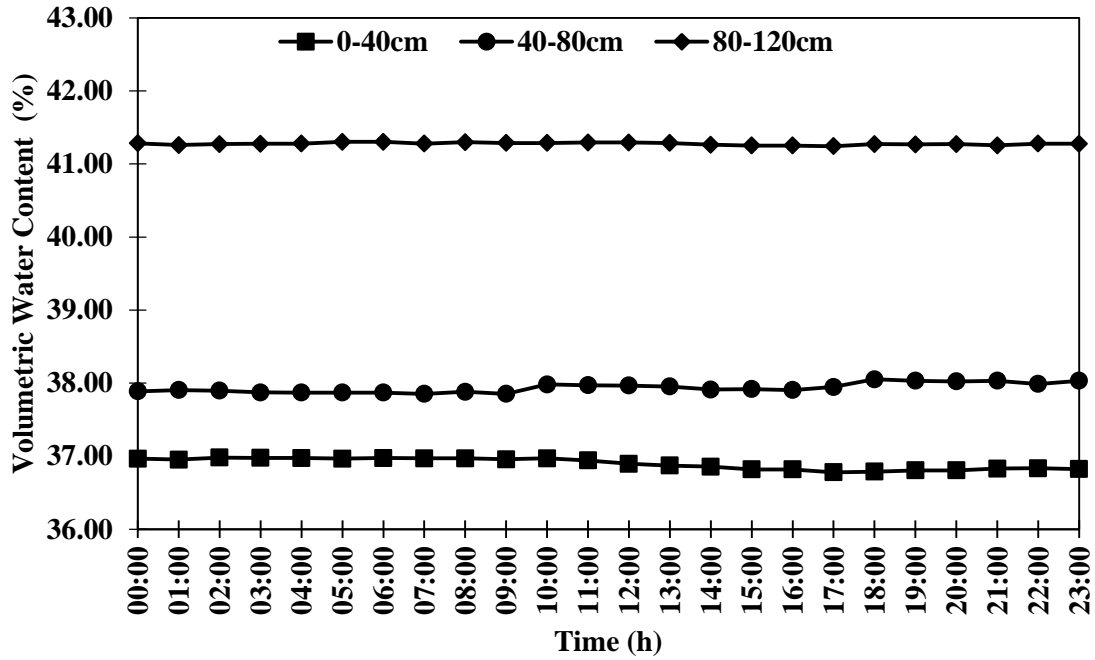


Figure 4.53 Temporal variation of % VWC in three soil profile depths during experimental set up 5 on 15/09/2019 at site 3

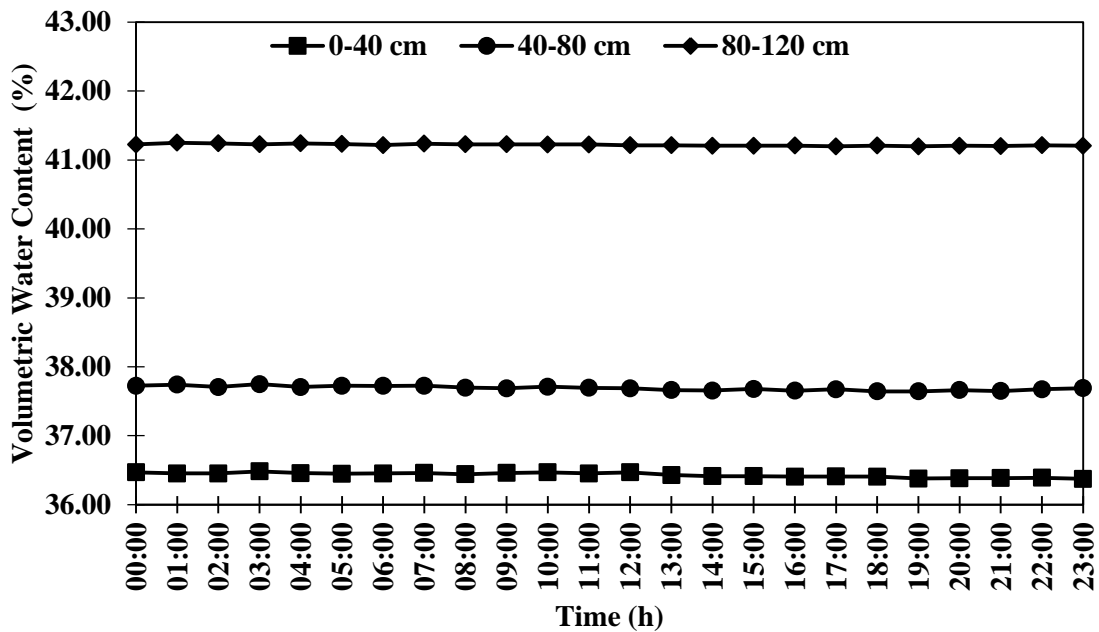


Figure 4.54 Temporal variation of % VWC in three soil profile depths during experimental set up 5 on 19/09/2019 at site 3

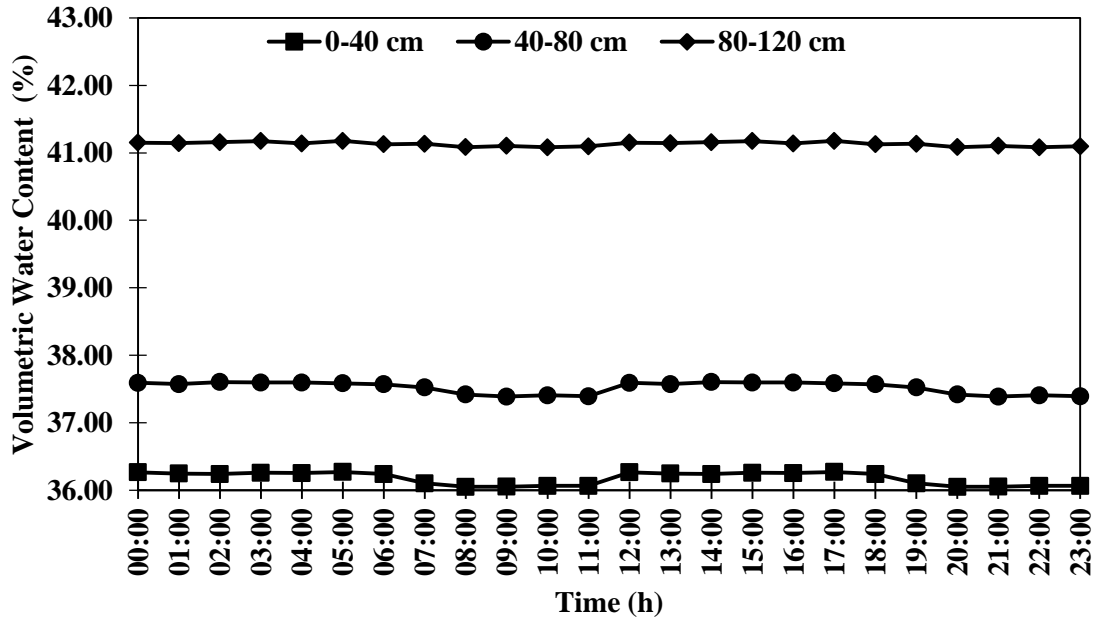


Figure 4.55 Temporal variation of % VWC in three soil profile depths during experimental set up 5 on 21/09/2019 at site 3

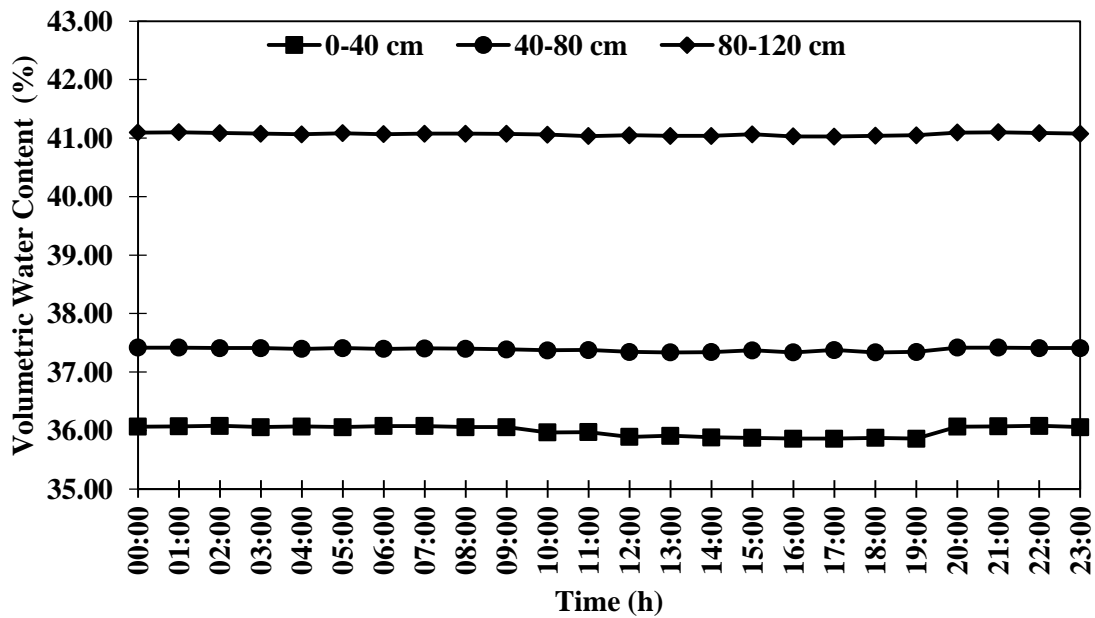


Figure 4.56 Temporal variation of % VWC in three soil profile depths during experimental set up 5 on 22/09/2019 at site 3

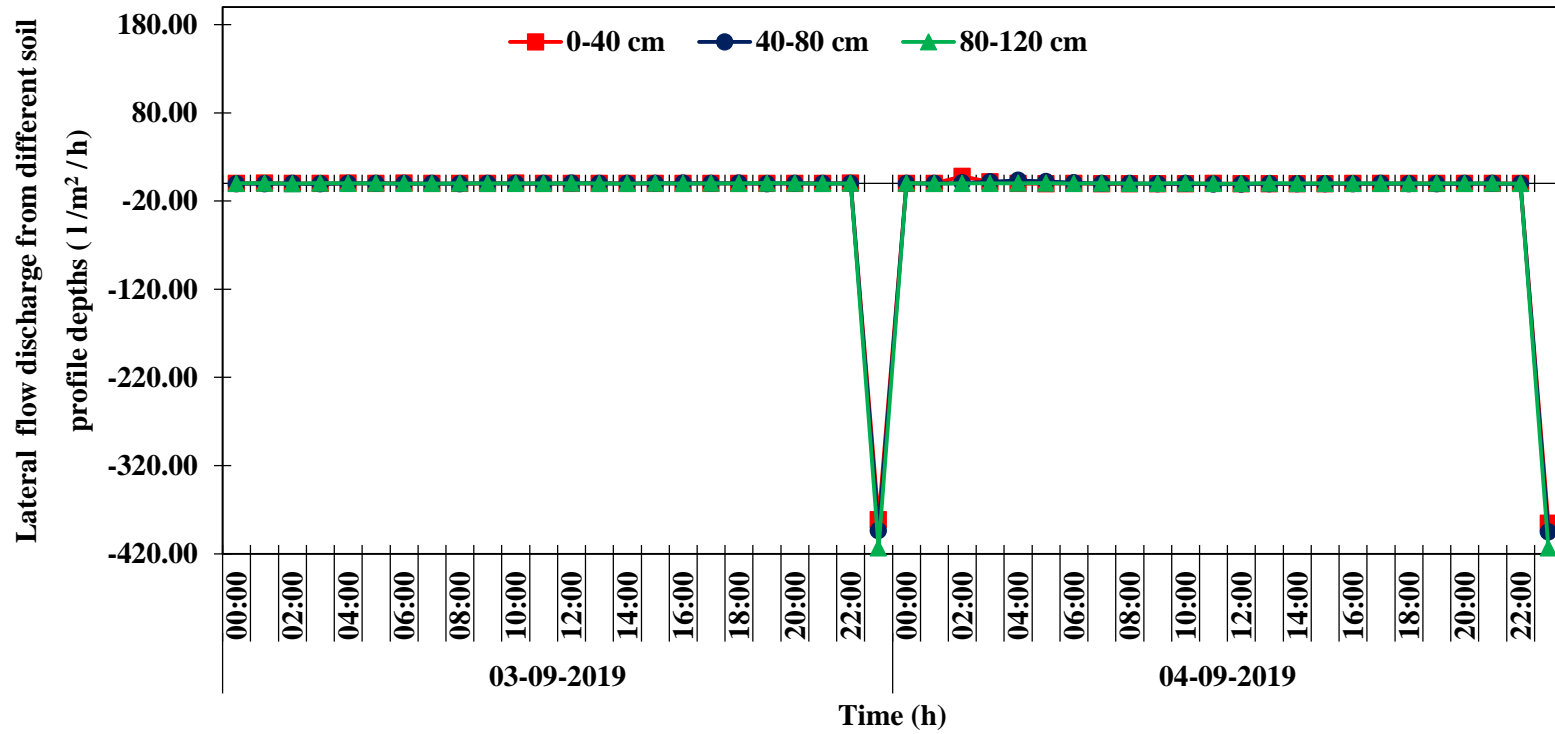


Figure 4.57 Temporal variation of lateral flow discharge from three soil profile depths during experimental set up 5 from 03/09/2019 to 04/09/2019 in site 3

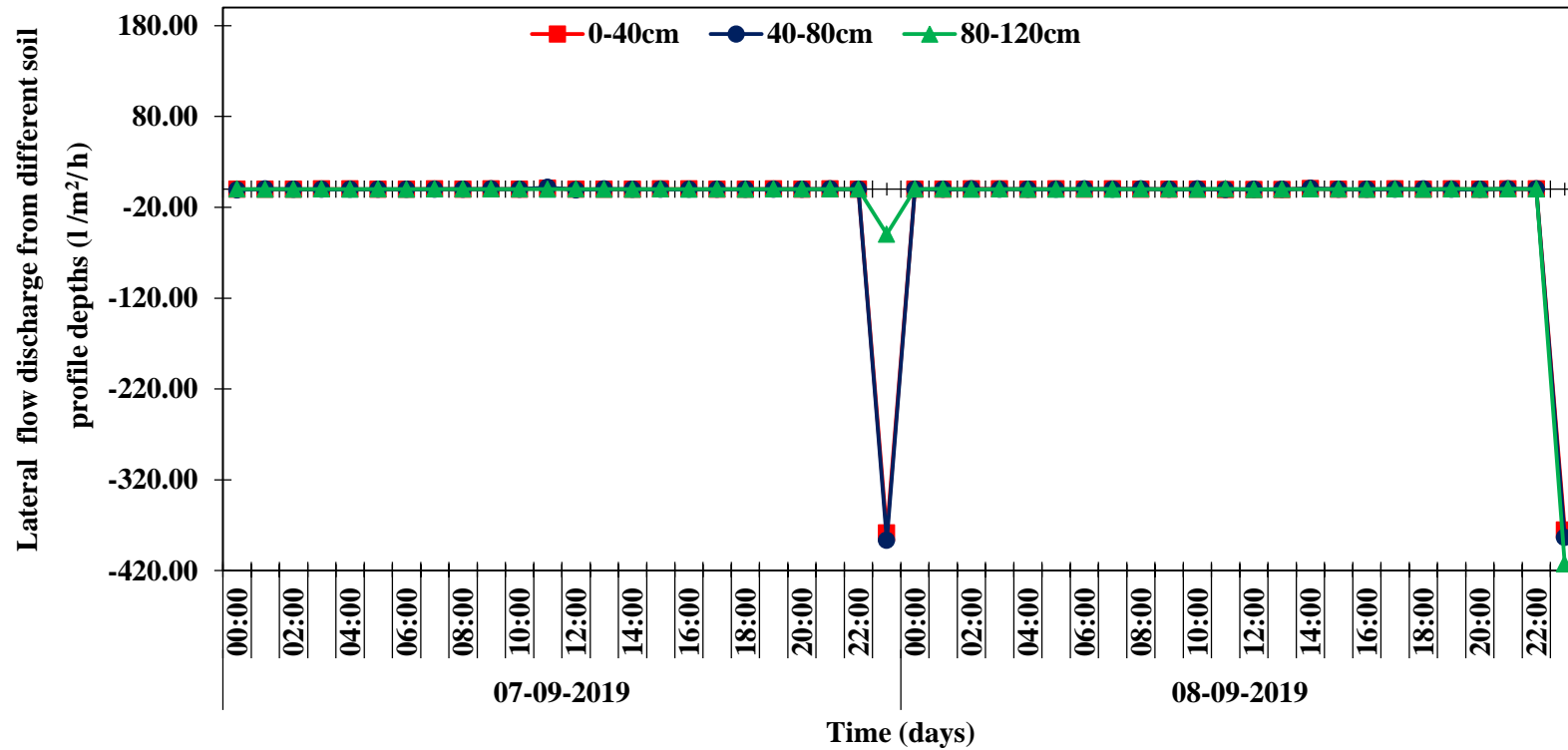


Figure 4.58 Temporal variation of lateral flow discharge from three soil profile depths during experimental set up 5 from 07/09/2019 to 08/09/2019 in site 3

The computed variation in daily lateral flow discharge for the representative days showed the effect of reduced rainfall on the daily discharge as shown in table 4.18.

Table 4.18 Variation in lateral flow discharge through different soil profile depths during experimental set up 5

Date	Average lateral flow discharge ($l/m^2/h$) at depths of		
	0-40 cm	40-80 cm	80-120 cm
03-09-19	0.14	0.09	0.17
04-09-19	3.18	1.65	0.20
06-09-19	0.09	0.09	0.17
07-09-19	0.19	1.92	0.02
08-09-19	0.18	0.22	0.24
09-09-19	0.09	0.22	0.20
10-09-19	0.15	0.18	0.13
11-09-19	0.15	0.15	0.16
12-09-19	0.10	0.16	0.14
15-09-19	0.15	0.47	0.14
19-09-19	0.10	0.21	0.14
21-09-19	0.34	0.60	0.21
22-09-19	0.31	0.23	0.17

The variation of lateral flow discharge with temporal variation of volumetric water content in Site 3 under natural rainfall conditions have been represented through table 4.19. The comparisons have been made for the representative durations in the day. The variation in both the quantities was proportional to each other. Similarly, daily lateral flow discharge from the three soil profile layers when compared to daily rainfall for the experimental set up 5, it was found to be proportional to one another as shown in figure 4.59

Table 4.19 Variation of Lateral Flow Discharge with Temporal Variation of Volumetric Water content in Site 3 under Natural Rainfall Conditions

Date	Time	Depths of Soil layers					
		0-40 cm		40-80 cm		80-120 cm	
		VWC (%)	Discharge ($l/m^2/h$)	VWC (%)	Discharge ($l/m^2/h$)	VWC (%)	Discharge ($l/m^2/h$)
4/9/2019	2:00	38.133	0	39.351	0	41.344	0
	3:00	38.928	7.95	39.393	0.42	41.333	0
	4:00	39.083	1.55	39.572	1.79	41.325	0
	5:00	39.068	0	39.905	3.33	41.344	0.19
	6:00	39.025	0	40.111	2.06	41.379	0.35
7/9/2019	11:00	37.85	0	38.664	0	41.372	0.0192
	12:00	37.95	1	38.85	1.86	41.302	0
	13:00	37.915	0	38.777	0	41.356	0.0648
	20:00	37.853	0.03	38.683	0	38.683	0.0192
	21:00	37.85	0	38.668	0	38.668	0.0132
	22:00	37.865	0.15	38.668	0	38.668	0.0048
21/9/2019	11:00	36.065	0	37.392	0	41.096	0.15
	12:00	36.267	2.02	37.593	2.01	41.151	0.55
	13:00	36.247	0	37.574	0	41.143	0

Date	Time	Depths of Soil layers					
		0-40 cm		40-80 cm		80-120 cm	
		VWC (%)	Discharge ($l/m^2/h$)	VWC (%)	Discharge ($l/m^2/h$)	VWC (%)	Discharge ($l/m^2/h$)
21/9/2019	14:00	36.24	0	37.605	0.31	41.158	0.15
	15:00	36.259	0.19	37.597	0	41.174	0.16

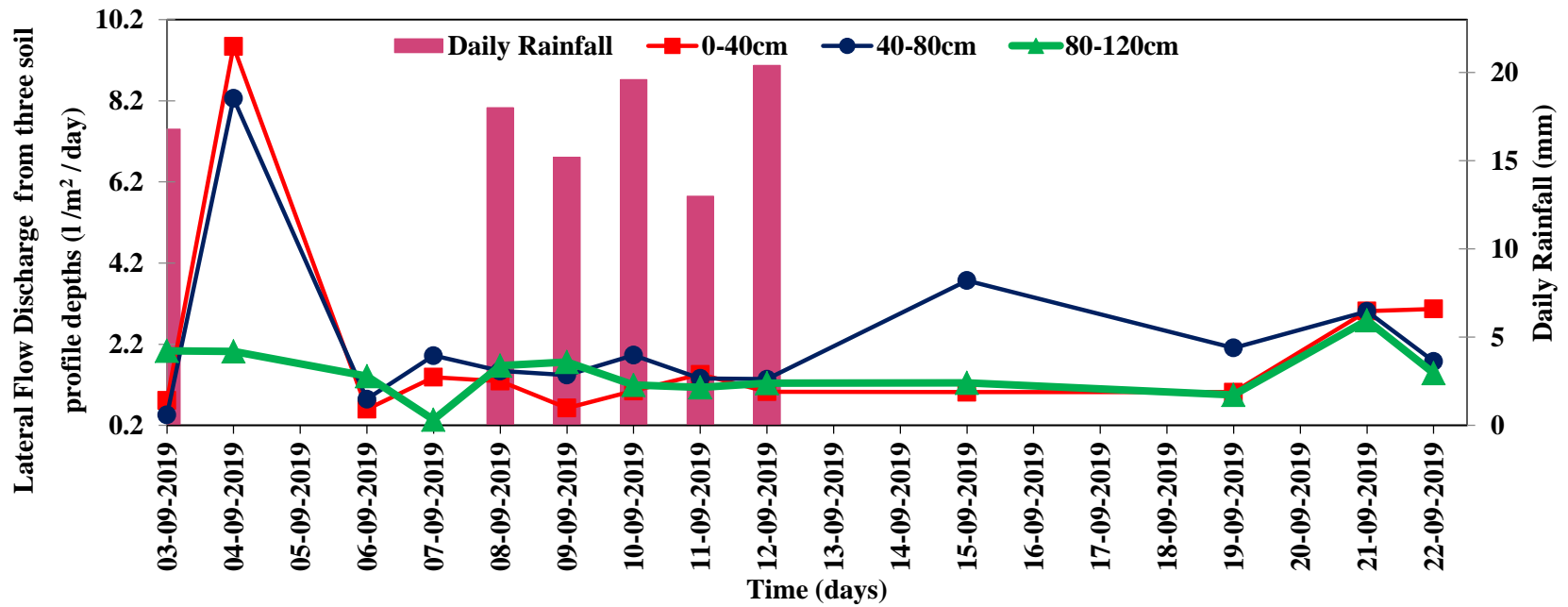


Figure 4.59 Daily lateral flow discharge from the three soil profile layers versus daily rainfall for the experimental set up 5 in site 3

A total discharge of 85.79 l from a cross sectional area of (2 m x 0.4 m) deep soil profile was obtained during the experimental period. The first 40 cm soil depth contributed 29.8 % of interflow out of the total subsurface flow produced from the trench face. Similarly, 36.8 % and 33.4 % of interflow was generated, from the soil depths of 40-80 cm and 80-120 cm respectively. Higher silt and sand minerals at 40-80 cm soil depth contributed to the higher discharge as compared to that from third soil depth. The calculated discharge rate obtained was 1.52 l/m²/day, 1.87 l/m²/day and 1.70 l/m²/day from soil depths of 0-40 cm, 40-80 cm and 80-120 cm respectively. The calculated seepage velocity was 0.2 cm/day, 0.36 cm/day and 0.56 cm/day from soil depths of 0-40 cm, 40-80 cm and 80-120 cm respectively. The hourly temporal variation of lateral flow discharge recorded from the monitoring trench from the soil layers at three different depths represented dips from all the soil layers in the experimental site. It can be attributed to the lower and intermittent rainfall pattern observed in the site throughout the experimental duration. Table 4.20 represents the average subsurface flow discharge through different soil profile depths recorded from three experimental sites under different experimental set ups. The highest discharge was recorded during simulated rainfall conditions.

Table 4.20 Average subsurface flow discharge through different soil profile depths recorded from three experimental sites under different experimental set ups.

Experimental site	Experimental set up	Depth of soil layers (cm)	Subsurface flow discharge (l/m ² /h)
Site 1	Under simulated rainfall conditions	0-40	34.26
		40-80	38.34
		80-120	55.65
Site 2	Line source trench @ 30 cm depth	0-40	1.699

Experimental site	Experimental set up	Depth of soil layers (cm)	Subsurface flow discharge ($l/m^2/h$)
Site 2	Line source trench @ 30cm depth	40-80	1.925
		80-120	1.606
	Line source trench @ 50cm depth	0-40	6.710
		40-80	5.895
		80-120	0.892
	Under natural rainfall conditions	0-40	7.569
		40-80	18.500
		80-120	6.320
	Site 3	Under natural rainfall conditions	0-40
40-80			2.299
80-120			1.471

The average subsurface flow discharge recorded from three experimental sites under varying experimental set ups and from soil layers of different depths also represented the heterogeneity of the soils in laterite terrain and their behaviour towards different modes of water application.

4.7 MONITORING LATERAL FLOW USING SALT TRACERS

4.7.1 Salt tracing in site 3

Mass estimation of salt tracer to be applied was done in laboratory on the basis of background chloride concentration/ electrical conductivity (EC) of water to be applied into the line source trench. On 13th October 2019 experimental site experienced rainfall of 40.1 mm. As, the rainfall had already saturated the soil column, only an initial volume of 500 l of salt solution was poured into the line source trench on the next day of rainfall. It was done in order to prevent overflowing

of applied water out of the trench. The pouring of tracer was carried out all at once in a single operation. The experiment was started on 14th October 2019 at 12:30 pm. The recorded variation in electrical conductivity and % VWC after tracer application on 14/10/2019 have been illustrated by figures 4.60 and figure 4.61.

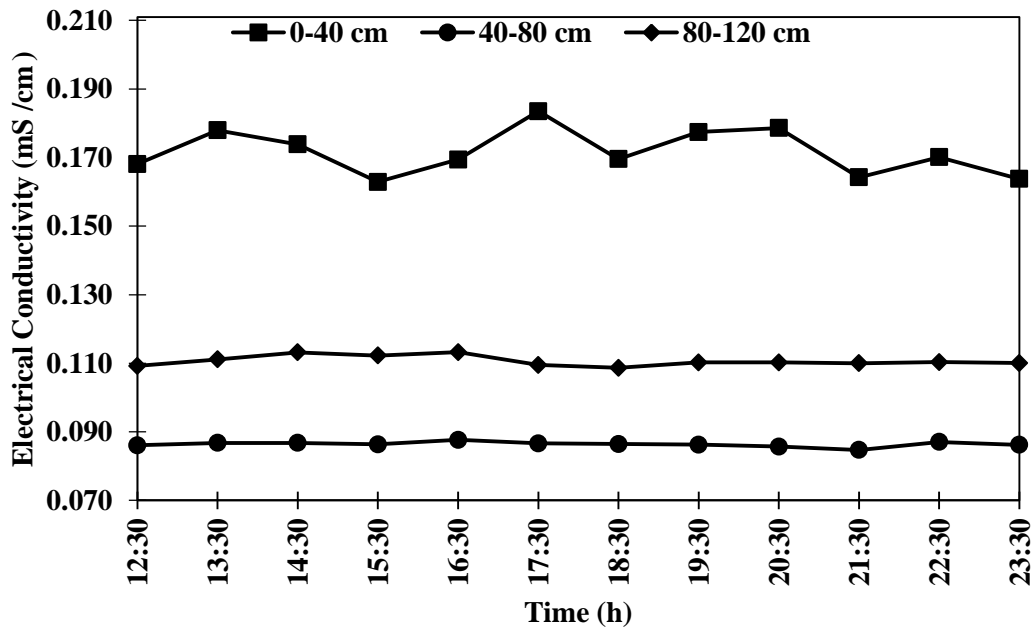


Figure 4.60 Spatial and temporal variation of EC after salt tracer application on 14/10/2019

The recorded electrical conductivity showed peak value of 0.185 mS/cm at 17:45 hrs, from first 40 cm soil depth which was approximately after five hours of tracer application. Second soil depth experienced the upsurge in its ionic response at about 16:15 hrs and gained peak EC value of 0.08 mS/cm. This event can be related to the outcome of the results obtained during the lateral flow monitoring in site 3, where soil section at 40-80 cm depth contributed maximum discharge compared to other depths. However, the third soil depth showed abrupt variations in electrical conductivity throughout the day after tracer application and gained peak EC of 0.11

mS/cm at 16:30 hrs. Depletion in electrical conductivity was experienced at soil depth of 80-120 cm after 16:30 hrs.

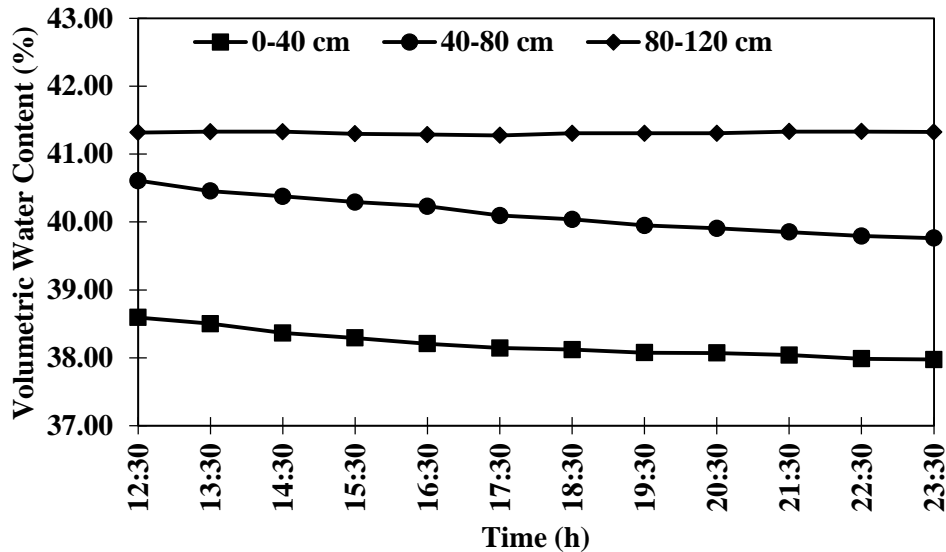


Figure 4.61 Spatial and temporal variation of % VWC after tracer application on 14/10/2019

The results of % VWC obtained on 14/10/2019 indicated dips at all the three observation points installed on the monitoring trench face. The disparity in percentage volumetric water content and corresponding electrical conductivity at different soil depths contrasted from each other. It may be due to the rainfall which occurred a day before the experiment was carried out (Wienhofer, J, 2009). The soil pores might have got completely saturated against the gravity, thus, resulting in no moisture increase laterally. This was validated from the % VWC variations observed in site 3 during north-east monsoon. Salt ions moved from a higher concentration gradient to a lower concentration gradient. Dispersion in cylindrical capillaries containing flowing fluids attains a parabolic velocity profile in a capillary of circular cross-section (Taylor, 1953). Thus, there are erratic variations in electrical conductivity with time, whereas no % VWC increases were recorded.

The experiment was repeated on 19th October 2019 by applying salt solution of volume 1000 l into the line source trench. Mass of salt (NaCl) applied was 120 g. On

18th October 2019 rainfall of magnitude 50.4 mm occurred in the site. The reiteration of the experiment was done to substantiate the processes and findings obtained through the tracer experiment carried out on 14th October 2019. The recorded variation in EC and % VWC after tracer application on 19/10/2019 have been illustrated by figures 4.62 and figure 4.63.

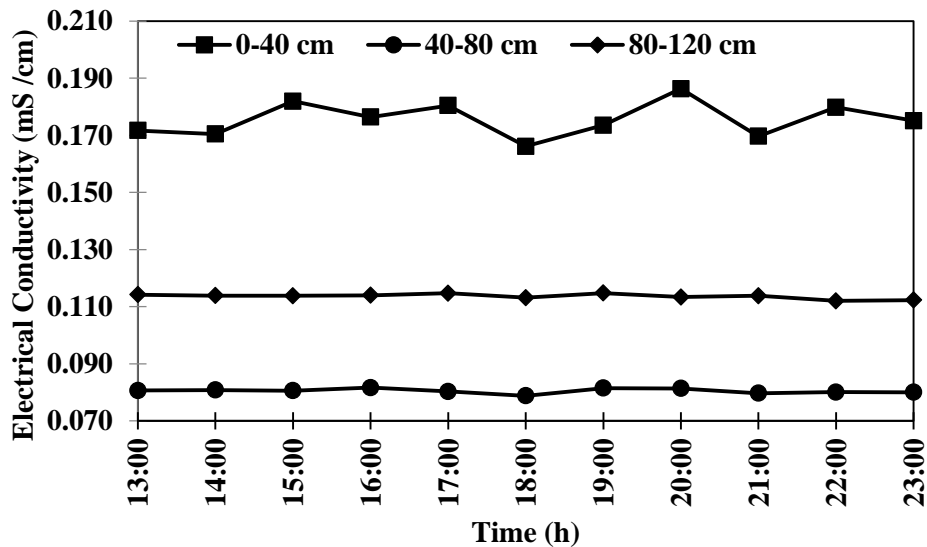


Figure 4.62 Spatial and temporal variation of EC after tracer application on 19/10/2019

The tracer solution was applied into the line source trench successively. The experiment was started at 14:00 hrs. First V_1 volume of salt tracer solution i.e. 500 l was applied into the trench. Subsequently, 500 l of salt tracer solution was again applied into the trench after the subsidence of initial application. Tracer application continued till 15:00 hrs. The results recorded on 19/10/2019 validated the results from the first tracer test carried out at site 3 on 14th October 2019. The experiment involved applying twice the volume of water which was applied in the previous experiment. It took an hour for the complete infiltration of salt solution. A peak value of 0.18 mS/cm was recorded at first soil depth, five hours after the tracer application was completed. Soil at depth of 40-80 cm exhibited EC at peak value of

0.08 mS/cm at 19:15 hrs which was almost an hour earlier than the first depth. The third depth continued to show abrupt variations and gained its peak EC of 0.11 mS/cm at 15:45 hrs.

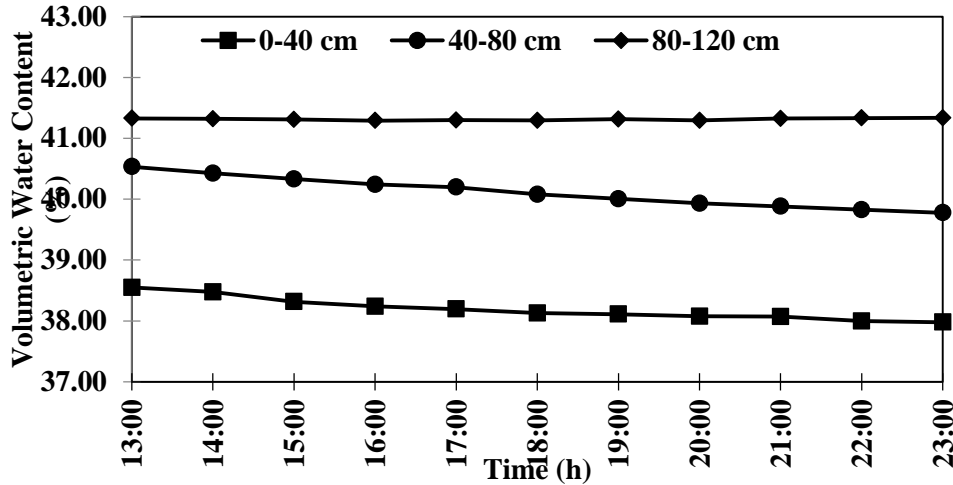


Figure 4.63 Spatial and temporal variation of % VWC after tracer application on 19/10/2019

Thus, the two iterative experiments carried out at site 3 established the fact that the applied tracer underwent a molecular diffusion due to the pre-saturated condition of soil. Initially the tracer molecules acquire a parabolic velocity profile while moving through the soil grains which may give rise to radial concentration gradients. This results in molecular diffusion of tracer molecules resulting into relative velocity products. This phenomenon triggers early breakthrough of salt ions at the monitoring nodes even when moisture variation is not detected. However, the tracer breakthrough curves did exhibit the variation in physical properties of soil at three different depths.

4.7.2 Salt tracing at Site 2

Tracer experiment in site 2 was carried out in post-monsoon duration. Prior to the application of salt tracer, saturation of soil column in between the trenches and of the line source trench was done. Subsequently, line source application trench was filled with water to a total volume V , i.e. V_1+V_2 .

Therefore,

$$V = V1 + V2$$

For site 2 $V = (\text{Volume of line source trench}) + (\text{Volume of soil column in between trenches})$

$$V = [(1m * 0.5m * 0.5m) + (2m * 0.5 * 1)] * 1000$$

$$= 1250 \text{ litres}$$

After saturating the soil through line source trench water application, salt solution was applied. The tracer experiment was carried out in two sets. The first one was accomplished on 13th November 2019 starting from 13:00 hrs. Total mass of tracer applied was 48 g in 1200 l of water. It was three times lesser than the calculated mass of tracer obtained from eq. 4.1. It was done to test the effect of tracer mass on the breakthrough detection through the soil layers in the experimental site. Tracer solution was applied continuously till the line source trench was completely filled. The second batch of water application was done as soon as the water in the trench started to descend. The variation in % VWC and electrical conductivity after tracer application on 13/11/2019 is shown from figure 4.64 and figure 4.65.

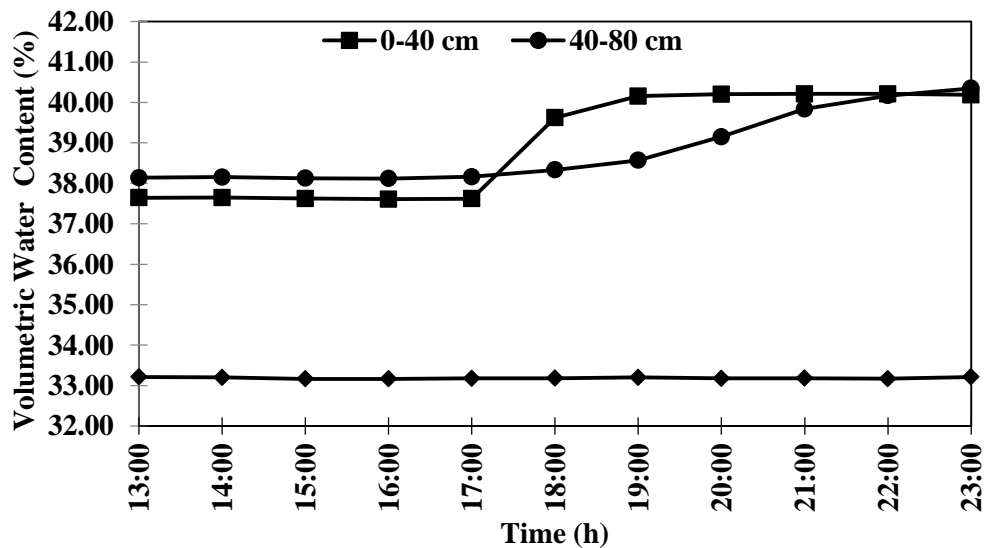


Figure 4.64 Spatial and temporal variation of % VWC after tracer application on 13/11/2019

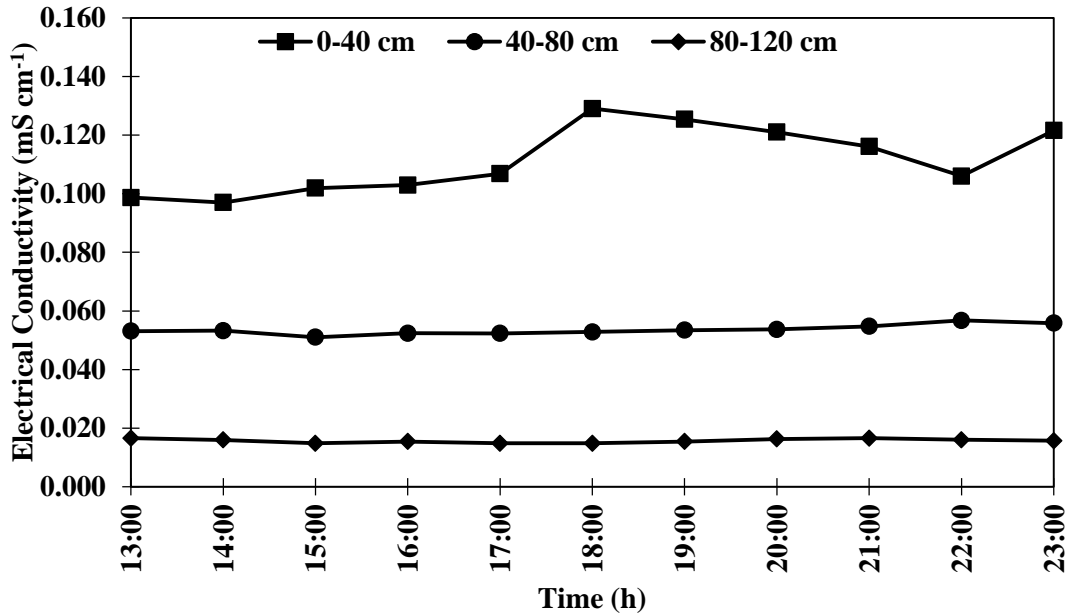


Figure 4.65 Spatial and temporal variation of EC after tracer application on 13/11/2019

According to the results obtained from tracer experiment at site 2, it was found that the recorded electrical conductivity from the three soil depths showed an arbitrary and unanticipated variation with time. However, this variation increased with time upto a single peak value, after which EC declined. A peak value of EC equal to 0.129 mS/cm was recorded at 18:00 hrs from first 40 cm of total soil depth under the study. This was exactly after five hours of tracer application in the line source trench. It was approximately same duration of time taken for the volumetric increase in site 2 during lateral flow monitoring under line source trench water application explained in section 4.9. Simultaneously, 40-80 cm of soil depth showed continuous dips and rise which kept on increasing with time till the peak value of EC was reached. However, the tracer breakthrough was not as postulated at this depth when compared with the lateral flow monitoring experiments conducted in the site. Further, the greater water holding capacity of finer soil at third soil depth on the monitoring trench face was also represented through the tracer breakthrough curve at

80-120 cm soil depth. The seepage velocity calculated was 5.70 cm/day, 4.25 cm/day and 0.38 cm/day for soil depths of 0-40 cm, 40-80 cm and 80-120 cm respectively.

The similarity of results with line source trench analysis explained in section 4.9 can be due to the application of same amount of water in the trench at similar time interval along with NaCl. Furthermore, the true velocity of interflow for the first soil layer recorded by the salt tracer breakthrough was obtained as 0.4 m/h which was similar to the true velocity of interflow recorded by TEROS12. The delayed breakthrough of NaCl at 40-80 cm and 80-120 cm of soil depths may be due to lower concentrations of salt. This assumption was validated through the second set of experiment.

The tracer experiment in site 2 was iterated on 16/11/2019 for analyzing the variation in subsurface flow with varying mass of tracer. Volume of water used for tracer dilution was 800 l. A tracer mass of 96 g was mixed in a tank of water thoroughly before applying into the line source trench. A better comprehension about lateral flow movement of the applied water in site 2 was inferred from second set of tracer experiment. Figure 4.66 and figure 4.67 represent the spatial and temporal variation of % VWC and EC recorded respectively on 16/11/2019.

The breakthrough of salt tracer was recorded from 17:00 hrs at 0-40 cm soil depth which attained a peak value of 0.133 mS/cm at 18:45hrs. Simultaneously, 40-80 cm of soil depth recorded a major breakthrough at 16:00 hrs before attaining a peak value of 0.060 mS/cm at 18:00 hrs. Breakthrough at 80-120 cm of soil depth was meagre and kept on differing between 0.21 mS/cm to 0.22 mS/cm even after attaining the peak value throughout the experiment. It can be attributed to a very low or negligible lateral flow recorded at third soil depth under experimentation. Early breakthrough of tracer at 40-80 cm soil depth indicated the highly porous nature of soil as compared to other two depths.

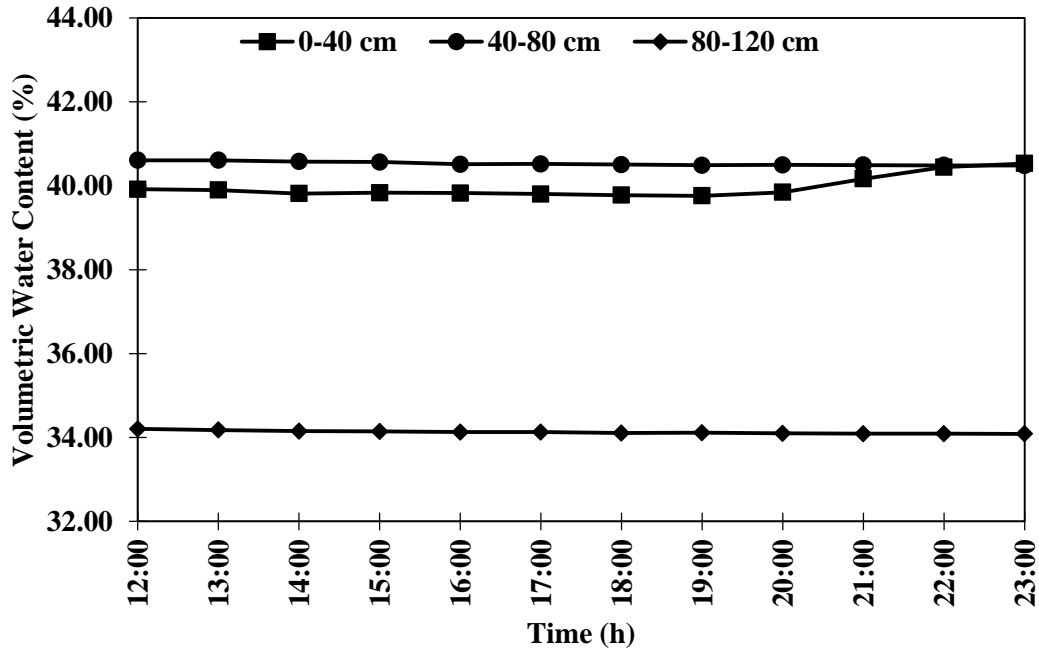


Figure 4.66 Spatial and temporal variation of % VWC after tracer application on 16/11/2019

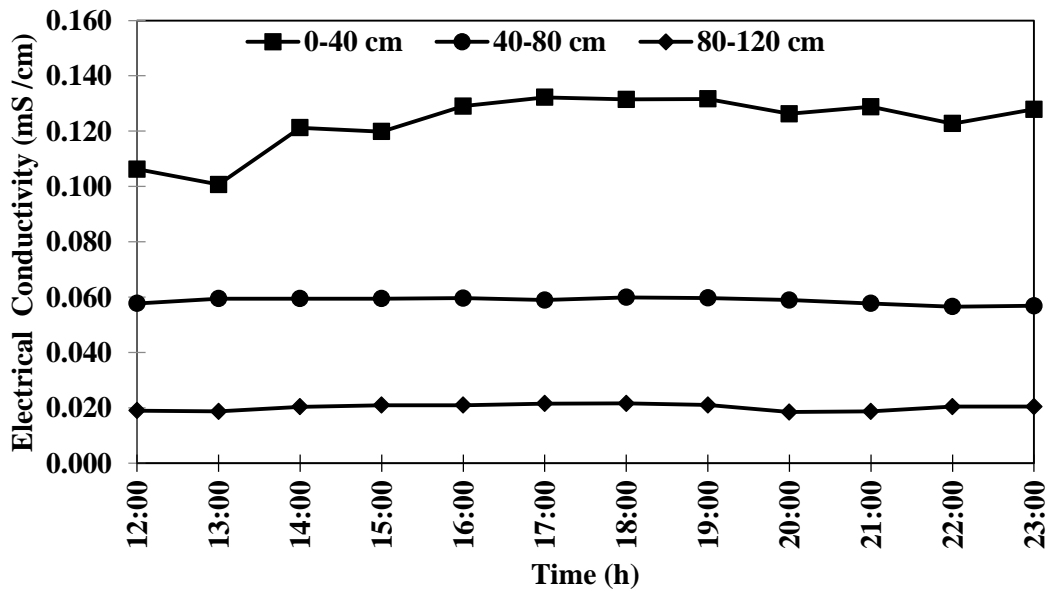


Figure 4.67 Spatial and temporal variation of EC after tracer application on 16/11/2019

Further, the experiment clearly exhibited the effect of greater soil surface area when exposed to water, resulted in maximum interflow with minimum deep percolation in the site. Thus, NaCl was proved to be an efficient tracer in monitoring lateral flow of water, specifically for upper soil depths. The mass of tracer to be applied greatly depends on the background chloride content or electrical conductivity of the water to be used to dilute salt tracer. From the experiment, it was concluded that mass of tracer to be applied in site 2 should result in an increase in EC, upto three times of its initial value to acquire better breakthrough signals. At greater soil depths the mineral content in laterite soils plays a crucial role in altering the tracer results. Further, from the series of experiments carried out in site 3 and 2 revealed that under rainfall conditions salt tracers are inefficient tracers. The values of true velocity of interflow recorded from the salt tracer breakthrough analysis in site 2 and 3 as tabulated in table 4.21 were found to be close to each other. It can be attributed to the similar soil texture in the two sites. The results of true velocity obtained through tracer analysis were found to be same as observed by the sensors.

Table 4.21 True velocity of interflow from the salt breakthrough analysis in site 2 and site 3

Experimental sites	Experimental set up for tracer	Depth of soil layer (cm)	True velocity of interflow from salt breakthrough (m/h)
Site 2	Tracer application through line source trench of 50 cm depth	0-40	0.40
		40-80	0.57
Site 3	Tracer application through line source trench of 50 cm depth	0-40	0.34
		40-80	0.50

4.8 BASE FLOW MONITORING

4.8.1 Pressure head analysis

The pressure head measurements were carried out weekly using a fibre measuring tape with a brass plumb bob tied at the bottom. The observations were recorded from 26/02/2019 to 1/09/2019. Water levels in observation well 1 reduced from the month of February. The month of April and till mid of May witnessed no pressure heads at the bottom surface of well 1 or the lowest levels of water table in the site. A gradual increase in water level was observed with the onset of south-west monsoon. The weekly pressure head variations in well 1 and well 2 are shown in figure 4.68 and figure 4.69. The pressure head variation pattern for both wells indicated the seasonal fluctuation of shallow wells in the site.

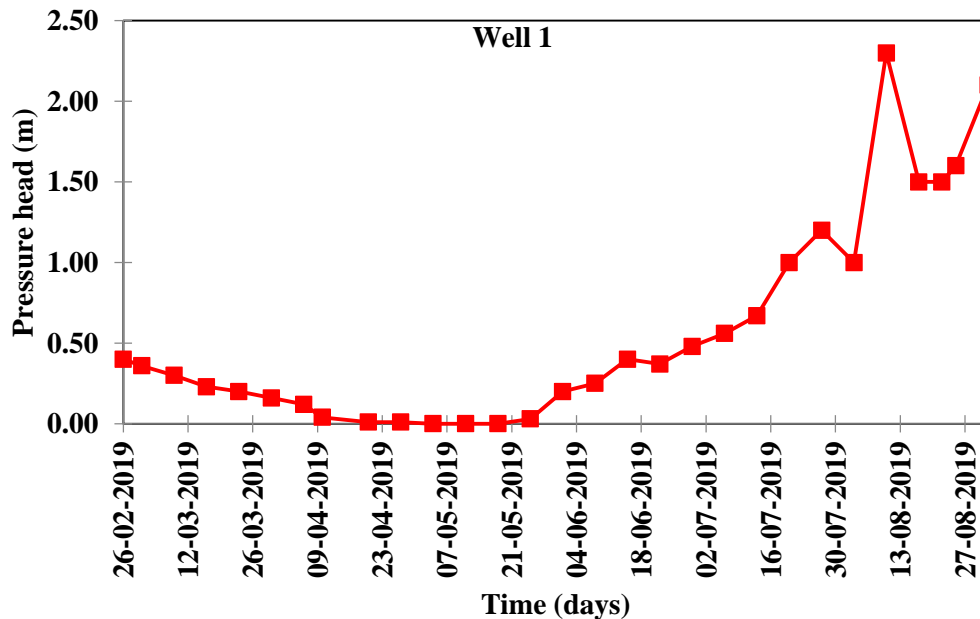


Figure 4.68 Pressure head variation in observation well 1

A total rainfall of 120 mm was observed from 24/05/2019 to 31/05/2019 as recorded by the non-recording rain gauge. Highest Pressure head in the observation well 1 was recorded as 2.3 m during the weekly observation in between 3/08/2019 to

10/08/2019 which was measured on 10/08/2019. The observations recorded from observation well 2 conformed to the rainfall observations.

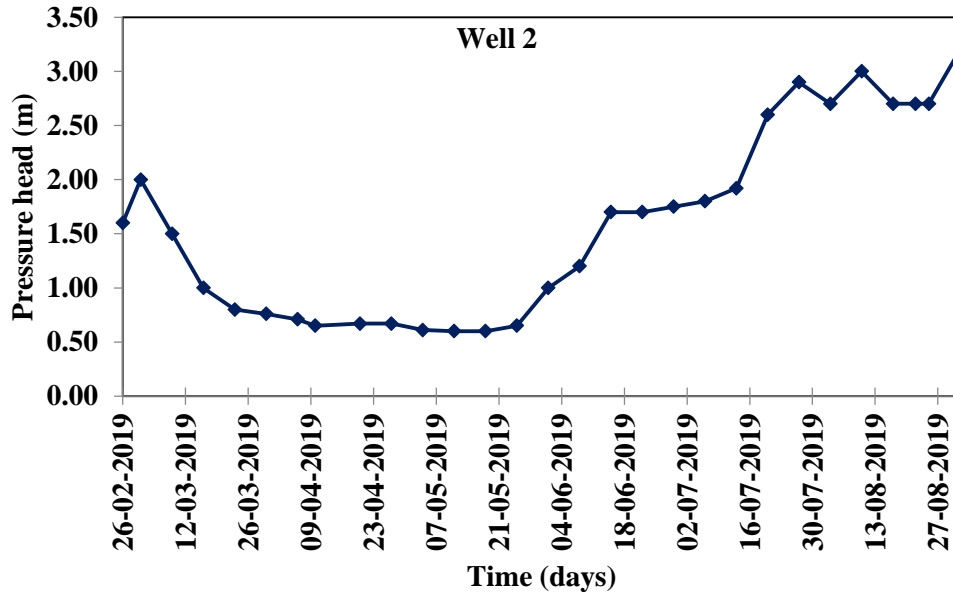


Figure 4.69 Pressure head variation in observation well 2

However, the least value recorded from observation well 2 was greater than that recorded in observation well 1. Apparently, it was due to greater depth of well 2 than observation well 1 and also due to its downslope location in the site which derived more subsurface flow into it. The calculated bottom elevations of wells are shown in table 4.22. The relative variation in total hydraulic head in well 1 and well 2 is represented in figure 4.70.

Table 4.22 Elevation head of observation wells 1 and 2

Well No	Depth of Well (m)	Site Elevation (m)	Bottom Elevation Head (m)
1	4.19	12.0	7.81
2	4.90	11.61	6.71

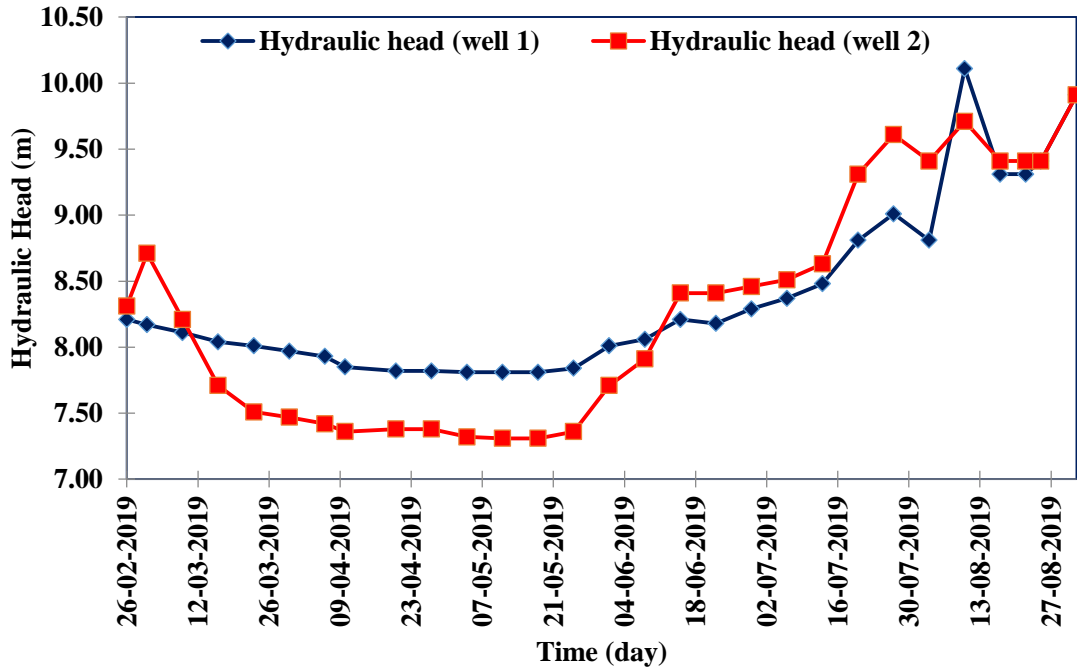


Figure 4.70 Hydraulic head variation of observation wells 1 and 2

4.8.1 Base Flow Monitoring using Salt Tracers

The injection of salt tracer (KCl) into the injection well 1 was carried out on 2nd February 2020 from 10:50 am to 11:00 am. The background salt concentration in the shallow injection and observation wells, recorded just before the tracer injection was 0.1 mS/cm. After injection, the tracer (KCl) concentration in injection well showed an increase till it reached a peak EC value of 3.00 mS/cm at 11:00 hrs as shown in figure 4.71. At 16:30 hrs the electrical conductivity recorded, was similar to the initial value observed prior to the injection of salt (KCl) tracer. Simultaneously, tracer recovery was noted from the monitoring wells A, B and C.

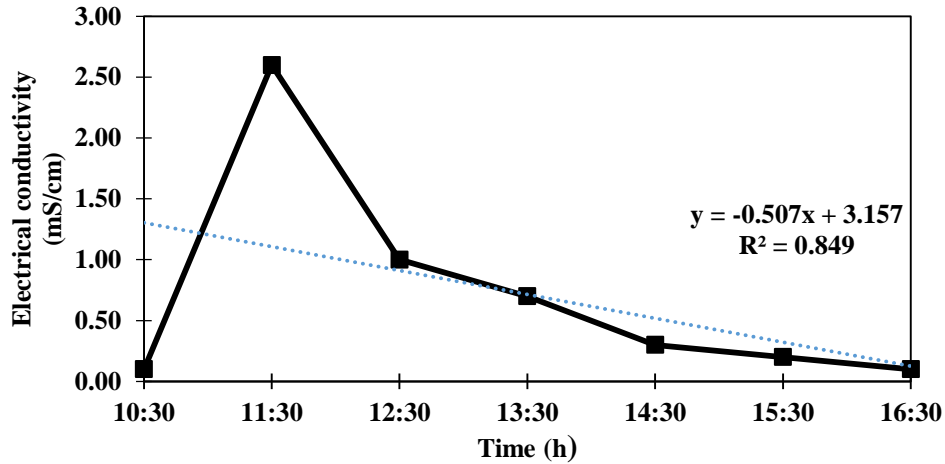


Figure 4.71 Temporal variation of electrical conductivity in injection well

A steady raise in EC was observed in well A from 11:30 hrs till a peak value of 0.145 mS/cm was recorded at 13:00 hrs. Breakthrough of salt (KCl) tracer in well B observed at 11:30 hrs was 0.110 mS/cm. Simultaneously, a major salt breakthrough was recorded from well C at 12:00 hrs with an EC value of 0.120 mS/cm. The recorded temporal variation of EC in observation wells signified the rapid movement of water through the shallow wells. The point dilution method for horizontal flow velocity determination was used for injection well 1 and for which the temporal variation of logarithmic tracer concentration is shown in figure 4.72.

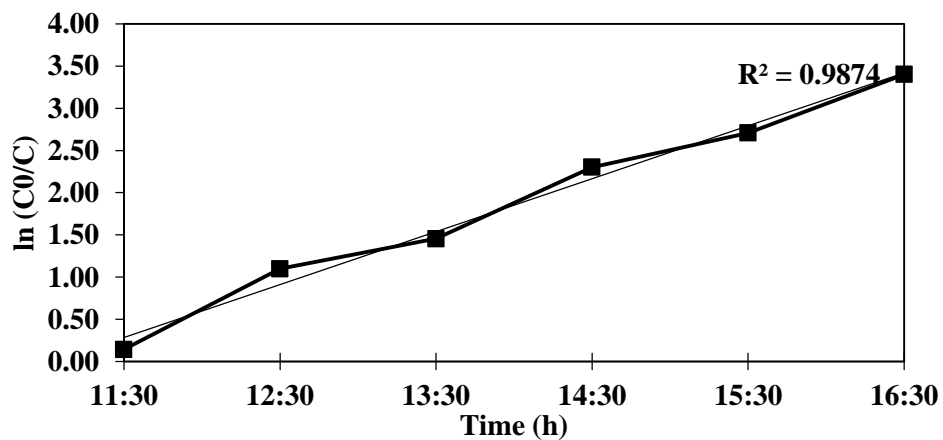


Figure 4.72 Temporal variation of logarithmic tracer concentration in injection well

The average apparent linear flow velocity calculated for injection well was 1.35 m/day and thereby the hydraulic conductivity was estimated as 80.4 m/day. The salt (KCl) tracer underwent dilution with time in well 1 which was evident through linear rise in the logarithmic concentration of tracer. The calculated value of hydraulic conductivity represented a porous shallow aquifer with apparently greater percentage of medium to fine sand (Domenico P.A *et al.*, 1998). The monitoring wells A, B and C recorded a tracer recovery with increasing time duration. The column of water when observed in monitoring well B was found to be completely drained off whereas well C withheld the groundwater. Perhaps, it can be attributed to the terrain slope which was directing the subsurface flow of water towards the nearby pond. The field experimentation was further compared to United State Bureau of Reclamation Equation (USBR).

According to the equation,

$$K = 0.36 (d_{20})^{2.3} \quad (3.11)$$

Where, K is in cm/sec and d_{20} is in mm. The formula is most suitable when the value of uniformity coefficient, U_c is less than 0.5 (Cheng and Chen, 2007), which was applicable in the present experimental site with shallow wells. A horizontal hydraulic conductivity of 2.0×10^{-4} m/s was obtained which represented a shallow aquifer with medium to fine sand proportion. Thus, the experimental and mathematically derived equation results coordinated well with each other. An inverse analysis of horizontal hydraulic conductivity was carried out following the Darcy's law.

Thus, from equation (3.10)

$$\begin{aligned} \text{Hydraulic head} = h &= \left(\frac{v}{k}\right) * L & (3.12) \\ &= 0.019 \text{ m} \\ &= 1.9 \text{ cm} \end{aligned}$$

The hydraulic head difference between the injection well and monitoring well A was 2 cm prior to the experiment. Thus, the point dilution test was found to be an effective method in calculating horizontal conductivity and velocity of flow in lateritic shallow wells. Utilizing the hydraulic conductivity and hydraulic head calculated from the point dilution method and weekly pressure head analysis respectively, the velocity of groundwater flow was calculated. The velocity of flow through the analysis of weekly varying hydraulic head in site 1 was obtained as 1.0 m/day and the weekly variation is represented in figure 4.73.

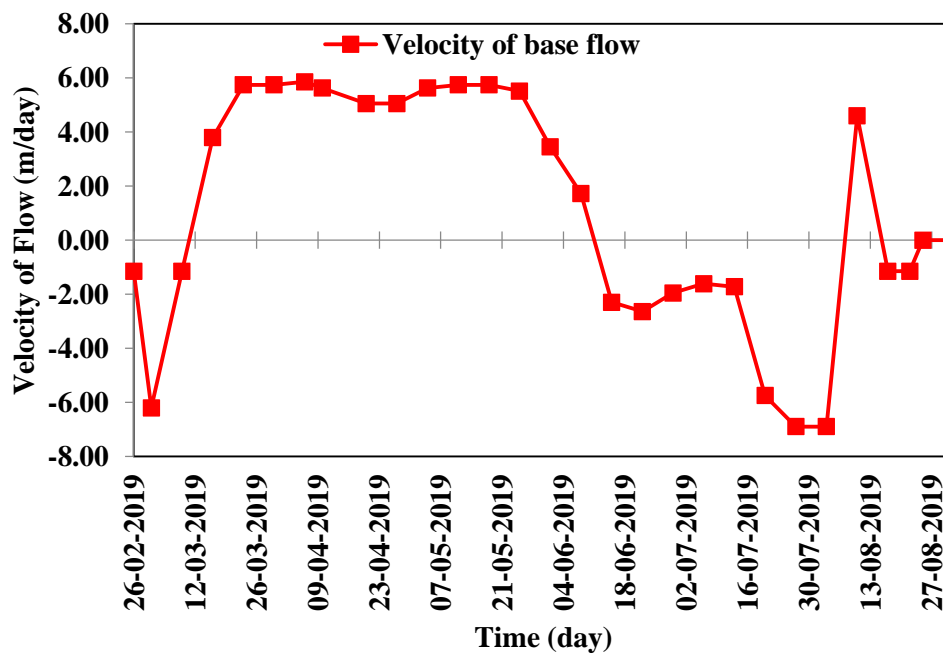


Figure 4.73 Weekly velocity of groundwater flow

Conversely, tracer breakthrough method for true velocity estimation in shallow wells resulted in an overestimation of velocity and thereby conductivity. The instant breakthrough in monitoring wells during tracer analysis can be attributed to pulse injection of tracer in the site. This instantaneous kind of tracer injection may lead to heterogeneous advection and hydrodynamic dispersion to the tracer plume (Becker et.

al. 2003). Thus, a continuous injection or dilution of salt tracers was found to be appropriate if reliable breakthrough of tracer has to be obtained.

4.9 NATURAL ISOTOPE ANALYSIS IN THE EXPERIMENTAL SITE

The presence of ^{18}O and ^2H is significant in tracing the origin of water in the hydrological cycle because they are constituents of water molecules. (Nyende et. al, 2013). The recorded values of δD (‰) and $\delta^{18}\text{O}$ (‰), represent the ratio of deuterium to hydrogen and oxygen-18 to oxygen-16 respectively as shown in table 4.22. The variation in these values depends upon the evaporation pattern.

Table 4.23 Stable isotope measurements

S.No	Sample ID	δD (‰)	$\delta^{18}\text{O}$ (‰)
1	BHAR01	-9.09	-2.06
2	BHAR02	-11.09	-1.81
3	BHBR02	-10.12	-2.21
4	OWAR01	-12.05	-2.30
5	OWAR02	-8.89	-2.12
6	OWBR01	-15.16	-2.42
7	OWBR02	-12.09	-2.23
8	PAR	-6.93	-1.62
9	PBR	11.46	2.73
10	RS	-1.26	0.43
11	SW03	-2.92	-0.88

The lighter molecules in water tend to evaporate faster as compared to heavier molecules. Subsequently, the isotopic concentration recorded from the residual water is the isotopic ratio calculation. The analysis indicated that all water bodies under the experimentation are shallow and represented closely related values of isotopic concentration. When compared with the local meteoric water line, (Warrier et. al, 2010) the results obtained were found to be very close to each other. It indicated that the major source of water replenishment was rainfall only. The pond water (PBR= 11.46 δ D (‰) and 2.73 δ ¹⁸O (‰) being an open source, indicated slightly enriched water due to the direct evaporation from a greater surface area.

4.10. MODELLING OF LATERAL FLOW USING HYDRUS-2D

The simulation of the two subsurface hydrological processes occurring in the site was carried out in HYDRUS-2D. The software accessibility was provided by Indian Institute of Technology (IIT, Mandi), Himachal Pradesh. Among the various experimental set ups described in section 4.9, installed at site 2 to monitor lateral flow, line application of water in 50 cm trench was used to simulate lateral flow through HYDRUS-2D. Since the point application of water through the trench was comparatively more controlled spatially and temporally, simulation using HYDRUS was considered to be more rendering. The problem was defined by dividing the flow region into finite element mesh as depicted in figure 4.74. The shapes of FE mesh were defined by the coordinates of the nodes that form the element corners (Simunek *et al.*, 1999). The water flow parameters were calculated using neural network prediction (Rosetta) model. The model was independently developed by Marcel Schaap at the U.S. Salinity Laboratory. HYDRUS coupled with Rosetta Lite DLL (Dynamically Linked Library) implements pedotransfer functions (PTFs) to predict van Genuchten water retention parameters and the saturated hydraulic conductivity (Ks) (Simunek *et al.*, 1999). The model was used to predict site specific parameters which are tabulated in table 4.23.

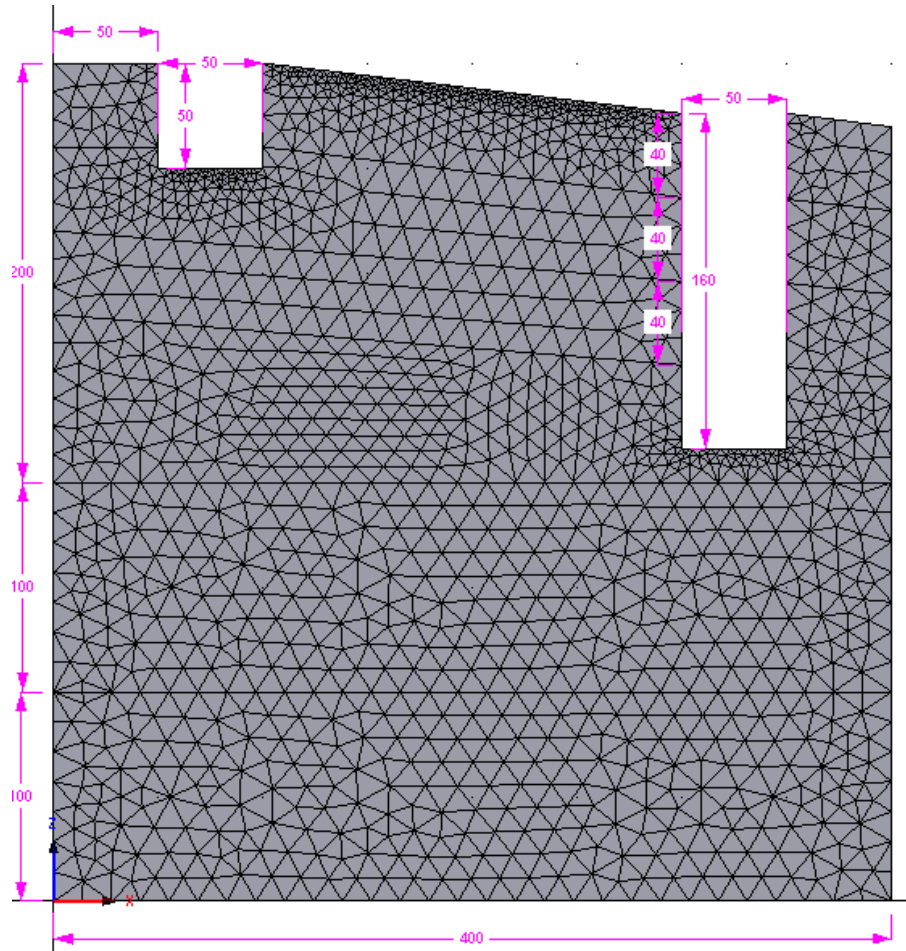


Figure 4.74 FE mesh with domain properties in HYDRUS-1D

Table 4.24 Material properties for water flow derived from Rosetta model

S.no	Name	θ_r	θ_s	α	n	K_s	l
1	Material 1	0.0404	0.4489	0.0392	1.5335	8.232917	0.5
2	Material 2	0.0408	0.4787	0.0368	1.4582	10.10542	0.5
3	Material 3	0.0397	0.4339	0.0336	1.4777	5.902083	0.5

Where,

θ_r = Residual soil water content

θ_s = Saturated soil water content

α , n = Empirical coefficients affecting the shape of the hydraulic functions

K_s = Saturated hydraulic conductivity

l = Tortuosity parameter in the conductivity function

Material 1, 2, and 3 represents the soil layers at depths of 0-40 cm, 40-80 cm and 80-120 cm respectively.

The simulation to analyse lateral flow was carried out for duration of 24 hours. The simulated volumetric water content recorded a similar pattern of lateral flow upsurge with time as that of the observed volumetric water content recorded in the field and has been illustrated in figure 4.75 (a). The temporal variation of simulated pressure head at three different observation nodes is shown in figure 4.75 (b). Observation node N1 representing 0-40 cm of soil depth recorded the highest volumetric water content. Even though with a greater porosity measured at soil depth of 40-80 cm, the soil depth recorded lesser variation compared to that at soil depth of 0-40 cm during this specific experimental set up. This was noted both during experimental observation and simulation of the hydrological process through HYDRUS-2D. This can be attributed to the position of TEROS 12 sensor which was installed at a depth of 60 cm from the soil surface. It was found from the observations that the simulated and observed results showed greater lateral flow of water when line application of water is done through deeper soil profile in site 2. The calculated correlation coefficient between the simulated and observed values of volumetric water content was obtained are shown from figure 4.76 to figure 4.78. It established the efficacy of HYDRUS-2D in simulating lateral flow in the site.

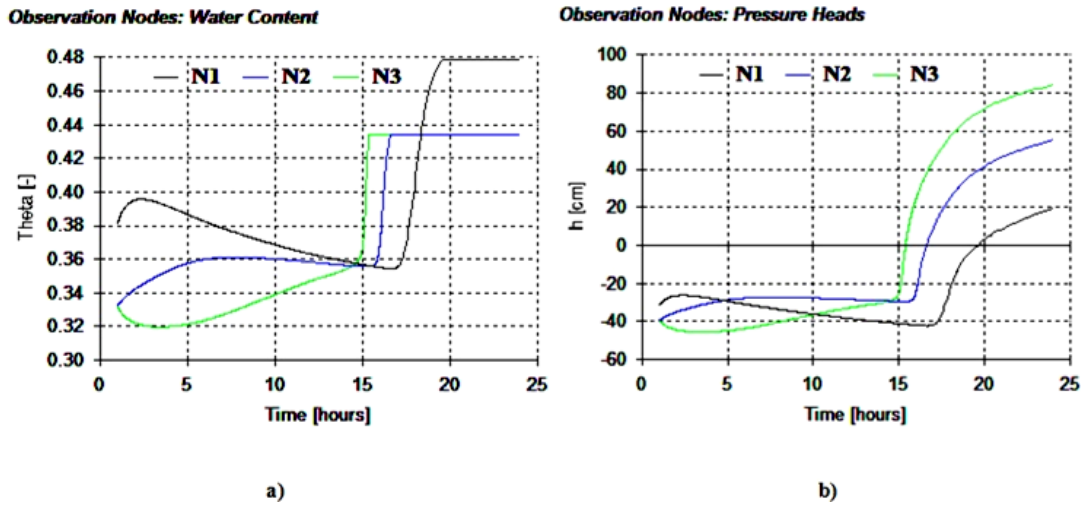


Figure 4.75 (a) Temporal variation of simulated VWC (%) at three different observation nodes in site 2, (b) Temporal variation of simulated pressure head at three different observation nodes in site 2

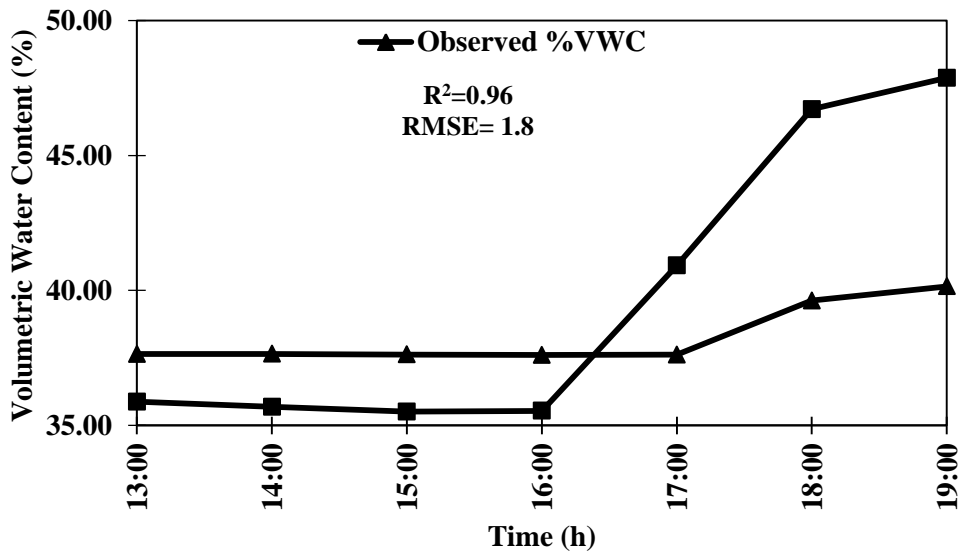


Figure 4.76 Simulated and observed % VWC for soil depth of 0-40 cm in site 2

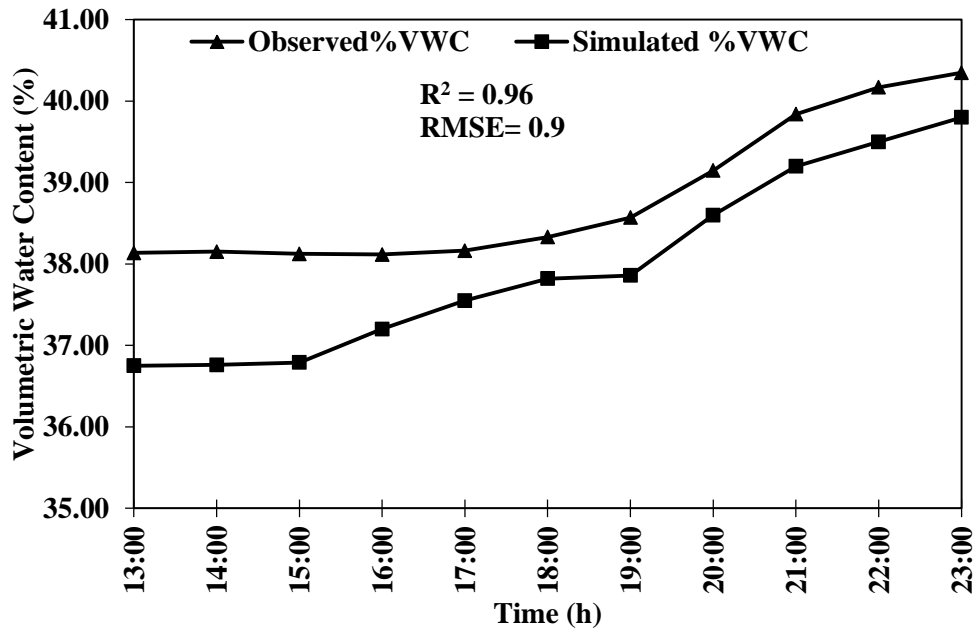


Figure 4.77 Simulated and observed % VWC for soil depth of 40-80 cm in site 2

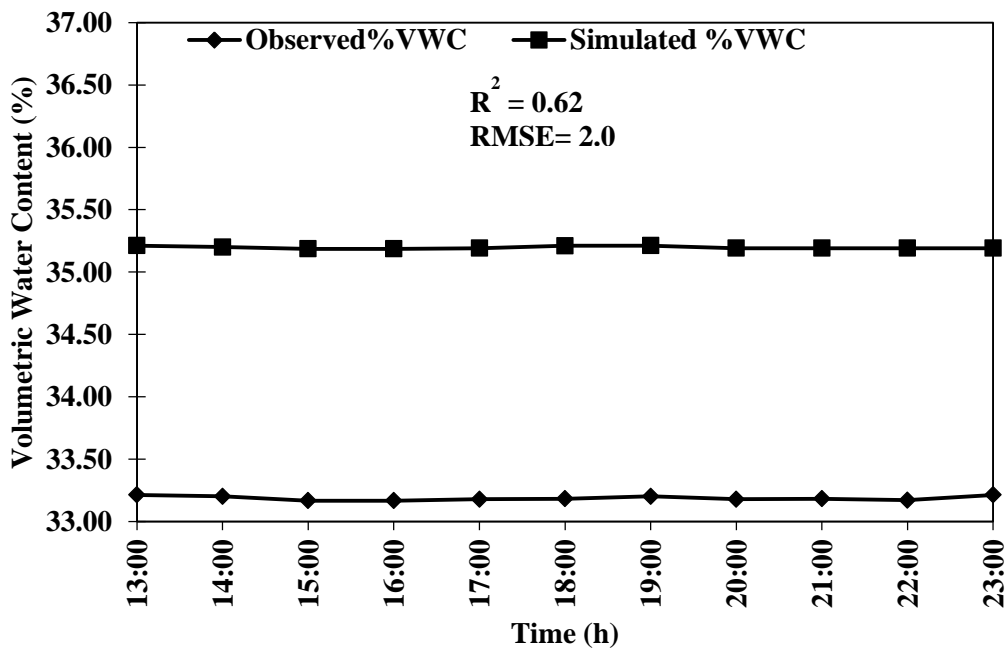


Figure 4.78 Simulated and observed % VWC for soil depth of 80-120 cm in site 2

The slight variations observed in the simulated % VWC when compared to observed % VWC at 0-40 cm depth may be attributed to the assumptions of negligible specific plant root water uptake in a day and the effect of varying soil temperature on lateral flow movement in the site. Subsequently, at soil depths of 40-80 cm and 80-120 cm the degree of correlation coefficient reduced. The observed values of % VWC at these two depths didn't show any relative increase. The simulated and observed % VWC at soil depth of 80-120 cm was found to be constant at 43.9 % and 33.2 - 33.1 % respectively. It can be fairly attributed from the results that a greater interval of temporal data may provide greater insight into the drainage pattern of the soil profile in the site. As the present research was entirely focused on addressing the velocity of subsurface flow and its pattern, the experiment was stopped when the soil reached its maximum water holding capacity. Thus, the lower soil depths of 40-80 cm and 80-120 cm showed a decline in their respective degree of correlation in between the simulated and observed values of % VWC. The cumulative variable boundary flux curve for the 50 cm line source trench as shown in figure 4.79 indicated the variation of cumulative flux with time across the line source trench boundary. It represented the high porosity and lateral conductivity of water in the site.

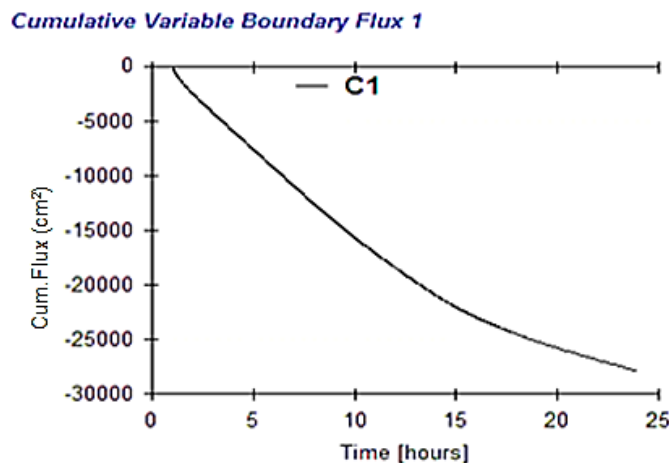


Figure 4.79 Temporal variation of cumulative flux across line source trench in site 2

The corresponding soil water retention curves for the three different soil profile depths (material 1, 2 and 3) for monitoring trench face in site 2 are indicated in figure 4.80.

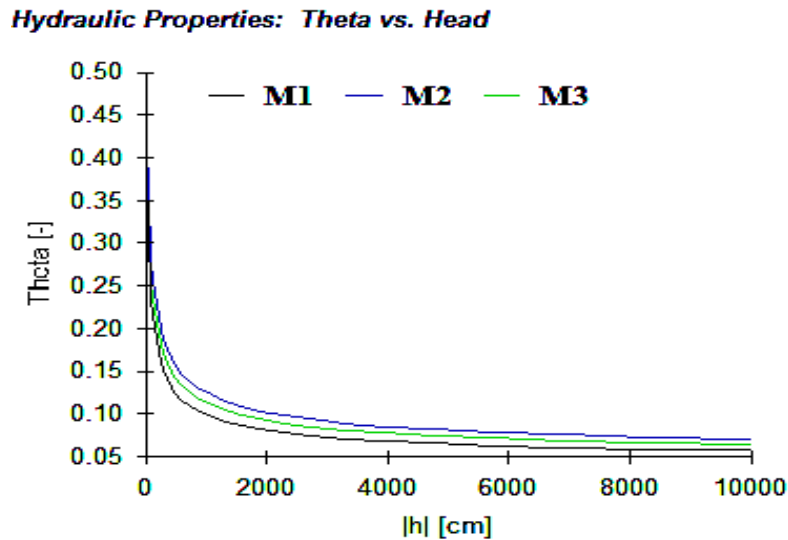


Figure 4.80 Soil water retention curve for soil materials at three different soil depths in site 2

The soil water retention curve clearly indicated larger sand pores at all the three soil depths affirming greater percentage of sand in site 2. Highest soil water retention capacity of soil material at soil profile depth of 40-80 cm was observed when compared to soil materials at other two profile depths. This was established from the highest porosity value and lowest value of bulk density at 40-80 cm of soil depth as described in section 4.4. Similarly, the rate of drainage from the soil profile depth of 40-80 cm was higher as compared to other soil profiles under the observation.

The simulated two dimensional movement of water for the representative duration in site 2 has been exhibited from figure 4.81 to figure 4.88.

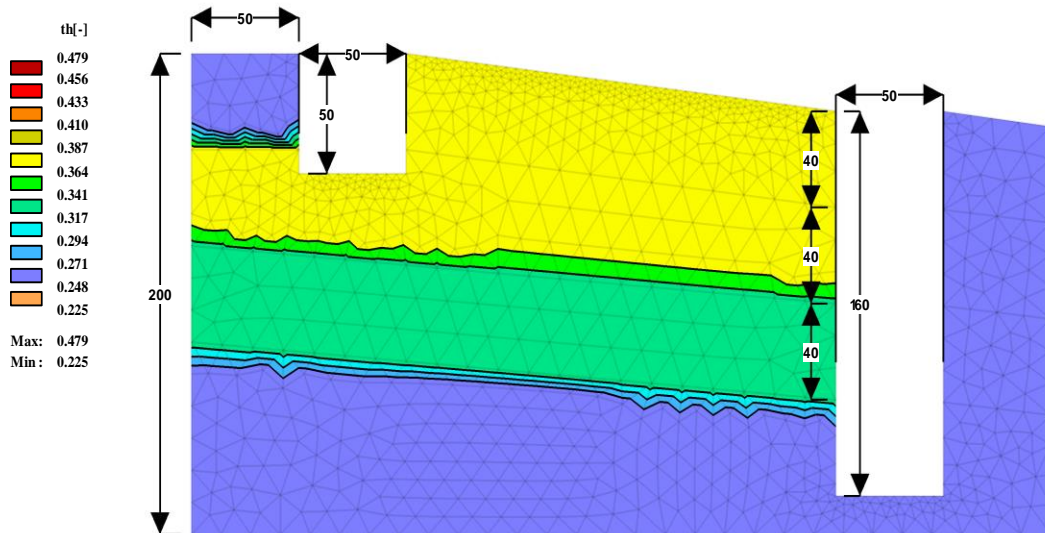


Figure 4.81 Simulated two dimensional distribution of water content in the soil profile at $t = 0$ in site 2

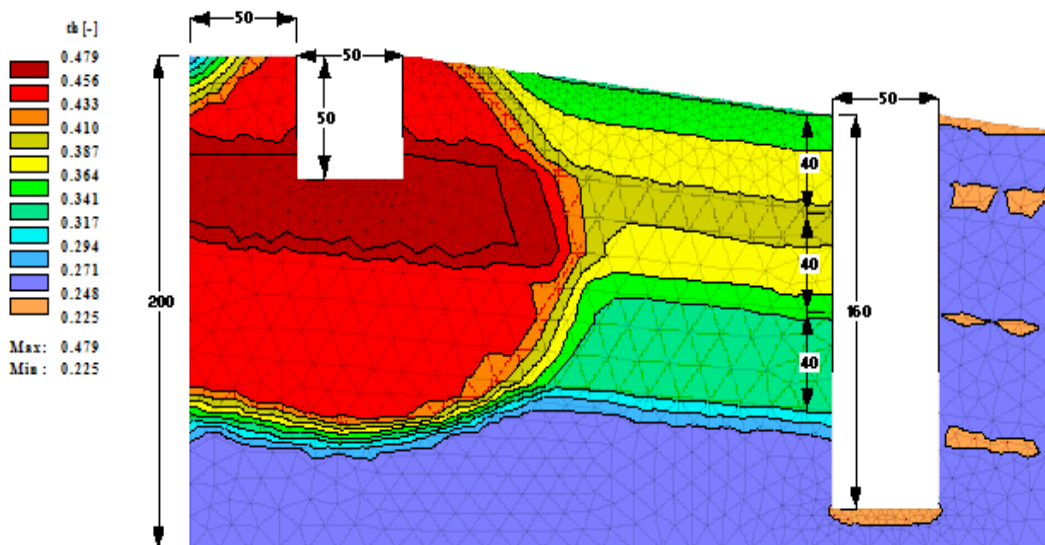


Figure 4.82 Simulated two dimensional distribution of water content in the soil profile at $t = 1h$ after line application of water in site 2

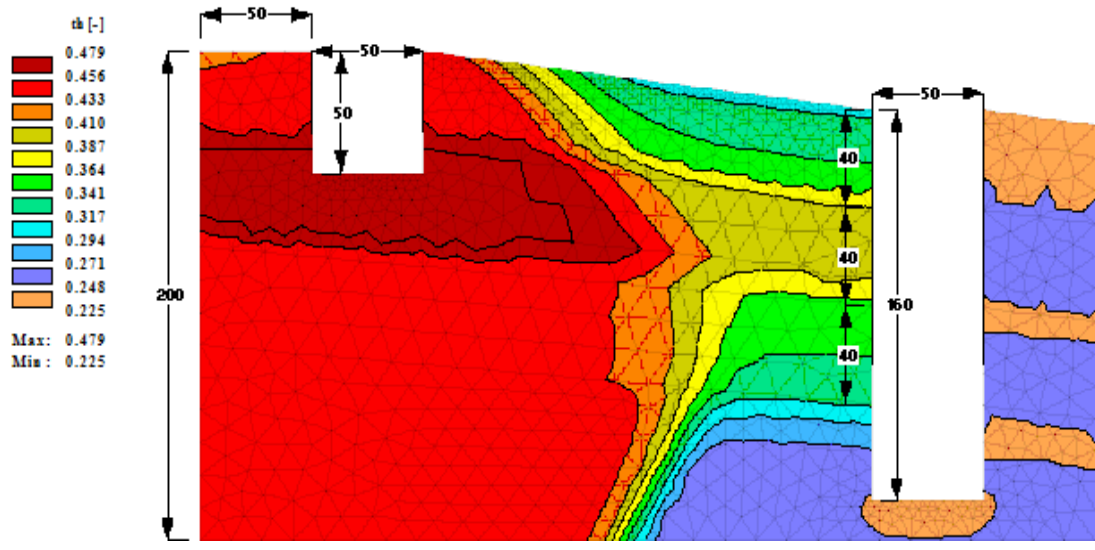


Figure 4.83 Simulated two dimensional distribution of water content in the soil profile at $t = 4$ h after line application of water in site 2

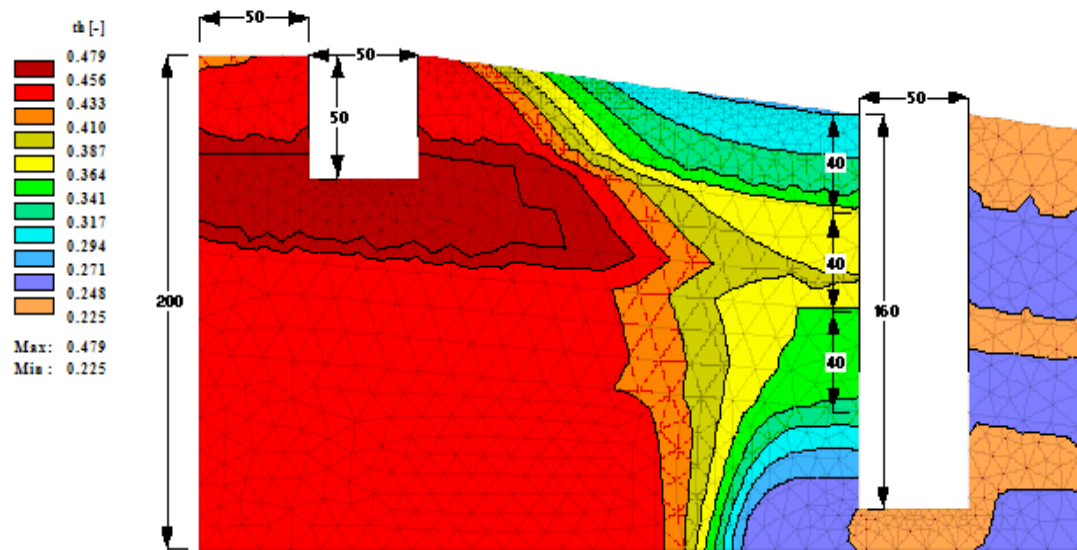


Figure 4.84 Simulated two dimensional distribution of water content in the soil profile at $t = 8$ h after line application of water in site 2

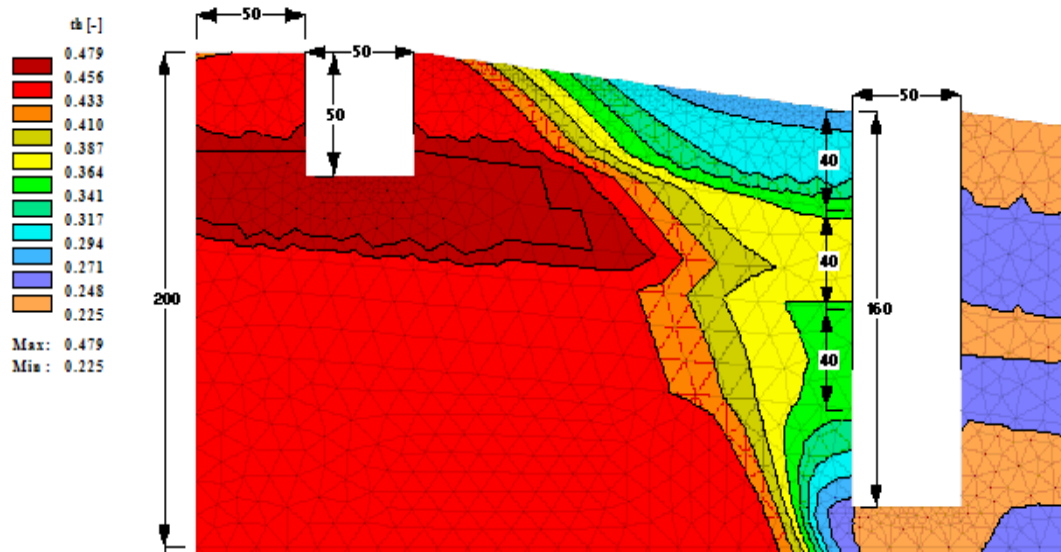


Figure 4.85 Simulated two dimensional distribution of water content in the soil profile at $t = 12$ h after line application of water in site 2

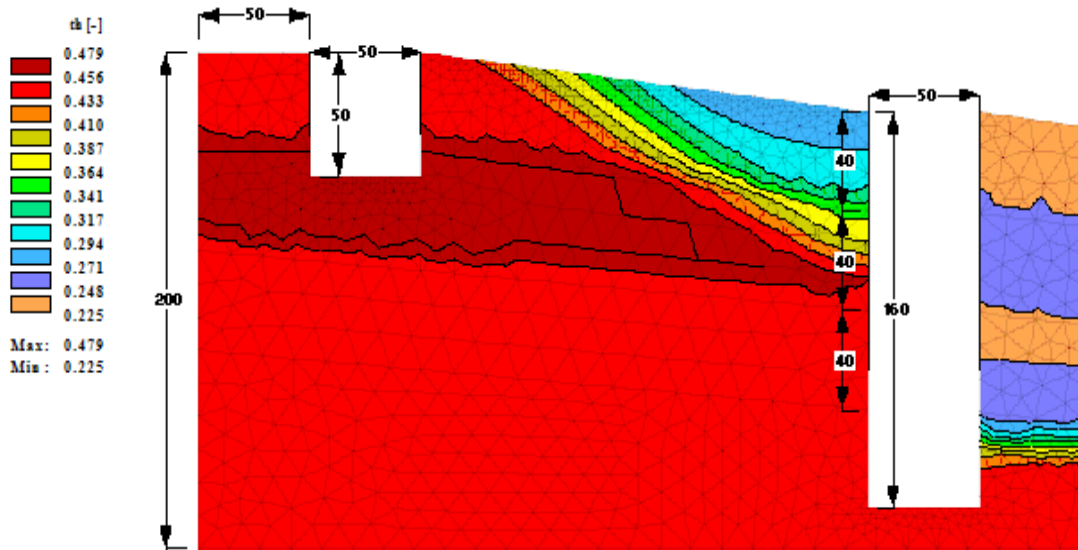


Figure 4.86 Simulated two dimensional distribution of water content in the soil profile at $t = 16$ h after line application of water in site 2

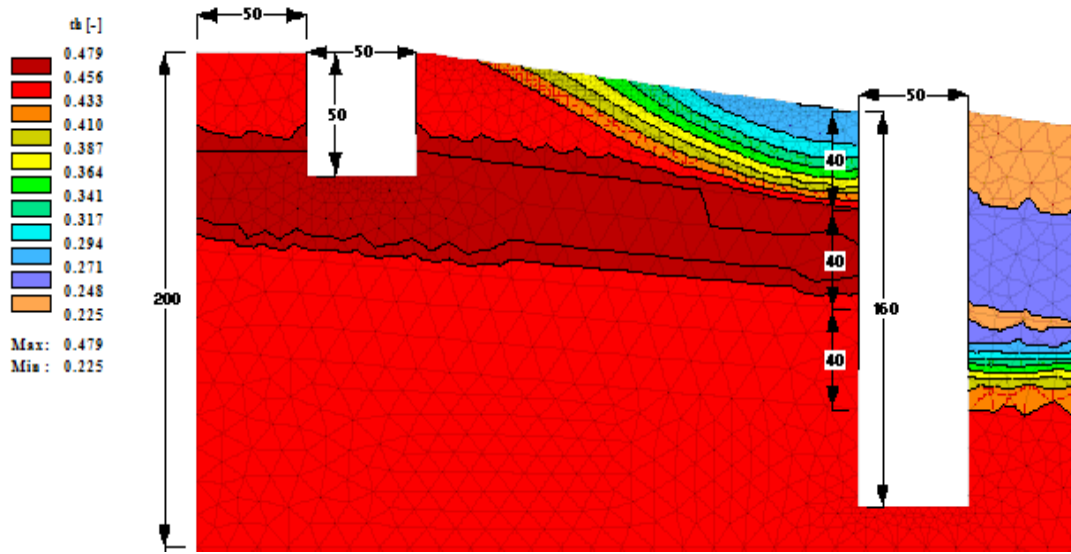


Figure 4.87 Simulated two dimensional distribution of water content in the soil profile at t =18 h after line application of water in site 2

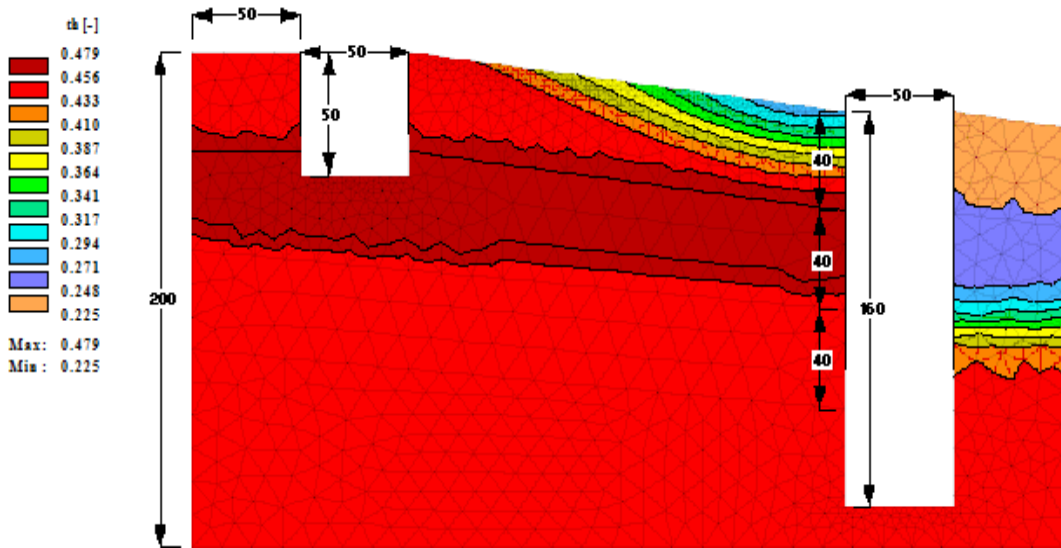


Figure 4.88 Simulated two dimensional distribution of water content in the soil profile at t =20 h after line application of water in site 2

The 0th hour represented the initial percentage of volumetric water content in the site prior to the application of water in line source trench. The first sensor was installed at a depth of 40 cm from the soil surface to represent the volumetric water content variation from the soil depth of 0-40 cm at the site. Simultaneously, the second and third sensors were installed at 60 cm and 120 cm soil depths respectively. A boundary condition of no flux was chosen for the bottom boundary of domain. Although the simulation was carried out for 24 hour duration, similar distribution of % VWC variation was observed in simulated and observed values from 13th hour of experimentation. Minimum value of simulated water content distribution was observed at other side of the monitoring trench. A major advancement of applied water plume was observed as lateral flow in between the soil depth of 30 cm to 60 cm. It was recorded by the sensor installed at 40 cm depth which represented maximum % VWC in between $t = 16$ to $t = 17$. The simulated velocity of flow matched with the observed velocity recorded by the sensors in the field. A rapid upsurge and decline in % VWC was represented by the soil layer at 34 cm to 60 cm of soil profile.

4.11 MODELLING OF BASE FLOW USING HYDRUS-2D

The two dimensional simulation of water movement, assessed through salt (KCl) tracer was carried out for the initial set up installed at site 1. The set up chosen for the simulation is shown in figure 4.89. The simulation was carried out for a period of 24 hours. A standard solute and water transport simulation was chosen in HYDRUS-2D. The simulated salt (KCl) tracer breakthrough in monitoring well A noted at observation node N1 in site 1 is shown in figure 4.90. The simulated and observed pattern of tracer (KCl) plume represented a similar temporal breakthrough in the monitoring well which has been represented by figure 4.91. The calculated coefficient of correlation was obtained as 73.1%. The correlation coefficient represented a fairly good correlation between the simulated and observed entities.

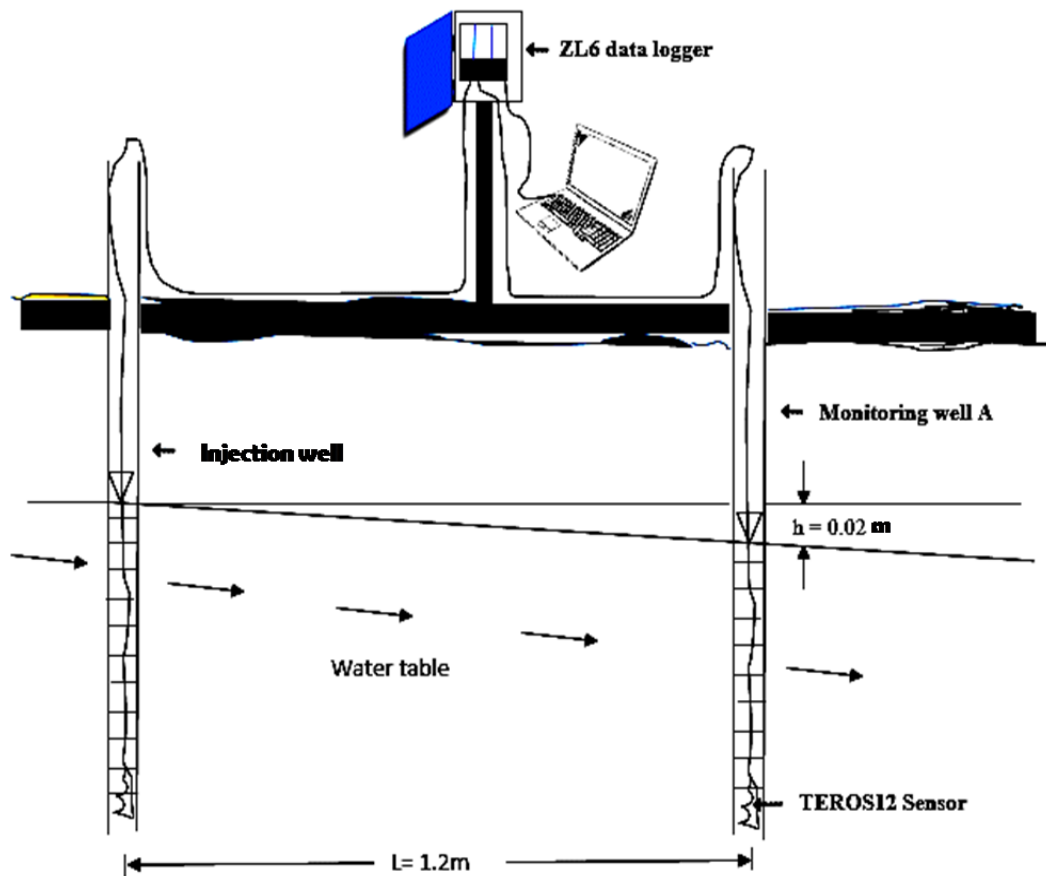


Figure 4.89 Field set up for simulation of velocity of flow in shallow wells in site 1

However, the R^2 value obtained can be attributed to the molecular diffusion of solute in free water and soil air (Leij et.al, 1999) which was assumed zero for the present research. The two dimensional solute concentration distributions for the representative duration after the solute pulse injection in site 1 have been shown from figure 4.92 to figure 4.98.

Observation Nodes: Concentration

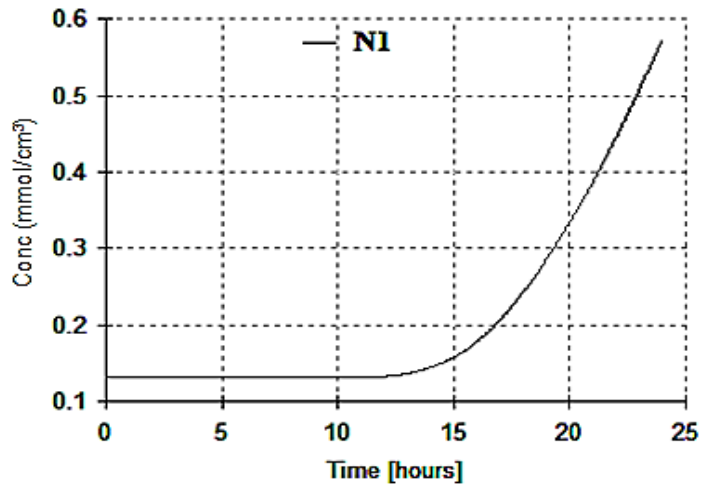


Figure 4.90 Simulated salt (KCl) tracer breakthrough in monitoring well A at observation node N1 in site 1

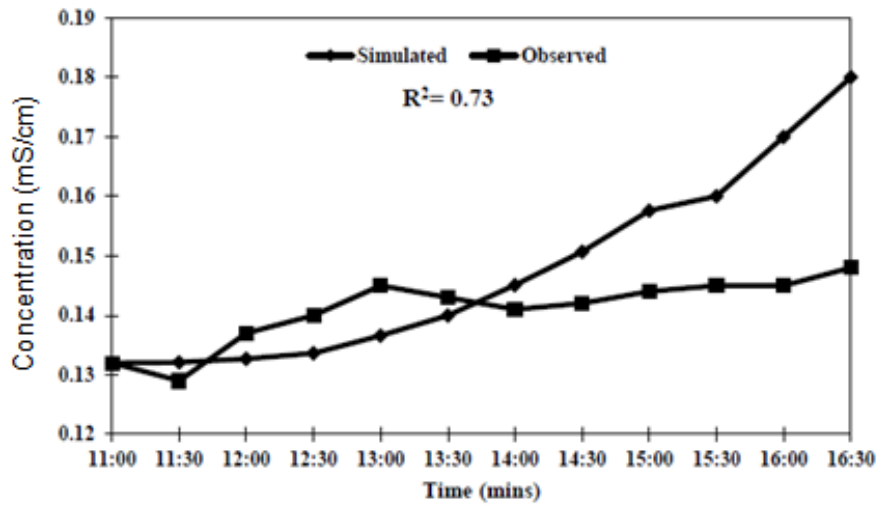


Figure 4.91 Simulated and observed salt (KCl) tracer breakthrough in monitoring well A at site 1

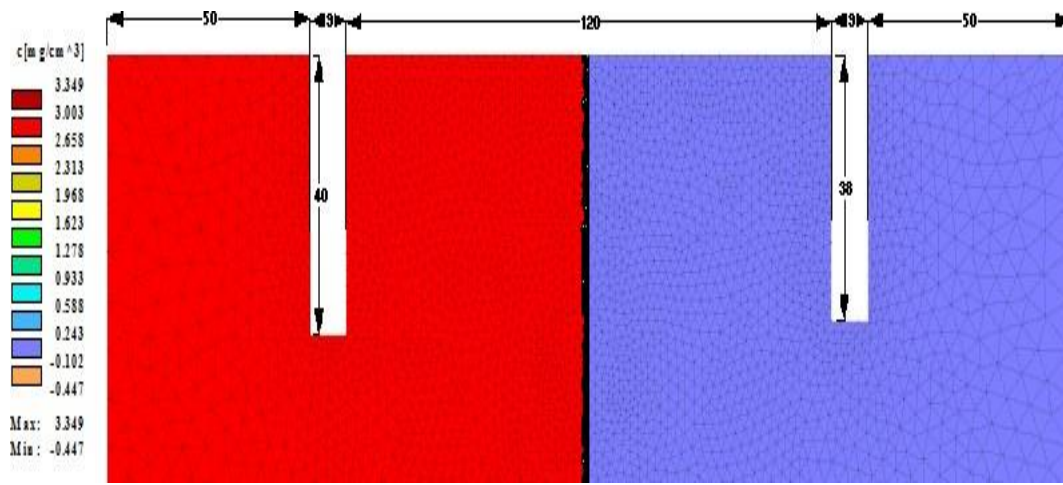


Figure 4.92 Simulated two dimensional distribution of salt tracer in the soil profile at $t = 0$ h in site1

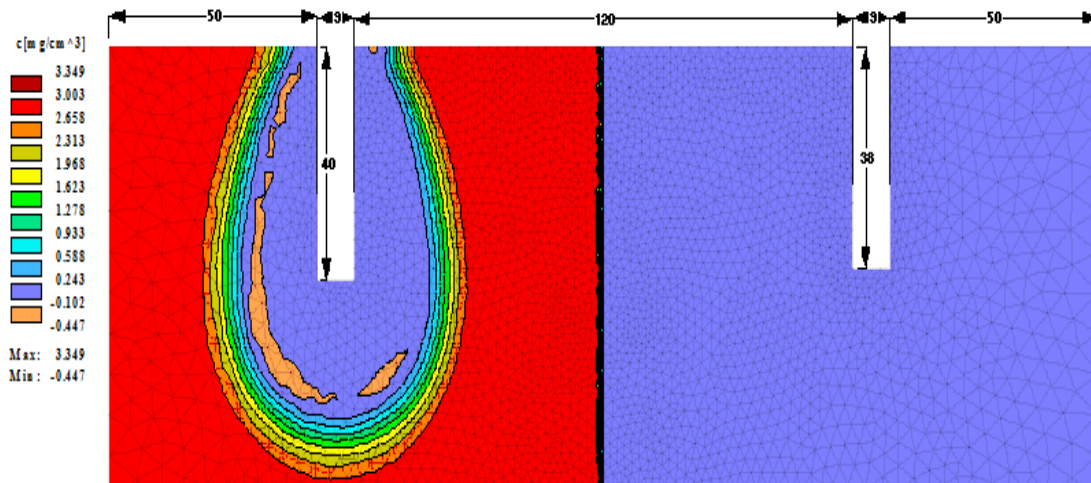


Figure 4.93 Simulated two dimensional distribution of salt tracer in the soil profile at $t = 1$ h in site1

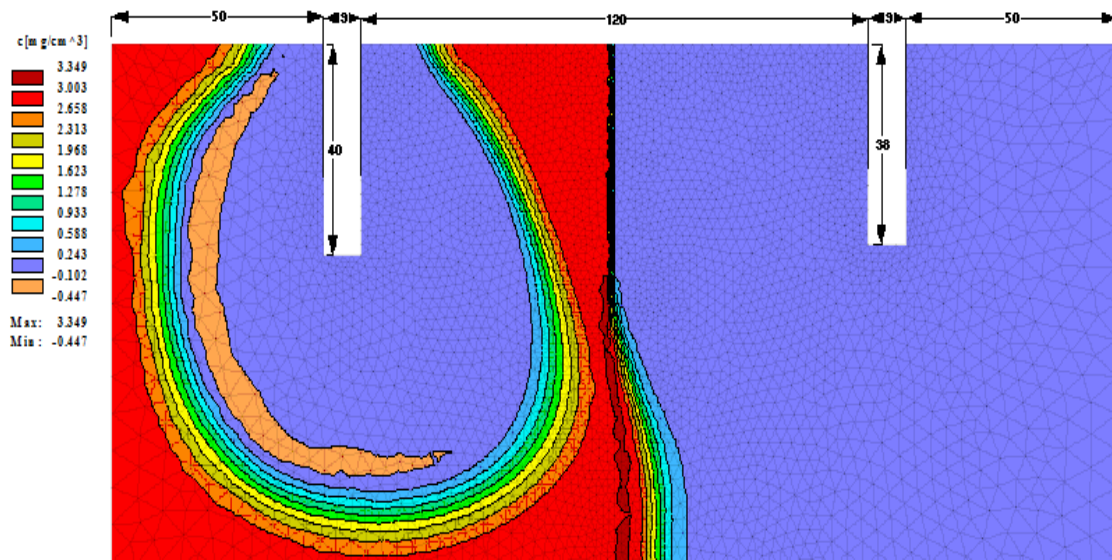


Figure 4.94 Simulated two dimensional distribution of salt tracer in the soil profile at $t = 4$ h in site1

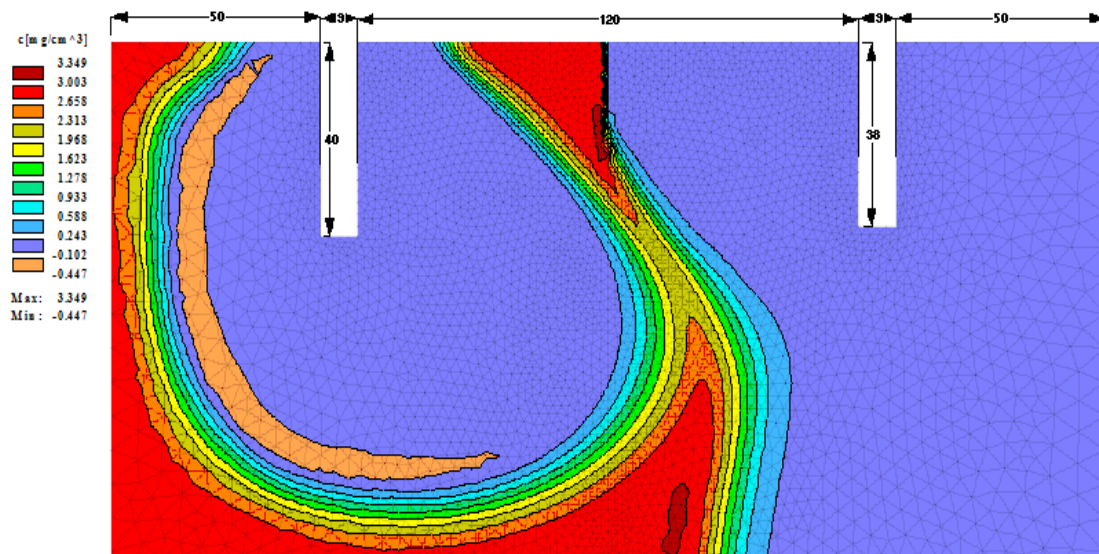


Figure 4.95 Simulated two dimensional distribution of salt tracer in the soil profile at $t = 8$ h in site1

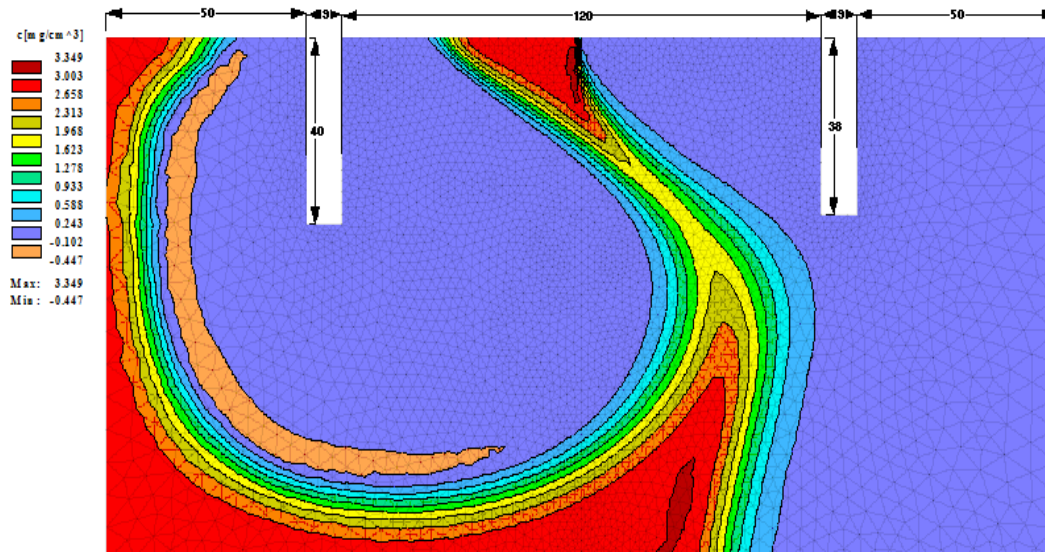


Figure 4.96 Simulated two dimensional distribution of salt tracer in the soil profile at $t = 12$ h in site1

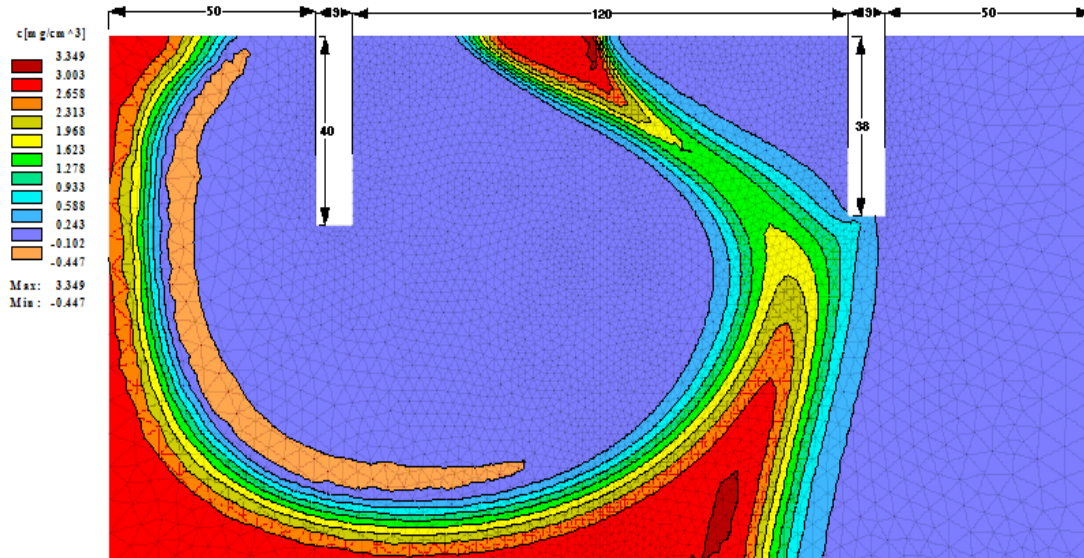


Figure 4.97 Simulated two dimensional distribution of salt tracer in the soil profile at $t = 16$ h in site1

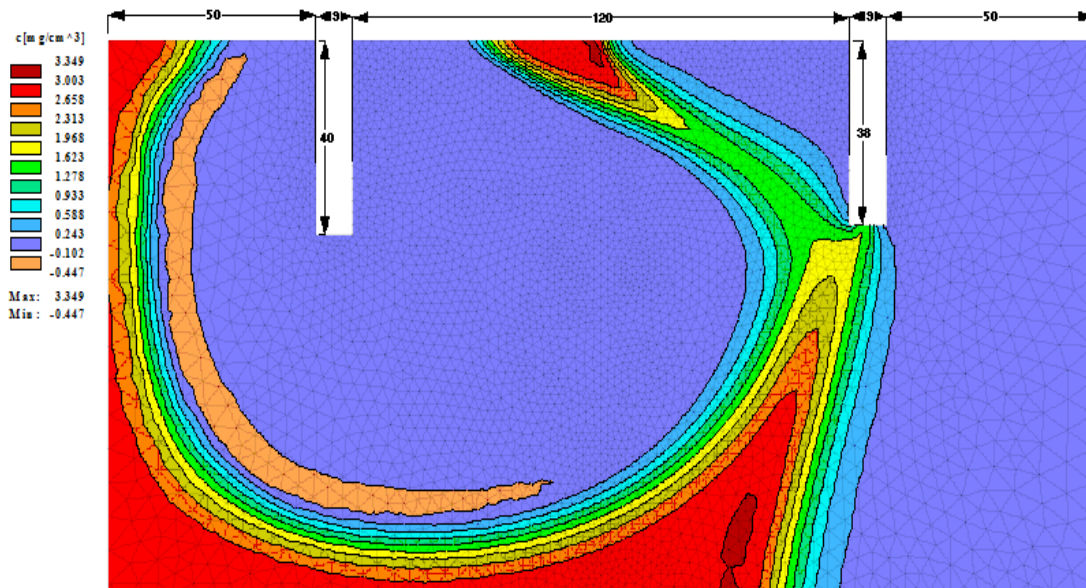


Figure 4.98 Simulated two dimensional distribution of salt tracer in the soil profile at t = 20 h in site1

The two dimensional simulated solute distribution was done in the vertical XZ plane. The solute concentration at observation node 1 recorded an increase at 11:30 h. The slight variation recorded was 0.132 mmol/cm^3 from the initial concentration of 0.130 mmol/cm^3 . The temporal variation of simulated and observed breakthrough of tracer recorded by TEROS12 sensor was found in correlation with each other. The rapid diffusion of salt (KCl) tracer can be attributed to decreasing solvent density which was apparently due to pulse injection of tracer.

4.12 INTERVENTIONS FOR GROUND WATER RECHARGE AND STORAGE

This study, which was intended to investigate, determine and predict lateral flow and base flow, has made a thorough experimentation and analysis of the process mentioned above. Practical utility of this work will go unfulfilled if interventions for groundwater recharge and storage are not given as recommendations based on the findings from the study. Therefore, some of the interventions possible for lateritic terrain for conserving water are given below.

It could be inferred from this study that lateral flow takes place in a soil profile depth of 30-100 cm which is predominantly the root zone. It is also seen that the main factor inhibiting the downward movement of water in the soil profile (deep percolation) is the presence of entrapped air in the soil pore space which blocks the downward movement of water. The entrapped air from the soil pores should escape to make way for the water to move downward for it to reach the groundwater storage.

Hence, recharge of groundwater has to be done by pits or trenches deeper than 1 m to 1.5 m. The downward movement of water from the pits will help major portion of this water to reach groundwater storage. All concentrated surface runoff has to be recharged in this fashion. In the case of continuous slope, to make the groundwater recharge more effective, trenches of 1 m to 1.5 m depth can be constructed at regular intervals across the slope. These trenches can be partially filled with locally available stone to avoid the undesirable attributes of deep trenches in agricultural land. Trenching and lining of the downslope face of the trench with polythene film and then backfilling of the trench with soil can also be adopted if presence of trenches on the ground needs to be eliminated altogether. Deep rooted trees can be planted as a line across the slope at regular intervals to intercept the lateral flow and to direct the subsurface flow in the downward direction to reach groundwater reservoir.

All buildings and impervious surfaces such as roads and pavements should have recharge pits of depth 1.5 m to 2 m to avoid the concentrated runoff moving directly to the neighbouring drain channel. The Central and State governments should bring a necessary law enforcement in this regard to make it obligatory by all sections of the society.

SUMMARY AND CONCLUSIONS

A study has been undertaken to monitor, and quantify two important hydrological phenomenon taking place in the land phase of the hydrological cycle as these two processes are very important from the point of view of in-situ water conservation. Understanding micro level water balance is very essential for suggesting site specific and scientific water conservation plans. At the same time, quantitative information on subsurface water flow phenomenon is very rare and inadequate. Therefore, this study has been proposed to determine the lateral and base flow taking place in a lateritic terrain, one of the common landforms in the midland of Kerala State, India. The study envisages determining lateral flow at different depth ranges of the root zone by monitoring the soil moisture using different techniques and also through salt tracers. Base flow monitoring has been made through the water table recordings of observation wells and through the application of salt tracer and environmental isotopes.

Further, the study has been extended to modelling of the lateral flow and base flow phenomena with the help of HYDRUS-2D software, so that the result of the study can be used in other areas too. The HYDRUS-2D model has been calibrated for both lateral flow and base flow. Thus, the model can be made use of for the estimation of subsurface flow phenomena in the terrains with similar environmental settings.

To carry out the field study and data collection three different sites at K.C.A.E.T Tavanur, Kerala campus have been identified and different field experiments were carried out. Different experimental set ups involved different techniques for the inducement of lateral flow such as simulation of rainfall by micro-sprinkling, line application of water in shallow trenches and natural rainfall. Lateral flow was monitored by observing the soil moisture variations at the vertical faces of the trenches made upto root zone depth. Salt tracer was also employed to monitor the movement of lateral flow and EC measurements were made to record

the breakthrough of salt.

In order to monitor the base flow, observation wells were constructed at closer distance apart and their water table was measured at periodic intervals. Salt tracer injections were made to the upper most well and its impact in other lower-positioned wells was monitored. Further, isotope study was also carried out to understand more on the base flow movement in the lateritic terrain.

The various results obtained from this study have been summarized below:

1. The rainfall recorded for two years have shown considerable variations in the monthly rainfall at the study area. The total number of rainy days recorded for the study area in 2018 and 2019 were 121 days and 117 days respectively. The area registered a total rainfall of 3322 mm and 2615 mm in the year 2018 and 2019 respectively. The August month of 2018 recorded the highest rainfall of 1104 mm whereas a deficit was recorded in August, 2019 with a monthly recorded rainfall of 597 mm.
2. Though the three experimental sites were geographically very close to one another, soil texture at each site showed significant variations. It represented the heterogeneity of soil layers with respect to spatial variation and layers.
3. The calculated lateral flow from soil moisture data obtained from 2 m deep soil profile in experimental site 1 accounted for 10.06 % of the total simulated rainfall. Out of the total lateral flow recorded at site 1 26.37 %, 30.03 % and 43.59 % took place through soil depth ranges of 0-40 cm, 40-80 cm and 80-120 cm respectively. The variations are attributed by the changes in soil bulk density and the relative presence of macropores.
4. In site 2, the soil horizon depth of 40-80 cm had the least bulk density and

the highest porosity as compared to the other two depths under observation. The recorded rate of interflow discharge was also the highest at 40-80 cm soil profile depth. Thus, a direct correlation was found in between the soil bulk density and interflow discharge rate.

5. In the case of line application of water for inducing lateral flow the experiment was conducted through a 30 cm deep trench. It represented the tortuosity of the soil layers in site2. A diffused form of soil water movement was noted when enough opportunity time was provided for the water to recede during the intermittent water application in the site. The average calculated lateral flow discharge rate from the three lateral cross-sectional areas were 10.44 $l/m^2/day$, 13.35 $l/m^2/day$ and 18.58 $l/m^2/day$ for soil depth ranges of 0-40 cm, 40-80 cm and 80-120 cm respectively. The average seepage velocity obtained was 2.13 cm/day, 2.42 cm/day and 3.7 cm/day from the soil depths of 0-40 cm, 40-80 cm and 80-120 cm respectively.

When water was applied as a single pulse in site 2 through a 50 cm deep trench the travel time and residence time taken by the soil water reduced and was discrete for different soil depths. With the application of water equal to the volume of line source trench and volume of soil to be wetted in between monitoring and line source trench, the interflow rate of discharge calculated for the observation nodes were 28.12 $l/m^2/day$, 23.50 $l/m^2/day$ and 2.05 $l/m^2/day$ respectively. The average seepage velocity of flow calculated was 5.7 cm/day, 4.27 cm/day and 0.41 cm/day for the three successive soil depths. Thus, when a pulse injection of water of volume, enough to wet the soil column in between line source and monitoring trench was applied, the soil layer with greater porosity conveyed the maximum soil water with greater seepage velocity and minimum vertical infiltration into the soil.

During natural rainfall conditions of south west monsoon in site 2, a similar pattern of lateral flow movement was observed with an average discharge rate of 13.35 l/m²/day, 27.67 l/m²/day and 9.48 l/m²/day through soil profile depths of 0-40 cm, 40-80 cm and 80-120 cm respectively.

6. The experiments carried out during the north-east monsoon season at site3. An interflow of mere 1.52 l/m²/day, 1.87 l/m²/day and 1.70 l/m²/day was recorded from the successive soil depths under experimentation. Subsequently, the average seepage velocity calculated was 0.2 cm/day, 0.36 cm/day and 0.56 cm/day from soil depths of 0-40 cm, 40-80 cm and 80-120 cm respectively.
7. It became evident from the experiments conducted in site 2 and site 3 that NaCl undergoes molecular diffusion due to the pre-saturated condition of soil due to the monsoon rains. Breakthrough of salt ions at the monitoring nodes was earlier to the detection of soil moisture by the sensors.
8. The efficacy and detection of salt (NaCl) tracer in an experiment relies on the background salt concentration of the solution and the mass of tracer used. Through the tracer experiment at site2, it was seen that the mass of tracer to be applied should result in an increase in EC upto three times of its initial value to give an appreciable breakthrough signals.
9. The average apparent linear flow velocity and the estimated hydraulic conductivity through the shallow observation well were obtained as 1.35 m/day and 80.3 m/day respectively. The calculated value of hydraulic conductivity represented a shallow aquifer with apparently greater percentage of medium to fine sand in the experimental site (Domenico P.A

et al., 1998).

10. The observed and the simulated distribution of volumetric water content by HYDRUS-2D exhibited a correlation coefficient of 96.4 %. It established the efficiency of HYDRUS-2D in simulating lateral flow for the lateritic terrain.

The following conclusions can be drawn from the study:

1. The physical properties of the soil show considerable variation even for small geographical separations and with respect to minor profile depth variations in laterite terrains.
2. Continuous soil moisture monitoring using calibrated capacitance based soil moisture sensors is an accurate and effective method of determining lateral flow.
3. It is seen that the most important physical property of the soil which govern the lateral flow is bulk density effective porosity and soil texture.
4. The percentage of lateral flow to the total rainfall received depends upon the physical properties of the soil, land slope and the intensity and duration of precipitation.
5. NaCl can be treated as an effective tracer to monitor the subsurface flow; however molecular diffusion of the salt due to antecedent moisture content remains as a hindrance to its use during rainy season.
6. KCl has been proved to be an effective salt in the study of base flow monitoring even though it is subject to diffusion in free water.
7. HYDRUS-2D software could predict the lateral flow discharge with a correlation coefficient of 96.4 % and base flow with 73 %.
8. The study suggests that though the infiltration capacity of the lateritic soil is

very high, major portion of the infiltrated water moves laterally without reaching water table. To augment groundwater recharge, more preferential flow in the vertical direction has to be enhanced through the presence of deep rooted vegetation. Else mechanical barriers to check lateral flow and to divert that in the downward direction are required.

The following suggestions are given for future research in this area:

1. A mineralogical analysis for deeper soil profiles in the site, prior to the installation of experimental set ups would be of considerable assistance in understanding the subsurface hydrological processes in a lateralized crystalline and the tertiary rock formations.
2. Monitoring trenches of greater depth and horizon will aid in identifying the appropriate water harvesting structures depending upon the heterogeneous macroscopic and microscopic characteristics of deeper soil profiles. It will also aid in better simulation of the subsurface movement of water.
3. Simultaneous analysis of event rainfall and percentage volumetric water content variation at different soil depths may help in the precise estimation of velocity of interflow through different soil profiles.
4. A prior laboratory analysis of tracers is suggested to infer diffusion of solute in free water and soil air.
5. Injection of tracers may produce reliable breakthroughs during the post monsoon season. Thus, the experiments need to be carried out accordingly. After a salt tracer experiment has been conducted in a field it is essential to leach out the remaining salts from the field before carrying out a new experiment.

REFERENCES

- Aayog, N.I.T.I., 2019. Composite Water Management Index: a tool for water management.
- Anderson, A.E., Weiler, M., Alila, Y. and Hudson, R.O., 2009. Dye staining and excavation of a lateral preferential flow network. *Hydrology and Earth System Sciences*, 13(6), pp.935-944.
- Anderson, A.E., Weiler, M., Alila, Y. and Hudson, R.O., 2009. Subsurface flow velocities in a hillslope with lateral preferential flow. *Water Resources Research*, 45(11).
- Anderson, M.G. and Burt, T.P., 1990. Process studies in hillslope hydrology: an overview. In *Process studies in hillslope hydrology* (pp. 1-8).
- Anderson, M.G. and Burt, T.P., 1990. Process studies in hillslope hydrology: an overview. In *Process studies in hillslope hydrology* (pp. 1-8).
- Assefa, K.A. and Woodbury, A.D., 2013. Transient, spatially varied groundwater recharge modelling. *Water Resources Research*, 49(8), pp.4593-4606.
- Becker, M.W. and Shapiro, A.M., 2003. Interpreting tracer breakthrough tailing from different forced-gradient tracer experiment configurations in fractured bedrock. *Water Resources Research*, 39(1).
- Beven, K. and Germann, P., 1982. Macropores and water flow in soils. *Water resources research*, 18(5), pp.1311-1325.
- Brocca, L., Morbidelli, R., Melone, F. and Moramarco, T., 2007. Soil moisture spatial variability in experimental areas of central Italy. *Journal of Hydrology*, 333(2-4), pp.356-373.
- Brouyere, S., 2003. Modelling tracer injection and well-aquifer interactions: A new mathematical and numerical approach. *Water resources research*, 39(3).

- Cheng, C. and Chen, X., 2007. Evaluation of methods for determination of hydraulic properties in an aquifer–aquitard system hydrologically connected to a river. *Hydrogeology Journal*, 15(4), pp.669-678.
- Chow, L., Xing, Z., Rees, H.W., Meng, F., Monteith, J. and Stevens, L., 2009. Field performance of nine soil water content sensors on a sandy loam soil in New Brunswick, Maritime Region, Canada. *Sensors*, 9(11), pp.9398-9413.
- Crave, A. and Gascuel-Oudoux, C., 1997. The influence of topography on time and space distribution of soil surface water content. *Hydrological processes*, 11(2), pp.203-210.
- Dandekar, A.T., Singh, D.K., Sarangi, A. and Singh, A.K., 2018. Modelling vadose zone processes for assessing groundwater recharge in semi-arid region. *Current Science*, 114(3), pp.608-618.
- Datta, S., Taghvaeian, S., Ochsner, T.E., Moriasi, D., Gowda, P. and Steiner, J.L., 2018. Performance assessment of five different soil moisture sensors under irrigated field conditions in Oklahoma. *Sensors*, 18(11), p.3786.
- Dean, T.J., Bell, J.P. and Baty, A.J.B., 1987. Soil moisture measurement by an improved capacitance technique, Part I. Sensor design and performance. *Journal of Hydrology*, 93(1-2), pp.67-78.
- Deshpande, R.D., Bhattacharya, S.K., Jani, R.A. and Gupta, S.K., 2003. Distribution of oxygen and hydrogen isotopes in shallow groundwaters from Southern India: influence of a dual monsoon system. *Journal of Hydrology*, 271(1-4), pp.226-239.
- Devlin, J.F., Schillig, P.C., Bowen, I., Critchley, C.E., Rudolph, D.L., Thomson, N.R., Tsoflias, G.P. and Roberts, J.A., 2012. Applications and implications of direct groundwater velocity measurement at the centimetre scale. *Journal of contaminant hydrology*, 127(1-4), pp.3-14.
- Domenico, P.A. and Schwartz, F.W., 1998. *Physical and chemical hydrogeology* (Vol. 506). New York: Wiley.

- Dominguez-Nino, J.M., Arbat, G., Rajj-Hoffman, I., Kisekka, I., Girona, J. and Casadesús, J., 2020. Parameterization of Soil Hydraulic Parameters for HYDRUS-3D Simulation of Soil Water Dynamics in a Drip-Irrigated Orchard. *Water*, 12(7), p.1858.
- Du, E., Jackson, C.R., Klaus, J., McDonnell, J.J., Griffiths, N.A., Williamson, M.F., Greco, J.L. and Bitew, M., 2016. Interflow dynamics on a low relief forested hillslope: Lots of fill, little spill. *Journal of Hydrology*, 534, pp.648-658.
- Essouayed, E., Annable, M.D., Momtbrun, M. and Atteia, O., 2019. An innovative tool for groundwater velocity measurement compared with other tools in laboratory and field tests. *Journal of Hydrology X*, 2, p.100008.
- Evett, S.R., Tolk, J.A. and Howell, T.A., 2006. Soil profile water content determination: Sensor accuracy, axial response, calibration, temperature dependence, and precision. *Vadose Zone Journal*, 5(3), pp.894-907.
- Fen-Chong, T., Fabbri, A., Guilbaud, J.P. and Coussy, O., 2004. Determination of liquid water content and dielectric constant in porous media by the capacitive method. *Comptes Rendus Mecanique*, 332(8), pp.639-645.
- Flury, M. and Wai, N.N., 2003. Dyes as tracers for vadose zone hydrology. *Reviews of Geophysics*, 41(1).
- Francesca, V., Osvaldo, F., Stefano, P. and Paola, R.P., 2010. Soil moisture measurements: Comparison of instrumentation performances. *Journal of irrigation and drainage engineering*, 136(2), pp.81-89.
- Freer, J., McDonnell, J.J., Beven, K.J., Peters, N.E., Burns, D.A., Hooper, R.P., Aulenbach, B. and Kendall, C., 2002. The role of bedrock topography on subsurface storm flow. *Water Resources Research*, 38(12), pp.5-1.
- Gao, Z., Zhu, Y., Liu, C., Qian, H., Cao, W. and Ni, J., 2018. Design and test of a soil profile moisture sensor based on sensitive soil layers. *Sensors*, 18(5), p.1648.
- Gat, J.R., 1996. Oxygen and hydrogen isotopes in the hydrologic cycle. *Annual Review of Earth and Planetary Sciences*, 24(1), pp.225-262.

- Gerke, H.H. and Van Genuchten, M.T., 1993. A dual-porosity model for simulating the preferential movement of water and solutes in structured porous media. *Water resources research*, 29(2), pp.305-319.
- Germann, P. and Beven, K., 1981. Water flow in soil macropores I. An experimental approach. *Journal of Soil Science*, 32(1), pp.1-13.
- Germann, P.F., Edwards, W.M. and Owens, L.B., 1984. Profiles of bromide and increased soil moisture after infiltration into soils with macropores. *Soil Science Society of America Journal*, 48(2), pp.237-244.
- Ghasemizade, M. and Schirmer, M., 2013. Subsurface flow contribution in the hydrological cycle: Lessons learned and challenges ahead—A review. *Environmental earth sciences*, 69(2), pp.707-718.
- Ghodrati, M. and Jury, W.A., 1990. A field study using dyes to characterize preferential flow of water. *Soil Science Society of America Journal*, 54(6), pp.1558-1563.
- Gomez-Plaza, A., Martinez-Mena, M., Albaladejo, J. and Castillo, V.M., 2001. Factors regulating spatial distribution of soil water content in small semiarid catchments. *Journal of hydrology*, 253(1-4), pp.211-226.
- Gomo, M., 2019. Effects of Artefacts on Natural Gradient Single-Borehole Tracer Dilution Tests. *Natural Resources Research*, pp.1-9.
- Grayson, R.B., Western, A.W., Chiew, F.H. and Blöschl, G., 1997. Preferred states in spatial soil moisture patterns: Local and nonlocal controls. *Water resources research*, 33(12), pp.2897-2908.
- Halevy, E., Moser, H., Zellhofer, O. and Zuber, A., 1967. Borehole dilution techniques: a critical review. In *Isotopes in hydrology. Proceedings of a symposium*.
- Hardie, M., Lisson, S., Doyle, R. and Cotching, W., 2013. Determining the frequency, depth and velocity of preferential flow by high frequency soil moisture monitoring. *Journal of contaminant hydrology*, 144(1), pp.66-77.

- Harrington, G.A., Cook, P.G. and Herczeg, A.L., 2002. Spatial and temporal variability of ground water recharge in central Australia: a tracer approach. *Groundwater*, 40(5), pp.518-527.
- Harrington, G.A., Gardner, W.P. and Munday, T.J., 2014. Tracking groundwater discharge to a large river using tracers and geophysics. *Groundwater*, 52(6), pp.837-852.
- Hopp, L. and McDonnell, J.J., 2009. Connectivity at the hillslope scale: Identifying interactions between storm size, bedrock permeability, slope angle and soil depth. *Journal of Hydrology*, 376(3-4), pp.378-391.
- Ishida, S., Tsuchihara, T., Yoshimoto, S. and Imaizumi, M., 2011. Sustainable use of groundwater with underground dams. *Japan agricultural research quarterly: JARQ*, 45(1), pp.51-61.
- Jackson, C.R., 1992. Hillslope infiltration and lateral downslope unsaturated flow. *Water Resources Research*, 28(9), pp.2533-2539.
- Jacques, D., Šimůnek, J., Mallants, D. and van Genuchten, M.T., 2003. The HYDRUS-PHREEQC multicomponent transport model for variably-saturated porous media: Code verification and application. *MODFLOW and More*, pp.23-27.
- Kienzler, P.M. and Naef, F., 2008 (a). Subsurface storm flow formation at different hillslopes and implications for the 'old water paradox'. *Hydrological Processes: An International Journal*, 22(1), pp.104-116.
- Kienzler, P.M. and Naef, F., 2008 (b). Temporal variability of subsurface stormflow formation. *Hydrology and Earth System Sciences*, 12(1), pp.257-265.
- Kim, H.J., Sidle, R.C. and Moore, R.D., 2005. Shallow lateral flow from a forested hillslope: Influence of antecedent wetness. *Catena*, 60(3), pp.293-306.
- Kumar, P., 2004. Layer averaged Richard's equation with lateral flow. *Advances in Water Resources*, 27(5), pp.521-531.
- Kumar, U.S., Sharma, S. and Navada, S.V., 2008. Recent studies on surface water-groundwater relationships at hydro-projects in India using environmental

- isotopes. *Hydrological Processes: An International Journal*, 22(23), pp.4543-4553.
- Kung, K.J., Kladvko, E.J., Gish, T.J., Steenhuis, T.S., Bubenzer, G. and Helling, C.S., 2000. Quantifying preferential flow by breakthrough of sequentially applied tracers silt loam soil. *Soil Science Society of America Journal*, 64(4), pp.1296-1304.
- Larocque, M., Cook, P.G., Haaken, K. and Simmons, C.T., 2009. Estimating flow using tracers and hydraulics in synthetic heterogeneous aquifers. *Groundwater*, 47(6), pp.786-796.
- Lee, K.S. and Kim, Y., 2007. Determining the seasonality of groundwater recharge using water isotopes: a case study from the upper North Han River basin, Korea. *Environmental Geology*, 52(5), pp.853-859.
- Leij, F.J. and Van Genuchten, M.T., 1999. Principles of solute transport. *Agricultural drainage*, 38, pp.331-359.
- Leterme, B., Gedeon, M. and Jacques, D., 2013, March. Groundwater recharge modelling of the Nete catchment (Belgium) using the HYDRUS-1D–MODFLOW package. In *Proceedings of the 4th International Conference HYDRUS Software Applications to Subsurface Flow and Contaminant Transport Problems, Prague, Czech Republic* (Vol. 2122).
- Leterme, B., Mallants, D. and Jacques, D., 2012. Sensitivity of groundwater recharge using climatic analogues and HYDRUS-1D. *Hydrology and Earth System Sciences*, 16(8), pp.2485-2497.
- Liu, H.H., Doughty, C. and Bodvarsson, G.S., 1998. An active fracture model for unsaturated flow and transport in fractured rocks. *Water Resources Research*, 34(10), pp.2633-2646.
- Lu, N., Kaya, B.S. and Godt, J.W., 2011. Direction of unsaturated flow in a homogeneous and isotropic hillslope. *Water Resources Research*, 47(2).

- Ly, M., Hao, Z., Liu, Z. and Yu, Z., 2013. Conditions for lateral downslope unsaturated flow and effects of slope angle on soil moisture movement. *Journal of hydrology*, 486, pp.321-333.
- Malicki, M.A., Plagge, R., Renger, M. and Walczak, R.T., 1992. Application of time-domain reflectometry (TDR) soil moisture miniprobe for the determination of unsaturated soil water characteristics from undisturbed soil cores. *Irrigation Science*, 13(2), pp.65-72.
- Martel, E.A., 1913. Sur les expériences de fluorescéine à grandes distances. *Comptes Rendus de l'Académie de Sciences*, 157, pp.1102-1104.
- Mastrocicco, M., Prommer, H., Pasti, L., Palpacelli, S. and Colombani, N., 2011. Evaluation of saline tracer performance during electrical conductivity groundwater monitoring. *Journal of contaminant hydrology*, 123(3-4), pp.157-166.
- Matula, S., Batkova, K. and Legese, W.L., 2016. Laboratory performance of five selected soil moisture sensors applying factory and own calibration equations for two soil media of different bulk density and salinity levels. *Sensors*, 16(11), p.1912.
- McCord, J.T. and Stephens, D.B., 1987. Lateral moisture flow beneath a sandy hillslope without an apparent impeding layer. *Hydrological Processes*, 1(3), pp.225-238.
- McIntosh, J., McDonnell, J.J. and Peters, N.E., 1999. Tracer and hydrometric study of preferential flow in large undisturbed soil cores from the Georgia Piedmont, USA. *Hydrological Processes*, 13(2), pp.139-155.
- McLaughlin, M.J., 1981. A review of the use of dyes as soil water tracers. *Water SA*, 8(4), pp.196-201.
- Merlin, O., Walker, J., Panciera, R., Young, R., Kalma, J. and Kim, E., 2007. Soil moisture measurement in heterogeneous terrain. *Proc. Int. Congr. MODSIM*, pp.2604-2610.

- Millington, R.J. and Quirk, J.P., 1961. Permeability of porous solids. *Transactions of the Faraday Society*, 57, pp.1200-1207.
- Miyazaki, T., 1988. Water flow in unsaturated soil in layered slopes. *Journal of Hydrology*, 102(1-4), pp.201-214.
- Nimmo, J.R., 2006. Unsaturated Zone Flow Processes. *Encyclopedia of Hydrological Sciences* 13: 150.
- Nyberg, L., 1996. Spatial variability of soil water content in the covered catchment at Gårdsjön, Sweden. *Hydrological Processes*, 10(1), pp.89-103.
- Nyende, J., van Tonder, G. and Vermeulen, D., 2013. Application of isotopes and recharge analysis in investigating surface water and groundwater in fractured aquifer under influence of climate variability. *J Earth Sci Clim Change*, 4(4).
- Pathak, S.P. and Singh, T., 2014. An analysis on groundwater recharge by mathematical model in inclined porous media. *International scholarly research notices*, 2014.
- Peters, R. and Klavetter, E.A., 1988. A continuum model for water movement in an unsaturated fractured rock mass. *Water Resources Research*, 24(3), pp.416-430.
- Philip, J.R., 1991. Hillslope infiltration: Planar slopes. *Water Resources Research*, 27(1), pp.109-117.
- Piccinini, L., Fabbri, P. and Pola, M., 2016. Point dilution tests to calculate groundwater velocity: an example in a porous aquifer in northeast Italy. *Hydrological Sciences Journal*, 61(8), pp.1512-1523.
- Pullare, Nandakumaran. (2012). Changes in ground water utilization in Kerala - Causes & Consequences. 10.13140/RG.2.1.4956.1769.
- Qiu, Y., Fu, B., Wang, J. and Chen, L., 2001. Soil moisture variation in relation to topography and land use in a hillslope catchment of the Loess Plateau, China. *Journal of Hydrology*, 240(3-4), pp.243-263.
- Roxy, M.S., Sumithranand, V.B. and Renuka, G., 2010. Variability of soil moisture and its relationship with surface albedo and soil thermal diffusivity at

- Astronomical Observatory, Thiruvananthapuram, south Kerala. *Journal of Earth System Science*, 119(4), pp.507-517.
- Sathian, K.K. and Symala, P., 2009. Calibration and validation of a distributed watershed hydrologic model. *Indian Journal of Soil Conservation*, 37(2), pp.100-105.
- Schaap, M.G., Leij, F.J. and Van Genuchten, M.T., 2001. Rosetta: A computer program for estimating soil hydraulic parameters with hierarchical pedotransfer functions. *Journal of hydrology*, 251(3-4), pp.163-176.
- Shaji, E., 2013. Groundwater quality management in Kerala. *Online International Interdisciplinary Research Journal*, 3(3), pp.63-68.
- Simunek, J., 2015. Estimating groundwater recharge using HYDRUS-1D. *Engineering Geology and Hydrogeology*, 29, pp.25-36.
- Simunek, J., Šejna, M. and Van Genuchten, M.T., 1999. *The HYDRUS-2D software package for simulating the two-dimensional movement of water, heat, and multiple solutes in variably-saturated media: Version 2.0*. US Salinity Laboratory, Agricultural Research Service, US Department of Agriculture.
- Sinai, G. and Dirksen, C., 2006. Experimental evidence of lateral flow in unsaturated homogeneous isotropic sloping soil due to rainfall. *Water Resources Research*, 42(12).
- Sloan, P.G. and Moore, I.D., 1984. Modelling subsurface stormflow on steeply sloping forested watersheds. *Water Resources Research*, 20(12), pp.1815-1822.
- Stumm, W. and Morgan, J.J., 1970. *Aquatic chemistry; an introduction emphasizing chemical equilibria in natural waters*.
- Taylor, G.I., 1953. Dispersion of soluble matter in solvent flowing slowly through a tube. *Proceedings of the Royal Society of London. Series A. Mathematical and Physical Sciences*, 219(1137), pp.186-203.

- Teschemacher S., Rieger, W. and Disse, M., 2019. Experimental Investigation of Lateral Subsurface Flow Depending on Land Use and Soil Cultivation. *Water*, 11(4), p.766.
- Tonkul, S., Baba, A., Şimşek, C., Durukan, S., Demirkesen, A.C. and Tayfur, G., 2019. Groundwater recharge estimation using HYDRUS 1D model in Alaşehir sub-basin of Gediz Basin in Turkey. *Environmental monitoring and assessment*, 191(10), pp.1-19.
- Topp, G.C., Davis, J.L. and Annan, A.P., 1980. Electromagnetic determination of soil water content: Measurements in coaxial transmission lines. *Water resources research*, 16(3), pp.574-582.
- Twarakavi, N.K.C., Simunek, J. and Seo, S., 2008. Evaluating interactions between groundwater and vadose zone using the HYDRUS-based flow package for MODFLOW. *Vadose Zone Journal*, 7(2), pp.757-768.
- Udayakumar, G. and Mayya, S.G., 2014. Semi impervious subsurface barrier for water conservation in lateritic formations. *Journal of The Institution of Engineers (India): Series A*, 95(3), pp.151-156.
- Udayakumar, G., Mayya, S.G. and Ojoawo, S.O., 2015. Estimation of lateral subsurface flow in lateritic formations using well hydrograph analysis. *Aquatic Procedia*, 4, pp.1062-1069.
- Van Genuchten, M.T., 1980. A closed-form equation for predicting the hydraulic conductivity of unsaturated soils. *Soil science society of America journal*, 44(5), pp.892-898.
- Van Schaik, N.L.M.B., Schnabel, S. and Jetten, V.G., 2008. The influence of preferential flow on hillslope hydrology in a semi-arid watershed (in the Spanish Dehesas). *Hydrological Processes: An International Journal*, 22(18), pp.3844-3855.
- Vereecken, H., Huisman, J.A., Bogaen, H., Vanderborght, J., Vrugt, J.A. and Hopmans, J.W., 2008. On the value of soil moisture measurements in vadose zone hydrology: A review. *Water resources research*, 44(4).

- Warrier, C.U., Babu, M.P., Manjula, P., Velayudhan, K.T., Hameed, A.S. and Vasu, K., 2010. Isotopic characterization of dual monsoon precipitation—evidence from Kerala, India. *Current Science*, pp.1487-1495.
- Weiler, M., and F. Naef (2003). An experimental tracer study of the role of macropores in infiltration in grassland soils, *Hydrol. Processes*, **17**, 477–493.
- Western, A.W., Zhou, S.L., Grayson, R.B., McMahon, T.A., Blöschl, G. and Wilson, D.J., 2004. Spatial correlation of soil moisture in small catchments and its relationship to dominant spatial hydrological processes. *Journal of Hydrology*, 286(1-4), pp.113-134.
- Wienhofer, J., Germer, K., Lindenmaier, F., Färber, A. and Zehe, E., 2009. Applied tracers for the observation of subsurface stormflow at the hillslope scale. *Hydrology and Earth System Sciences*, 13(7), pp.1145-1161.
- Wilson, D.J., Western, A.W. and Grayson, R.B., 2004. Identifying and quantifying sources of variability in temporal and spatial soil moisture observations. *Water Resources Research*, 40(2).
- Wood, E.F., Sivapalan, M., Beven, K. and Band, L., 1988. Effects of spatial variability and scale with implications to hydrologic modelling. *Journal of hydrology*, 102(1-4), pp.29-47.
- Woods, R. and Rowe, L., 1996. The changing spatial variability of subsurface flow across a hillside. *Journal of Hydrology (New Zealand)*, pp.51-86.
- Worthington, S.R. and Smart, C.C., 2016. Determination of tracer mass for effective groundwater tracer tests. *Carbonates and Evaporites*, 31(4), pp.349-356.
- Xu, X., Kalhor, S.A., Chen, W. and Raza, S., 2017. The evaluation/application of Hydrus-2D model for simulating macro-pores flow in loess soil. *International Soil and Water Conservation Research*, 5(3), pp.196-201.
- Zaslavsky, D. and Sinai, G., 1981. Surface hydrology: V—In-surface transient flow. *Journal of the Hydraulics Division*, 107(1), pp.65-94.

**ASSESSMENT OF LATERAL FLOW AND BASE FLOW FOR EFFECTIVE
INTERVENTIONS IN WATER CONSERVATION**

By

JYOTHY NARAYANAN

(2016-28-004)

Abstract

Submitted in partial fulfillment of the requirement for the degree of

Doctor of Philosophy

In

Agricultural Engineering

(Soil and Water Engineering)

Faculty of Agricultural Engineering and Technology

Kerala Agricultural University



Department of Soil and Water Conservation Engineering

**KELAPPAJI COLLEGE OF AGRICULTURAL ENGINEERING AND
TECHNOLOGY**

TAVANUR-679573, MALAPPURAM (DT)

KERALA, INDIA

2021

ABSTRACT

Subsurface movement of water has a vital role in the availability of water of an area, such that vertical downward movement of water from root zone region will recharge the groundwater and the lateral movement from the soil moisture or groundwater reservoir will tend to diminish it. The vertical downward movement of infiltrated water gets partially blocked and the accumulated water will induce interflow/lateral flow from a point of higher hydraulic gradient towards the lower hydraulic gradient. The midlands in the State of Kerala are predominantly covered with laterite soil underlain with hard laterite and crystalline rocks. Even though the state of Kerala receives an average annual rainfall of 3000 mm, it experiences severe dry spell during post-monsoon season as groundwater storage is not adequate to meet various demands. With growing variations in the characteristics of precipitation, increasing population and urbanization the infiltration opportunity time for rainwater has decreased resulting in further worsening of the situation. The pertaining issue requires a comprehensive investigation, learning and adoption of effective interventions for water conservation. The most hidden knowledge in this regard is the lack of quantitative information available on the movement of subsurface water.

Hence, the present study was carried out to understand two major hydrological processes viz., lateral flow / interflow and groundwater flow in lateritic soils. The research was conducted at KCAET Tavanur campus, Kerala Agricultural University, India. The interflow determination was done in three sites through five experimental set ups. The selected experimental sites were having varied vegetal cover, slope and soil texture. Different techniques were used for the inducement of lateral flow such as rainfall simulation using micro-sprinklers, application of water in trenches and the natural rainfall. Interflow was monitored at three different soil depth zones of 0-40 cm, 40-80 cm and 80-120 cm on the vertical face of the trench made at the downslope side of the water application site. Further, salt (NaCl) tracer was used to determine lateral flow by analyzing salt breakthrough which was recorded through electrical

conductivity variations at the monitoring trench face. Tracer analysis for interflow estimation was done through 2 experimental set ups in site 2 and site 3. Base flow monitoring was done through salt (KCl) tracer through five observation wells constructed for this purpose. Instantaneous injection of KCl tracer was done in the injection well and salt breakthrough analysis was carried out in nearby monitoring wells. The study also included simulation of lateral flow and groundwater flow using HYDRUS-2D software. The study revealed that among various soil physical properties, the lateral flow discharge greatly depends on bulk density of soil and soil texture. Further, it was found that an instantaneous application of water on the soil surface and in trench results in more lateral flow than gentle application rates. It was proved from the experiments that NaCl can be treated as an effective tracer to monitor the subsurface flow though molecular diffusion of the salt due to antecedent moisture content remains as a hindrance to its use during rainy season. The study has established that though the infiltration capacity of the lateritic soil is very high, major portion of the infiltrated water moves laterally without reaching the water table. Thus, to increase the groundwater recharge, it is essential to enhance vertical preferential flow through deep rooted vegetation or by deep trenches and pits. Adopting subsurface mechanical barriers which can intercept and divert the interflow to downward direction is also appears to be effective. Further, simulation of lateral flow and base flow using HYDRUS-2D software predicted the lateral flow discharge with a correlation coefficient of 96.4 %. The prediction accuracy of the model for base flow was 73%.



Laboratory Calibration of Capacitance-Based Soil Moisture Sensor to Monitor Subsurface Soil Moisture Movement in Laterite Soil

Jyothy Narayanan^{1*} and K. K. Sathian²

¹Kellapaji College of Agriculture Engineering and Technology, Tavanur, Kerala, India.

²Dean (Agricultural Engineering), Kelappaji College of Agricultural Engineering and Technology, Tavanur, Kerala, India.

Authors' contributions

This work was carried out in collaboration between both authors. Both authors read and approved the final manuscript.

Article Information

DOI: 10.9734/IJPSS/2021/v33i1730558

Editor(s):

(1) Dr. Sangita Sahni, Dholi, Dr. Rajendra Prasad Central Agricultural University, India.

Reviewers:

(1) Manuel Filipe Pereira da Cunha Martins Costa, University of Minho, Portugal.

(2) Sofyan A Taya, Islamic university of Gaza, Palestine.

Complete Peer review History: <https://www.sdiarticle4.com/review-history/71185>

Original Research Article

Received 24 May 2021
Accepted 27 July 2021
Published 03 August 2021

ABSTRACT

Subsurface soil moisture movement in the unsaturated zone plays a critical role in the replenishment of groundwater table. This comprehension can be vital for the terrain with lateritic soil followed by the charnockite bedrock system. The conventional techniques to determine the subsurface soil moisture and its movement is cumbersome owing to high cost, large scale time consumption, field drudgery and greater possibility of manual errors. Among many other modern technologies for the measurement of volumetric water content, capacitance-based moisture sensors are capable and less expensive, thus, making them highly suitable for the research scholars worldwide. The study involves the use of TEROS 12 moisture sensors. The capacitance-based sensor TEROS 12, equipped with advanced soil moisture technique curtails the constraints in the conventional technique of soil moisture assessment and can provide precise measurements if suitably calibrated for the site specific soils. The study involves a soil specific calibration of TEROS 12 moisture sensor which was performed for the laterite soil to incorporate the sensor with the automated soil moisture monitoring system. The reliability of the sensor TEROS 12 was assessed by comparing its moisture measurements with that of the gravimetric method. The

*Corresponding author: E-mail: jyothy89narayanan@gmail.com;

calibration was performed for three TEROS 12 moisture sensors in order to monitor the interflow at three varying soil depths in the vadose zone. The R^2 values obtained from the calibration of sensors at depths of 0-0.4 m, and 0.8-1.2 m were 0.996, 0.994 and 0.992 respectively. Further, during validation it was found that the new measurements coordinated with the gravimetric measurements to a greater extent and increased the preciseness as compared to that of uncalibrated values of moisture contents, thereby establishing TEROS 12 capacitance-based sensor as a reliable and cost effective moisture sensor.

Keywords: Calibration; capacitance-based sensor; TEROS 12; interflow; soil moisture movement.

1. INTRODUCTION

Analysis of soil water movement plays a vital role in understanding various hydrological processes and their efficient simulation through hydrological models. However, there is only limited knowledge available regarding soil moisture movement in the subsurface soil strata as it is influenced by a number of forces and heterogeneous characteristics of the substrata [1,2]. Thus, real-time monitoring of soil moisture movement in the vadose zone is highly essential to interpret the groundwater recharge and preferential flow characteristics of the soil [3]. Direct measurement and thereby the characterization of vadose zone is quite challenging as it needs to carry out the investigations deeper than one or two meters below the soil surface. Additionally, direct measurements involve invasive methods of collecting soil samples in order to carry out laboratory examinations. Thus, direct measurements cannot be convenient and reliable owing to the rapidity in spatial and temporal variation of soil moisture movement [4].

Among the various methods used for monitoring the soil moisture movement, optical sensors, sensors using the electromagnetic technique namely, Time Domain Reflectometer TDR and Frequency Domain Reflectometer FDR (Capacitance-Based Sensor) are used, being convenient in handling and for the acquisition of real time data. Electric permittivity and magnetic permeability μ are the basic physical parameters describing electromagnetic properties of a medium [5]. An optical sensor is a device in which light interacts with the substance to be detected (measurand) and converts light affected by the measurand substance into electrical signal which gives information about the analyte [6]. Interaction between light and matter is of high significance to a wide variety of interesting applications [7]. Since optical fiber utilizes light rays instead of electrical signals, it is less affected by weather changes [8]. Time Domain

Reflectometer (TDR) is an electronic device that works on the principle of radar based on transmitting signals into the medium and collecting reflected signals [9]. TDR determines dielectric constant and consequently permittivity and water content (direct related) of the medium, which is soil, via wave propagation transmitted by two parallel embedded metal probes with the utmost accuracy [9,10]. Although, Time Domain Reflectometer (TDR) is precise but, it has limited wide scale applicability due to the cost of investment and discrepancy of data in high saline soils [11,12]. Conversely, capacitance-based sensors are cheaper as compared to the former and utilize high frequency to withstand the variations due to salinity and temperature [13]. The output of capacitive moisture sensors depends on the complex relative permittivity ϵ^* of the soil (dielectric medium) [14]. However, capacitance-based sensor needs to be calibrated specifically for the soil under the study for very precise results [15]. TEROS12 moisture sensor by the METER Group, Inc. USA, is a commercially available moisture sensor that assures consistency, robust construction, a large volume influence of 1010 ml, and data reliability at a cost which is affordable. The capacitance-based soil moisture sensor TEROS 12 has been already company calibrated for mineral soils and soilless media [16]. However, the sensor has not been calibrated for its accuracy in the laterite terrain at different soil profiles with varying soil aggregation and texture. Hence, the present study was carried out (i) to examine the accuracy and reliability of TEROS 12 capacitance-based moisture sensor using the conventional gravimetric and core sampling methods, (ii) to develop a calibration function for the site specific soil, (iii) to validate the calibrated sensor results, (iv) to integrate the calibrated moisture sensor to a data acquisition system.

2. MATERIALS AND METHODS

TEROS 12 capacitance-based soil moisture sensor as illustrated in Fig. 1 is a METER Group

product. It has three needles. Soil moisture is measured in between needle 1 and needle 2. The sensor measures electrical conductivity (EC) between needle 2 and needle 3. A thermistor is embedded to measure the temperature. It measures the dielectric permittivity or the ability of medium (soil) to get polarized by creating an electromagnetic field.

An oscillating wave of 70 MHz is supplied by the sensor to the sensor needles, which gets charged depending upon the dielectric property of medium. The charge time taken by the needles is recorded by the TEROS 12 microprocessor and provides the output in the form of a raw value based on the substrate dielectric property. The raw value is converted to volumetric water content (VWC) by a calibration equation specific to the substrate. The configuration for the TEROS 12 moisture sensors and its data collection was done by the ZL6 data logger (Fig1-b, c). ZL6 logger is a plug-n-play data logger for field research endeavours. A weather resistant enclosure houses the data logger thereby making the device compatible for long term outdoor operations. The collected data from the logger was transmitted to the ZENTRA cloud web service via cellular communication which was furnished in the ZENTRA Utility software. ZENTRA Utility was used to set all the configuration parameters required for the logger and real time sensor measurements were performed at the study site. The calibration was carried out for a lateritic terrain to monitor subsurface soil moisture movement. To analyse the soil moisture movement and its characteristics using TEROS 12 a trench of dimension 1.5 m x 0.6 m x 1.6 m (length x width x height) was dug in the experimental site. Three different soil profile depths i.e. 0-0.4 m, 0.4-0.8 m and 0.8-1.2 m were selected to determine the variation in volumetric water content with soil depth. Calibration was carried out for three TEROS 12 sensors separately for the three soil profile depths following the phases as explained below.

2.1 Field Data Acquisition and Analysis

Soil samples from the trench were collected (Fig 2.a) from the study site to determine the major index properties i.e. bulk density, specific gravity and type of the soil at three different profile depths from the trench face. Adequate care was taken while extracting the soil core samples so as to prevent excessive invasion of soil from the trench face. Subsequently, field data acquisition

was carried out in two phases. The first phase involved installation of TEROS 12 capacitance-based soil moisture sensors along with ZL6 data logger at the study site (Fig 2. b & c). The three TEROS 12 moisture sensors were marked as 1, 2 and 3 as per the sequence of their insertion at different soil depths. The tines of the moisture sensors were carefully inserted in all the three soil profile depths in the study site. The insertion was carried out carefully particularly, at 2nd and 3rd soil depths (0.4-0.8 m and 0.8-1.2 m). Proper care was taken to avoid the bending or breakage of the sensor tines, considering the presence of lateritic clay clods and compact soil, usually occurring at greater soil depths. The stereo plug connector of the moisture sensors were connected to sensor input ports inside the ZL6 data logger. A TEROS 12 sensor comes with a standard 5 m cable. The excess cable was secured during this experiment as it needs to be protected against the damage caused by rodents and other animals (Fig 2.d). Data logger was configured through ZENTRA Utility interface. Subsequently, the sensor configuration was done by providing a measurement interval of fifteen minutes and the sensor type information was supplied to the respective ports. Desired preferences for the volumetric water content, temperature and electrical conductivity measurements were set through the ZENTRA Utility interface. Subsequently, the sensor readings were scanned for all three soil depths at different time to obtain the real time soil moisture data.

The second phase of field data acquisition was for the gravimetric moisture content analysis. Soil samples from the three profile depths of 0-0.4 m, 0.4-0.8 m and 0.8-1.2 m were collected carefully from the vicinity of the TEROS 12 sensors creating the least / no disturbance to the moisture sensors and depicting the representative sample in the volume of influence of moisture sensor at the same time.

The samples were taken after noting down the sensor readings so as to ensure no discrepancy in the sensor data. The collected soil samples were kept in oven at a temperature of 105^oC for 24 hours after removing their lids. Mandatory calculations and comparisons were done among the results obtained from both phases of field data acquisition.

2.2 Sensor to Sensor Variability Analysis

Sensor to sensor variability analysis was performed for different soil moisture contents. A

calibration container of size 0.295 m x 0.225 m x 0.12 m (L x W x H) was used to perform the analysis. This was done by inserting two TEROS12 moisture sensors at different points in the calibration container for the same volumetric water content. Adequate caution was taken to prevent insertion of one sensor in the holes created by the other sensor. The coefficient of variation between the sensors was calculated at each varying moisture contents for the soil sample taken from a depth of 0-0.4 m from the trench face.

2.3 Soil Sample Preparation and Calibration of Sensor

Following the comparative analysis of the soil moisture obtained from the capacitance- based moisture sensor TEROS 12 and that from the gravimetric method, soil sample from the first profile depth of 0-0.4 m was taken. The calibration procedure preferred was “Method A” for soil specific calibration of METER soil moisture sensors. It is a method recommended by the METER group for higher accuracy and is based on weighing the entire sample of calibration. The collected soil sample from the study site was air-dried for 24 hours (Fig 3.a). The air dried sample was run through a sieve of 0.002 m size after breaking the larger clods. A plastic container was used as a calibration container (Fig 3.b). The container was packed with the soil to match field bulk density, of 0-0.4 m soil profile depth. This was done using the dry density value which was calculated through the core sample analysis in the laboratory. Subsequently, the air dried soil was packed upto a height of eight meter in the plastic container in

such a way, that it matched the field bulk density of soil. The procedure was carried out gradually by adding the soil in layers and also by compacting it after every layer so as to minimize the voids. TEROS 12 moisture sensor was inserted vertically directly into the soil filled in the container, avoiding any air gaps between the sensor tines and the soil. Raw moisture data from the sensor was collected and noted down. Soil sample of about 0.015 Kg was collected in the moisture can for gravimetric moisture content determination. Water was added in the dry soil to about ten percent of the total soil volume to raise the volumetric water content by ten percent (Fig.3.c). The soil was thoroughly mixed by overturning, until the mixture became homogeneous. The soil sample was filled again into the plastic calibration container in layers and with each layer light compaction was done to minimize the voids. Raw value of raised volumetric water content was recorded by the TEROS 12 sensor. At this point sensor to sensor variation was also determined using sensor 2 (Fig.3.d).

The above procedure was repeated to yield five calibration points. The calibration of sensor 1 was opted for the soil profile depth of 0-0.4 m. Similarly, sensor 2 and sensor 3 were calibrated for soil profile depths of 0.4-0.8 m and 0.8-1.2 m respectively. Proper care was taken to maintain the same bulk density of the sample throughout the calibration process, by packing the soil sample in the calibration container to the same height while raising the volumetric water content. The whole procedure was carried out at room temperature. Raw data from the sensor obtained via ZENTRA Utility was then tabulated.

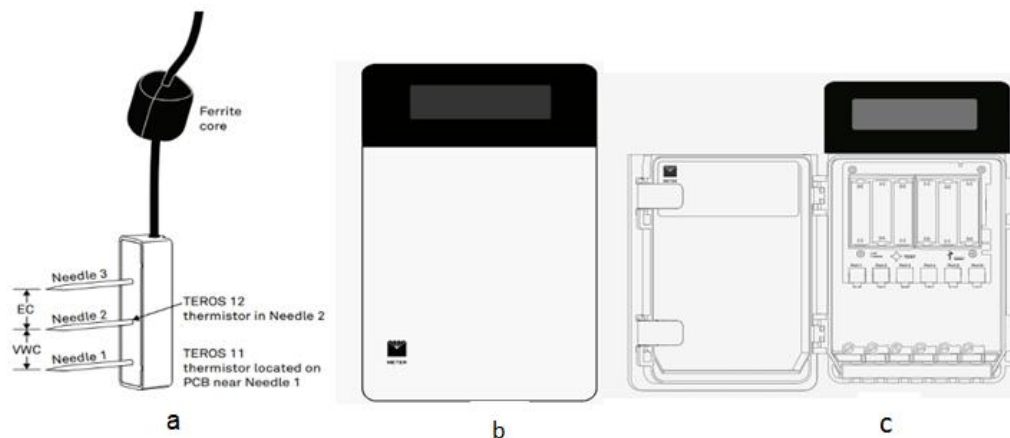


Fig. 1. a) TEROS 12 Sensor, b) Exterior of TEROS 12 Sensor, c) Interior of Sensor

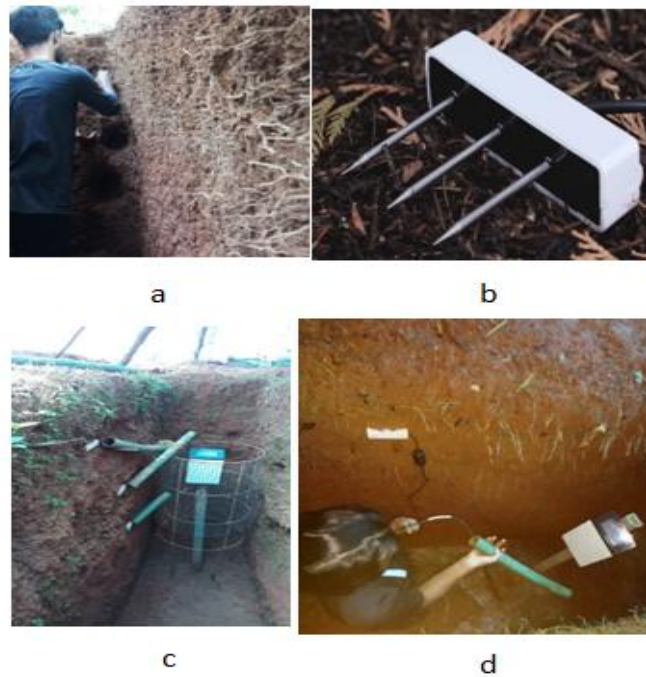


Fig. 2. a) Core cutter Sampling , b) TEROS 12 Sensor, c) Installation of TEROS 12 Sensor in the trench, d) Prevention from the rodent damage

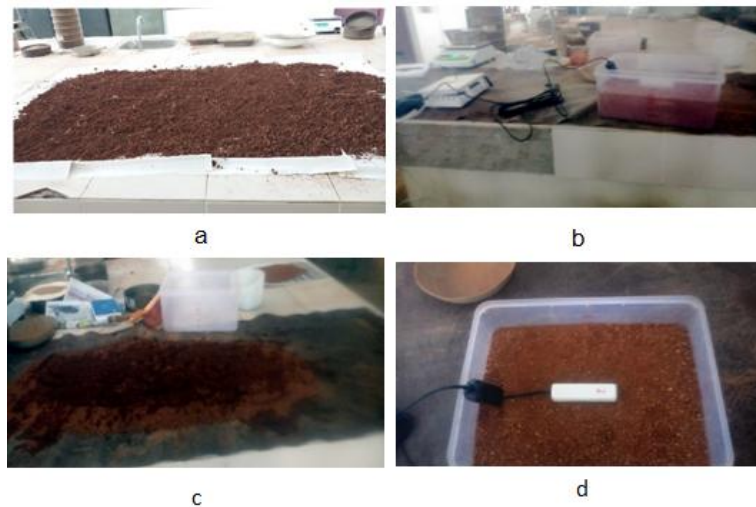


Fig. 3.a) Air drying of site specific soil , b) Addition of water to raise VWC of soil, c) Compaction of soil in plastic container to attain field BD, d) Insertion of TEROS 12 sensor

2.4 Integration of TEROS 12 moisture sensor with ZENTRA Cloud Software

Once the calibration functions were determined for all the three soil moisture sensors specific for the respective soil profile depths, it can be applied to the METER sensor data. In the

present study the calibration function was applied using ZENTRA Cloud software. Coefficients of new calibration function were added along with ancillary data obtained from field analysis. Once the coefficients for new calibration function were fed in the ZENTRA Cloud validation was carried out.

2.5 Validation of the Generated Calibration Function

The developed calibration function was validated by determining volumetric water contents in the site specific soil samples. The first soil profile depth of 0-0.4 m at the study site represented sandy loam type of soil and the other two depths contain loamy sand. The calibration procedure as prescribed in TEROS 12 user manual resulted in calculated coefficients which were put in the calibration equation via ZENTRA cloud software. The validation was performed for all the three soil profile depths with varying moisture content soil samples: oven dried, air dried, samples with volumetric water contents of 20%, 30% and 40%.

3. RESULTS AND DISCUSSIONS

The major soil index properties were identified. Bulk density was calculated using the core cutter method following equation 1. Specific gravity was calculated using pycnometer test and equation 2. Sieve analysis provided the grain size distribution of the soil. The textural classification was carried out by opting USDA textural classification triangle.

$$\rho = \frac{M_s}{V} \quad (1)$$

Where, ρ is soil bulk density, M_s is the mass of oven dry soil and V is bulk volume of the soil.

$$G = \frac{M_2 - M_1}{(M_2 - M_3) - (M_3 - M_4)} \quad (2)$$

Where, G is the specific gravity of soil, M_1 is mass of empty Pycnometer, M_2 is mass of the Pycnometer with dry soil, M_3 is mass of the Pycnometer and soil and water, M_4 is mass of Pycnometer filled with water only. The site specific soil index properties have been depicted in Table 1. The results which were determined by the capacitance-based soil moisture sensor TEROS 12 involved volumetric water content, soil temperature and electrical conductivity. The measurements were stored in ZL6 data logger.

The retrieval of data was done through ZENTRA Utility interface software. The gravimetric water content measurements were carried out for all the three profile depths. The collection of soil samples for laboratory analysis was done exactly at the same time for which the TEROS 12 moisture sensor data were analysed. The volumetric water content, θ (m^3 / m^3) of the site specific soil was obtained using equation 3 where, W_g (kg/kg , %) is the gravimetric water content of the sample, ρ_d (kg/m^3) and ρ_w (kg/m^3) are the dry bulk density of the soil and density of water respectively.

$$\theta = W_g \frac{\rho_d}{\rho_w} \quad (3)$$

The spatially varying data obtained from gravimetric analysis and TEROS 12 moisture sensors were then compared. Subsequently, it was revealed that the values predicted by TEROS 12 sensors were not precise (Table2).

3.1 Results of Gravimetric Analysis and Moisture Sensor for the Three Soil Profile Depths

The gravimetric analysis and volumetric water content determination through TEROS 12 moisture sensor was carried out in the lateritic terrain simultaneously. The textural classification of the site specific soil revealed sandy loam soil type at first profile depth and loamy sand at the other two profile depths. The comparison between the moisture contents obtained from gravimetric analysis and TEROS 12 moisture sensors depicted that TEROS 12 moisture sensor recorded a variation of (-5%) at a depth of 0-0.4 m, (-12%) variation at 0.4-0.8 m depth and (+3%) variation at 0.8-1.2 m depth.

3.2. Results of Sensor to Sensor Variability Analysis

The Sensor to sensor variability analysis was carried out prior to the calibration for the predetermined soil moisture content sample. It

Table 1. Index properties of the site specific soil

Soil index properties of the site specific soil			
Depth	Bulk Density (kg/m^3)	Specific Gravity	Type of Soil
0-0.4 m	1230	2.42	Sandy Loam
0.4-0.8 m	1110	2.49	Loamy Sand
0.8-1.2 m	1260	2.54	Loamy sand

Table 2. Comparison of TEROS 12 moisture sensor readings to gravimetric measurements

S.No.	Before calibration			Before calibration		
	TEROS 12 Measurements Volumetric Water Content (%)			Gravimetric Measurements Volumetric Water Content (%)		
	0-0.4 m	0.4-0.8 m	0.8-1.2 m	0-0.4 m	0.4-0.8 m	0.8-1.2 m
1	40.3	41.3	34.6	42.4	47.3	33.52

was performed only for the soil depth of 0-0.4 m. Samples at different moisture contents (air dry, 10%, 20%, 30%, 40%) were used to test sensor to sensor variability.

The values of Coefficient of Variation as shown in Table 3 depicted no significant sensor to sensor variability. Thus, calibration of one sensor was only required for a particular depth and type of soil with specific bulk density.

3.3 Calibration of TEROS 12 Capacitance-Based Moisture Sensor for Site Specific Laterite Soil

The comparison between the moisture measurements taken by gravimetric analysis and TEROS 12 moisture sensor depicted variations. Thus, in order to obtain precise measurements sensor calibration was performed using Calibration A method used for the TEROS 12 moisture sensor by the METER group. The calibration resulted in an equation with calculated coefficients for all the three soil depths of the trench separately. Fig. 4, Fig. 5 and Fig. 6 depicts the calibration curves (CC) for all the three soil depths in the trench. Calibrated coefficients were obtained through the calibration equations 4, 5, and 6 for the three respective soil profile depths of 0-0.4 m, 0.4-0.8 m and 0.8-1.2 m. In equations 4, 5, and 6 the x values represent raw moisture data and the y values represent actual VWC values in m^3 / m^3 . Subsequently, the calibrated coefficients were fed through ZENTRA cloud to determine the calibrated and site specific precise values of Volumetric water content of the soil.

$$y = 9.610e^{-10}x^3 - 7.362e^{-6}x^2 + 1.892e^{-2}x - 1.596 \dots \dots (4)$$

$$y = 1.891e^{-9}x^3 - 1.457e^{-5}x^2 + 3.734e^{-2}x - 3.145 \dots \dots (5)$$

$$y = 1.164e^{-9}x^3 - 8.902e^{-6}x^2 + 2.274e^{-2}x - 1.905 \dots \dots (6)$$

The values of coefficient of determination i.e. R^2 obtained for the moisture sensors were 9.964,

9.941 and 9.922 for the depths 0-0.4 m, 0.4-0.8 m and 0.8-1.2 m respectively.

3.4 Insertion of Calibrated Function for TEROS 12 Sensor through ZENTRA Cloud

The calibrated coefficients obtained from equations 4, 5 and 6 were fed in the polynomial equations through ZENTRA cloud to obtain calibrated values of volumetric water content.

3.5. Data Validation with the Conventional Gravimetric Method

Validation of the developed calibrated function was done by measuring the site specific moisture contents. This was done by installing the TEROS 12 moisture sensors in the experiment site along with the ZL6 data logger. All the three sensors were installed carefully in the trench face at depths of 0-0.4 m, 0.4-0.8 m and 0.8-1.2 m. Proper caution was taken while connecting the moisture sensors to the data logger, such that sensor 1 which was calibrated for first soil depth (sandy loam soil, BD=1.23) was connected to the first port in the data logger and successively for the other two soil depths (loamy sand, BD=1.11, BD= 1.26 respectively) sensor 2 and Sensor 3 were connected to the second and third ports in the data logger. The calibrated volumetric water content was obtained directly from ZENTRA cloud. The soil samples for gravimetric moisture content analysis were collected in a set of three from all the three soil depths. Three soil samples from each depth were taken so as to obtain a representative sample from the volume of influence of TEROS 12 moisture sensor for a better comparison and thus validation of sensor. The comparative results represented a significant reduction in the variation between the results obtained through capacitance-based moisture sensor and gravimetric moisture content analysis. The Root Mean Square Error (RMSE) was calculated for soil moisture contents derived by different calibrated functions. The RMSE values for the three depths were 0.13, 0.16 and 0.20 respectively. The percentage variation in the

Table 3. Coefficient of Variation among the three sensors at various pre-determined soil moisture contents

M.C	Sensor 1	Sensor 2	Sensor3	Mean	SD	CV (%)
Air Dry	1974.5	1960.5	1980.9	1972.0	10.4	0.5
10%	2083.1	2059.1	2071.3	2071.1	12.0	0.6
20%	2255.3	2246.2	2255.6	2252.3	5.3	0.2
30%	2660.3	2659.2	2640.8	2653.4	11.0	0.4
40%	2924.1	2930.6	2945.2	2933.3	10.8	0.3

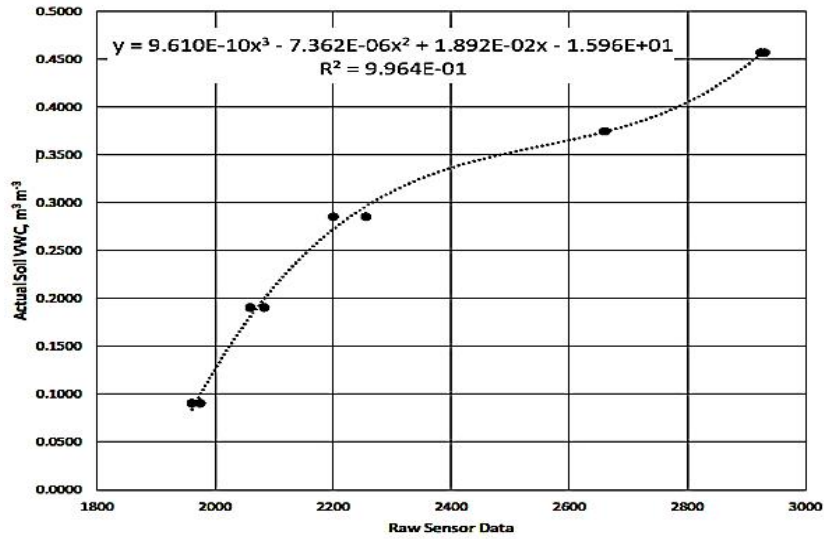


Fig. 4. Calibration curve for sensor 1 (for soil profile at 0-0.4 m)

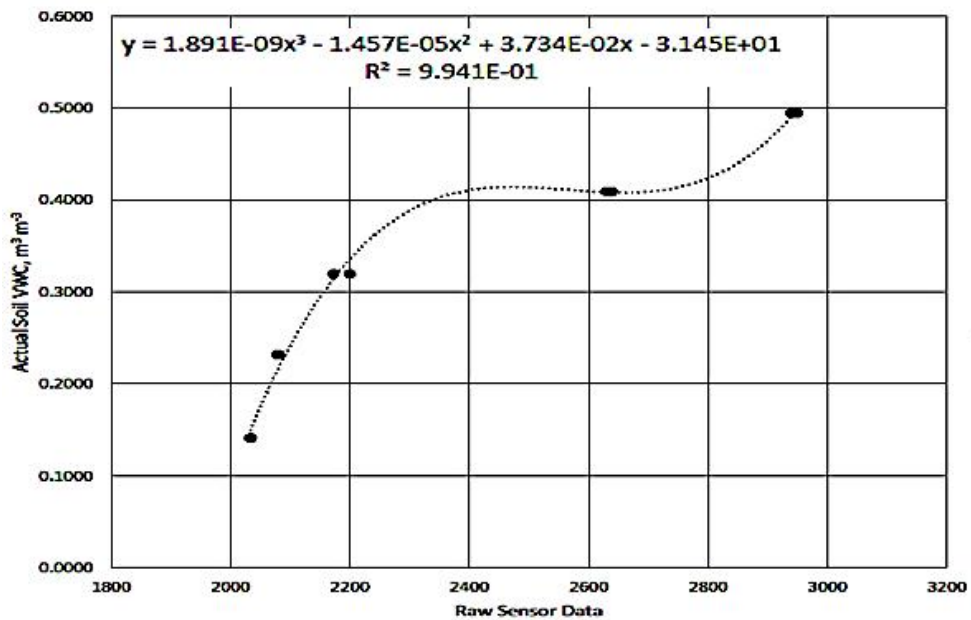


Fig. 5. Calibration curve for sensor 2 (for soil profile at 0.4-0.8 m)

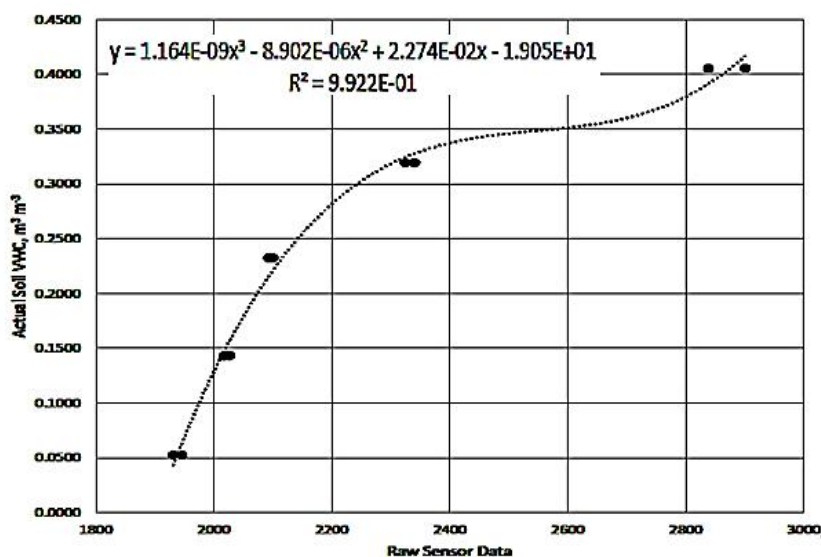


Fig. 6. Calibration curve for sensor 3 (for soil profile at 0.8-1.2 m)

volumetric water content for the depths 0-0.4 m, 0.4-0.8 m and 0.8-1.2 m were reduced after calibration to (+1.7%), (+3.9%) and (-1.8%) respectively. Thus, the data prediction by the capacitance-based TEROS 12 moisture sensor was improved.

4. CONCLUSIONS

The study involved evaluation of the accuracy and reliability of TEROS 12 capacitance-based sensor under field conditions. The study also established the reliability of calibration method A provided by the sensor company. The main purpose of installing the moisture sensor was to study the high spatial and temporal variation of lateral flow of water in the laterite soil. The TEROS 12 sensor is not sensitive to variation in soil texture and EC because it runs at a high measurement frequency which was identified during the study. Therefore, its generic calibration equation should result in reasonable absolute accuracy according to the METER group (Pullman). But, the site chosen for the study had unusual decrease in bulk density and greater porosity at a soil depth of 0.4-0.8 m as compared to the depths of 0-0.4 m and 0.8-1.2 m. Moreover the site represented a lateritic terrain. Thus, a reliability check was essential before completely relying on the sensor measurements. The developed soil specific calibration equation for the site specific soil performed satisfactorily during the sensor validation procedure for the determination of

volumetric water content of soil in the field. Hence, TEROS 12 sensor can be used successfully to determine the VWC of mineral soils with appropriate calibration. The sensor is highly suitable for the experiments involving greater temporal variation for long duration. Additionally, the results suggest that the accuracy of sensor greatly depends upon the bulk density and texture of soil.

However, while working at varying soil depths or profile (on the trench face) with TEROS 12 sensors it is essential to create least disturbance at the experimental site before and after installing the sensors. It is also important to investigate the effect of varying bulk densities of the soil profile on the sensor measurements. The results depicted a positive error at the first two depths of the soil profile suggesting higher porosity as the calibration will be too wet at the dry end due to the filling up of pore with air. This positive error was highest for the second depth. The third depth noticed negative error which suggested lower porosity as the calibration will be too dry at the wet end due to the filling of pore spaces with water. Further studies should be undertaken to include the effects of soil mineralogy, and organic matter content on the sensor measurements and its calibration.

DISCLAIMER

The products used for this research are commonly and predominantly use products in our

area of research and country. There is absolutely no conflict of interest between the authors and producers of the products because we do not intend to use these products as an avenue for any litigation but for the advancement of knowledge. Also, the research was not funded by the producing company rather it was funded by personal efforts of the authors.

ACKNOWLEDGEMENTS

I would like to present my foremost thanks to my supervisor Dr.Sathian K.K, *Dean of the Institution, Professor and Head*, Dept. of SWCE, Tavanur, Kerala for providing his valuable guidance. I am grateful to Kerala Agricultural University for the required funding to acquire the advanced capacitance based sensors and data logger in order to accomplish this study. I would like to present my thanks to Mr. Adarsh S.S for his sincere help during laboratory tests for the calibration of TEROS 12 sensors.

COMPETING INTERESTS

Authors have declared that no competing interests exist.

REFERENCES

1. Bouma J. Soil morphology and preferential flow along macropores. *Agricultural Water Management*. 1981;3.4:235–50. Available: [https://doi.org/10.1016/0378-3774\(81\)90009-3](https://doi.org/10.1016/0378-3774(81)90009-3)
2. Fares Ali, Ripendra Awal, Haimanote K. Bayabil, ‘Soil water content sensor response to organic matter content under laboratory conditions. *Sensors (Switzerland)*. 2016;16.8. Available:<https://doi.org/10.3390/s16081239>
3. Nimmo, John R. Unsaturated Zone Flow Processes. *Encyclopedia of Hydrological Sciences*. 2005;2299–2322. Available:<https://doi.org/10.1002/0470848944>.
4. Gao, Zhenran, Yan Zhu, Cheng Liu, Hongzhou Qian, Weixing Cao, Jun Ni. Design and Test of a Soil Profile Moisture Sensor Based on Sensitive Soil Layers. *Sensors (Switzerland)*, 2018;18.5. Available:<https://doi.org/10.3390/s18051648>
5. Taya SA. Slab waveguide with air core layer and anisotropic left-handed material claddings as a sensor. *Opto-Electronics Review*. 2014;22(4):252-257.
6. Taya SA, Shaheen SA. Binary photonic crystal for refractometric applications (TE case). *Indian Journal of Physics*. 2018;92(4):519-527.
7. Taya SA. P-polarized surface waves in a slab waveguide with left-handed material for sensing applications. *Journal of Magnetism and Magnetic Materials*. 2015;377:281-285.
8. Al-Ashi NE, Taya SA, El-Naggar SA, Vigneswaran D, Amiri IS. Optical fiber surrounded by a graphene layer as an optical sensor. *Optical and Quantum Electronics*. 2020;52(3):1-10.
9. Dwevedi A, Kumar P, Kumar Y, Sharma YK, Kayastha AM. Soil sensors: detailed insight into research updates, significance, and future prospects. In *New pesticides and soil sensors*. Academic Press. 2017;561-594.
10. Fen-Chong, Teddy, Antonin Fabbri, Jean Pierre Guilbaud, Olivier Coussy. Determination of liquid water content and dielectric constant in porous media by the capacitive method. *Comptes Rendus – Mecanique*. 2004;332(8):639–45. Available:<https://doi.org/10.1016/j.crme.2004.02.028>
11. Blonquist Jr JM, Jones SB, Robinson DA. A time domain transmission sensor with TDR performance characteristics. *Journal of hydrology*. 2005;314(1-4):235-245.
12. Nagahage, Ekanayaka Achchillage Ayesha Dilrukshi, Isura Sumeda Priyadarshana Nagahage, and Takeshi Fujino. Calibration and validation of a low-cost capacitive moisture sensor to integrate the automated soil moisture monitoring system. *Agriculture (Switzerland)*. 2019;9(7). Available: <https://doi.org/10.3390/>
13. Kojima Y, Shigeta R, Miyamoto N, Shirahama Y, Nishioka K, Mizoguchi M, Kawahara Y. Low-cost soil moisture profile probe using thin-film capacitors and a capacitive touch sensor. *Sensors*, 2016; 16(8):1292.
14. Kelleners TJ, Soppe RWO, Robinson DA, Schaap MG, Ayars JE, Skaggs TH. Calibration of capacitance probe sensors using electric circuit theory. *Soil Science Society of America Journal*, 2004;68 (2):430-439.
15. Chow, Lien, Zisheng Xing, Herb W. Rees, Fanrui Meng, John Monteith, Lionel Stevens. field performance of nine soil

water content sensors on a sandy loam soil in new brunswick, maritime region, Canada. *Sensors*. 2009;9.11:9398–9413. Available:<https://doi.org/10.3390/s91109398>
16. Meter group, 'Teros 11/12'. 2019;30.

© 2021 Narayanan and Sathian; This is an Open Access article distributed under the terms of the Creative Commons Attribution License (<http://creativecommons.org/licenses/by/4.0>), which permits unrestricted use, distribution, and reproduction in any medium, provided the original work is properly cited.

Peer-review history:

*The peer review history for this paper can be accessed here:
<https://www.sdiarticle4.com/review-history/71185>*